An International ICT Journal
Featuring Industry-University-Institute Cooperation

ISSN 1673-5188
CN 34-1294/TN

ZTE COMMUNICATIONS

中兴通讯技术(英文版)

https://zte.magtechjournal.com

June 2026, Vol. 24 No. 2

Special Topic:
AI-Agent Communication Network (ACN): Architecture, Protocols and Key Technologies

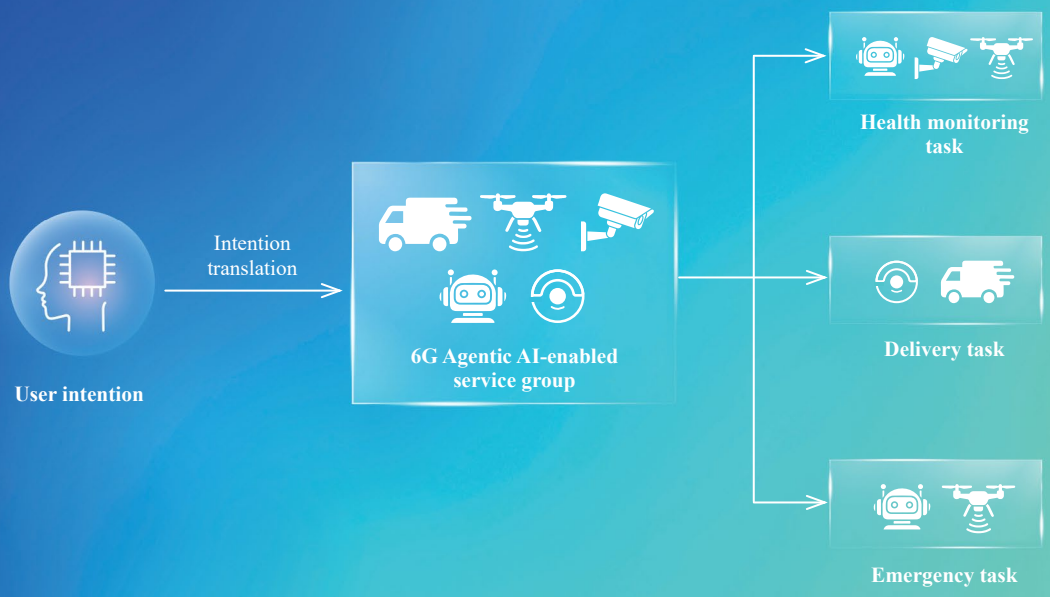

(See Fig. 9 on P. 49)

ISSN 1673-5188
06>

The 10th Editorial Board of ZTE Communications

CONTENTS

ZTE COMMUNICATIONS
June 2026 Vol. 24 No. 2 (Issue 95)

Special Topic ▶ AI-Agent Communication Network (ACN): Architecture, Protocols and Key Technologies

Industry-Academia Co-Research ▶

Serial parameters: CN 34–1294/TN*2003*q*16*102*en*P*¥30.00*2200*11* 2026-06

Special Topics for 2026

	Special Topic	Leading Guest Editor
1	Achievements of ZTE's Industry-University-Institute Cooperation Projects	Xu Chengzhong (University of Macau, China)
2	**AI-Agent Communication Network (ACN): Architecture, Protocols and Key Technologies**	**Sun Tao (China Mobile Research Institute, China)**
3	Reconfigurable Antenna Systems for Next-Generation Mobile Communications	Yang Kun (Nanjing University, China)
4	Goal-Oriented Joint Semantic and Channel Coding for Future Communications	Yuan Jinhong (University of New South Wales, Australia)

ZTE Communications Guidelines for Authors

Remit of Journal

ZTE Communications publishes original theoretical papers, research findings, and surveys on a broad range of communications topics, including communications and information system design, optical fiber and electro-optical engineering, microwave technology, radio wave propagation, antenna engineering, electromagnetics, signal and image processing, and power engineering. The journal is designed to be an integrated forum for university academics and industry researchers from around the world.

Manuscript Preparation

Manuscripts must be typed in English and submitted electronically in MS Word (or compatible) format. The word length is approximately 3 000 to 8 000, and no more than 8 figures or tables should be included. Authors are requested to submit mathematical material and graphics in an editable format.

Abstract and Keywords

Each manuscript must include an abstract of approximately 150 words written as a single paragraph. The abstract should not include mathematics or references and should not be repeated verbatim in the introduction. The abstract should be a self-contained overview of the aims, methods, experimental results, and significance of research outlined in the paper. Three to eight carefully chosen keywords must be provided with the abstract.

References

Manuscripts must be referenced at a level that conforms to international academic standards. All references must be numbered sequentially intext and listed in corresponding order at the end of the paper. References that are not cited in-text should not be included in the reference list. References must be complete and formatted according to *ZTE Communications* Editorial Style. A minimum of 10 references should be provided. Footnotes should be avoided or kept to a minimum.

Content and Structure

ZTE Communications seeks to publish original content that may build on existing literature in any field of communications. Authors should not dedicate a disproportionate amount of a paper to fundamental background, historical overviews, or chronologies that may be sufficiently dealt with by references. Authors are also requested to avoid the overuse of bullet points when structuring papers. The conclusion should include a commentary on the significance/future implications of the research as well as an overview of the material presented.

Peer Review and Editing

All manuscripts will be subject to a two-stage anonymous peer review as well as copyediting, and formatting. Authors may be asked to revise parts of a manuscript prior to publication.

Biographical Information

All authors are requested to provide a brief biography (approx. 100 words) that includes email address, educational background, career experience, research interests, awards, and publications.

Acknowledgments and Funding

A manuscript based on funded research must clearly state the program name, funding body, and grant number. Individuals who contributed to the manuscript should be acknowledged in a brief statement.

Address for Submission

http://mc03.manuscriptcentral.com/ztecom

Guest Editorial >>>

Special Topic on AI-Agent Communication Network (ACN): Architecture, Protocols and Key Technologies

Guest Editors

Sun Tao

Cui Yong

AI agents, whether embodied as physical entities or existing as software, are developing extremely fast and are believed to be vital for 6G and the whole Internet in the future. The communication network shall evolve to meet the great potential increase in the number of agents. AI agents are expected to become new users but with quite different traffic patterns, varying quality of service (QoS) requirements, and multi-modality data. They may also rely on the network to gain facilitated capabilities such as computing, sensing, and data. It is important to enable these AI agents to communicate with each other securely at any time and anywhere to accomplish assigned tasks. By leveraging AI agents, the communication system may undergo a revolutionary change toward a new generation. Embodied AI agents in network elements (e. g. , terminals, access, core and transport networks) will make the system run actively, dynamically, and autonomously. It can be seen that AI agents are bringing a new paradigm for network services as well as for the network itself. It is worthwhile for both industry and academia to devote effort to making this happen toward the AI era.

In this special issue, we aim to explore the AI-Agent Communication Network (ACN) from the perspectives of architecture, protocol and key technologies. In view of the community's interest in this area, as well as the timing of 6G standardization, we believe this special issue is the right time to show how the community views this important area and, as a trigger, to further explore this.

The first paper, titled "AI Agent Centric Network: New Network Design Paradigm and Related Key Technologies", proposes a paradigm shift for future 6G wireless networks from traditional human-centric, connectivity-oriented designs to AI Agent-Centric (AA-Centric) networks. To realize this vision, the paper introduces key supporting technologies, including a new functional system framework, a layered wireless network architecture, multi-level large language model collaboration, and enhanced protocols for agent-to-agent and agent-to-non-agent interaction.

The second paper, titled "Toward AI-Agent-Native 6G Networks: A Survey on Protocols, Multimodal Coordination, and ISCC-Driven Dynamic Networking", explores AI-agent-native 6G networks, shifting from the Internet of Things (IoT) to the Internet of Agents (IoA) with AI agents as core users. It analyzes unique agentic traffic (bursty semantic streams, ultra-reliable low-latency flows) and proposes agent-centric key value indicators (KVIs). It introduces Agentic Syntax for intent-based signaling, multi-agent coordination via Integrated Sensing, Communication, and Computing (ISCC) technologies, and network embedded agents (NEAs). A Deep-Agentic-Network Architecture (DAN-Arch) is proposed, vertically integrating physical sensing and reasoning flows. Finally, challenges in energy efficiency, standardization, and governance are discussed to guide future research.

The third paper, titled "Training Optimization for Complex Reasoning Tasks in ACN: Dynamic Batch-Aware Advantage Weighting for Agentic RAG", addresses reward sparsity and low sample efficiency in training Agentic retrieval-augmented generation (RAG) for complex reasoning in 6G ACN. It pro-

DOI: 10.12142/ZTECOM.202602001
Citation: (Format 1): Sun T, Cui Y. Editorial: AI-Agent Communication Network (ACN): architecture, protocols and key technologies [J]. ZTE Communications, 2026, 24(2): 1–2. DOI: 10.12142/ZTECOM.202602001
Citation: (Format 2): T. Sun and Y. Cui, "AI-Agent Communication Network (ACN): architecture, protocols and key technologies," *ZTE Communications*, vol. 24, no. 2, pp. 1 – 2, Jun. 2026. doi: 10.12142/ZTECOM.202602001.

poses dynamic batch-aware advantage weighting (DB-AW), a lightweight reinforcement learning (RL) module built on group relative policy optimization (GRPO), with two core components: difficulty-aware weighting (amplifying advantages for challenging samples) and batch filtering (removing zero-gradient groups). Evaluated on HotpotQA, NQ, and 2Wiki datasets, DB-AW delivers 15% – 18% accuracy gains on Qwen2.5-3B/7B and LLaMA3.2-3B, while lifting the effective update rate from 68% to 100%. It reduces training costs and enables scalable agent deployment in ACN.

The fourth paper, titled "Internet of Agents: Design of the Protocol System", designs a protocol system for the IoA, addressing identity management, dynamic networking, and semantic routing challenges in large-scale agent collaboration. It classifies agents into user agents and service agents, proposing a three-layer architecture with management, control, and routing protocols. Key designs include unified agent identification, capability registration, Domain Name System (DNS)-based service discovery, task-driven networking, and semantic routing. The system extends existing Internet protocols and introduces semantic awareness to enable scalable, secure cross-domain agent collaboration, laying a foundation for an open, large-scale agent ecosystem.

The fifth paper, titled "The Dawn of 6G: Empowering a User-Centric Ecosystem with Agentic AI", proposes AA6NS, an Agentic AI-enabled 6G network service framework for user-centric ecosystems. It integrates Agentic AI across 6G's application, core, and RAN layers, enabling intent-driven orchestration, adaptive QoS management, and dynamic multi-device service group coordination. The framework supports physical AI applications such as smart delivery, elderly care, and emergency rescue, translating user intents into real-time network actions. Key capabilities include task-level packet data unit (PDU) sessions, service awareness, and group management, laying the foundation for intelligent, adaptive human-machine collaboration in 6G.

The sixth paper, titled "Intent-Driven Control System for Heterogeneous Agent-Oriented Networking (HaoNet)", tackles dynamic, high-frequency agent interactions. HaoNet has three core traits: task-driven operation, distributed collaboration, and closed-loop intelligence. A three-layer architecture integrating Intent-Driven Network (IDN) maps high-level intents to network actions. Key technologies include Monitor-Analyze-Plan-Execute over a shared Knowledge (MAPE-K) adaptive loops, large language model (LLM)-based intent processing, and large-small model collaboration. Smart home and smart factory scenarios verify the system's ability to boost policy consistency, reliability, and task efficiency in dynamic agent networks.

The seventh paper, titled "Mitigating Semantic Drift in Multi-Agent Communication: A Dynamic Neuro-Symbolic Approach", addresses semantic drift in LLM-based multi-agent communication, where heterogeneous agents assign conflicting meanings to shared terms. It proposes DOA, a dynamic ontology alignment framework with a semantic prober, neuro-symbolic aligner, and consensus vault. DOA dynamically reconciles local ontologies in real time, grounding dialogue in a shared evolving ontology. Evaluated in supply chain and healthcare scenarios, DOA boosts task success rates by 31.5% and cuts communication overhead by 50%, outperforming raw natural language and fixed-schema baselines.

ACN is a new and important topic. The papers above span new ideas on architecture, mechanisms, and protocols, covering both mobile networks and the Internet in general. As this special issue is being generated, OpenClaw is booming. It can be expected that more AI agent applications, frameworks, and platforms will emerge. The open-source and industry ecosystem is also key to this area. In summary, we hope this special issue is a big step toward identifying the open problems, attracting more attention from the community to work together, and designing the system for the era of AI tokens and AI-agent worlds.

Biographies

Sun Tao received his BS degree in automation (2003) and PhD degree in control science and engineering (2008), both from Tsinghua University, China. He has been with China Mobile Research Institute since 2008. He is now the Chief Expert at China Mobile. He has more than ten years of experience in mobile network architecture design, IP technology research, and standardization, and served as the Vice Chair of 3GPP SA2 (System Architecture). He currently serves as Vice Chair of 3GPP SA.

Cui Yong received his BE degree (1999) and PhD degree (2004) both in computer science and engineering from Tsinghua University, China. He is currently a full professor in the Computer Science Department at Tsinghua University. He has published over 100 papers in refereed conferences and journals, receiving several Best Paper Awards. He has co-authored more than 10 Internet standard documents (RFCs). His major research interests include mobile cloud computing and network architecture. He served or serves on the editorial boards of *IEEE TPDS*, *IEEE TCC*, and *IEEE Internet Computing*. He also acted as a working group co-chair at IETF.

AI Agent Centric Network: New Network Design Paradigm and Related Key Technologies

Duan Xiangyang[1,2], Yang Li[1,2], Zhang Kangjie[1,2], Sun Wenwen[1,2], Xie Feng[1,2], Niu Li[1,2]

(1. State Key Laboratory of Mobile Network and Mobile Multimedia, Shenzhen 518055, China;
2. ZTE Corporation, Shenzhen 518057, China)

DOI: 10.12142/ZTECOM.202602002

https://kns.cnki.net/kcms/detail/34.1294.TN.20260519.1450.004.html, published online May 20, 2026

Manuscript received: 2026-04-11

Abstract: The diverse and heterogeneous terminal artificial intelligence (AI) agents and network-element AI agents are flourishing in a flywheel-like manner. The new characteristics of their capabilities and behaviors will reshape the service paradigm and traffic logic of future mobile information networks. This article first elaborates on the dynamics of the intertwined and integrated development of the AI agent/robot industry and the wireless communication industry. Then, based on an analysis of the new capabilities and behavioral characteristics of terminal AI agents and network-element AI agents, the article deduces a new design paradigm for future AI agent-centric (AA-Centric) networks, which includes seven core features: intent-driven, proactive service, distributed collaboration, efficient customization, deterministic guarantee, online evolution, and infinite generation. Guided by this new paradigm, the new architecture of 6G networks is further deduced, and the key supporting technologies are expounded. Finally, it is concluded that AI agents play a crucial role in driving the innovation of future network architectures and the ultimate expansion of capabilities.

Keywords: 6G wireless system; AI agent; AA-Centric design; system capability characteristics; system behavior characteristics

Citation (Format 1): Duan X Y, Yang L, Zhang K J, et al. AI agent centric network: new network design paradigm and related key technologies [J]. ZTE Communications, 2026, 24(2): 3 - 15. DOI: 10.12142/ZTECOM.202602002

Citation (Format 2): X. Y. Duan, L. Yang, K. J. Zhang, et al., "AI agent centric network: new network design paradigm and related key technologies," *ZTE Communications*, vol. 24, no. 2, pp. 3 - 15, Jun. 2026. doi: 10.12142/ZTECOM.202602002.

1 Introduction

Industry predictions indicate that the number of artificial intelligence (AI) agents is expected to grow exponentially in the future, and their diversity in type and capability may exceed that found among humans. These AI agents are equipped with multi-modal perception, autonomous decision-making, and large-scale collaboration capabilities, enabling them to process information and perform tasks at speeds and scales beyond those of human users. As a result, they will become primary service objects for future 6G networks, profoundly impacting network service paradigms and integrated traffic patterns[1-3].

Large language model (LLM) technologies are driving the application of AI agents to a new level, and have already demonstrated strong perception, reasoning, and execution capabilities for digital tasks in the digital world. As AI agents continue to advance, their applications will be deployed on future AI agent terminals, evolving into super-applications and reshaping the user interaction paradigm at the terminal side. Simultaneously, the capabilities of AI agents are also being integrated into future intelligent network entities, becoming super components of the network, significantly enhancing the network's self-intelligence and service agility, and driving the emergence of on-demand and flexible network operations and service paradigms[4-6]. The brain-like intelligence of AI agents is driving the application of embodied robots to a new level, enabling them to perform multi-modal perception, autonomous decision-making, and complex physical tasks (such as autonomous driving, warehouse logistics, and domestic services). Monolithic non-networked robots are inherently constrained by their physical form, limited computational resources, perceptual range, and communication capacity. Therefore, networked robots are poised to become the dominant trend, enabled by cellular connectivity and capable of collaborative operation and on-demand capability expansion. Cellular networked robot terminals will emerge as new

This work is supported by the National Science and Technology Major Project of China under Grant No. 2025ZD1304800.

mobile users and change the service paradigm of future wireless networks from serving humans to serving devices and intelligent agents[7-8].

In recent years, the convergence of AI agents and wireless communications has garnered significant attention from both academia and industry, driving the evolution toward AI-native 6G architectures. From an academic research perspective, several pioneering studies have laid important foundations for the AI Agent-Centric (AA-Centric) network paradigm. Chen[9] presented a comprehensive analysis of mobile AI agent use cases in 6G, including AI agent-based network automation, handheld personalized agents, connected robotics, and wearable AI agents, and proposed a novel system architecture supporting agent-application collaboration and multi-modal data transmission. Liu[10] proposed a 6G native AI architecture, introducing the Quality of AI Service (QoAIS) concept and a three-layer architecture comprising a data plane, an intelligence plane, and extended control/user planes. Furthermore, Zhang[11] proposed a scalable multi-agent reinforcement learning (MARL) framework for radio resource allocation in multi-cell wireless networks, demonstrating that distributed Multi-Agent Proximal Policy Optimization (MAPPO) algorithms can achieve quality of service (QoS) performance comparable to centralized methods.

In terms of industrial standardization and architecture design, 3GPP has initiated extensive studies on AI-native 6G architectures in Release 20, focusing on wireless AI frameworks that enable autonomous AI operation between devices and the network across all layers[12]. The IETF has also contributed significantly through several Internet-Drafts: Zhao[13-14] proposed an AI agent architecture for network digital twin, integrating AI agents with digital twin technology to enable autonomous network management; Tong[15] presented network AI agent use cases and requirements in 6G, proposing a three-layer framework comprising a central intelligence layer, a service agent layer, and an atomic capability layer; and Duan[16] discussed use cases and requirements of AI agent communication for 6G, exploring potential frameworks for Agent-to-Agent (A2A) communications. Additionally, the European 6G-INTENSE project[17] proposed an intent-driven native AI architecture supporting compute-network abstraction and sensing at the deep edge, adopting the intent-based networking (IBN) paradigm across all layers with natural language intent specification capabilities.

Currently, the AI agent/robot industry and the wireless communication industry are integrating and promoting each other in their development. The new achievements in AI agent/robot technologies will greatly promote the further development and even innovation of the wireless communication industry. On the other hand, future 6G wireless networks will also provide more powerful and efficient interconnection and empowerment guarantees for various AI agent/robot terminals, consequently helping to explore more extensive new applications of AI agents/robots. Compared with traditional human-centric, connectivity-oriented 5G/5G-advanced (5G-A) networks, the core innovation of this work lies in the proposal of an AA-Centric 6G network paradigm oriented toward AI agents. This new paradigm shifts the primary service objects from humans to AI agents and robots, overcoming the limitations of passive connectivity, static configuration, and centralized management inherent in conventional architectures. It enables an AI native network characterized by intent-driven operation, proactive services, distributed collaboration, deterministic assurance, and online evolution. This paper systematically introduces new network functions, a new hierarchical architecture, and multi-agent collaboration mechanisms, addressing existing gaps in 5G-A related to identity, behavior, QoS, and security, and providing a comprehensive design framework and technical support for the deep integration of AI agents and 6G networks.

2 Three Key Supports for Further Development of Wireless Communication Industry

In the mid-stage of 5G networks, the wireless communication industry once faced difficulties, with the demand-driven application of pure Communication Technology (CT) technologies showing weak momentum. To achieve the breakthrough toward intelligent, ubiquitous, and service-oriented 6G, it is widely acknowledged that the advancement of generalized AI agent terminals, embodied robots, and novel AI agent network entities will play a pivotal enabling role in the evolution of wireless communications.

2.1 New Generalized AI Agent Terminals

New generalized AI agent terminals refer to a new generation of diverse and heterogeneous terminals that integrate various AI agent applications or agents. They can help regular users unlock more abundant over-the-top (OTT) applications, network-intelligent services, and latent capabilities, further promoting users' digital consumption experience and efficiency. Taking the personal digital assistant, a terminal AI agent application, as an example, users can more easily and efficiently perform tasks such as intelligent search, task management, and content creation through natural language interaction. 5G networks still have some deficiencies in supporting and guaranteeing applications of the personal digital assistant type, so the related capabilities need to be improved and optimized in future 6G wireless networks[18-20]. For example, if a personal digital assistant needs to read and comprehend screen content, the network must support high uplink bandwidth. Real-world tests show that real-time screen reading typically requires an uplink rate of 2.5 Mbit/s, while simultaneous real-time screen reading and multi-stream live broadcasting can require uplink speeds of up to 8 Mbit/s.

As shown in Table 1, the network requirements of personal digital assistants include authentication and authorization, behavior supervision, traffic scheduling, QoS guarantee, cross-layer collaboration, and user experience guarantee. Agents can

Table 1. New 6G network requirements for the personal digital assistant

Category	Authentication & Authorization	Behavior Supervision	Traffic Scheduling	QoS Guarantee	Cross-Layer Collaboration	Reliability
5G-A status	Non-unified	None	Relatively weaker uplink	Static, e.g., 100 ms window	Terminal-cloud	Moderate reliability (99.99%)
6G new requirements	Unified and seamless	Enhanced identification	Enhanced uplink capability	Dynamic, e.g., 10 ms window	Terminal-network-cloud	High reliability (99.999%)

QoS: quality of service 5G-A: 5G-advanced

continuously provide personalized services for users across terminals and scenarios, which requires unified and continuous identity authentication and authorization from the network. Agents can automatically or on behalf of users initiate behaviors and sensitive operations, which requires the network to identify, audit, and control the behavior of AI agents, preventing abuse and violations. The service of AI agents is highly dependent on real-time data interaction and cloud AI reasoning, and has higher requirements for network latency, bandwidth, and reliability than 5G networks. The current 5G-A network mainly focuses on single terminals and sessions, lacking unified identity authentication, behavior supervision, and dynamic QoS guarantee at the AI agent level, which makes it difficult to support seamless migration of AI agents among multiple devices and meet the high real-time requirements for 5G-A networks. For 6G, it is necessary to build an AA-Centric network service system, and strengthen unified identity authentication, fine-grained behavior supervision, intelligent traffic identification and hierarchical QoS guarantee, as well as multi-layer collaboration among terminals, networks, and the cloud, to promote the evolution of the network toward greater intelligence, security, and efficiency.

2.2 Embodied Robots

Embodied robots refer to AI agent robots that have a physical body and can perceive the surrounding environment in the real physical world, interact with people and objects, and autonomously complete complex tasks. Embodied robots typically consist of three main components: the body, the cerebellum, and the brain. However, their appearance, task execution capabilities, and intelligence levels vary greatly, and their dependence on cellular networks also differs. For numerous future industrial and household application scenarios, various types of embodied robots will become the most valuable area of technology and application. They will not only generate significant new-quality productive forces in fields such as production, transportation, logistics, and security, but also gradually enter regular households to become important intelligent companions for people[21]. Taking the application of nursing robots as an example, regular users can achieve tasks such as care and supervision, household collaboration, and safety monitoring through natural language interaction. 5G networks still have some deficiencies in supporting and guaranteeing such applications, so the related capabilities need to be improved and optimized in future 6G wireless networks[22–23]. For example, achieving smoother and more human-like movements imposes stringent requirements on network latency and reliability. Specifically, during task execution, the robot transmits real-time video to the network, which analyzes the video content and then issues corresponding action commands. In this process, the communication round-trip latency must be kept within 10 ms, with a reliability of at least 99.99%, and the computational processing latency should also be controlled within 30 ms. Otherwise, the smoothness of the robot's movements will be noticeably degraded.

As shown in Table 2, nursing robots serve in sensitive scenarios such as home and medical care, involving high-value assets and private information. They require precise identity authentication, authorization, and access control from the network to prevent illegal access and abuse of permissions. The robots have the ability for autonomous decision-making and automatic execution, so the network needs to achieve fine-grained behavior recognition, real-time auditing, and compliance supervision to promptly detect and block abnormal or illegal operations and ensure users' personal safety and property safety. When multiple robots work collaboratively, the net-

Table 2. New 6G network requirements for embodied robots

Category	Identity Authentication	Behavior Control	Task-Oriented Networking	QoS Guarantee	Cross-Layer Collaboration	Security
5G-A status	Centralized trust	Lack of constraints	>20 ms static networking	Static, e.g., 100 ms window	Device-network-cloud collaboration	Weak
6G new requirements	Distributed trust	Enhanced constraints	<10 ms dynamic networking	Dynamic, e.g., 10 ms window	Multi-agent collaboration	Strong

QoS: quality of service 5G-A: 5G-advanced

work needs to support efficient, low-latency dynamic networking and information sharing to achieve task collaboration and resource scheduling. The traffic of nursing robots is highly dependent on the seamless transmission of multiple data, such as high-definition video, real-time voice, and environmental perception. The network needs to have dynamic traffic identification, hierarchical scheduling, and end-to-end high-quality transmission capabilities. The current 5G-A network is unable to achieve refined authorization at the robot level and lacks real-time behavior supervision and traceability. The networking and coordination mechanism of 5G-A network relies on static configuration, while QoS guarantee is difficult to dynamically adjust according to traffic, and the overall security is insufficient. In the future, the network needs to establish a consistent and distributed trusted identity authentication and authorization system, strengthen real-time supervision and auditing capabilities at the behavior level, natively support dynamic networking and intelligent collaborative scheduling of multiple robots, finally, achieving end-to-end QoS dynamic guarantee based on traffic scenarios, enhancing multi-agent collaboration and task security, and supporting the safe and large-scale deployment of robots in various industries.

2.3 New AI Agent Based Network Entity

AI agent network entities refer to new types of wireless network entities that integrate or combine the capabilities and roles of different AI agents, such as base stations with AI agents, core networks (CNs) with AI agents, and network management with AI agents. Currently, wireless network management products have already embedded network operation and maintenance AI agents, and the 3rd Generation Partnership Project (3GPP) is actively exploring use cases of AI agents network entities[24–25].

Traditional network entities or network functions (NFs) are based on experts' design capability, preset regulation processes, and automated configuration. They show several weaknesses and pain points when facing various environments and uncertain task services, such as slow deployment and launch, slow service response, rigid service processes, and unreasonable exception handling. Therefore, future 6G wireless networks need to consider appropriately applying new AI agent network entities.

As shown in Table 3, traditional 5G network entities have significant deficiencies in intelligence, planning, orchestration, collaboration, flexibility, update, and evolution. Most network entities rely on preset regulations and manual configuration, and are not flexible in responding to complex and variable traffic and abnormal situations. They lack global perception and collaborative optimization capabilities, making it difficult to achieve intelligent collaboration among multiple nodes. The intelligent capabilities are mainly concentrated in network management or application servers, lacking native AI agents for the network foundation, making it difficult for new services to be arranged on demand, and upgrades of new services are mostly offline. The 6G network entities need to possess native and inherent AI agent capabilities, enabling proactive services and on-demand orchestration. They should be able to flexibly generate processes based on real-time traffic and environmental changes, and actively optimize resource allocation, service paths, and security policies. At the same time, they should support strong collaboration among network entities to achieve global optimal traffic scheduling and service guarantee, and continuously improve capabilities through online evolution. The new AI agent network entities do not completely replace traditional network entities; instead, they are oriented toward specific new network services and tasks, forming a more flexible and organic scheduling and collaboration support. By adopting AI agent network entities, the 6G network will achieve self-sensing, self-decision-making, and self-optimization, providing strong support for diverse innovative scenarios and ultimate experiences.

Overall, various types of AI agents/robots have put forward new multi-dimensional demands in terms of functions, performance, paradigms, and characteristics for the future 6G wireless networks. These demands have greatly promoted the development of the wireless communication industry and have become the key driving force for future industry technological innovation and business model upgrades. It can be foreseen that the development trend and market rhythm of the future wireless communication industry will integrate with the AI agent/robot business model and promote each other, forming a new pattern of symbiotic development between AI agents/robots and the wireless communication industry.

3 Analysis of New Capabilities and Behavioral Characteristics of AI Agents/Robots

Traditional intelligent terminals and ubiquitous Internet of Things (IoT) terminals mainly focus on dynamic data collection and transmission-related services. As a result, pre-6G wireless networks have been characterized by a connectivity-centric design paradigm, emphasizing efficient and reliable

Table 3. New 6G network requirements for AI agent network entity

Category	Intelligence	Planning Capability	Orchestration	Collaboration	Process Flexibility	Evolution & Updates
5G-A status	External/built-in	Passive service	No	Weak	Predefined, rigid	Offline upgrade
6G new requirements	Natively embedded	Proactive service	On-demand	Strong	Flexible	Online evolution

5G-A: 5G-advanced

data transmission. However, new terminals represented by various types of AI agents/robots have undergone significant changes in their capabilities and behavioral characteristics, posing higher requirements for computation, communication, and collaboration. This will fundamentally determine the new capability characteristics and system design paradigm of future 6G wireless networks, shifting the focus toward AA-Centric networks.

3.1 Capability Characteristics

As shown in Table 4, the new capability characteristics of terminals represented by AI agents/robots are mainly reflected in six aspects: perception, interaction, autonomy, cognition, adaptability, and learnability. In recent years, breakthroughs in technologies such as large-scale pre-training models, multi-modal perception, and reinforcement learning have enabled agents and robots to possess the capabilities of environmental perception, multi-modal interaction, and autonomous planning. Agents can perform deep environmental perception and achieve seamless human-machine and machine-machine interaction by integrating multi-modal data such as voice, vision, and touch. Leveraging the reasoning and learning capabilities of LLMs, agents exhibit deep reasoning and a high degree of autonomy, as evidenced by their ability to independently plan tasks, make decisions, and adjust their behaviors dynamically. Through group collaboration and experience sharing, agents continuously achieve self-evolution and reinforcement learning, and possess the capability of cross-scenario task processing and collaborative optimization. Unlike traditional terminals that primarily perform simple measurements with limited interaction and low autonomy, AI agents are distinguished by their environmental perception, multi-modal interaction, autonomous planning, deep reasoning, flexible adaptation, and reinforcement learning. These features position them as a key force driving the advancement of network intelligence.

3.2 New Behavior Characteristics

As shown in Table 5, AI agent/robot terminals, due to their certain independent and autonomous behavioral capabilities, can exhibit new behavioral characteristics different from those of traditional human users, such as behavioral predictability and coordination, dynamic QoS requirements, proficiency in self-learning and optimization, and a high degree of data openness. Future 6G wireless networks can leverage these new features to intelligently optimize the task execution of AI agent-based terminals as appropriate.

AI agents show high predictability in communication and computing behaviors. Their task processes usually revolve around clear goals, presenting strong planning and regularity, which is conducive to precise network scheduling and service guarantee. In group collaboration scenarios, AI agents have efficient coordination capabilities, and the network can uniformly schedule and allocate resources for multiple AI agents, thereby improving overall task efficiency and resource utilization. Facing complex tasks and dynamic environments, AI agents require networks with highly dynamic and resilient capabilities. This demand is especially pronounced in key business processes, where requirements for bandwidth, latency, and computing power far exceed those of traditional terminals, calling for continuous improvement in network self-adaptive ability and reliability. AI agents generally have self-learning and continuous optimization capabilities, which enable them to continuously improve task adaptability and execution efficiency through reinforcement learning and experience sharing, while also placing higher demands on data transmission, model synchronization, and edge-cloud collaboration, requiring the self-evolution and optimization of the network foundation. Compared with traditional terminals, data collection from AI agents is more convenient and offers greater openness and usability. Data ownership is clear, and privacy constraints tend to be lower in some scenarios, depending on the data type and application context, than those typically associated with traditional terminals. This provides a rich data foundation for network intelligent management, behavior analysis and service innovation, and facilitates the intelligent operation and continuous innovation of wireless networks.

Table 4. New capability features of AI agent/robot representative terminals

Category	Perception	Interactivity	Autonomy	Cognition	Adaptability	Learnability
Traditional terminals	Simple measurement	Basic interaction	Weak autonomy	Limited reasoning	Low adaptability	Almost none
AI agents/robots	Environmental sensing	Multi-modal interaction	Autonomous planning	Deep reasoning	Flexible adaptation	Reinforcement learning

Table 5. New behavioral features of AI agent/robot representative terminals

Category	Predictability	Coordination	QoS Requirements	Self-Learning and Optimization	Data Openness
Traditional terminals	Highly random	Low cooperativeness	Static requirements	Almost none	Highly private, difficult to utilize
AI agents/robots	Highly predictable	Highly coordinated	Dynamic, extreme performance	Continuous self-evolution	Easily collected and utilized

Overall, the three types of AI agents (generalized terminals with personal digital assistants, embodied robots, and network entity agents) have a very broad space for innovation and application. Although they have different behavioral characteristics and technological development paces, all of them will drive the 6G wireless network to evolve toward higher-level intelligence, service orientation, strong resilience, high guarantee, and security. The design of 6G networks and multi-dimensional service capabilities urgently needs to break through traditional old paradigms at an early stage to lay a solid foundation for the future network architecture to meet the diverse, complex, and uncertain demands of multiple types of AI agents/robots.

4 New Design Paradigm and Core Characteristics of Future AA-Centric Network

As shown in Fig. 1, the evolution of wireless networks is undergoing a paradigm shift: from human-oriented to thing/machine-oriented, and then to AI agent-oriented. In the future era of ubiquitous AI agents/robots (with a total number far exceeding that of humans), the design, operation and maintenance paradigms of wireless networks will shift from human-centric to AA-Centric. Under the old human-centric paradigm, business logic and operational models mainly revolve around people, with AI merely serving as an auxiliary tool. The intelligence on the terminal side is directly driven by human users, while the intelligent capabilities on the network side rely on manual operation. Its main design goal is to improve quality, reduce costs and increase efficiency. In the future, under the new paradigm of AA-Centric, business logic and operational models will mainly revolve around the independent and autonomous development of agents. On the terminal side, agents/robots can independently analyze, make decisions and execute tasks based on task requirements, while humans mainly act as responsible users for behavior supervision. On the network side, network traffic services are supported and guaranteed by network entities/network management agents in a distributed and dynamic collaborative manner. The design goals have been upgraded to intelligent self-generation of the network and expansion of service content, among others.

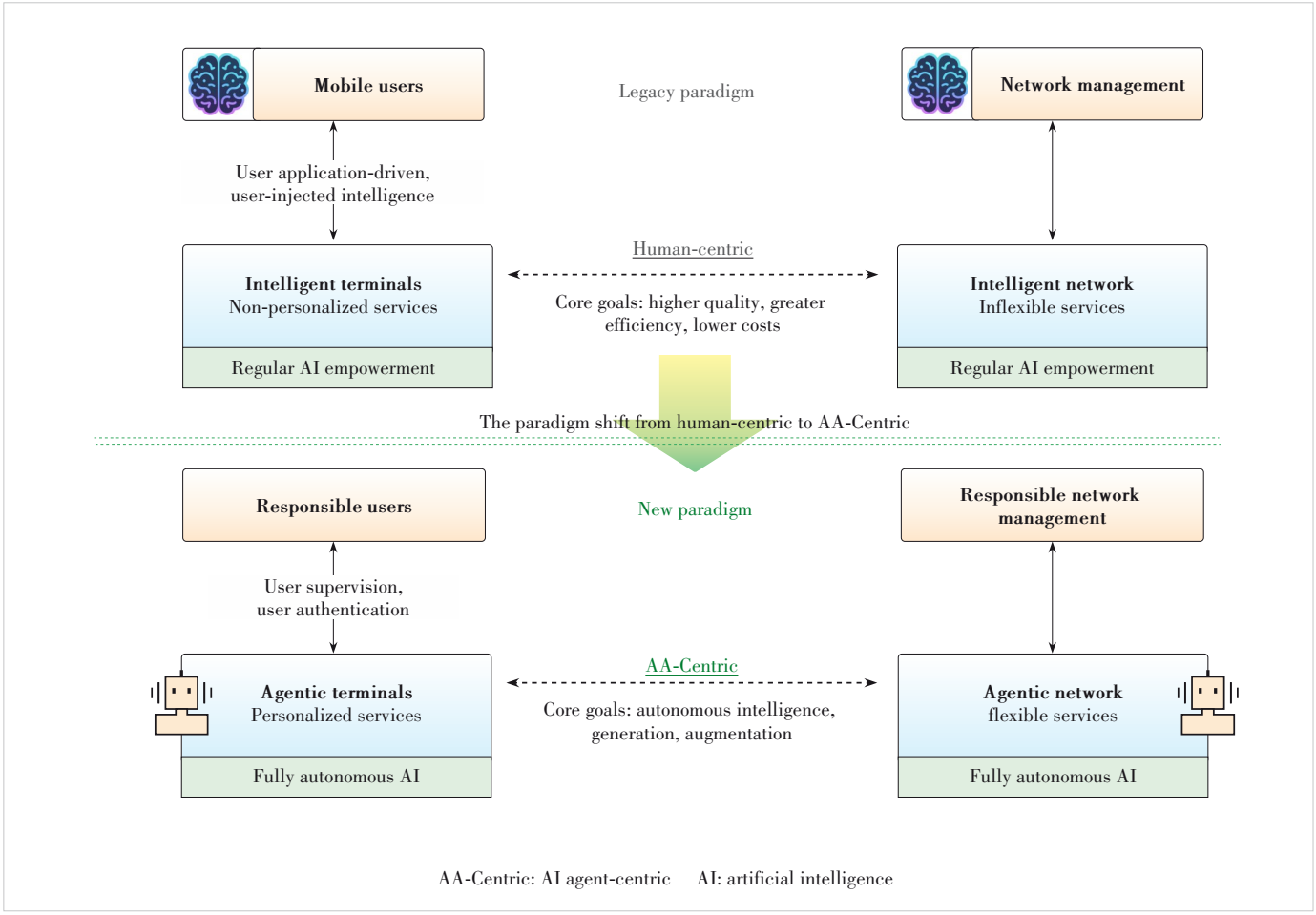

Figure 1. New AA-Centric paradigm of wireless networks

As AI agents and robots are widely used in various services and scenarios, the design, operation and maintenance of future wireless networks are accelerating toward a new AA-Centric paradigm, which is reflected in the seven core characteristics summarized in Table 6.

First, intention-driven operation will become a core feature of 6G networks. The service requests initiated by agents can carry complex traffic goals and contexts. The network needs to identify and understand their operation purposes and service preferences, optimize resource scheduling and service matching, and realize the transformation from connection guarantee to intention recognition and response. Second, proactive service becomes the evolution direction of the network. Based on the insight into agent behavior and business models, the network actively conducts resource planning, service recommendation, and experience optimization. Through intelligent analysis and prediction, it proactively identifies needs and risks, actively pushes new services, and improves service creativity. Third, distributed collaboration capability is significantly enhanced. The network needs to support distributed collaboration among multi-agents, realize efficient information exchange and task synchronization, and meet the group collaboration requirements of complex tasks. Fourth, efficient customization becomes fundamental. The network needs to flexibly customize service parameters such as bandwidth, delay, and computing power according to the agent's traffic type and real-time status to realize efficient utilization of resources and meet diverse and dynamic needs. Fifth, the deterministic guarantee of the network needs to be enhanced. For key scenarios such as industrial automation and telemedicine, the network needs to provide lower delay, higher reliability, and more powerful security for agent applications to ensure the stable operation of critical tasks. Sixth, online evolution becomes an important feature. The network needs to dynamically optimize parameters and functions based on real-time data and feedback, and have the ability of self-learning and continuous adjustment to adapt to the continuous changes of agents and traffic environments. Finally, the network needs to quickly respond to the demand for innovation and generation; that is, the network needs to support the dynamic introduction and on-demand deployment of new functions and services, and continuously expand service capacity and the ecosystem.

In summary, there are seven core characteristics derived from the requirements of agents/robots for 6G wireless networks in practical communication and computing applications: intention-driven operation, proactive service, distributed collaboration, efficient customization, deterministic guarantee, online evolution, and service generation. They represent the key capabilities of 6G networks to cope with the complexity of agent tasks, the expansion of collaboration scale, the frequent update of traffic services, and the high reliability of key scenarios. AA-Centric is not only reflected in the original design stage of 6G networks but will also run through all aspects of network operation and maintenance as well as traffic and applications, and become an important guiding principle and core evolution goal throughout the design state, operation state, maintenance state, operation and maintenance state, and application state.

5 Key Technologies for AA-Centric Wireless Network

This chapter will elaborate on a number of key supporting technologies, mainly around the functional system, network architecture, the collaboration between large and small models, and other aspects.

5.1 New Function Set and System Framework

Future 6G wireless networks must be extended with several new key functions to meet the requirements arising from the new characteristics of AI agent/robot behavior. Firstly, the network should have the ability to proactively predict the behavior of AI agent/robot terminals. The communication and computing requirements of AI agents/robots are goal-oriented, centered around specific tasks, and display predictable patterns. The network needs to dynamically perceive and predict their behavior, and realize the pre-optimization of communication and computing resource allocation and task planning, so as to improve the efficiency and quality of network service response. Secondly, when multiple AI agents/robots jointly execute complex tasks, they often require cooperative task allocation and resource coordination. The network needs to be task-centered, enabling dynamic arrangement and collaborative scheduling of AI agent/robot groups, so as to adapt to the complexity of networking and dynamic resources. In addition, in response to the increasingly dynamic and differentiated requirements brought by AI agents/robots operating in diverse

Table 6. Seven core characteristics of future AA-Centric wireless networks

Category	Intention-Driven Operation	Proactive Service	Distributed Collaboration	Efficient Customization	Deterministic Guarantee	Online Evolution	Service Generation
Human-centric (legacy paradigm)	Partial human intention	Passive response	Weak, centralized control	Personalization	Basic guarantee	Almost none	Almost none
AA-Centric (new paradigm)	Any goal/task intention	Proactive orchestration	Ubiquitous, distributed coordination	Customization	Enhanced guarantee	Online iteration	Scenario/content generation

AA-Centric: AI agent-centric

environments and scenarios, the network needs to further enhance its QoS guarantee capabilities. The network also needs to provide a suitable learning and evolution platform for AI agents/robots to support mutual learning and experience data sharing among agents. Through network-side collaboration, agent/robot can not only realize their own capability improvement and expansion, but also achieve overall intelligence evolution through group collaboration. Finally, as AI agents/robots can generate massive amounts of data, it is necessary to establish efficient mechanisms for data management and value realization to support the safe and open use of data. Compared with traditional network architectures, the new function set and system framework require the introduction of multiple types of agents as well as the assurance of distributed collaboration among agents at different levels. In addition, the novel characteristics of next-generation networks will have a significant impact on network functions, necessitating their careful consideration during system design. The new functional system framework is illustrated in Fig. 2.

Under the new function and system framework centered on AI agents, the aforementioned functions can be implemented via corresponding network entity AI agents. For instance, behavior prediction AI agents, task coordination AI agents, QoS dynamic guarantee AI agents, learning and evolution AI agents, and data openness AI agents are deployed respectively in the radio access network (RAN) and the CN. The behavior prediction AI agent dynamically models and predicts the environment state and task requirements of AI agents/robots based on historical records and real-time perception data. The task coordination AI agent automatically allocates sub-tasks, schedules links and computing power for multi-agent/robot joint tasks, according to network status and the individual capabilities of the group. The QoS dynamic guarantee AI agent evaluates terminal traffic requirements and network environment changes in real time, and flexibly adjusts link strategies and service priorities. The learning and evolution AI agent provides distributed learning and knowledge transfer capabilities, supporting the sharing of experience and model synchronization upgrades among AI agents. The data openness AI agent establishes a secure sharing and capitalization mecha-

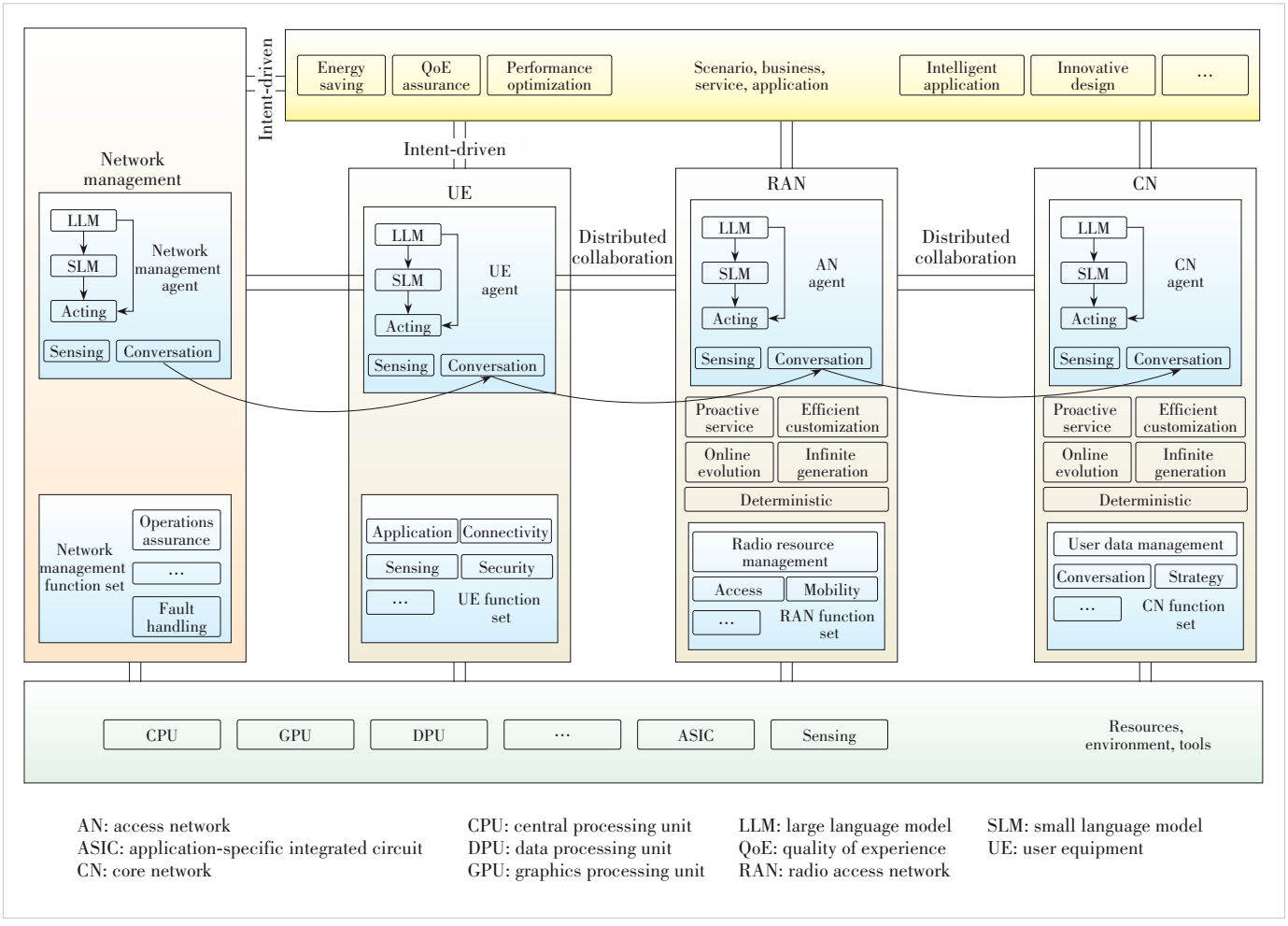

AN: access network
ASIC: application-specific integrated circuit
CN: core network
CPU: central processing unit
DPU: data processing unit
GPU: graphics processing unit
LLM: large language model
QoE: quality of experience
RAN: radio access network
SLM: small language model
UE: user equipment

Figure 2. New AA-Centric functional system framework

nism for data to realize efficient circulation and compliance utilization of data among multi-agents/robots and the external ecosystem. On the whole, the 6G network can efficiently support and extend the diverse needs of AI agents/robots through the modular and collaborative functional architecture of network entity AI agents.

5.2 New Wireless Network Architecture

By leveraging their new capabilities in autonomous decision-making, environmental perception, and task-oriented operation, AI agents and robots are transforming wireless networks from mere connectivity platforms into organizers and enablers of tasks. As shown in Fig. 3, the future wireless network is layered and can cooperate across domains, including the wireless network infrastructure layer, the AI agent task enabling layer, and the AI agent task application layer. As a unified heterogeneous hardware and digital intelligence foundation, the wireless network infrastructure layer provides basic resources to support agent task traffic services. The middle agent task enabling layer provides and opens multi-dimensional capabilities such as communication, computing, intelligence, data, and security on demand, thereby supporting and hosting task execution for the agent task application layer above. The agent task application layer provides agent-enabled capability guarantees for business applications, multi-factor collaboration, as well as network operations and maintenance. The new wireless network architecture adopts an overlay design, adding an AI application layer on top of the existing architecture, and incorporating advanced capabilities in intelligence, computing, data, and security that extend beyond traditional communication functions within the network.

At the RAN level, the core requirement of AI agents/robots for the network is the bidirectional cooperation between the RAN and AI agent-based terminals. Traditional RAN treats terminals as passive receivers or senders of data, while AI agent terminals require the RAN to be able to sense the environment and assist in their decision-making processes. The RAN architecture needs to establish an agent state per-

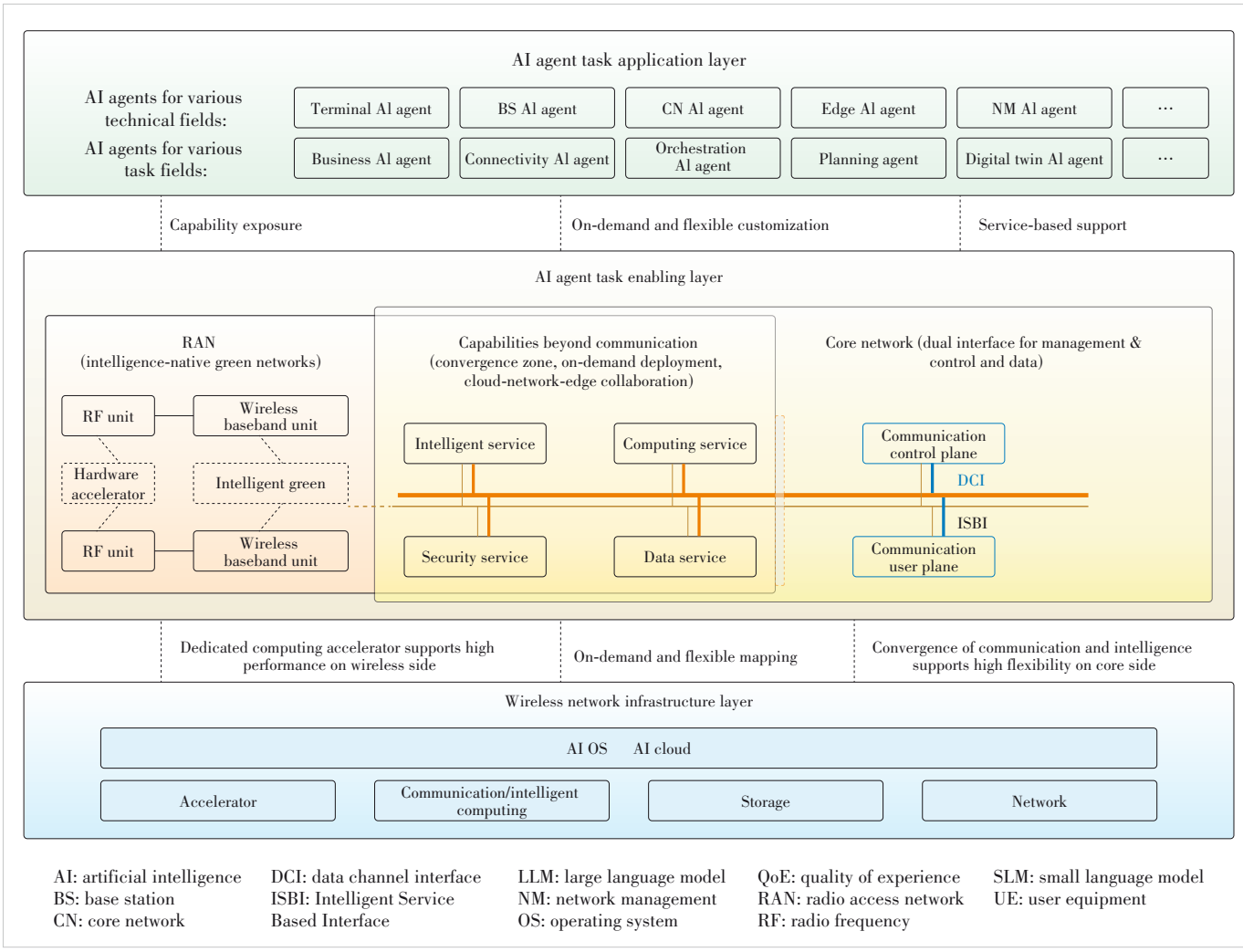

AI: artificial intelligence
BS: base station
CN: core network
DCI: data channel interface
ISBI: Intelligent Service Based Interface
LLM: large language model
NM: network management
OS: operating system
QoE: quality of experience
RAN: radio access network
RF: radio frequency
SLM: small language model
UE: user equipment

Figure 3. New AA-Centric wireless network architecture

ception and prediction framework to identify its behavior pattern, movement trajectory, and resource demands, and dynamically adjust resource allocation accordingly. The RAN evolves from a passive and reactive access network to an active and collaborative participant, providing AI agents with network and environmental information beyond their own perception capabilities.

At the CN level, AI agents/robots require a network architecture that enables intent-driven network services (i.e., services configured based on intentions or desired outcomes specified by AI agents). The traditional CN is based on predefined service templates and static policy regulations, which are difficult to adapt to the variable task requirements of AI agents. The future CN needs to understand the intentions of AI agents and automatically map them into network configurations, achieving a transition from static templates to dynamic function combinations for service definition. The CN will shift from a provider of service catalogs to an assistant for AI agent tasks, being able to understand and respond to what the AI agent wants to accomplish, thus simplifying the interaction process between AI agents and the network.

At the end-to-end network architecture level, AI agents/robots need to achieve task-driven end-to-end collaboration through the network. When AI agents perform complex tasks, they require cross-layer and cross-domain collaborative support. However, in traditional network architectures, resource management and service deployment are in different layers and domains, making it difficult to achieve unified coordination. The future end-to-end network architecture needs to break through the limitations of traditional vertical layering and horizontal domain division, establish a task-centered resource collaboration mechanism, and achieve overall optimization of multi-dimensional resources such as sensing, computing, storage, and communication. The network transforms from physical infrastructure into a task execution environment, which can reshape its own structure according to the requirements of AI agent tasks and provide mapping from task intentions to network resources.

5.3 Collaboration Among Multi-Level Network LLMs

The AA-Centric wireless network architecture includes domain-level LLMs, system-level LLMs, and function-level LLMs, corresponding to global decision-making, system coordination, and intelligent implementation of specific functions, respectively. Together, they form a multi-model collaborative architecture featuring hierarchical progression and coordinated evolution[26]. The domain-level LLM, as a global Mixture of Experts (MoE), has a parameter scale of over 10 billion, coordinating the management of various system-level LLMs and providing pre-trained models for downstream tasks. It continuously performs parameter fine-tuning using the activation data and experience parameters provided by system-level LLMs, thereby achieving self-evolution of the network's global intelligence. The system-level LLM is responsible for the comprehensive scheduling and functional integration of multiple systems within a specific domain, with approximately 10 billion parameters activated. Through techniques such as pruning, quantization, and distillation, the system-level LLM can efficiently remove irrelevant experts, reduce storage and computing consumption, and improve inference efficiency through pre-filling and dynamic redundancy strategies. At the same time, the system-level LLM can continuously fine-tune itself based on feedback from function-level models, achieving dynamic management and optimization of multiple function-level LLMs. The function-level LLM, distilled from the system-level LLM, focuses on the implementation of specific functions and has approximately 1 billion activated parameters. The function-level LLM achieves large-scale reinforcement learning and supervised fine-tuning, retaining the system-level reasoning chain capability while continuously strengthening specific function performance for actual scenarios.

As shown in Fig. 4, large and small AI models complement each other in the 6G network, jointly supporting the efficient, flexible, and low-cost evolution of the endogenous intelligent network. Large models excel at global optimization and cross-domain collaboration, making them suitable for complex tasks such as dynamic allocation of network resources, but they rely on high computing power and large amounts of data, resulting in higher inference latency. Small models, with their lightweight and efficient advantages, quickly handle local optimization problems, such as base station load balancing and local energy-saving management. To achieve optimal performance, in the cloud-network-terminal architecture, distributed computing should be adopted to schedule large and small models as needed to various network entities, forming a multi-level and collaboratively evolving AI agent network function system. The new paradigm based on the hierarchical large models not only expands the depth and breadth of network intelligence, but also provides a solid foundation for the future AA-Centric network.

5.4 Collaboration Among AI Agents and Non-Agents

In the future, various AI agents will be widely deployed on terminals, networks, and cloud platforms[27–28]. The 6G wireless network will serve as a bridge for connecting and coordinating various AI agents, capable of supporting scenarios such as single-domain AI agent task execution, multi-domain multi-agent collaboration, and flexible networking. The layered cross-domain collaborative applications among AI agents in the 6G wireless system are typically discussed at three different levels: single-domain intelligence, cross-domain collaborative intelligence, and networking-level intelligence. These require systematic optimization of network interfaces and communication protocols at different levels to meet the diverse needs for multi-agent collaboration and resource sharing, and to accelerate the evolution of wireless networks toward self-

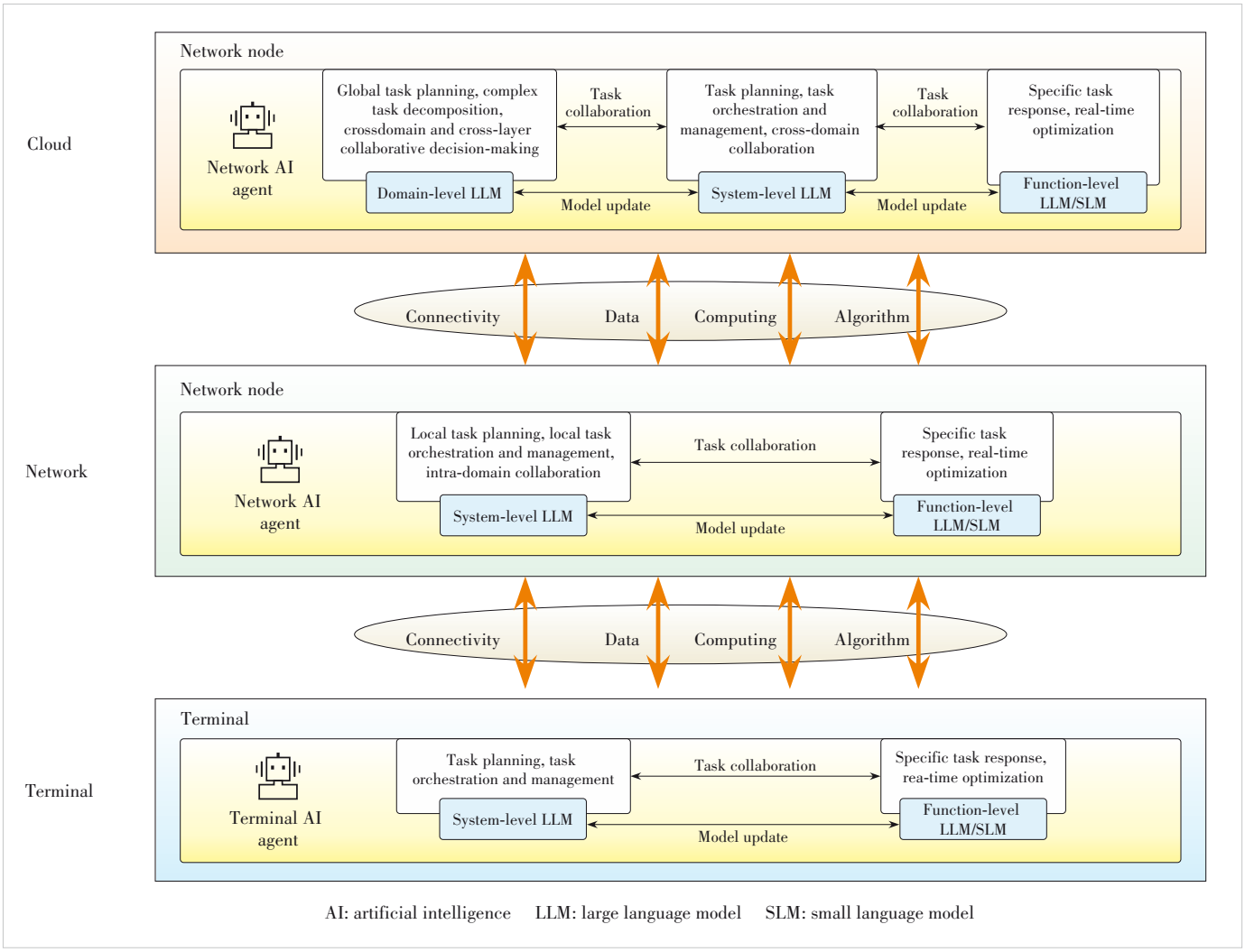

Figure 4. Multi-factor collaboration between large and small AI models in 6G wireless systems

intelligent networks with collaborative intelligence. The industry has proposed various AI agent communication protocols such as A2A, Model Context Protocol (MCP), and Agent Network Protocol (ANP) [29]. For example, A2A supports direct message transmission and collaboration among AI agents, while MCP is used for sharing model context and capability information between AI agents, tools, or services. ANP enables dynamic registration, discovery, addressing, and networking of AI agents. These protocols lay the foundation for efficient collaboration and resource sharing among multiple AI agents. However, most of these protocols originated in the fields of the Internet and distributed computing, making it difficult for them to meet the unique requirements of wireless communication networks in terms of real-time performance, reliability, and multi-layered security. In the future, it will be necessary to customize and optimize AI agent communication protocols based on the characteristics of 6G wireless networks, promote the deep integration of wireless networks and the AI agent ecosystem, and achieve efficient collaboration and self-intelligent evolution of ubiquitous AI agents.

6 Key Challenges in AA-Centric Network

Deploying various AI agents over wireless networks introduces technical challenges across multiple dimensions, as shown in Table 7.

Communication-computation integration represents a fundamental architectural challenge in AA-Centric networks. In conventional wireless networks, communication and computation are managed as independent systems. However, in AA-Centric networks, the end-to-end performance of agent tasks is jointly determined by both inference latency and transmission latency. Multi-agent collaboration pipelines impose certain determinism requirements on end-to-end latency, yet existing QoS mechanisms are designed primarily around the wireless link and offer limited visibility into computation-side latency characteristics.

Table 7. Some key challenges in AA-Centric network

Challenges	Current State	Key Challenges to solve
Communication-computation integration	Resource management and computation scheduling are decoupled	Joint optimization of inference and transmission latency; existing QoS mechanisms cannot enforce end-to-end determinism across the compute domain
Semantic-agnostic protocol stack	Protocol stack operates as a bitpipe; QoS defined solely by bandwidth, latency, and priority	No mechanism to differentiate semantic criticality; task-aware resource management is absent
Traffic burstiness	Scheduling assumes stationary traffic; GBR/non-GBR targets continuous flows	Agent coordination induces synchronous bursts; existing schedulers and buffers are ill-suited
Large-scale many-to-many access	5G NR scheduling is point-to-point; group communication support is limited	Many-to-many patterns are structurally mismatched with existing access mechanisms
Semantic transmission efficiency	Semantic communication remains pre-standardization	Token sequences impose high overhead; no compression or coding methods optimized for task-level metrics

AA-Centric: AI agent-centric GBR: guaranteed bit rate NR: new radio QoS: quality of service

Joint optimization of radio resource scheduling and inference task scheduling therefore remains an open problem.

Semantic unawareness of the protocol stack poses another challenge at the network protocol level. Existing protocol stacks are designed around bit-level transport, with QoS defined in terms of bandwidth, latency, priority, etc. In AA-Centric networks, during agent communication, the task-level importance of transmitted content varies considerably, yet current mechanisms lack the capability to identify and differentiate such AA semantics, making fine-grained, task-oriented resource management difficult to achieve.

Beyond these, AA-generated traffic burstiness, large-scale many-to-many access, and semantic transmission efficiency are challenges broadly shared with general wireless network evolution. The collaborative communication patterns characteristic of AA networks further amplify these issues to some extent, while also providing concrete application contexts for emerging research directions such as semantic communications.

7 Conclusions

Currently, AI agents and robots have emerged as crucial carriers of new quality productive forces and social services. Wireless network services will evolve toward universality, diversification, and customization. The AI agent/robot industry and the wireless communication industry have become closely integrated and have achieved convergent growth. The rapid iteration of AI agent and robot technologies is greatly driving the direction and pace of wireless communication industry development, fueling the reinvention and advancement of wireless communication networks. In the future, the paradigm of wireless networks will gradually shift from human-centric to AA-Centric, featuring seven core characteristics: intention-driven operation, proactive services, distributed collaboration, efficient customization, deterministic guarantee, online evolution, and infinite generation. These features need to be supported by key technologies such as new function and system frameworks, wireless network architectures, collaboration among multi-level network LLMs, and collaboration between AI agents and non-agent entities. Consequently, the AA-Centric paradigm is poised to become a key guiding principle and ultimate goal for the design, operation, and application of future wireless networks. Nevertheless, the pervasive deployment of AI agents and robots introduces critical challenges in data management, security, and ethics, necessitating further investigation and systematic safeguards.

References

[1] Xie F, Yang L, Chen L, et al. New requirements of 6G intelligent endogenous 2.0 and agent-based network architecture design [J]. Mobile communications, 2025, 49(1): 9 – 15
[2] Pan J P, Cai L, Yan S, et al. Network for AI and AI for network: challenges and opportunities for learning-oriented networks [J]. IEEE network, 2021, 35(6): 270 – 277. DOI: 10.1109/MNET.101.2100118
[3] Wang C X, You X H, Gao X Q, et al. On the road to 6G: visions, requirements, key technologies, and testbeds [J]. IEEE communications surveys & tutorials, 2023, 25(2): 905 – 974. DOI: 10.1109/comst.2023.3249835
[4] Pennanen H, Hänninen T, Tervo O, et al. 6G: the intelligent network of everything [J]. IEEE access, 2025, 13: 1319 – 1421. DOI: 10.1109/access.2024.3521579
[5] Yang Y, Ma M L, Wu H Q, et al. 6G network AI architecture for everyone-centric customized services [J]. IEEE network, 2023, 37(5): 71 – 80. DOI: 10.1109/mnet.124.2200241
[6] Zheng Y T, Cheng X Z, Wang J Y. Research and application of AI agent empowering network operations [J]. ZTE technology journal, 2025, 31(5): 19 – 24. DOI: 10.12142/ZTETJ.202505004
[7] Zhang P, Niu K, Wang X Y, et al. ComAI: the convergence of communication and artificial intelligence [J]. IEEE communications surveys & tutorials, 2026, 28: 2163 – 2197. DOI: 10.1109/COMST.2025.3608174
[8] Duan X D, Huang Z L, Lu L, et al. AI agent communication network (ACN): a new network paradigm for 6G [J]. Journal on communications, 2025, 46(11): 332 – 346. DOI: 10.11959/j.issn.1000-436x.2025203
[9] Chen Z Q, Sun Q, Li N, et al. Enabling mobile AI agent in 6G era: architecture and key technologies [J]. IEEE network, 2024, 38(5): 66 – 75. DOI: 10.1109/MNET.2024.3422309
[10] Liu G Y, Chen T J, Cui Y P, et al. 6G native AI wireless network architecture for QoAIS guarantee [J]. Mobile communications, 2025, 49(1): 2 – 8. DOI: 10.3969/j.issn.1006-1010.20241125-0006
[11] Zhang Y M, Guo D N. Multi-agent reinforcement learning for multi-cell

spectrum and power allocation [J]. IEEE transactions on communications, 2025, 73(8): 5980 – 5992. DOI: 10.1109/TCOMM.2025.3534565
[12] Yang L, Wang X Y, Duan X Y, et al. Key technologies and future outlook of agent-centric network technology framework [J]. Information and communications technologies, 2025, 19(2): 4 – 11. DOI: 10.3969/j.issn.1674-1285.2025.02.002
[13] Zhao J, Pang R, Zhang S, et al. AI agent architecture for network digital twin [R]. IETF, 2026
[14] Zhao J, Wang M X, Wu B, et al. AI based network management agent (NMA): concepts and Architecture [R]. IETF, 2026
[15] Tong L, Ao S, Wang A J, et al. Network AI agent use cases and requirements in 6G [R]. IETF, 2025
[16] Du Z P. Use cases and requirements of AI agent communication from 6G aspect [R]. IETF, 2025.
[17] Boutouchent A, Mekrache A, Ksentini A, et al. 6G-INTENSE: intent-driven native artificial intelligence architecture supporting network-compute abstraction and sensing at the deep edge [J]. IEEE vehicular technology magazine, 2025, 20(1): 44 – 54. DOI: 10.1109/mvt.2024.3525001
[18] Ling S, Xu C, Song J H. Network deep perception and adaptive communication method for robotic teleoperation, 2025, 49(5): 75 – 81. DOI: 10.3969/j.issn.1006-1010.20250107-0001
[19] Li K Y, Zhu Y P, Yu S X, et al. Ai-driven terminals: advances in intent recognition, multimodal interaction, and AI collaboration [C]//Proceedings of IEEE 6th International Seminar on Artificial Intelligence, Networking and Information Technology (AINIT). IEEE, 2025: 1 – 5. DOI: 10.1109/AINIT65432.2025.11035635
[20] Liu E J, Li X, Tan Z, et al. Current status, trends, and policy recommendations for the AI-phone industry development [J]. Robot industry, 2025 (6): 18 – 35. DOI:10.19609/j.cnki.cn10-1324/tp.2025.06.005
[21] Liu M L, Ding Y H, Ma X Q, et al. Research on the development of embodied intelligence technology [C]//Proceedings of IEEE International Conference on Pattern Recognition, Machine Vision and Artificial Intelligence (PRMVAI). IEEE, 2025: 1 – 7. DOI: 10.1109/PRMVAI65741.2025.11108525
[22] Liu Y K, Wang Q J, Zhu Z L, et al. Embodied artificial intelligent industrial robot: system architecture, key technologies and case study [J]. Computer integrated manufacturing systems, 2025, 31(12): 4513-4541. DOI: 10.13196/j.cims.2024.Z21
[23] Jin L M, Wang H C, Gu J C, et al. Research on low-altitude embodied artificial intelligence-enabled spectrum management and control technology [J]. Journal of data acquisition & processing, 2025, 40(1): 45 – 55. DOI: 10.16337/j.1004-9037.2025.01.004
[24] Duan X D, Huang Z L, Lu L, et al. Agent communication network enabling new service provisioning and network architecture evolution [J]. Communications world, 2025(24): 5 – 6. DOI: 10.13571/j. cnki. cww.2025.24.015
[25] Duan X D, Sun T, Lu L, et al. Internet of agents: conception, architecture and key technologies [J]. Telecommunications science, 2025, 41(10): 1 – 10. DOI: 10.11959/j.issn.1000-0801.2025221
[26] Sun F P, Qian Z T. Key technologies and applications of high level autonomous networks [J]. ZTE technology journal, 2024, 30(4): 77 – 82. DOI: 10.12142/ZTETJ.202404012
[27] Gu H X, Zhao L Q, Han Z, et al. AI-enhanced cloud-edge-terminal collaborative network: survey, applications, and future directions [J]. IEEE communications surveys & tutorials, 2024, 26(2): 1322 – 1385. DOI: 10.1109/COMST.2023.3338153
[28] Wang Z Q, Zhou J Z, Han K F. 6G AI-native network with edge-device collaboration [J]. ZTE technology journal, 2025, 31(4): 29 – 33. DOI: 10.12142/ZTETJ.202504005
[29] Ehtesham A, Singh A, Gupta G K, et al. A survey of agent interoperability protocols: model context protocol (MCP), agent communication protocol (ACP), agent-to-agent protocol (A2A), and agent network protocol (ANP) [PP/OL]. V2. arXiv (2025-05-23) [2026-01-13]. https://doi. org/10.48550/arXiv.2505.02279

Biographies

Duan Xiangyang is the Deputy General Manager of Technology Planning at ZTE Corporation and a professor-level senior engineer. He is responsible for technology pre-research planning and technical cooperation at ZTE. He has received one first prize of the National Science and Technology Progress Award, several first prizes of provincial and ministerial science and technology progress awards, and one first prize of the China Institute of Communications Technological Invention Award. His main research interests are in network communication systems technology.

Yang Li (yang.li8@zte.com.cn) is a professor-level senior engineer and serves as the chief engineer for 6G technology pre-research at ZTE Corporation. He is the head (senior expert) of the Algorithm Department's Nanjing team, with 20 years of experience in wireless technology pre-research and standardization. He has authored and co-authored more than 30 technical papers, white papers, and technical monographs in the field of communications. His main research interests include strategic planning and system design for ODICT industry development, intelligent future wireless networks and digital twin applications, integrated communication, sensing, computing, intelligence, trust technologies, and vertical industry applications.

Zhang Kangjie is an engineer in wireless communications technology R&D at ZTE Corporation. He received his Ph.D. degree in communication engineering from Beijing University of Posts and Telecommunications (BUPT), China. He has published over 10 SCI-indexed papers. His research interests include 6G RAN architecture design and 6G AI agent communication protocols.

Sun Wenwen is a wireless technology pre-research engineer at ZTE Corporation. She received her master's degree from Southeast University, China and her bachelor's degree from Xi'an Jiaotong University, China. Her main research interests include 6G native intelligence and new service applications, such as digital twin and data plane technologies.

Xie Feng, PhD, is the head of 6G access network architecture and chief wireless architecture expert at ZTE Corporation, as well as the academic leader of the State Key Laboratory of Mobile Network and Mobile Multimedia Technology, China. He received his bachelor's degree from Peking University, China and his Ph.D. degree from Nanyang Technological University, Singapore. He has conducted short-term research at BT Innovation Centre, UK and the University of Hong Kong, China. Since joining ZTE, he has served as subproject manager for WiMAX/LTE standard pre-research, head of 5G access network architecture pre-research, and chief designer for 5G RAN prototype and product protocol design.

Niu Li received her master's degree from Beijing Jiaotong University, China in 2008. She is currently a pre-research engineer at ZTE Corporation in Beijing, China. Her research interests include IoT communications, satellite communications, and 5G/6G communications.

Toward AI-Agent-Native 6G Networks: A Survey on Protocols, Multimodal Coordination, and ISCC-Driven Dynamic Networking

Zhang Xiaotian[1], Xiao Han[1], Wang Dan[2], Huang Zhenglei[2], Xu Changqiao[1]

(1. Beijing University of Posts and Telecommunications, Beijing 100876, China;
2. China Mobile Communications Group Co., Ltd., Beijing 100032, China)

DOI: 10.12142/ZTECOM.202602003

https://kns.cnki.net/kcms/detail/34.1294.TN.20260422.1331.002.html, published online April 22, 2026

Manuscript received: 2025-02-03

Abstract: As 6G approaches, the proliferation of large language models (LLMs) and embodied intelligence is driving a paradigm shift from the Internet of Things (IoT) to the Internet of Agents (IoA). However, traditional network architectures, designed for content-agnostic data transmission, struggle to accommodate the bursty, reasoning-driven traffic patterns and rigorous multimodal synchronization requirements of autonomous agents. This paper surveys the AI-agent communication network (ACN), aiming to bridge the gap between static network resources and dynamic agent tasks. We analyze the evolution from bit-oriented transmission to agentic syntax protocols, which enable intent-based signaling and semantic compression. Furthermore, we explore mechanisms for multi-agent collaborative consensus and distributed decision-making under the constraints of unstable wireless environments. We critically focus on task-driven dynamic networking, examining how integrated sensing, communication, and computing (ISCC) and network-embedded agents (NEA) facilitate the real-time generation of task graphs and intent-aware traffic scheduling. To synthesize these technologies, we propose a reference framework, the Deep-Agentic Network Architecture (DAN-Arch), which vertically integrates physical-layer sensing with application-layer reasoning flows. Finally, open challenges regarding energy efficiency, cross-domain governance, and 3GPP standardization pathways are discussed to guide future research towards a fully agent-native 6G ecosystem.

Keywords: AI-agent communication network (ACN); 6G architecture; network-embedded agent (NEA); integrated sensing, communication, and computing (ISCC); multi-agent coordination

Citation (Format 1): Zhang X T, Xiao H, Wang D, et al. Toward AI-agent-native 6G networks: a survey on protocols, multimodal coordination, and ISCC-driven dynamic networking [J]. ZTE Communications, 2026, 24(2): 16 - 25. DOI: 10.12142/ZTECOM.202602003

Citation (Format 2): X. T. Zhang, H. Xiao, D. Wang, et al., "Toward AI-agent-native 6G networks: a survey on protocols, multimodal coordination, and ISCC-driven dynamic networking," *ZTE Communications*, vol. 24, no. 2, pp. 16 - 25, Jun. 2026. doi: 10.12142/ZTECOM.202602003.

1 Introduction

The evolution of mobile communication networks has historically focused on connecting humans and physical objects, culminating in the massive machine-type communications of the 5G era[1]. As 6G approaches, a shift is underway due to the proliferation of large language models (LLMs) and the maturation of embodied artificial intelligence, giving rise to AI agents as a new class of network users[2]. Unlike passive terminals, these agents possess autonomy, reasoning capabilities, and the ability to execute complex tasks. This transition marks the emergence of the Internet of Agents (IoA), where the network's function evolves from the transmission of bits to the orchestration of intent and knowledge[3]. As illustrated in Fig. 1, this shift transforms the role of 6G networks from bit-transparent pipes to intent-aware cognitive substrates.

In this context, the AI-agent communication network (ACN) emerges as a necessary architectural framework. While 5G introduced "AI for Network" (AI4Net) to optimize performance, ACN represents the inverse "Network for AI" (Agent4Net) approach[4]. In an agent-native network, the infrastructure must

This work is supported by the National Science and Technology Major Project of China on Mobile Information Networks under Grant No. 2025ZD1304700, the National Natural Science Foundation of China (NSFC) under Grant Nos. 62301070, 62225105 and 62394323. It is also funded by the Beijing University of Posts and Telecommunications-China Mobile Communications Group Co., Ltd. Joint Institute, the Research Initiation Project for Introduced Talents of BUPT under Grant No. 2025KYQD12, and the Foundation of the State Key Laboratory of Networking and Switching Technology, Beijing University of Posts and Telecommunications, under Grant No. NST20250303.

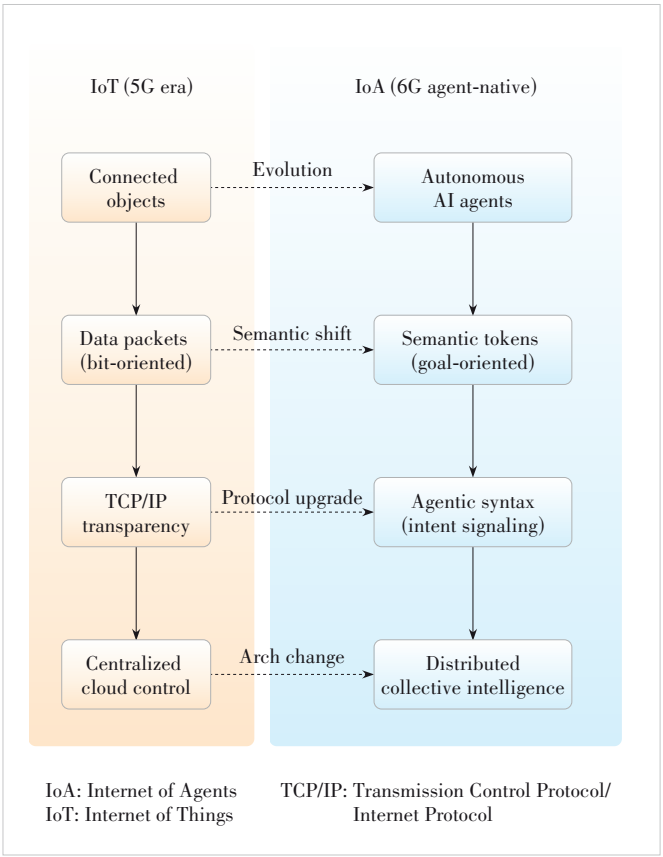

Figure 1. Evolution from IoT to IoA

accommodate unique traffic patterns, such as the bursty token streams generated by chain-of-thought (CoT) reasoning processes[5] and the high-precision synchronization required by multimodal sensory data[6]. Traditional Transmission Control Protocol/Internet Protocol (TCP/IP) and static resource allocation, designed for content-agnostic delivery, are insufficient for the semantic consistency and dynamic collaboration required by autonomous agents. Furthermore, the physical layer capabilities of 6G, particularly integrated sensing, communication, and computing (ISCC), provide a foundation for agent collaboration. Concepts such as network-embedded agents (NEA) suggest that network elements, base stations and core nodes, will evolve into intelligent agents capable of forming dynamic topologies based on task requirements. This article surveys the key technologies required for an agent-native 6G network. We analyze agentic traffic characteristics, the evolution of agentic syntax for intent-based signaling, and mechanisms for multi-agent coordination. A key contribution is the proposal of Deep-Agentic Network Architecture (DAN-Arch), a framework vertically integrating the ISCC physical foundation with logical reasoning flows. Finally, we discuss challenges regarding energy efficiency, standardization, and governance.

To distinguish our architectural focus from recent advances, Table 1 maps prior literature against the proposed 6G-DAN-Arch. While existing works have pioneered payload-centric optimizations—such as generative AI-assisted 3D semantic communication[7], multimodal human-robot visuo-tactile quality of service (QoS)[8], and joint source-channel vibrotactile codecs[9] —our framework fundamentally shifts the focus to control-plane signaling and intent-aware topologies.

2 Agentic Traffic Characteristics in 6G Scenarios

As 6G networks evolve to interconnect autonomous agents, traffic patterns are undergoing a transformation distinct from the streaming or browsing traffic of previous generations. AI agents generate traffic intrinsically linked to reasoning processes, environmental interactions, and physical control loops. This section analyzes these patterns and proposes a key value indicator (KVI) system tailored for the agent-native era.

2.1 New Traffic Patterns Driven by Typical 6G Applications

1) Extreme ultra-reliable low latency communication (xURLLC) for embodied agents

Embodied AI, such as industrial collaborative robots, imposes synchronization requirements exceeding 5G capabilities. These agents operate in high-frequency control loops where multimodal sensory data—combining machine vision, haptic feedback, and telemetry—must align with actuation commands. In 6G scenarios utilizing sub-THz bands, this manifests as microsecond-level isochronous streams. Unlike human users tolerant to millisecond-level jitter, embodied agents require deterministic networking where the "Age of Information" is minimized to prevent control instability. The traffic is characterized by high-density, periodic, short packets demanding near-zero packet loss[10].

2) Semantic streams and token bursts driven by generative AI

Software agents powered by LLMs introduce non-periodic,

Table 1. Comparison of architectural features: 6G agentic traffic vs traditional traffic

Architecture Plane	Prior Work Focus (semantic communication and 5G)	Proposed 6G-DAN-Arch (Agent-Native)
Collective intelligence	Generative 3D & vibrotactile codecs[7, 9]	Agentic syntax & distributed consensus
ISCC control	Reactive multimodal QoS[8]	Predictive ISCC task-triggered slicing
Agentic resource	Edge-cloud offloading	NEA

6G-DAN-Arch: 6G Deep-Agentic Network Architecture ISCC: integrated sensing, communication, and computing NEA: network-embedded agent QoS: quality of service

bursty traffic distinct from traditional packet switching. The interaction involves CoT reasoning, where transmission is punctuated by inference latency. Consequently, traffic exhibits an "Inference-Transmission" duty cycle, resulting in unpredictable bursts of tokens. As communication shifts to semantic payloads (e. g., vectors or knowledge graphs), bandwidth requirements may decrease, but sensitivity to semantic noise increases[11]. The network must handle variable-length, high-entropy payloads that do not conform to standard Poisson distribution models.

3) Traffic in space-air-ground integrated networks (SAGIN)

The core of 6G agent mobility lies within the SAGIN architecture. Unmanned aerial vehicles (UAVs) and satellite-based agents create a three-dimensional heterogeneous environment[12]. Traffic in this domain is defined by the physical characteristics of the non-terrestrial topology: long propagation delays and frequent topology changes due to high-speed mobility. For instance, a drone swarm performing collaborative sensing generates massive uplink throughput in short bursts while traversing different beam coverage areas. This creates rapid fluctuations in channel quality, requiring the network to accommodate traffic that is tolerant of propagation delays but highly sensitive to handover interruptions and routing convergence times. Table 2 summarizes these characteristics.

2.2 6G Key Value Indicator System for ACN

To measure the performance of networks serving AI agents, traditional QoS metrics must be augmented with agent-centric KVIs.

1) Task success rate (TSR): Moving beyond "bit-level" reliability[13], TSR measures "goal-level" reliability. To preserve application-layer privacy and avoid deep packet inspection (DPI), the network does not infer outcomes from payloads. Instead, TSR is measured via explicit agent reporting—a lightweight acknowledgment token sent to the network control plane upon task completion or failure.

2) Semantic accuracy: In semantic scenarios, the bit error rate (BER) is less relevant than semantic accuracy. This measures the fidelity of meaning preservation, ensuring the decoded intent matches the sender's encoded intent, even if bits are altered.

3) Global energy efficiency (GEE): Since agents consume power for both reasoning and interaction, 6G must optimize GEE. This evaluates the energy cost per successful task inference, encouraging offloading to nodes where the combined cost of transmission and computation is minimized. The definitions are detailed in Table 3.

3 6G AI-Native Protocols and Agentic Syntax

To accommodate agentic traffic, the protocol stack must evolve from the transparent TCP/IP model to the "goal-oriented" agentic syntax. This layer unifies semantic understanding with network signaling.

Table 2. 6G agentic traffic characteristics vs traditional traffic

Traffic Category	Typical Application Scenario	Temporal Pattern	Payload Type	Key Network Requirement
Legacy mobile broadband	4K/8K video streaming, web browsing	Continuous or periodic	High-redundancy bitstreams	Throughput (Mbit/s)
xURLLC (Embodied)	Industrial robots, haptic feedback	Isochronous, high-frequency	Short control packets	Deterministic latency (<0.1 ms), jitter control
Generative AI streams	Large language models, CoT reasoning	Non-periodic, bursty (token spikes)	Semantic vectors, knowledge graphs	Semantic fidelity, burst tolerance
NTN swarm telemetry	UAV swarms, satellite IoT	Intermittent, topology-dependent	State updates, sparse data	Routing convergence, topology robustness

CoT: chain-of-thought NTN: non-terrestrial networks xURLLC: extreme ultra-reliable low latency communication
IoT: Internet of Things UAV: unmanned aerial vehicle

Table 3. Proposed KVIs for agent-centric networks

KVI	Definition	Target Optimization Goal	Comparison with 5G QoS
Task success rate	The probability that a group of agents successfully completes a specific mission within constraints	Maximizes mission outcome (e.g., "target found")	Shifts from bit-level reliability (99.999%) to goal-level reliability
Semantic accuracy	The fidelity of meaning preservation between the sender's intent and receiver's understanding	Minimizes semantic errors in vector transmission	Replaces BER; allows bit loss if meaning is preserved
Global energy efficiency	The energy cost per successful task inference (J/task)	Minimizes total communication and computation cost	Shifts from bit/J to inference/J

BER: bit error ratio KVI: key value indicator QoS: quality of service

3.1 Evolution from Transparent Bit Transmission to Semantic Protocols

The foundation of ACN lies in semantic communication (SemCom), which shifts focus from accurate symbol transmission to precise meaning conveyance[14 - 15]. Semantic protocols allow agents to exchange extracted feature vectors or semantic knowledge graphs rather than raw data. This resolves the token burst challenge by utilizing shared knowledge bases (KBs) to achieve high compression ratios, filtering out redundancy while preserving core logic[16]. The communication channel transforms from a pipe carrying bits into a medium that filters and refines knowledge.

3.2 Design of the Agentic Syntax Layer

The agentic syntax layer defines how intents are encoded, signaled, and negotiated within the 6G stack. It is embedded above the new non-access stratum (NAS) signaling layer and below collective intelligence interfaces, as shown in Fig. 2.

1) New NAS and 6G signaling enhancement: It is crucial to distinguish agentic syntax from payload-oriented SemCom, which compresses data into features[17]. Agentic syntax operates strictly at the control plane. We propose a minimal viable intent signaling unit (ISU) header comprising Agent-ID, Capability-Req, Task-Priority, and Context-Digest. In the Signaling-as-Reasoning sequence, an agent transmits the ISU (fewer than 100 bytes to avoid congestion); the first-hop NEA parses the intent to pre-allocate a micro-slice; the semantic payload follows. To ensure backward compatibility, a rollback strategy triggers a fallback to standard IP forwarding if legacy core networks fail to parse the ISU.

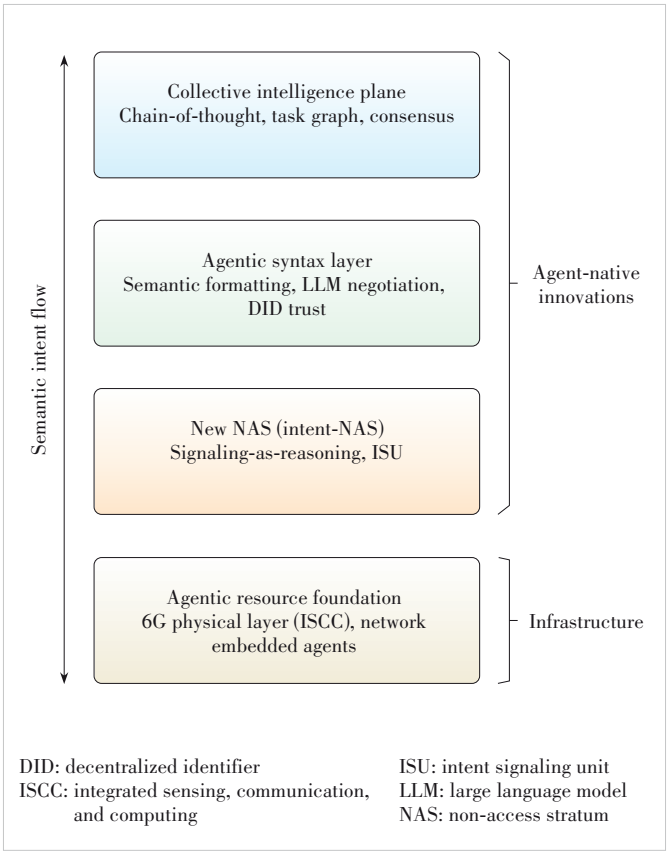

Figure 2. Agentic syntax protocol stack

2) LLM-driven protocol self-negotiation: Given agent heterogeneity, static standards are impractical. By leveraging LLMs, the agentic syntax layer supports protocol self-negotiation. Communicating agents dynamically agree on coding schemes and semantic vocabulary before transmission. For example, agents may switch from text-based to dense vector protocols upon detecting a stable channel, optimizing semantic accuracy.

3.3 Cross-Domain Identity and Trust

As agents operate across the SAGIN, they traverse trust boundaries. ACN introduces a decentralized identifier (DID) system based on 6G endogenous security. Unlike a SIM card, an agent-DID binds a software agent to its ownership and reputation history. The network performs continuous trust assessment, verifying DIDs during collaborative tasks to ensure agents create valid semantic outputs and the integrity of collective intelligence.

4 Multi-Agent Coordination and 6G Consensus Mechanisms

With agentic syntax established, agents require coordination to execute complex tasks. In 6G communications, coordination evolves from centralized orchestration to distributed, perception-aware consensus.

4.1 Task Decomposition and Distributed Collective Intelligence

In large-scale ACNs, single agents often lack sufficient resources. We propose a Cloud-Edge-End collaborative framework based on the Mixture-of-Experts (MoE) paradigm. Cloud-level agents act as strategic planners decomposing goals; Edge-level agents (at base stations or mobile edge computing nodes) distribute sub-tasks based on latency requirements; and End-level agents execute actions. This hierarchical approach transforms coordination into a collaborative inference challenge, requiring the network to synchronize the "Prompt State" across the continuum to maintain logical consistency.

4.2 Coordination Optimization Driven by 6G Sensing

A distinct advantage of the 6G ACN is the availability of ISCC capabilities. Unlike traditional multi-agent systems (MAS) requiring explicit telemetry exchange, the 6G infrastructure provides "Sensing-as-a-Service"[18]. By analyzing channel state information (CSI) and radar echoes, the network constructs a real-time environmental digital twin. This shared ground truth reduces state synchronization traffic. Agents can

employ distributed decision-making algorithms, such as federated reinforcement learning[19], to align behaviors. For instance, UAV swarms can adjust formations based on network sensing data rather than peer-to-peer telemetry. This closed-loop coordination is depicted in Fig. 3.

4.3 Interoperability for Heterogeneous Agents

To prevent intelligence silos among diverse models, cross-model interoperability is essential. We propose a Semantic Handshake Protocol where agents exchange Model Cards—metadata describing modalities and context windows—before collaboration. Additionally, the network can deploy semantic translators at the edge using lightweight adapter models to convert semantic vectors[20] between latent spaces, enabling alignment across vendor boundaries.

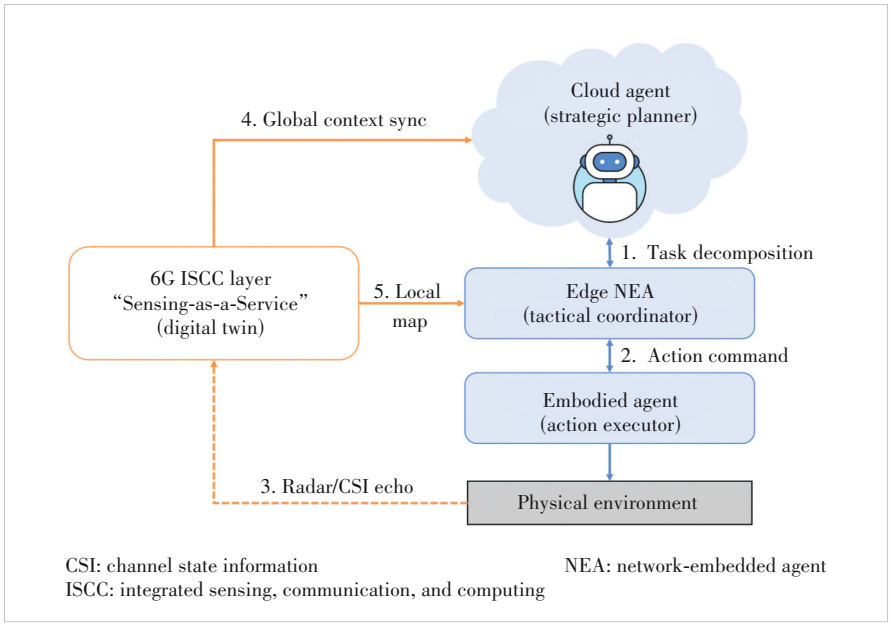

Figure 3. Multi-agent coordination loop

5 Task-Driven Dynamic Networking and Task Graph Generation

The network topology in 6G must physically adapt to support high-level agentic behaviors. This section explores the evolution towards a task-driven network where topology is reconstructed based on the real-time task dependency graph.

5.1 Dynamic Task Graph Generation

The connection between agent reasoning and resource allocation is the dynamic task graph. As agents engage in CoT reasoning, they generate logical dependencies (e.g., Perceive → Retrieve → Act). The network control plane maps this flow to a physical directed acyclic graph (DAG)[21]. We propose a CoT-to-DAG mapping mechanism (Fig. 4). When an agent initiates a mission, the intent is parsed to generate a graph where nodes represent capabilities (e. g., Vector Database Lookup) and edges represent flow requirements. Unlike static service function chaining (SFC), this graph possesses topology flexibility, updating instantly if environmental conditions or agent logic change.

While dynamic DAG parsing incurs computational setup latency, it avoids creating a bottleneck in xURLLC scenarios through predictive template matching. For high-frequency, repetitive embodied tasks, the network caches pre-compiled DAG templates. When the ISU matches a known intent, the topology is instantiated instantly (<1 ms), bypassing the full parsing latency.

5.2 6G NEA Architecture

To execute the dynamic task graph efficiently, the execution environment cannot be limited to distant clouds or user terminals. The network infrastructure itself—base stations (BS), user plane functions, and routers—must evolve into NEAs[22].

In the NEA architecture, network elements are no longer passive forwarders but active agents equipped with inference engines. NEAs possess self-organization capabilities, allowing them to autonomously form "On-Demand Subnets" based on the task graph.

• Scenario: In a high-speed vehicular platoon scenario, a roadside unit acting as an NEA can temporarily bond with the vehicular agents to form a local, ultra-low-latency subnet for cooperative collision avoidance.

• Mechanism: Once the task concludes, the NEA dissolves the subnet and releases resources back to the common pool. This flash networking capability is critical for optimizing the energy efficiency KVI, as resources are only committed when a valid task graph exists.

5.3 A-DNS and Intent-Based Routing

In a global-scale 6G ecosystem, particularly within Non-Terrestrial Networks (NTNs) covering remote areas, agents need a mechanism to discover peers based on capabilities rather than physical locations. The legacy IP-based domain name system (DNS) maps names to addresses, but it cannot map "intents" to "providers".

We review the evolution towards an agent DNS (A-DNS). A-DNS introduces a new resolution layer: intent-to-capability mapping[23].

• Query: Instead of querying www. service. com, an agent queries intent: {action: "analyze_seismic_data", constraint: "low_power"}.

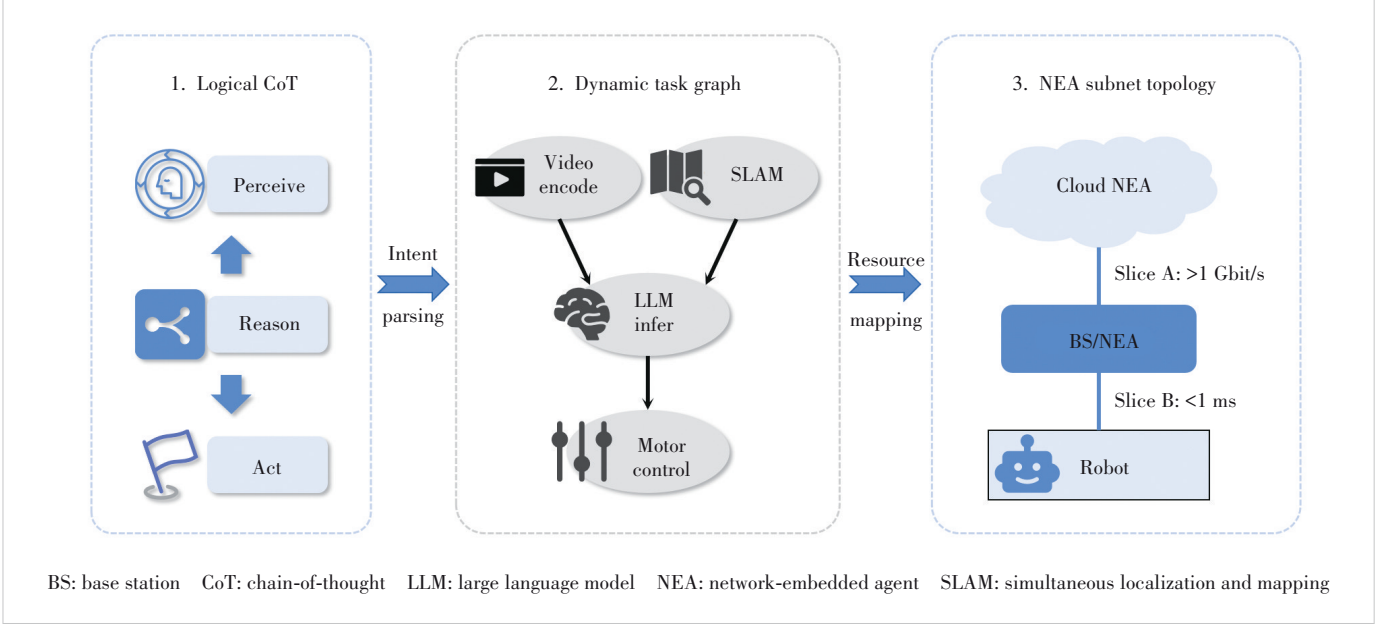

Figure 4. CoT to task graph to topology

• Resolution: The A-DNS resolves this intent to the DID of the most suitable NEA or service agent currently available in the satellite-terrestrial footprint.

Consequently, routing evolves from the Shortest Path (IP metric) to the Most Capable Path (Intent metric). Data packets are routed not necessarily to the nearest node, but to the node that possesses the specific model weights or sensing data required to fulfill the corresponding task function in the task graph.

6 ISCC-Driven Intelligent Traffic Scheduling

Following the generation of the dynamic task graph and the establishment of the NEA topology discussed in Section 5, the final critical step in the ACN lifecycle is the allocation of physical resources to execute these tasks. Traditional cellular scheduling algorithms, such as Proportional Fair or Round Robin, optimize for aggregate throughput or fairness among users but fail to account for the logical dependencies and semantic value of agentic traffic. In the 6G era, traffic scheduling must evolve from a packet-centric approach to an intent-centric paradigm, leveraging the unique capabilities of ISCC to optimize resource utilization across the spatial, temporal, and computational domains.

6.1 Intent-Aware and Precision Resource Scheduling

The core principle of intent-aware scheduling is that not all data packets are created equal; their value is determined by their role in the agent's current reasoning process. In the context of the ACN, the network scheduler utilizes the weighted task graph generated in the previous stage as its primary input. By analyzing the topology of the task graph, the scheduler can identify the critical path[24], that is, the sequence of subtasks that strictly determines the overall completion time of the mission. Resources are then allocated preferentially to nodes and links along this critical path. For instance, a high-priority obstacle recognition inference task may be assigned to a dedicated millisecond-level time slot on a mmWave band to ensure immediate execution, while a parallel log synchronization task is relegated to a sub-6 GHz background channel. This differentiation ensures that limited spectrum resources directly contribute to task success rates rather than merely maximizing bit-level throughput. Furthermore, this mechanism supports multi-band dynamic allocation, where the network seamlessly switches an agent's data stream between Terahertz bands for bursty, high-bandwidth semantic transfers and lower-frequency bands for reliable control signaling, depending on the real-time requirements of the intent[25].

6.2 Deep Integration of Sensing, Communication, and Computing

ISCC provides a revolutionary mechanism for traffic scheduling by introducing physical environmental awareness into the resource allocation loop. In traditional networks, the scheduler reacts to channel quality indicator (CQI), which are often outdated due to processing delays. In an ISCC-driven ACN, the network utilizes ubiquitous sensing capabilities—such as radar echoes and radio imaging—to construct a real-time digital twin of the physical environment. This allows the scheduler to predict the mobility trajectory of embodied agents with high precision. For example, if the ISCC system detects that a UAV agent is about to fly behind a building, the scheduler can proactively trigger a handover to a satellite link or a reconfigurable intelligent surface reflected path before the line-of-sight link is blocked.

Moreover, ISCC enables the joint optimization of communi-

cation and computation resources, often referred to as the communication-computation trade-off[26]. The scheduler continuously evaluates the energy and latency costs of transmitting data versus computing it locally. If the ISCC sensing data indicates that the wireless channel is degrading due to environmental clutter, the network control plane may direct the NEA to execute a model partitioning strategy, forcing the agent to perform early-exit inference locally rather than offloading raw data to the cloud. This cross-layer optimization ensures that the network operates at the optimal point of the energy-latency curve.

6.3 Predictive Traffic Control and Self-Evolving Policies

To handle the bursty and non-periodic nature of agentic traffic described in Section 2, ACN scheduling must shift from reactive flow control to predictive traffic shaping. By analyzing historical interaction logs and the current CoT status of agents, the network can employ AI-based prediction models to forecast upcoming traffic bursts. For instance, if an agent is detected entering a complex reasoning phase, the scheduler anticipates a subsequent surge in token generation and preallocates uplink grants, thereby eliminating the scheduling request latency. This predictive capability is further enhanced by self-evolving network policies. Through reinforcement learning (RL), the scheduler learns from the outcomes of past task executions. If a particular scheduling policy led to a timeout in a multi-agent consensus task, the RL agent applies a negative reward and adjusts its policy to reserve larger guard bands for similar synchronization tasks in the future. This closes the loop between application-level metrics and physical-layer resource management, enabling the network to autonomously adapt to the evolving intelligence of its users.

7 Proposed Framework: 6G-DAN-Arch

Given the technological evolutions discussed in the preceding sections, ranging from agentic traffic analysis and semantic protocols to distributed coordination and ISCC-driven scheduling, it becomes evident that a piecemeal evolution of current network architectures is insufficient. The disparate requirements of autonomous agents demand a holistic architectural transformation. To this end, we propose 6G-DAN-Arch. Unlike the traditional open systems interconnection (OSI) model, which enforces strict horizontal decoupling, DAN-Arch advocates for a vertically integrated design where the logical reasoning flows of agents are deeply coupled with the physical sensing and computing resources of the 6G infrastructure. This reference framework is structured into three unified planes: the agentic resource foundation plane, the ISCC control plane, and the collective intelligence plane. A systematic comparison between the traditional AI4Net paradigm and the proposed Agent4Net architecture is presented in Table 4, highlighting the shift towards intent-awareness and dynamic topology.

7.1 Architecture Design Logic and Planes

The foundation of the architecture is the agentic resource foundation plane. This layer represents the physical evolution of the network infrastructure, where traditional base stations and routers are upgraded to NEAs as discussed in Section 5. In the DAN-Arch, these NEAs serve as the execution substrate, integrating ubiquitous sensing capabilities with endogenous computing power. By creating a standardized hardware abstraction layer, this plane presents the raw physical resources—spectrum, computing cores, and sensing apertures—as unified "agentic capabilities" rather than isolated hardware parameters. This allows upper layers to subscribe to resources based on capability logic, such as requesting a "visual processing node", rather than a specific server IP address. The overall architecture of the proposed 6G-DAN-Arch, integrating NEAs, ISCC control, and collective intelligence, is summarized in Fig. 5.

Above the foundation lies the ISCC control plane, which

Table 4. Architectural comparison: 5G AI4Net vs 6G Agent4Net

Feature Dimension	Traditional 5G/AI4Net	Proposed 6G/Agent4Net
Primary user	Humans and passive IoT sensors	Autonomous AI agents & embodied robots
Core function	Transparent data pipe (content-agnostic)	Intelligent substrate (intent-aware)
Protocol stack	TCP/IP + standard NAS	Agentic syntax and new NAS (intent-signaling)
Resource scheduling	Reactive (based on channel quality/CQI)	Predictive (based on task graph & ISCC)
Network topology	Static/semi-static slicing	Dynamic (task-triggered ephemeral subnets)
Routing mechanism	IP address (shortest path)	A-DNS (capability-based routing)
Role of AI	AI optimizes the network (overlay)	Network is built for AI (native design)

A-DNS: agent domain name system
Agent4Net: Network for AI
AI4Net: AI for Network
CQI: channel quality report
IoT: Internet of Things
ISCC: integrated sensing, communication, and computing
NAS: non-access stratum
TCP/IP: Transmission Control Protocol/Internet Protocol

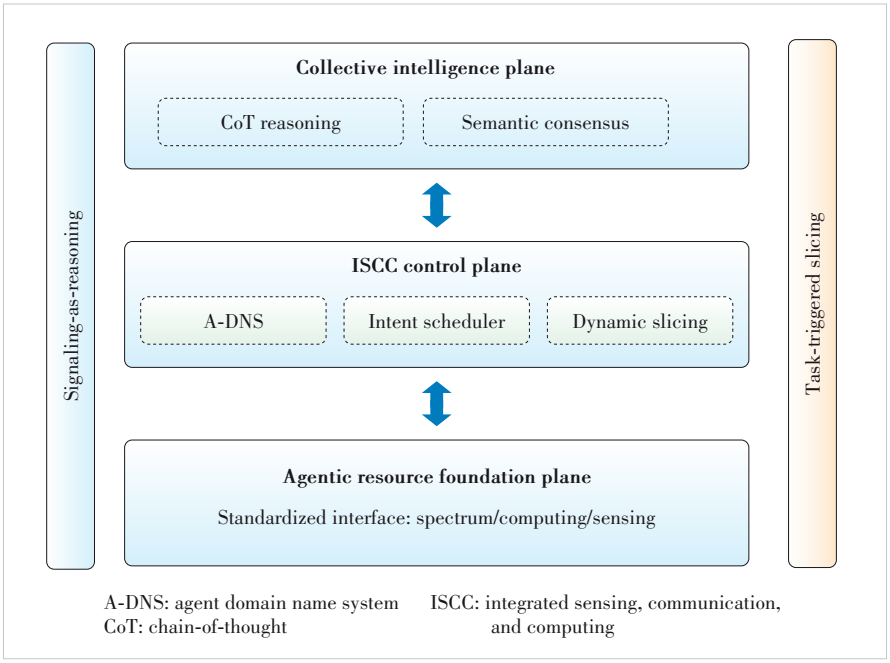

Figure 5. DAN-Arch framework

functions as the operating system of the ACN. This plane is responsible for the intent-based routing and intelligent scheduling mechanisms detailed in Section 6. Its core function is to translate the abstract semantic intents received from the upper layer into concrete physical network configurations. It maintains a dynamic global view of the network topology and the physical environment via ISCC updates. Crucially, this plane hosts the A-DNS and the dynamic task graph parser. It acts as the bridge that maps the logical dependencies of an agent's task directly to the optimal topology of NEAs, ensuring that the fluidity of the physical network configuration matches the cognitive fluidity of the users.

The uppermost layer is the collective intelligence plane. This plane operates at the level of agentic syntax and semantic knowledge, managing the lifecycle of collaborative tasks. It is responsible for parsing CoT reasoning processes, managing semantic knowledge bases, and executing the distributed consensus algorithms described in Section 4. By decoupling semantic synchronization from the underlying data transport, this plane ensures that diverse agents can achieve logical alignment and intent interoperability regardless of their physical location or hardware vendor.

7.2 Core Mechanisms: Signaling-as-Reasoning and Task-Triggered Slicing

The 6G-DAN-Arch is empowered by two novel mechanisms that distinguish it from legacy AI-enabled networks. The first is the signaling-as-reasoning mechanism. In traditional networks, control plane signaling is strictly used for connection management. In DAN-Arch, we propose expanding the new NAS protocol to carry reasoning tokens directly within the signaling header. When an agent initiates a request, the signaling message contains not just connection parameters but also a snapshot of the agent's current inference state. This allows NEAs along the signal path to perform in-network inference, pre-loading relevant model weights or caching semantic context before the payload data even arrives. This creates a network environment where the signaling flow effectively functions as a distributed chain of thought, significantly reducing the latency of multi-step inference tasks.

The second core mechanism is task-triggered dynamic slicing. Consider an end-to-end visuo-tactile collaboration case where a robotic arm intends to lift a fragile object. Triggered by the agent's ISU (about 80 bytes overhead), the control plane uses cached templates to instantiate a visuo-tactile micro-slice (about 0.8 ms setup latency). Instead of waiting for reactive scheduling requests, the ISCC radar tracks the robot's trajectory and predictively allocates a burst of sub-THz bandwidth just before physical contact, ensuring <0.1 ms deterministic latency required for tactile feedback. Upon task completion, an explicit TSR acknowledgment triggers immediate slice teardown. This end-to-end orchestration yields a total setup and execution latency of about 1.2 ms, effectively eliminating traditional packet-centric scheduling bottlenecks.

8 Future Directions and Challenges

While the DAN-Arch framework and the associated key technologies present a viable path toward an Agent-Native 6G network, several profound challenges remain to be addressed before widespread industrial deployment can be realized. These challenges span the domains of sustainability, standardization, and cross-domain governance, defining the research roadmap for the latter half of the decade.

8.1 The Energy Efficiency Paradox in Hyper-Connected Intelligence

The first critical challenge lies in the energy sustainability of the ACN. AI agents are inherently energy-intensive, requiring substantial power for both large-model inference and high-speed semantic communication. As the density of agents increases, there is a risk that the energy gains achieved through 6G spectral efficiency improvements will be negated by the exponential growth in computational power consumption. A potential paradox emerges where optimizing for higher semantic accuracy or faster task completion inadvertently leads to un-

sustainable carbon footprints. Future research must focus on the joint optimization of communication and computation energy consumption, developing a global utility function that penalizes excessive reasoning steps or redundant transmissions. Innovations in green semantic communication, which dynamically degrades semantic precision to save energy during non-critical tasks, and the integration of backscatter communications or ambient IoT for zero-energy passive agents will be pivotal. The network must evolve not only to schedule bandwidth but also to act as a global energy orchestrator, balancing the battery life of embodied terminals against the urgency of their tasks.

8.2 Standardization Pathways Toward 3GPP Release 20 and Beyond

From an industrial perspective, the standardization of ACN interfaces is the prerequisite for multi-vendor interoperability. While 3GPP Release 18 and 19 have successfully laid the groundwork for AI4Net, focusing on AI-enabled air interfaces and mobility management, the transition to Agent4Net requires a more radical standardization effort in Release 20 and beyond. Key open issues include the standardization of the agentic syntax signaling header within the NAS protocol to ensure that diverse agents can express intents in a unified format. Furthermore, the definition of the NEA requires consensus on the architectural split between communication and computing functions within the core network and the radio access network. There is a pressing need for the industry to define a standardized "agent interface" (comparable to the Uu interface for mobiles) that exposes 6G ISCC sensing and compute capabilities to third-party agents in a secure, measured manner.

8.3 Security, Sovereignty, and Ethical Governance

The autonomous nature of AI agents introduces novel security vectors. A minimal threat model for the ACN includes injection attacks (fabricating ISUs to drain slice resources), tampering (altering intents to disrupt tasks), replay attacks (triggering redundant topologies), and negotiation attacks (forcing downgrades to legacy protocols). To counter these, future architectures must incorporate baseline defenses: integrity protection via lightweight hashing in the ISU context-digest, hardware isolation (e. g., trusted execution environments) within NEAs for secure intent parsing, and strict policy rollback mechanisms that instantly isolate anomalous Agent-DIDs to default security postures. Issues of data sovereignty and sovereign semantic clouds remain essential for cross-border AI compliance.

9 Conclusions

The emergence of the ACN represents a fundamental transition from the IoT to the IoA, necessitating a network architecture that evolves from a passive data pipe to an intent-aware substrate. This survey has analyzed the unique traffic patterns of autonomous agents and the limitations of current protocols, proposing the adoption of agentic syntax and ISCC-driven coordination to address these challenges. By introducing the DAN-Arch framework, we demonstrate how NEAs and dynamic task graphs can align physical network topology with logical agent reasoning. While challenges in energy efficiency, standardization, and governance remain, the integration of these technologies establishes a viable roadmap for 6G to serve as the external cortex for collective intelligence.

References

[1] Letaief K B, Chen W, Shi Y M, et al. The roadmap to 6G: AI empowered wireless networks [J]. IEEE communications magazine, 2019, 57(8): 84 – 90. DOI: 10.1109/mcom.2019.1900271
[2] Chen Z Q, Sun Q, Li N, et al. Enabling mobile AI agent in 6G era: architecture and key technologies [J]. IEEE network, 2024, 38(5): 66 – 75. DOI: 10.1109/mnet.2024.3422309
[3] Wang C X, You X H, Gao X Q, et al. On the road to 6G: visions, requirements, key technologies, and testbeds [J]. IEEE communications surveys & tutorials, 2023, 25(2): 905 – 974. DOI: 10.1109/comst.2023.3249835
[4] Zhang Z Q, Xiao Y, Ma Z, et al. 6G wireless networks: vision, requirements, architecture, and key technologies [J]. IEEE vehicular technology magazine, 2019, 14(3): 28 – 41. DOI: 10.1109/mvt.2019.2921208
[5] Wei J, Wang X, Schuurmans D, et al. Chain-of-thought prompting elicits reasoning in large language models [PP/OL]. arXiv (2023-01-10) [2026-01-12]. http://arxiv.org/abs/2201.11903
[6] Nguyen D C, Ding M, Pathirana P N, et al. 6G Internet of Things: a comprehensive survey [J]. IEEE Internet of Things journal, 2022, 9(1): 359 – 383. DOI: 10.1109/jiot.2021.3103320
[7] Chen M K, Liu M H, Wang C Y, et al. Cross-modal graph semantic communication assisted by generative AI in the metaverse for 6G [J]. Research, 2024, 7: 342. DOI: 10.34133/research.0342
[8] Wang Z R, Chen M K, Liu Q. A review on multimodal communications for human-robot collaboration in 5G: from visual to tactile [J]. Intelligence & robotics, 2025, 5(3): 579 – 606. DOI: 10.20517/ir.2025.30
[9] Wang R J, Chen K M, Li S J, et al. Efficient semantic codec for real-time vibrotactile transmission [C]//The 33rd ACM International Conference on Multimedia. ACM, 2025: 12092 – 12101. DOI: 10.1145/3746027.3755630
[10] Saad W, Bennis M, Chen M Z. A vision of 6G wireless systems: applications, trends, technologies, and open research problems [J]. IEEE network, 2020, 34(3): 134 – 142. DOI: 10.1109/mnet.001.1900287
[11] Qin Z, Tao X, Lu J, et al. Semantic communications: principles and challenges [PP/OL]. arXiv (2022-06-27) [2026-01-12]. http://arxiv. org/abs/2201.01389
[12] Chen J, Zhang H, Xie Z. Space-air-ground integrated network (SAGIN): a survey [PP/OL]. arXiv (2023-07-27) [2026-01-12]. http://arxiv. org/abs/2307.14697
[13] Shao J W, Mao Y Y, Zhang J. Task-oriented communication for multidevice cooperative edge inference [J]. IEEE transactions on wireless communications, 2023, 22(1): 73 – 87. DOI: 10.1109/twc.2022.3191118
[14] Zhang P, Xu W J, Gao H, et al. Toward wisdom-evolutionary and primitive-concise 6G: a new paradigm of semantic communication networks [J]. Engineering, 2022, 8: 60 – 73. DOI: 10.1016/j.eng.2021.11.003
[15] Strinati E C, Barbarossa S. 6G Networks: beyond Shannon towards semantic and goal-oriented communications [PP/OL]. arXiv (2021-02-17) [2026-01-12]. http://arxiv.org/abs/2011.14844
[16] Liang C, Du H, Sun Y, et al. Generative AI-driven semantic communication networks: architecture, technologies and applications [PP/OL]. arXiv (2024-01-07) [2026-01-12]. http://arxiv.org/abs/2401.00124

[17] Dong R, She C Y, Hardjawana W, et al. Deep learning for hybrid 5G services in mobile edge computing systems: learn from a digital twin [J]. IEEE transactions on wireless communications, 2019, 18(10): 4692 – 4707. DOI: 10.1109/twc.2019.2927312
[18] Liu F, Zhou L F, Masouros C, et al. Toward dual-functional radar-communication systems: optimal waveform design [J]. IEEE transactions on signal processing, 2018, 66(16): 4264 – 4279. DOI: 10.1109/tsp.2018.2847648
[19] Yang Z, Chen M, Wong K-K, et al. Federated learning for 6G: applications, challenges, and opportunities [PP/OL]. arXiv (2021-01-05) [2026-01-12]. http://arxiv.org/abs/2101.01338
[20] Xie H Q, Qin Z J, Li G Y, et al. Deep learning enabled semantic communication systems [J]. IEEE transactions on signal processing, 2021, 69: 2663 – 2675. DOI: 10.1109/tsp.2021.3071210
[21] Vetriveeran D, Leena Sri R. Resource provisioning in fog computing—a survey [J]. ACM computing surveys, 2025, 57(12): 1 – 26. DOI: 10.1145/3744662
[22] Chen M, Hao Y X, Hwang K, et al. Disease prediction by machine learning over big data from healthcare communities [J]. IEEE access, 2017, 5: 8869 – 8879. DOI: 10.1109/access.2017.2694446
[23] Pang L, Yang C G, Chen D Y, et al. A survey on intent-driven networks [J]. IEEE access, 2020, 8: 22862 – 22873. DOI: 10.1109/access.2020.2969208
[24] Uysal E, Kaya O, Baghaee S, et al. Age of information in practice [PP/OL]. arXiv (2021-06-02) [2026-01-12]. http://arxiv.org/abs/2106.02491
[25] Akyildiz I F, Han C, Nie S. Combating the distance problem in the millimeter wave and terahertz frequency bands [J]. IEEE communications magazine, 2018, 56(6): 102 – 108. DOI: 10.1109/mcom.2018.1700928
[26] Mao Y Y, You C S, Zhang J, et al. A survey on mobile edge computing: the communication perspective [J]. IEEE communications surveys & tutorials, 2017, 19(4): 2322 – 2358. DOI: 10.1109/comst.2017.2745201

Biographies

Zhang Xiaotian received his BS degree in the School of Computer Science from Beijing University of Posts and Telecommunications (BUPT), China in 2024. He is currently working toward a doctoral degree in the School of Computer Science, BUPT. His research interests include multi-agent communication and AI.

Xiao Han (xiaohan@bupt.edu.cn) is currently an associate professor with the State Key Laboratory of Networking and Switching Technology, Beijing University of Posts and Telecommunications, China. His research interests include immersive media transmission, online learning, AIGC video services, and generative AI.

Wang Dan is a project manager with the China Mobile Research Institute, China Mobile Communications Group Co., Ltd. She has been actively engaged in standardization research on AI-native and agent-oriented communication networks and has served as a principal contributor to the SA2 NET4AI direction. He work focuses on network architecture evolution, intelligent agent communication, and standardization pathways for integrating AI agents into future mobile networks.

Huang Zhenglei is a director, researcher, and senior engineer with the China Mobile Research Institute, China Mobile Communications Group Co., Ltd., China. He serves as the leader of the Agent Communication Network Working Subgroup under CCSA TC5 WG12. His research interests include future network architecture, intelligent communication networks, agent communication networks, and standardization for AI-native mobile communication systems.

Xu Changqiao received his PhD degree from the Institute of Software, Chinese Academy of Sciences (ISCAS) in January 2009. He was an assistant research fellow and research and development project manager at ISCAS from 2002 to 2007. He was a researcher at Athlone Institute of Technology, Ireland, and a jointly trained PhD candidate at Dublin City University, Ireland, from 2007 to 2009. He joined Beijing University of Posts and Telecommunications (BUPT), China in 2009. He is currently a professor with the State Key Laboratory of Networking and Switching Technology and the Director of the Network Architecture Research Center, BUPT. His research interests include network security, mobile networking, multimedia communications, and future Internet technology. He has published over 200 technical papers in prestigious international journals and conferences, including *IEEE Communications Magazine*, *IEEE/ACM Transactions on Networking*, *IEEE Transactions on Mobile Computing*, INFOCOM, and ACM Multimedia.

Training Optimization for Complex Reasoning Tasks in ACN: Dynamic Batch-Aware Advantage Weighting for Agentic RAG

Chen Yu[1], Li Fan[2], Wu Jie[3], Gao Weipeng[1], Ouyang Ye[1]

(1. AsiaInfo Technologies (China) Co., Ltd., Beijing 100193, China;
2. Network Optimization Center, China United Network Communications Co., Ltd., Beijing 100031, China;
3. China United Network Communications Co., Ltd., Guangzhou Branch, Guangzhou 510630, China)

DOI: 10.12142/ZTECOM.202602004

https://kns.cnki.net/kcms/detail/34.1294.TN.20260515.0959.002.html, published online May 19, 2026

Manuscript received: 2026-01-15

Abstract: With the emergence of AI-agent communication networks (ACN) in the 6G era, the efficient training of agents for complex reasoning tasks has become a critical capability for scalable ACN deployment. As a representative complex reasoning task, retrieval-augmented multi-hop question answering (e.g., agentic retrieval-augmented generation) requires agents to perform multi-step reasoning through reflection, planning, and tool-use mechanisms. However, reinforcement learning training still faces reward sparsity and sample efficiency challenges, limiting agents' rapid evolution and adaptability. We propose dynamic batch-aware advantage weighting (DB-AW), integrating two core components at the batch level: the difficulty-aware weighting component dynamically amplifies positive advantages based on long-term success rates, directing learning toward learnable yet challenging samples; and the batch filtering component removes zero-variance groups, ensuring each update contains non-zero gradient signals. Experiments show that DB-AW achieves 18%, 17%, and 15% relative improvements on Qwen2.5-7B, Qwen2.5-3B, and LLaMA3.2-3B, respectively, while improving the effective update rate from 68% to 100%, significantly reducing agent training costs. As a lightweight and reusable algorithmic module, DB-AW can be readily integrated into methods such as group relative policy optimization (GRPO), providing a practical pathway for efficient training of complex reasoning agents in ACN.

Keywords: Agentic RAG; AI-agent communication network; batch filtering; difficulty-aware weighting; multi-hop question answering; reinforcement learning

Citation (Format 1): Chen Y, Li F, Wu J, et al. Training optimization for complex reasoning tasks in ACN: dynamic batch-aware advantage weighting for agentic RAG [J]. ZTE Communications, 2026, 24(2): 26 - 32. DOI: 10.12142/ZTECOM.202602004

Citation (Format 2): Y. Chen, F. Li, J. Wu, et al., "Training optimization for complex reasoning tasks in ACN: dynamic batch-aware advantage weighting for agentic RAG," *ZTE Communications*, vol. 24, no. 2, pp. 26 - 32, Jun. 2026. doi: 10.12142/ZTECOM.202602004.

1 Introduction

As 6G networks evolve toward intelligence, AI-agent communication networks (ACN) have emerged as an infrastructure supporting massive agent interconnection[1]. Through core capabilities such as digital identity management, flexible networking, and multi-agent collaboration, ACN provides a secure and efficient communication environment for agents, empowering diverse application scenarios including intelligent customer service, network operations, and knowledge-based question answering (QA). In these applications, complex reasoning tasks (such as multi-hop question answering, multi-step planning, and code generation) pose higher requirements for agents' reasoning capabilities.

Agentic retrieval-augmented generation (Agentic RAG), as a representative complex reasoning task, provides powerful support for multi-hop question answering scenarios through agentic workflows including reflection, planning, and tool use, enabling iterative refinement and multi-step reasoning[2]. Commonly used benchmarks include HotpotQA[3], WikiMultihopQA[4], and MuSiQue[5], with NQ[6] as an open-domain reference.

Reinforcement learning (RL) is widely applied to optimize performance, but deploying and training agents for complex reasoning tasks (represented by Agentic RAG) in ACN environments faces severe challenges:

First, training efficiency bottlenecks limit agent-scale deployment. Multi-hop reasoning tasks' high difficulty leads to severe reward sparsity in outcome-based RL. Training contains numerous zero-variance batches, producing ineffective gradient updates. This not only reduces individual agent training speed but also limits the rapid iteration and evolution capabilities of agent populations in ACN, a limitation

that is particularly prominent when ACN needs to support massive parallel agent training.

Second, learning bias affects agent generalization. Policies tend to over-focus on "easy samples," failing to direct learning toward samples near the competence frontier with appropriate challenges, limiting generalization improvement. This affects agents' adaptation capabilities in the diverse task scenarios of ACN, disadvantaging flexible deployment in complex network environments.

How to efficiently integrate "difficulty-aware" and "sample efficiency improvement" optimization ideas into mainstream training algorithms like group relative policy optimization (GRPO) for complex reasoning tasks remains a worthwhile endeavor.

We propose dynamic batch-aware advantage weighting (DB-AW). DB-AW introduces two core components: difficulty-aware advantage weighting and batch filtering. Without changing reward formulation, we dynamically amplify positive advantages based on long-term historical success rates following within-group normalization, directing learning toward samples near the competence frontier. At the batch level, we identify and filter out zero-variance groups, ensuring each update contains non-zero gradient signals and significantly improving effective update steps per unit of computation.

The main contributions are summarized as follows.

1) An RL optimization method for complex reasoning tasks in ACN: Using Agentic RAG multi-hop QA as a representative scenario and addressing training challenges such as reward sparsity and learning bias, we propose DB-AW with two synergistic components:

• Difficulty-aware advantage weighting: It dynamically amplifies positive advantages based on long-term success rates after within-group normalization.

• Batch filtering: We introduce the first batch-level zero-variance group filtering mechanism for Agentic RAG scenarios. It operates without task-specific designs, maintaining lightweight and general applicability.

DB-AW optimizes GRPO training through gradient reweighting without altering reward definition.

2) Empirical validation and analysis: Under controlled setup, we validate DB-AW's effectiveness on HotpotQA, NQ, and 2Wiki. DB-AW achieves 18%, 17%, and 15% relative improvements on Qwen2.5-7B, Qwen2.5-3B, and LLaMA3.2-3B, respectively, validating cross-model generalization.

2 Related Work

2.1 Agentic RAG

Agentic RAG introduces reflection, planning, and tool use into retrieval-augmented pipelines, forming "think→retrieve →rethink" iterative loops[2]. ReAct [7], Self-RAG [8], and Reflexion[9] implement closed-loop control. Search-o1[10] achieves autonomous knowledge supplementation through Agentic RAG mechanisms.

2.2 GRPO in Agentic RAG

GRPO[11] balances "no value network" and "sample efficiency" through group relative advantages and ratio clipping. Search-R1[12] implements multi-turn alternating reasoning-retrieval. R1-Searcher[13] proposes two-stage RL: Stage-1 learns retrieval calling and Stage-2 focuses on effective utilization. Despite their demonstrated effectiveness, challenges remain, such as reward sparsity, sample distribution imbalance, and zero-gradient updates.

2.3 ACN and Multi-Agent Training Research

The emergence of ACN raises new training requirements. Research shows that multi-agent collaboration incurs high communication overhead (up to 15 times token consumption[14]) and suffers from low training efficiency. While offline MARL[15] and parameter sharing[16] make progress in multi-agent training, efficient individual agent training remains the foundation for scalable ACN deployment. This paper focuses on training optimization of individual Agentic RAG agents in ACN, laying the groundwork for multi-agent collaborative training.

2.4 Reinforcement Learning Improvement Algorithms

OHEM[17] and curriculum learning[18] emphasize "learnable yet challenging" samples. Decoupled clip and dynamic sampling policy optimization (DAPO)[19] integrates dynamic sampling, asymmetric clipping, and length penalties, achieving significant results in mathematical reasoning but potentially harming reasonable long-chain reasoning in Agentic RAG (e.g., HotpotQA). RLOO and REINFORCE++[20-21] improve performance from variance and robustness perspectives, while DPO and SimPO[22-23] simplify alignment through preference signals.

We propose DB-AW, introducing "difficulty-aware advantage weighting+batch filtering" at the batch level. Batch filtering draws inspiration from DAPO's zero-variance removal strategy but is tailored for Agentic RAG without imposing task-specific length penalties, therefore maintaining lightweight design and general applicability.

3 Methodology

We elaborate on DB-AW and improve training efficiency and sample utilization through batch-aware strategies within the GRPO framework. The core philosophy is to identify and filter ineffective training groups at the batch level while dynamically adjusting advantage weights based on sample difficulty, thereby directing learning toward learnable yet challenging samples and significantly improving training effectiveness without increasing computational overhead.

As shown in Fig. 1, DB-AW's complete training loop consists of five key stages: 1) data sampling and reward computa-

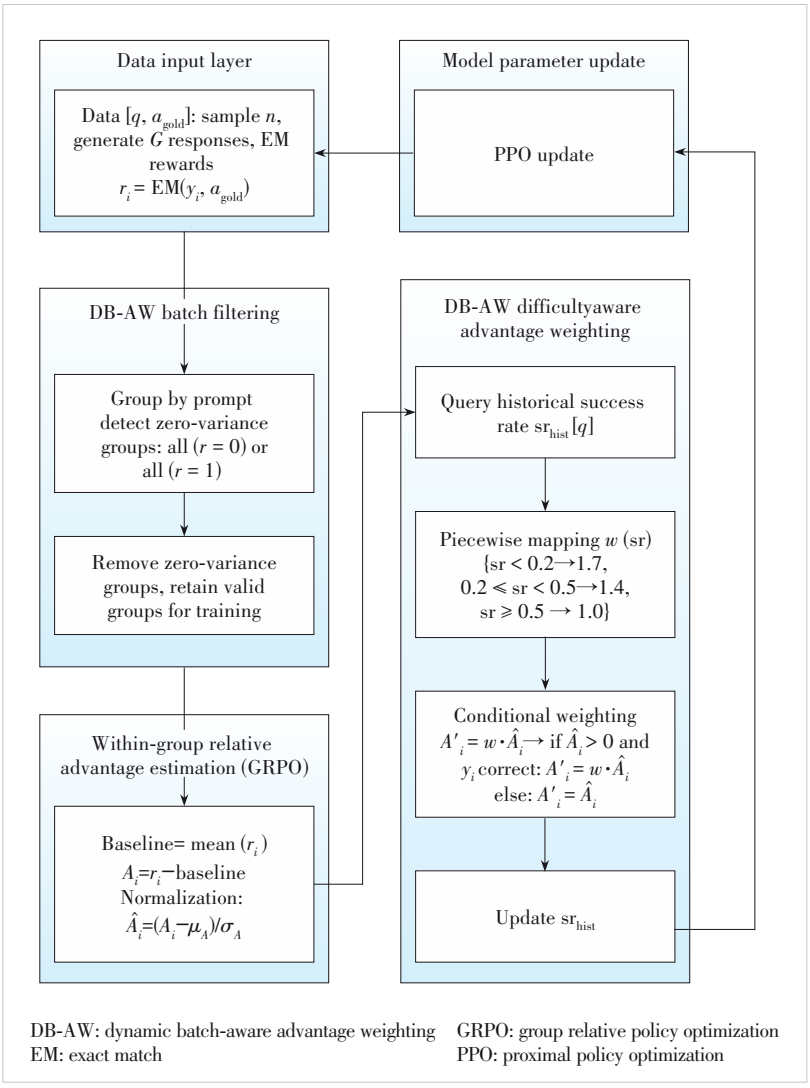

DB-AW: dynamic batch-aware advantage weighting
EM: exact match
GRPO: group relative policy optimization
PPO: proximal policy optimization

Figure 1. Overview of DB-AW training framework

tion; 2) batch filtering (Component 1), which removes zero-variance groups to ensure that each update contains effective gradient signals; 3) within-group advantage estimation, computing relative advantages following standard GRPO; 4) difficulty-aware weighting (Component 2), which dynamically amplifies positive advantages based on the prompt's long-term historical success rate; and 5) policy gradient update and history tracking, executing proximal policy optimization (PPO) updates using weighted advantages and statistic updates through exponential moving average (EMA).

The name DB-AW reflects three characteristics: "dynamic" refers to the dynamic adjustment of weights based on sample difficulty; "batch-aware" emphasizes batch-level optimization decisions; and "advantage weighting" indicates the method's final effect on GRPO's advantage estimation.

3.1 Problem Formulation and Base Algorithm: GRPO

1) Problem formulation: We formulate the Agentic RAG RL training task based on GRPO. Given an input sample x, the model generates interleaved structured tags: it reasons within <think> ⋯</think>; triggers retrieval through <tool call> {...} </tool call>; receives the reinjected result as <tool response>; and outputs the answer in <answer> ⋯ </answer>.

2) Loss masking: During training, we sample G responses per prompt. In all experiments, we set G = 4 due to the high interaction cost of multi-turn retrieval (each prompt requires multiple tool calls). We mask out external retrieval tokens in <tool response> and compute policy objectives only on model-generated tokens, avoiding meaningless fitting of retrieved text. In general, larger G can yield more stable group-relative advantage estimates but increases computation and tool usage.

3) Reward design: We adopt outcome-based sparse signals, using exact match (EM) as the sole outcome-based reward.

4) Relative advantages are calculated using the within-group mean as the baseline b = mean ($\{r_i\}$), and $A_i = r_i - b$. The objective function adopts GRPO's ratio clipping (PPO style, no value network) with KL regularization to monitor distribution drift.

3.2 DB-AW: Difficulty-Aware Advantage Weighting Component

1) Motivation: Dynamic weighting for learnable yet challenging samples improves sample efficiency. We adopt "weighting after within-group normalization", avoiding offset introduced by within-group de-meaning and normalization.

2) Method: Track the historical success rate sr_{hist} using the prompt key, updated via within-group average accuracy. Computation flow is shown as follows.

• Historical success rate tracking. We track sr_{hist} at the question (prompt) level using a $prompt_{key}$ (either a question ID if available, or a hash of normalized question text) as the unique identifier. The tracker is independent of retrieved evidence and random seeds.

• EMA update. After each training step, we compute $sr_{current}$ as the within-group mean accuracy for that prompt and update the tracker with an EMA: $sr_{hist}[prompt_{key}] \leftarrow \alpha\ sr_{current} + (1 - \alpha) \cdot sr_{hist}[prompt_{key}]$, where α defaults to 0.3 (recommended range: [0.2, 0.5]).

• Cold start. For a new $prompt_{key}$, we initialize sr_{hist} to 0.5, which maps to w = 1.0 (i. e., no re-weighting). Difficulty-

aware amplification is applied only after at least one update is observed for that prompt.

3) Design choice: We amplify only correct samples with positive standardized advantage. Our goal is to amplify the scarce, informative gradient signals that correspond to successful solutions on difficult prompts (e. g., sr < 0.2 for smaller backbones). These successes serve as high-quality demonstrations of correct retrieval and reasoning. We avoid additionally increasing penalties for failures on very hard prompts, which can make training unstable and overly conservative under sparse outcome rewards. Note that failed samples (reward = 0) still contribute their standard negative gradients via GRPO; DB-AW does not suppress error-correction signals. With a binary EM reward, we cannot distinguish "nearly correct" failures; finer-grained process rewards could address this and are left for future work.

a) Obtain within-group advantages $A_i = r_i - \text{mean}(\{r\})$;

b) Normalize $A^i = (A_i - \text{mean}(A))/\text{std}(A)$;

c) Compute weight w based on sr_{hist} (piecewise mapping): $\text{sr} < 0.2 \rightarrow w = 1.7$ (difficult); $0.2 \leqslant \text{sr} < 0.5 \rightarrow w = 1.4$ (medium); $\text{sr} \geqslant 0.5 \rightarrow w = 1.0$ (easy);

d) Weight only positive advantages of correct samples: if $A^i > 0$ and the sample is correct, then $A_i' = w \cdot A^i$; otherwise $A_i' = A^i$.

4) Rationale: With fixed rewards, we perform difficulty-aware scaling on advantages to shift the learning focus toward learnable samples near the competence frontier, alleviating advantage estimation bias under extreme distributions.

Algorithm 1. DB-AW: difficulty-aware advantage weighting component

Require: prompt x, group responses $\{y_i\}_{i=1}^{G}$, rewards $\{r_i\}_{i=1}^{G}$, historical success rate $\text{sr}_{\text{hist}}[x]_i$
Ensure: weighted advantages $\{A_i\}_{i=1}^{G}$
$\text{sr} < -\text{sr}_{\text{hist}}[x]$
return $\{A_i\}_{i=1}^{G}$
// Compute within-group advantages and normalization
baseline ← mean ($\{r_i\}$), $\mu_A \leftarrow 0$, $\sigma_A \leftarrow 1$
for $i = 1$ to G **do**
$A_i \leftarrow r_i -$ baseline
end for
$\mu_A \leftarrow$ mean ($\{A_i\}$), $\sigma_A \leftarrow$ std($\{A_i\}$)
for $i = 1$ to G **do**
$A_i \leftarrow (A_i - \mu_A)/\sigma_A$
end for
// Difficulty weight mapping
$\text{sr} \leftarrow \text{sr}_{\text{hist}}[x]$
if $\text{sr} < 0.2$ **then**
$w \leftarrow 1.7$ {difficult samples}
else if $\text{sr} < 0.5$ **then**
$w \leftarrow 1.4$ {medium difficulty}
else
$w \leftarrow 1.0$ {easy samples}
end if
// Weight positive advantages of correct samples
for $i = 1$ to G **do**
if $A_i > 0$ **and** y_i is correct **then**
$A_i' \leftarrow w \cdot A_i$
else
$A_i' \leftarrow A_i$
end if
end for
return $\{A_i'\}_{i=1}^{G}$

5) Filtering scope and distribution shift: Batch filtering is applied only within a single training step at the batch level. For each batch containing n prompts, each prompt forms a group of G responses (totaling $n \times G$ samples). If a prompt's group yields all-0 or all-1 rewards, it is skipped in the current update. This filtering is not persistent: the same prompt can be included in later steps if resampling yields mixed rewards, ensuring that extremely hard prompts are not permanently excluded. KL regularization further mitigates the forgetting of already-solved prompts (note that for $\text{sr} \geqslant 0.5$, we use $w = 1.0$).

6) Effective update rate: We define the effective update rate as the ratio of mixed-reward groups to total groups per training step, averaged across steps. By construction, filtering removes zero-variance groups, ensuring an effective update rate of 100% for DB-AW, while baseline GRPO can be substantially lower under sparse rewards.

3.3 DB-AW Batch Filtering Component

1) Motivation: Under group sampling, if within-group rewards are all 0 (all incorrect) or all 1 (all correct), gradient signals approach zero, wasting resources and reducing convergence speed. We adopt lightweight group-level filtering to address this.

2) Method: For G responses per prompt, if $\{r_i\}$ is all 0 or all 1, it is identified as a zero-gradient group and removed, retaining only non-zero variance groups for training. Filtering is executed after determining token-level rewards but before advantage estimation, allowing subsequent statistics to inherit non-zero gradient signals.

3) Rationale: By removing zero-variance groups, we ensure that each update contains non-zero gradient signals, avoiding ineffective computation and improving training efficiency.

Algorithm 2. DB-AW batch filtering component

Require: batch $B = \{(x_j, \{r_j, 1, r_j, 2, \cdots, r_j, G\})\}_j|_{=}^{B}|$
Ensure: filtered batch B'
$B' \leftarrow \varnothing$
for each prompt x_j in B **do**
rewards ← $\{r_j, 1, r_j, 2, \cdots, r_j, \text{G}\}$
if all (rewards == 0) **or** all (rewards == 1) **then**
continue {Skip zero-variance groups}
else

7: $B' \leftarrow B' \cup \{(x_j, \text{rewards})\}$ {Retain effective groups}
8: **end if**
9: **end for**
10: **return** B'

4 Experiments

We validate DB-AW's effectiveness on HotpotQA, NQ, and 2WikiMultihopQA. This section details the setup and comparison methods, presents the main results, including cross-model generalization and algorithm comparison, and provides an ablation study on component contributions and synergistic effects.

4.1 Experimental Setup

Datasets: HotpotQA (complex multi-hop reasoning), Natural Questions (open-domain QA), and 2WikiMultihopQA (structured multi-hop reasoning).

Research positioning: Considering the high computational cost of Agentic RAG RL training (where each round requires multiple group responses and search engine interactions), we conduct a controlled comparison on small-to-medium datasets (500/2 000 samples). Our research focuses on validating the proposed algorithmic mechanism's improvement relative to the baseline under the same resource constraints, not on pursuing absolute performance on large datasets.

Controlled experimental principles: All comparison methods use exactly the same datasets, training steps, and hyperparameter configurations, with fixed random seeds and multiple runs averaged. The main metric is Accuracy (strict EM), with unified decoding hyperparameters and retrieval budget.

4.2 Baselines and Variants

GRPO serves as the baseline. DAPO integrates four core technologies. DB-AW (Filtering Only) uses only batch filtering. DB-AW (Weighting Only) uses only difficulty-aware weighting. DB-AW (Full) has both components enabled.

4.3 Implementation Details

Models: Qwen2.5-3B-Instruct (main), Qwen2.5-7B-Instruct (larger version), and LLaMA3.2-3B-Instruct (different architecture). Configuration: n_agent=4 – 6, group size G = 4, and max turns = 3 – 4.

Training hyperparameters: lr = 1e-6, warmup ratio = 0.2 – 0.5, and Kullback-Leibler (KL) coefficient = 0.003 – 0.005.

Rewards and Evaluation: EM is used as the sole outcome-based reward. The main metric is Accuracy (strict EM).

4.4 Main Results

To validate DB-AW's effectiveness relative to mainstream RL methods, we compare the GRPO baseline, DAPO, and DB-AW (full) using the same dataset size and training steps across three models.

Algorithm effectiveness: DB-AW (Full) significantly outperforms GRPO and DAPO across all models and datasets. It achieves the highest relative improvement on Qwen2.5-7B (+18.2%), followed by Qwen2.5-3B (+17.2%) and LLaMA3.2-3B (+15.2%). In contrast, DAPO shows limited improvement (2.7% – 3.4%).

Cross-model generalization: DB-AW achieves significant improvements across all three models (15% – 18%), demonstrating robust generalization across varying parameter scales and model architectures.

DAPO applicability: DAPO's limited improvement suggests that its overlength penalty may hinder valid long-chain reasoning in Agentic RAG. In contrast, DB-AW focuses on two core components without task-specific penalties, thereby maintaining lightweight, general applicability while achieving superior performance.

4.5 Ablation Study

To evaluate component contributions and synergistic effects, we conduct an ablation study within the GRPO framework on Qwen2.5-3B-Instruct.

Accuracy Improvement: Weighting alone achieves a 13.8% improvement, filtering contributes +5.9%, and the full combination reaches +17.2%, indicating that the com-

Table 1. Main results: cross-model generalization (2 000 samples, validation accuracy)

Base Model	Method	HotpotQA	NQ	2Wiki	Avg	Improvement over GRPO
Qwen 2.5-3B	GRPO	0.23	0.49	0.15	0.290	-
	DAPO	0.25	0.49	0.16	0.300	+3.4%
	DB-AW (Full)	**0.31**	**0.53**	**0.19**	**0.340**	**+17.2%**
Qwen 2.5-7B	GRPO	0.25	0.52	0.17	0.313	-
	DAPO	0.27	0.52	0.18	0.323	+3.2%
	DB-AW (Full)	**0.33**	**0.57**	**0.21**	**0.370**	**+18.2%**
LLaMA 3.2-3B	GRPO	0.21	0.45	0.13	0.263	-
	DAPO	0.22	0.45	0.14	0.270	+2.7%
	DB-AW (Full)	**0.26**	**0.49**	**0.16**	**0.303**	**+15.2%**

DAPO: Decoupled Clip and Dynamic Sampling Policy Optimization
DB-AW: dynamic batch-aware advantage weighting
GRPO: group relative policy optimization

Table 2. Ablation study on Qwen2.5-3B-Instruct (2 000 samples, validation accuracy)

Configuration	HotpotQA	NQ	2Wiki	Avg
GRPO (baseline)	0.23	0.49	0.15	0.290
DB-AW (Filtering Only)	0.26	0.50	0.16	0.307 (+5.9%)
DB-AW (Weighting Only)	0.29	0.52	0.18	0.330 (+13.8%)
DB-AW (Full)	**0.31**	**0.53**	**0.19**	**0.340 (+17.2%)**

DB-AW: dynamic batch-aware advantage weighting

bined method outperforms either single component.

Training efficiency: Filtering significantly improves effective update steps by raising the non-zero gradient group ratio from 68% to 100%. Weighting directs focus toward learnable yet challenging samples through difficulty-aware amplification.

Component synergy: The full configuration (+17.2%) significantly exceeds the expected simple addition (≈+14%), indicating that batch filtering provides cleaner gradient signals for difficulty-aware weighting, while weighting enables more effective utilization of filtered samples, forming a virtuous cycle.

5 Conclusions

Addressing Agentic RAG RL training challenges in ACN, we propose DB-AW. Within the GRPO framework, DB-AW introduces two core components: difficulty-aware advantage weighting and batch filtering, which significantly reduce zero-gradient updates and increase the number of non-zero gradient updates per computation unit. Experiments show DB-AW achieves relative improvements of approximately 18%, 17%, and 15% on Qwen2.5-7B, Qwen2.5-3B, and LLaMA3.2-3B, respectively, validating its effectiveness and cross-model generalization.

DB-AW provides a practical pathway for efficient Agentic RAG training in ACN. Experiments show that DB-AW improves the effective update rate from 68% to 100% while maintaining performance, significantly reducing ineffective agent-environment interactions. This has important implications for scalable agent deployment in ACN:

1) Reduced training costs: Fewer ineffective interactions lead to less computational consumption, facilitating massively parallel agent training in ACN. In scenarios where ACN needs large-scale agent deployment, DB-AW's efficiency significantly reduces overall training overhead.

2) Accelerated agent evolution: Efficient training enables agents to quickly adapt to ACN's diverse task scenarios, improving the network's overall intelligence. By directing learning toward the competence frontier, DB-AW helps agents more rapidly enhance generalization on complex reasoning tasks.

3) Support for distributed extension: DB-AW's lightweight and reusable properties lay the foundation for multi-agent collaborative training extension. Batch filtering and difficulty-aware weighting can be conveniently migrated to distributed scenarios, supporting multi-agent knowledge sharing and experience transfer.

Future work is outlined as follows:

1) Multi-agent collaborative training extension: We will extend DB-AW to multi-agent collaborative training in ACN, investigating knowledge sharing and experience transfer mechanisms and exploring efficient gradient aggregation in distributed environments.

2) Larger-scale validation: While we have validated DB-AW on small-to-medium datasets (500/2 000 samples), future work can evaluate scalability and transferability on larger datasets (e.g., the full HotpotQA) and more ACN applications (e.g., intelligent customer service and network operations).

3) Dense reward design exploration: This paper focuses on simple EM-based outcome reward, without studying structured dense rewards such as format scores and process rewards. Future work should systematically explore the role of dense rewards, design principles, and their compatibility with advantage ranking in Agentic RAG RL.

References

[1] China Mobile. AI-Agent communication network white paper [R]. 2025
[2] Singh A, Ehtesham A, Kumar S, et al. Agentic retrieval-augmented generation: a survey on agentic RAG [PP/OL]. arXiv (2025-04-01) [2026-02-06]. https://arxiv.org/abs/2501.09136
[3] Yang Z L, Qi P, Zhang S Z, et al. HotpotQA: a dataset for diverse, explainable multi-hop question answering [PP/OL]. arXiv (2018-09-25) [2026-02-06]. https://arxiv.org/abs/1809.09600
[4] Ho X, Nguyen A K, Sugawara S, et al. Constructing a multi-hop QA dataset for comprehensive evaluation of reasoning steps [C]//The 28th International Conference on Computational Linguistics. International Committee on Computational Linguistics, 2020: 6609 – 6625. DOI: 10.18653/v1/2020.coling-main.580
[5] Trivedi H, Balasubramanian N, Khot T, et al. MuSiQue: multihop questions via single-hop question composition [J]. Transactions of the association for computational linguistics, 2022, 10: 539 – 554. DOI: 10.1162/tacl_a_00475
[6] Kwiatkowski T, Palomaki J, Redfield O, et al. Natural questions: a benchmark for question answering research [J]. Transactions of the association for computational linguistics, 2019, 7: 453 – 466. DOI: 10.1162/tacl_a_00276
[7] Yao S Y, Zhao J, Yu D, et al. ReAct: synergizing reasoning and acting in language models [PP/OL]. arXiv (2022-10-06) [2026-02-06]. https://arxiv.org/abs/2210.03629
[8] Asai A, Wu Z Q, Wang Y Z, et al. Self-RAG: learning to retrieve, generate, and critique through self- reflection [PP/OL]. arXiv (2023-10-17) [2026-02-06]. https://arxiv.org/abs/2310.11511
[9] Shinn N, Cassano F, Berman E, et al. Reflexion: language agents with verbal reinforcement learning [PP/OL]. arXiv (2023-03-20) [2026-02-06]. https://arxiv.org/abs/2303.11366
[10] Li X X, Dong G T, Jin J J, et al. Search-o1: agentic search-enhanced large reasoning models [PP/OL]. arXiv (2025-01-09) [2026-02-06]. https://arxiv.org/abs/2501.05366
[11] Shao Z H, Wang P Y, Zhu Q H, et al. DeepSeekMath: pushing the limits of mathematical reasoning in open language models [PP/OL]. arXiv (2024-02-05) [2026-02-06]. https://arxiv.org/abs/2402.03300
[12] Jin B W, Zeng H S, Yue Z R, et al. Search-R1: training LLMs to reason and leverage search engines with reinforcement learning [PP/OL]. arXiv (2025-03-12) [2026-02-06]. https://arxiv.org/abs/2503.09516
[13] Song H T, Jiang J H, Min Y Q, et al. R1-searcher: a novel two-stage outcome-based RL approach for search-enhanced large reasoning models [PP/OL]. arXiv (2025-03-12) [2026-02-06]. https://arxiv. org/abs/2503.05592
[14] Song Y, Ramaneti K, Sheikh Z, et al. Agent data protocol: unifying datasets for diverse, effective fine-tuning of LLM agents [PP/OL]. arXiv (2025-10-28) [2026-02-06]. https://arxiv.org/abs/2510.24702
[15] Eldeeb E, Alves H. Offline multi-agent reinforcement learning for 6G communications: fundamentals, applications and future directions [PP/

OL]. arXiv (2026-01-01) [2026-02-06]. https://arxiv. org/html/2601.00321v1
[16] Christianos F, Papoudakis G, Rahman M A, et al. Scaling multi-agent reinforcement learning with selective parameter sharing [C]//The 38th International Conference on Machine Learning. PMLR, 2021: 1989 – 1998
[17] Shrivastava A, Gupta A, Girshick R. Training region-based object detectors with online hard example mining [C]//Conference on Computer Vision and Pattern Recognition (CVPR). IEEE, 2016: 761 – 769. DOI: 10.1109/cvpr.2016.89
[18] Soviany P, Ionescu R T, Rota P, et al. Curriculum learning: a survey [J]. International journal of computer vision, 2022, 130(6): 1526 – 1565. DOI: 10.1007/s11263-022-01611-x
[19] Yu Q Y, Zhang Z, Zhu R F, et al. DAPO: an open-source LLM reinforcement learning system at scale [PP/OL]. arXiv (2025-03-18) [2026-02-06]. https://arxiv.org/abs/2503.14476
[20] Ahmadian A, Cremer C, Gallé M, et al. Back to basics: revisiting reinforce style optimization for learning from human feedback in LLMs [PP/OL]. arXiv (2024-02-26) [2026-02-06]. https://arxiv. org/abs/2402.14740
[21] Hu J, Liu J K, Xu H T, et al. REINFORCE++: an efficient RLHF algorithm with robustness to both prompt and reward models [PP/OL]. arXiv (2025-11-10) [2026-02-06]. https://arxiv.org/abs/2501.03262
[22] Rafailov R, Sharma A, Mitchell E, et al. Direct preference optimization: your language model is secretly a reward model [PP/OL]. arXiv (2024-07-29) [2026-02-06]. https://arxiv.org/abs/2305.18290
[23] Meng Y, Xia M Z, Chen D Q. SimPO: simple preference optimization with a reference-free reward [PP/OL]. arXiv (2024-05-23) [2026-02-06]. https://arxiv.org/abs/2405.14734
[24] Schulman J, Wolskie F, Dhariwal P, et al. Proximal policy optimization algorithms [PP/OL]. arXiv (2017-07-20) [2026-02-06]. https://arxiv.org/abs/1707.06347
[25] Cui G Q, Yuan L F, Wang Z F, et al. Process reinforcement through implicit rewards [PP/OL]. arXiv (2025-02-03) [2026-02-06]. https://arxiv.org/abs/2502.01456
[26] Zhang E C, Yan X G, Lin W, et al. Learning like humans: advancing LLM reasoning capabilities via adaptive difficulty curriculum learning and expert-guided self-reformulation [C]//The Conference on Empirical Methods in Natural Language Processing. ACL, 2025: 6630 – 6644. DOI: 10.18653/v1/2025.emnlp-main.336

Biographies

Chen Yu received his ME degree in computer science from Southeast University, China in 2017. He currently serves as an AI algorithm engineer at the AI Lab of AsiaInfo Technologies. He holds 3 patents. His research interests include LLMs, reinforcement learning for agents, RAG, multi-agent systems, and the application of AI in telecommunications and enterprise intelligence.

Li Fan is a senior engineer at China Unicom Beijing Branch. He received his ME degree from Beijing University of Posts and Telecommunications. His research interests include 4G/5G network optimization, mobile network digital operation, intelligentization of mobile communication networks, intelligent optimization and operation and maintenance, and emerging mobile communication technologies.

Wu Jie received her BE degree from South China Normal University, China. She currently serves as an AI project expert in the Digitalization Department of China United Network Communications Group Co., Ltd., Guangdong Branch. She holds one patent and multiple software copyrights. Her research interests focus on cutting-edge technologies in artificial intelligence including machine learning, natural language processing (NLP), and multi-modal agents, as well as the innovative application and project management of AI.

Gao Weipeng (gaowp@asiainfo.com) received his ME degree from Jiangnan University, China. He currently serves as an algorithm engineer at the AI Lab of AsiaInfo Technologies. His research interests focus on LLM fine-tuning, time series forecasting, intelligent root cause analysis, agent communication protocols, and intelligent system modeling and optimization.

Ouyang Ye is the Chief Executive Officer and Chief Technology Officer at AsiaInfo Technologies, Co., Ltd. He received his BE degree from Southeast University, China, MS degrees from Tufts University and Columbia University, USA, and his PhD from Stevens Institute of Technology, USA. He has extensive experience in large-scale team management and R&D innovation in the ICT field. He focuses on cross-domain innovation and the commercialization of technologies in cellular networks, AI, and data science. He is also a professor and an IEEE Fellow.

Internet of Agents: Design of the Protocol System

Fu Yuexia, Liu Peng, Lu Lu, Duan Xiaodong
(China Mobile Research Institute, Beijing 100053, China)

DOI: 10.12142/ZTECOM.202602005
https://kns.cnki.net/kcms/detail/34.1294.TN.20260429.1856.004.html, published online April 30, 2026
Manuscript received: 2026-03-11

Abstract: With the rapid advancement of generative artificial intelligence (AI) and large language model (LLM) technologies, AI agents are gradually becoming the core service units in networks, and their communication mode is evolving from local collaboration to wide-area interconnection. The construction of the Internet of Agents (IoA) faces multiple challenges, such as identity management, dynamic networking, and semantic routing, which urgently requires the design of a network protocol system that adapts to its new traffic characteristics and collaboration needs. Based on the application scenarios of agent communication, this paper systematically analyzes the management, control, and routing requirements that multi-agent collaboration imposes on IP networks, proposes a three-layer functional architecture for the IoA, and designs a protocol suite covering management, control, and routing around key issues such as agent registration and identification, service discovery, capability sensing, and cross-domain traffic assurance. By extending existing Internet protocols and introducing a semantically aware routing mechanism, this paper provides a scalable, efficient, and secure approach to implementing a protocol for end-to-end agent collaboration, thereby contributing to the construction of an open, large-scale agent collaboration ecosystem.

Keywords: Internet of Agents; user agent; service agent; protocol framework

Citation (Format 1): Fu Y X, Liu P, Lu L, et al. Internet of agents: design of the protocol system [J]. ZTE Communications, 2026, 24(2): 33 - 42. DOI: 10.12142/ZTECOM.202602005
Citation (Format 2): Y. X. Fu, P. Liu, L. Lu, et al., "Internet of agents: design of the protocol system," *ZTE Communications*, vol. 24, no. 2, pp. 33 - 42, Jun. 2026. doi: 10.12142/ZTECOM.202602005.

1 Introduction

With the breakthrough in large language model (LLM) technology, LLM-based agents have demonstrated excellent autonomous perception, decision-making, and action capabilities across various tasks and are regarded as one of the important paths to achieve artificial general intelligence (AGI). While a single agent can handle specific tasks independently, complex scenarios often require the collaboration of multiple heterogeneous agents. The core challenge then lies in how to achieve efficient and reliable organization and interaction among these agents. This makes the Internet of Agents (IoA) protocol a key enabling technology.

Agent protocols are mainly divided into two categories. One is the agent interaction protocol, which is used to standardize the structured communication and collaboration mechanisms between agents[1 - 3]. For example, Anthropic's Model Context Protocol (MCP) focuses on the interaction between agents and external tools, while Agent Network Protocol (ANP), Agent-to-Agent (A2A), Agora, etc., are mainly oriented to direct communication and task coordination between agents[4 - 7]. Such protocols define message formats, session processes, and security rules, enabling multi-agent systems to achieve task allocation, knowledge sharing, and joint reasoning. The other is the agent network Internet protocol, which is responsible for connecting distributed agents in physical or virtual networks, and its foundation is the Transmission Control Protocol/Internet Protocol (TCP/IP) system and related underlying protocols, such as Wi-Fi, Ethernet, and Border Gateway Protocol/Interior Gateway Protocol (BGP/IGP) routing protocols[8 - 10]. With the development of agent applications towards real-time, collaborative, and cross-domain directions, the existing Internet architecture faces new requirements in terms of delay, reliability, and resource customization, promoting the continuous evolution of network layer protocols.

Nevertheless, most existing agent interaction protocols, including MCP, A2A, ANP, and Agora, focus on message exchange, tool invocation, and point-to-point coordination, while lacking unified specifications for agent service capability identifiers, agent capability sensing, task-driven network-

This work is supported by the National Key R&D Program of China under Grant No. 2024YFB2906701.

ing, and capability-oriented semantic routing. They rely heavily on traditional network addressing and lack support for semantic discovery, decentralized trust, and secure cross-domain scheduling in open, large-scale environments. The framework proposed in this paper comprises capability identification, capability control and management, and semantic routing as core components, which can effectively address the deficiencies of current protocols and be applied across different agent service providers and multiple domains. The standardization and optimization of the IoA protocol will be an important foundation for realizing a large-scale and open agent collaboration ecosystem.

The wide-area interconnection of agents may give rise to new behaviors such as message traffic management and transmission-reception control, thereby triggering new changes in Internet address naming, message forwarding, traffic control, and other aspects. Research on the IoA has emerged at home and abroad. Ref. [11] proposes that the IoA will be built based on cloud networks, with the bottom layer supported by the basic Internet, and looks forward to various types of agents relying on the Internet for interconnection and collaboration to complete tasks; Ref. [12] defines the concept of the IoA, proposes its architecture, including resource layer, management layer, collaboration layer, service layer, and user layer, and conceives five types of application scenarios and processes of the IoA.

On the basis of recent work, this paper further analyzes the protocol design challenges of the IoA, proposes a method for classifying agents into user agents and service agents, puts forward the protocol framework, and introduces the design of related key protocols, providing a reference for further application and promotion of the IoA.

2 Protocol Design Requirements for the Internet of Agents

With the development of AI agent technology, the independent work of single agents, local collaboration, and wide-area collaboration will become the mainstream interconnection modes, supporting various scenarios from personal tasks to cross-domain collaboration. The large-scale hybrid networking of physical and software agents will pose new systematic requirements for the management, control, and routing systems of the existing Internet.

The first is the agent management requirement, whose core is to realize unified identity management and full-life-cycle supervision. AI agents can be divided into user agents (which act on behalf of users to perform tasks) and service agents (which provide functions or services), and a unified registration and identification system should be established to be compatible with multi-source heterogeneous agents. The key points include standardized identification and registration of capabilities, performance monitoring and reliability assurance, and a charging mechanism for service calls and resource consumption.

The second is the IoA control requirement, which focuses on dynamically adaptive and policy-driven collaboration scheduling. To support flexible and secure collaboration, it is necessary to realize real-time discovery of capabilities and services, sensing of the status and load of service agents, dynamic networking, and fine-grained definition and cross-domain synchronization of user agent permissions, so as to ensure task-driven adaptive collaboration.

The third is the IoA routing requirement, which needs to realize semantically aware and differentiated traffic assurance. The new type of "implicit traffic" generated by the autonomous interaction of agents requires the routing mechanism to go beyond the traditional address-based strategy, support dynamic routing based on capabilities and task content, and integrate multiple forwarding methods such as unicast, anycast, and multicast. At the same time, it is necessary to distinguish between user-service interaction traffic and inter-service collaboration traffic, and implement intelligent scheduling and collaborative management according to their differences in bandwidth, delay, packet loss, etc.

3 Protocol Framework of the Internet of Agents

The IoA is a new type of overlay network built based on the IP network for agent interconnection, which meets the needs of flexible networking, autonomous communication, massive concurrency, etc., between agents. Based on the IoA architecture[13], this paper proposes a protocol view, which serves as the basis for the construction and implementation of its core protocols. Considering various factors such as the service object, main function, and permission of agents, this paper classifies agents into two categories: user agents and service agents.

The user agent parses the user's service intentions, automatically executes subsequent operations for the user, and interacts with other agents on behalf of the user, enabling the user to be unaware of the implementation details. Limited by human interaction, the interaction frequency is relatively low, and the traffic is mainly used for interaction instructions and execution results. The current Internet protocols can be adopted, and the information transmission content includes the instructions issued by users to agents and the feedback results of agents. In addition, such agents often form a deeply bound relationship with users, so authentication and authorization only occur in the early stage of establishing the relationship and regularly in the later stage, with a low frequency.

The service agent is mainly responsible for providing specific services, and interacts with user agents about service demand information, service execution result information, etc. Service agents need to register the services and capabilities they provide in the network for discovery and invocation by other agents. Their traffic is mainly the interac-

tion information between agents, including instructions, information, etc., and special protocols for inter-agent communication are adopted, including identification, addressing, etc. In addition, due to the task-driven agent collaborative networking, the initial authentication and authorization need to be triggered after each task group is established, so the authentication and authorization between service agents will be more frequent.

To meet the needs of agent identification, discovery, collaboration, and networking, the IoA protocol framework, which combines the networking view and architecture view, is divided into three major protocol suites: IoA Management Protocol, IoA Control Protocol, and IoA Routing Protocol, as shown in Fig. 1.

The IoA Management Protocol enables agents to interact with three types of platforms. First, they interact with the unified registration platform during network access registration to obtain agent identification information. Second, they interact with the unified service registration to register agent service capability information and its enabling information. Third, they interact with the management platform that obtains the performance information provided by services to evaluate the historical performance information of agent services. There are two kinds of identifiers in IoA: one is the agent identifier, used to identify the agent; the other is the agent service capability identifier, used to identify the agent service capability. Both identifiers need to be unified and verifiable. The IoA Management Protocol also includes protocols such as agent service orchestration, agent service operation, and agent service charging, supports the new task-based charging for agents, constructs an agent service evaluation system to support the performance and reputation evaluation of various agent service capabilities, and provides an agent capability exposure protocol to provide a unified capability calling platform, serving as a unified service operation entrance for agent users.

The IoA Control Protocol is used to support the sensing of agent service capability status. At the same time, it supports centralized agent service discovery to obtain information of agents participating in collaboration; supports task-driven networking implementation of multiple agents and performs traffic engineering according to service requirements. In addition, considering the implementation of multi-sessions between multiple agents, a transmission control protocol is used to ensure the transmission quality between multiple agents. Moreover, the control protocol can realize unified identification distribution, service discovery, networking routing, and other capabilities regardless of the access methods, supporting the agent communication requirements of 6G network and the integrated access and services under the trend of space-air-ground integration.

The IoA Routing Protocol is used to support the routing and forwarding of data between agents, including the intra-domain and inter-domain routing and forwarding protocols. It supports the semantic routing protocol based on the agent service capability identifier. It needs to support the adaptive routing protocol for multiple access methods such as mobile access, fixed access, and satellite access, which can realize the integrated and unified access of various access methods. In addition, it needs to support multi-modal routing protocols for voice, text, video, etc.

Based on the characteristics of the information to be transmitted by user agents and service agents, their service objects, and networking situations, Table 1 analyzes the demand characteristics of the two types of agents for management protocols, control protocols, and routing protocols.

4 Management Protocol Design for the Internet of Agents

4.1 Agent Registration and Identification Protocol

Both user agents and service agents require unified identification, but their capability types, registration information, permission information, and dependent trust roots are differ-

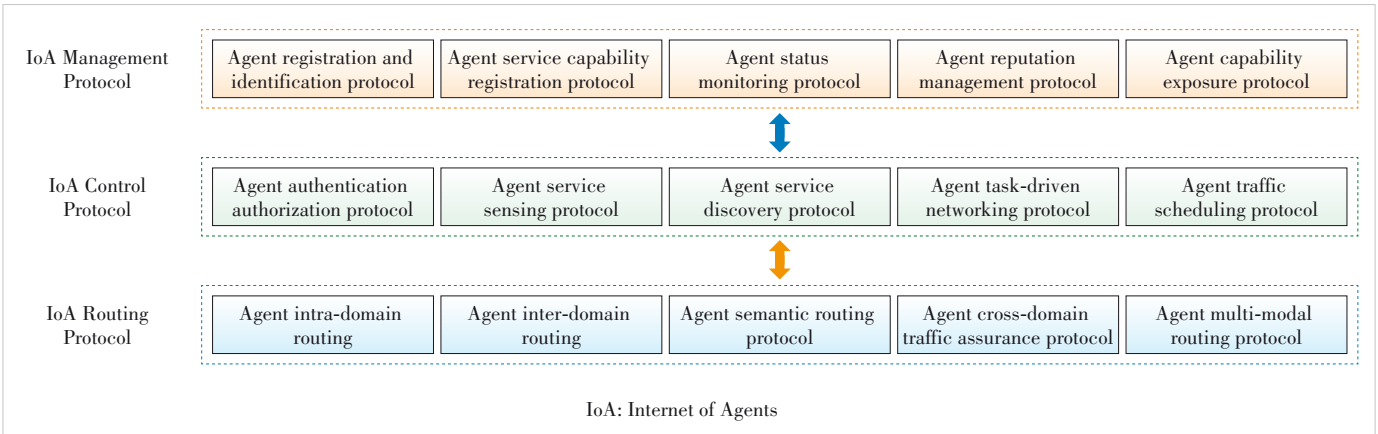

Figure 1. Protocol framework of the IoA

Table 1. Analysis of protocol requirements for user agents and service agents

Protocol Category	Specific Protocol	User Agent	Service Agent
IoA Management Protocol	Registration and Identification Protocol; Service Registration Protocol	Distribution of user agent identification information; association of user binding information	Distribution of service agent identification information and agent service capability identification information; registration and update of capability identification information
	Status Monitoring Protocol; Reputation Management Protocol	More direct user perception; demand for fixed-duration charging	Demand for service performance monitoring; task-based charging
IoA Control Protocol	Authentication and Authorization Protocol	Low frequency; consideration of user permission information	High frequency; consideration of agent service capability information and task group information
	Service Discovery Protocol	Small selection range, simple discovery mechanism; relatively fixed association with users	Large selection range; discovery based on service identification, combined with performance for optimization
	Service Sensing Protocol	Simple sensing information; infrequent status changes	Complex sensing information; frequent status changes
	Task-Driven Networking Protocol	Networking with users: local area, static network; networking among user agents: driven by multi-user collaboration, relatively static networking	Networking among service agents: task-driven networking, multi-agent networking; involving cross-domain networking
IoA Routing Protocol	Semantic Routing Protocol	Supporting IP-based routing and agent service capability identifier-based routing	Supporting IP-based routing and agent service capability identifier-based routing
	Cross-domain Traffic Assurance Protocol	Intra-domain routing	Inter-domain routing; demand for traffic engineering
	Multi-Modal Routing Protocol	Mainly transmitting interaction information between humans and agents, and task results of service agents	Mainly transmitting instructions, task related information, multi-modal, etc., among agents

IoA: Internet of Agents

ent. In the initial access and registration management stage, the management of user agents focuses on unified identity management, association with the affiliated user, and permission authentication, laying a foundation for subsequent service access and charging; the management of service agents focuses on service registration, service capability access verification, and maintenance of service capability dependency relationships, laying a foundation for subsequent service capability discovery and supply.

As shown in Fig. 2, user agents obtain identifiers assigned by the network operator they access through association with the user. User agents of different operators establish trust relationships through operators and follow a unified identification mechanism; service agents obtain identifiers assigned by their respective agent service providers. Service agents of different service providers establish trust relationships through the service providers and follow a unified identification mechanism; in addition, operators and service providers will also establish trust relationships, thereby enabling user agents across operators and service agents across service providers to establish trust relationships and realize the uniqueness and verifiability of identifiers.

As shown in Fig. 3, the access network operator issues a unified registration template to the user agent. After the user agent reports information according to the registration template, identifier distribution is carried out. In addition, after obtaining the identifier of the user agent, it is necessary to establish a binding relationship with the user and report information of the user agent, such as user association information, valid time, permission information, user agent type, and location information. Considering the security and privacy of user information, the relevant sensitive information is uniformly maintained by the access network operator. A new type of user agent registration template information can be defined. The issuance of such registration templates can be realized by extending existing registration protocols (e.g., Netconf), or a new user agent registration protocol can be defined to realize the flexible issuance and interaction of registration templates.

In addition, when the enabling information of the user agent or the associated user information changes (such as a current fault that makes it unable to provide services or changes in the bound user information), it is necessary to

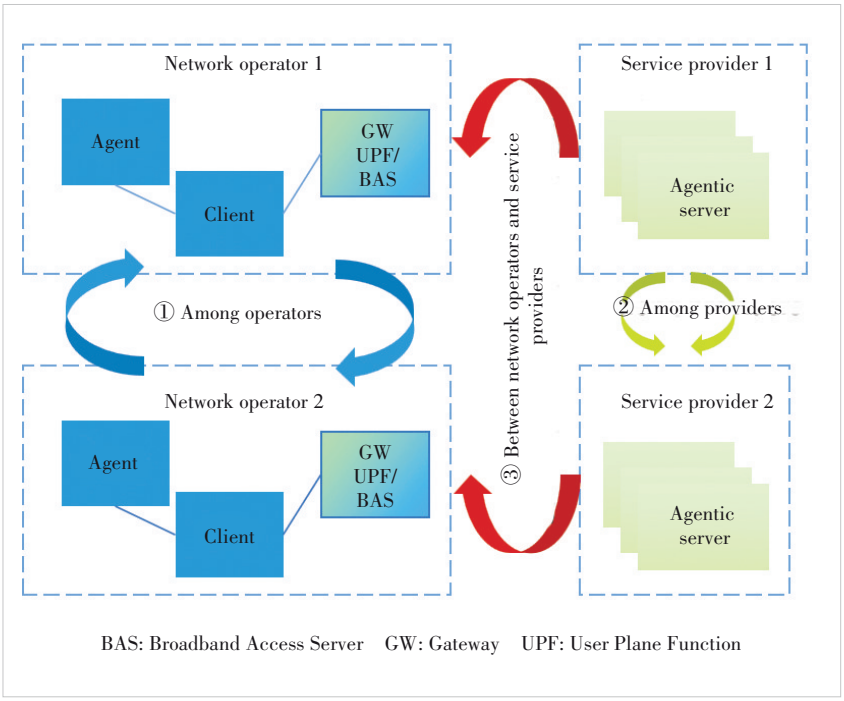

Figure 2. Classification view of agents in the IoA

synchronize the changes to the registration platform in a timely manner. A new type of update management message can be defined to update the changes in the attribute information of registered agents.

Service agents can be uniformly assigned agent identifiers by various agent service providers, which issue unified registration templates to the service agents. After the service agents report information according to the registration templates, identifier distribution is carried out. Optionally, a new type of service agent registration template can be defined, and its issuance can be realized by extending existing registration protocols, e.g., by extending interfaces based on the Representational State Transfer (REST) over HTTP. Various service agents establish mutual trust through service providers and maintain capability registration and verification information.

On the other hand, in addition to considering the identifier allocation for newly added agents, it is also necessary to support the identifier recovery mechanism for existing agents. For example, when an agent goes offline and no longer provides services, to ensure the effective allocation and utilization of identifiers, a new type of withdrawal message can be defined to recover the identifier of the agent for subsequent distribution.

4.2 Agent Service Capability Registration Protocol

After the initial identifier allocation of agents is completed, it is necessary to maintain the global agent service capability view of user agents and service agents in real time. Agents' services can be divided into two categories: self-services and open services[13]. Self-services can be used for agent maintenance, management, monitoring, etc., and are called by the registration or management platforms; open services are based on unified agent service capability identifiers to identify the same type of agent service capabilities.

Based on the unified identifiers of service agents, the initial registration and dynamic update of agent service capabilities need to be carried out. The service agent initiates a service capability registration request to the capability exposure platform, and the capability exposure platform sends an information template required for registration. According to the unified template, when registering service capabilities, the service agent needs to carry the agent identifier, IP address, service capability list, service capability binding information, and agent service capability dependency relationships, among which:

• Agent service capability binding information: This information is used to distinguish whether the agent service capability is an exclusive agent service capability or a shared agent service capability. It can be registered in the capability exposure platform. For example, if it is an exclusive service capability, its current binding relationship needs to be registered with no need to maintain its performance information, and the duration of the exclusive service capability can be further registered; if it is a shared service capability, its performance information needs to be main-

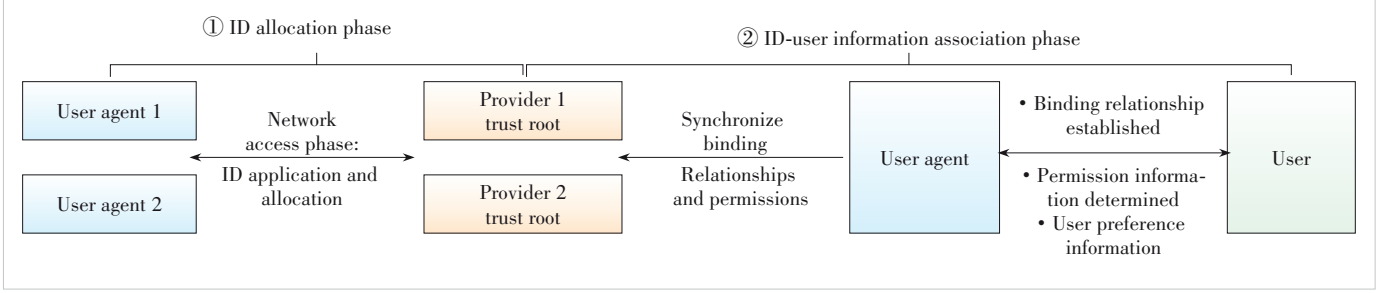

Figure 3. Registration diagram of user agents

tained in the later stage.

• Agent service capability dependency relationships: These are dependency relationships between some agent service capabilities, that is, the current service capability must cooperate with specific service capabilities to complete specific services. The dependency relationships need to be registered in the unified capability platform for reference when querying and discovering agent service capabilities.

As for the agent service capability identifier allocation, a standardized method for the identifier needs to be adopted. For different types of agent service capabilities, different metrics may be needed. The name space of the identifier employs a hierarchical, globally unique, and semantically extensible structured design compliant with unified agent capability identifier specifications, which explicitly characterizes the domain, capability type, interface version, and security attributes of agent service capabilities. Furthermore, a distributed trusted registration and resolution mechanism can be adopted to achieve dynamic identifier allocation, conflict detection, access control, and version evolution.

The capability exposure platform completes the agent service capability registration after verifying the identification information of the service agent. The above process can be realized by extending the interaction based on existing protocols, such as via the RESTful interface over HTTP, or by defining a new service capability registration and update protocol to implement processes such as service capability addition, update, and deletion. The capability exposure platform further generates a service capability information database based on the dimension of agent service capabilities. However, agent service capabilities may be added, deleted, or experience performance changes, so the service capability information needs to be updated, which can be realized through periodic, trigger-based, or active subscription methods. In a specific implementation, the network side can consider the popularity of the service capability demand on the request side and subscribe to updates for service capabilities with high popularity; or consider whether there is additional payment, and for paid agent capabilities, subscribe to update information.

• Periodic update: It only synchronizes the information of newly added/deleted agent service capabilities, and regularly synchronizes with the capability management platform.

• Trigger-based update: It only synchronizes the information of newly added/deleted agent service capabilities, or actively updates to the management platform when their service capability binding relationships change.

• Subscription-based update: The capability management platform can subscribe to the target service capability update information from the agent, and specify to receive active updates of agent service capabilities of specific types.

5 Control Protocol for the Internet of Agents

5.1 Agent Service Discovery Protocol

How to quickly and accurately discover suitable agents for task collaboration is an important issue in IoA. For the discovery of agent service capabilities, two technical routes have emerged currently: based on existing Internet infrastructure or building a new agent discovery mechanism.

Route 1: Build a new mechanism to obtain the agent identifier and agent IP, respectively, which can flexibly discover the required agent service capabilities without modifying the current infrastructure.

Route 2: Reuse the Domain Name System (DNS)[8] capability, initiate an "agent domain name request" to directly obtain the Agent IP, reuse the dynamic resolution and hierarchical mechanism of DNS, and require little modification on the user side; however, it needs to rely on DNS for ultra-large concurrent dynamic service discovery, as shown in Fig. 4.

As for Route 2, when a task request is initiated to the agent proxy, the proxy decomposes the instruction into multiple subservices and needs to connect to the corresponding service agents. The agent needs to initiate a DNS request based on the unified agent service capability identifier to achieve dynamic mapping from it to the IP address. This involves enhancing multiple functionalities, including the unified agent service capability identifier, adding agent service query and response packets, a hierarchical DNS mechanism, and dynamic resolution mapping.

Unified agent service "domain name": The unified agent service "domain name" could design identifiers similar to "domain name" to identify different agent service capabilities. Compatibility with the current system needs to be considered, and one alternative method could be considered: adding new information resource records based on the agent service "domain name" to store the mapping relationship between the agent service "domain name" and IP addresses. In this case, as shown in Fig. 5, a new fully qualified domain name (FQDN) can be defined, for example, based on a URL; a new type is defined to identify this as an agent service re-

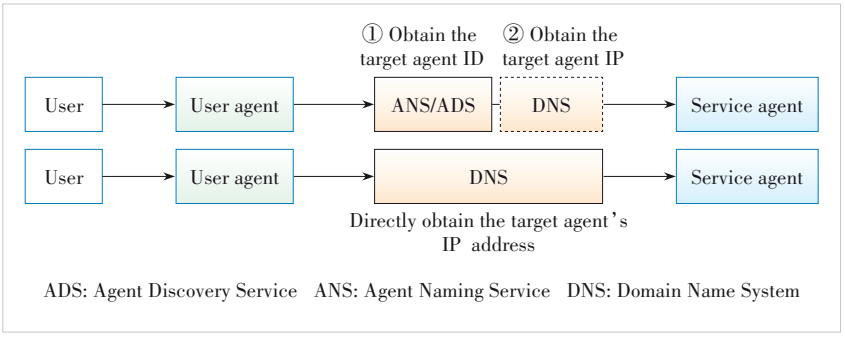

Figure 4. Two routes of agent service discovery

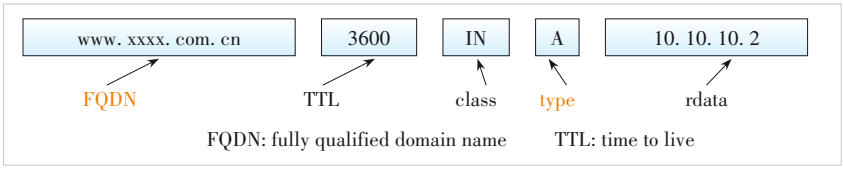

Figure 5. Example of the format of DNS domain name resource record

cord; the class defines whether the agent service capability identifier is for the local area or the Internet. The DNS reads the FQDN of the query packet and the packet type to determine whether it needs to query the information resource record of the corresponding agent service capability identifier.

Agent service query and response packets: New DNS query packet and response packet types can be introduced to identify the DNS request initiated by the agent, and to consider a DNS-side authentication mechanism that determines whether the current agent has permission to initiate a query. One alternative method is shown below:

• Identify the DNS message type, which can carry information in the Opcode field or Z field of the DNS message header, as shown in Table 2.

• When sending updates, send one or more update messages to the local DNS, with QCOUNT=0 (the number of questions) and ACOUNT (the number of answers) ⩾ 1; multiple agent service query information can be carried.

Hierarchical DNS mechanism: To improve response and resolution speed, agent service "domain name" resolution can also be carried out hierarchically and regionally, supporting the local DNS to store mapping information of nearby agent service capability identifiers, ensuring the stability and scalability of domain name resolution. The freshness and hit rate of locally cached mapping information need to be optimized using the AI/machine learning (ML) methods.

Dynamic resolution mapping: The DNS reads whether the query packet carries additional demand information, such as agent selection preferences (e. g., requesting an agent from the same agent provider), and whether there are capability dependency relationships to define priorities. In addition, agent capability performance information can be maintained, and selection can be made by combining demand information, geographical location, preference requirements, etc. The demand information translation and the mapping process need to consider multi-dimensional information, which may require the integration of AI and ML into these functionalities to improve accuracy and resolution performance.

The Agent Service Discovery Protocol adopts a centralized or DNS-like architecture for identifier-to-location resolution, emphasizing unified control and good compatibility, making it suitable for intra-domain, controllable and relatively static agent discovery.

Table 2. Format of DNS message header

Field	Description
QR (1 bit)	Query/response flag; 0 for query, 1 for response
Opcode (4 bit)	Operation code; 0 for standard query, 1 for reverse query, 2 for server status request; others are reserved bits
AA, TC, RD, RA	Refer to RFC 1035[14] for definitions
Z	Reserved bits
QCOUNT	Number of questions
ACOUNT	Number of answers

AA: authoritative answer flag RA: recursion available flag TC: truncated flag
DNS: Domain Name System RD: recursion desired flag

5.2 Agent Service Sensing Protocol

Considering that different users may have different requirements for the same type of agent service capability (e.g., recognition accuracy, response delay, preference for agents with a higher number of service occurrences, and agents with good service records), it is necessary to obtain the performance information of agent service capabilities to achieve differentiated matching.

Different grading dimensions of agent service capabilities can be determined according to different types of capabilities, such as capability response delay, capability response accuracy, maximum concurrent service number, capability calling cost, performance stability, and historical performance level. First, according to the agent service capability binding information, the list of currently available shared agent service capabilities is screened.

Two sensing methods, active performance reporting or on-demand pulling, can be supported, which can be realized through the RESTful interface with HTTP, etc.

When a capability actively reports performance information to the capability control platform, it can be registered at the new capability registration stage. Three methods of obtaining capability performance information can be supported: periodic, trigger-based, or active subscription.

• For the periodic acquisition method, different cycles can be set according to the service type: a longer cycle is set for long-term service agents, and a shorter cycle is set for short-term service agents.

• The trigger-based update method triggers an update when the agent capability change reaches a certain threshold. Different thresholds can be set according to the service type, such as a lower threshold for performance-sensitive agents and a higher threshold for performance-insensitive agents.

• The subscription-based update method allows the capability control platform to subscribe to target capability update information from the agent and specify to receive timely updates of the agent capabilities of specific capability types.

To save the maintenance cost of performance information,

the capability control platform can first maintain the capability list information. When a user requests a certain agent service capability, the platform can be triggered to actively initiate a capability performance query request to the corresponding agent service capability list. After receiving the performance information fed back by all capabilities in the capability list, further screening is carried out in combination with user requirements. Alternatively, the user's performance requirements are first extracted to generate a capability list, and after the capabilities in the capability list receive the demand information, they locally judge whether they meet the demand. If so, they return the specific capability performance information to the capability control platform.

In practice, agent service sensing can be performed by agent service providers with their own controllers and the required status information is then synchronized to the controller of the IoA. In this case, the interfaces between the controller of the IoA and other agent service providers are essential.

5.3 Agent Task-Driven Networking Protocol

Considering that when the performance of an agent deteriorates or a fault occurs, triggering a service agent to switch to a new agent requires the agent task proxy to initiate a new agent service discovery process and to carry additional information, such as the address information of the peer agent for collaboration. Before and after the switch, the agents perform the required context synchronization using task group identification information, service capability identifier, etc.

Therefore, during the agent task execution process, it is necessary to introduce an agent task status monitoring protocol to monitor the current agent's session connection status (including network status) with other agents, as well as the status of each agent, such as service response delay and uplink and downlink rates. When the network status information or agent status information deteriorates to a preset threshold, the switch process is triggered. The agent proxy then re-initiates a service discovery request and additionally carries demand information, which includes the target agent capability identification information, address information (which can carry the address information of the peer agent interconnected with the agent), etc.

The agent proxy receives the new agent information and synchronizes it to the relevant interconnected agents, re-establishing a session connection for task collaboration. When the agent service discovery function receives a new service discovery request, it re-selects a new agent in combination with the additional demand information, which could be carried via the extension of the DNS packet as shown in Fig. 6. To ensure the service continuity, the agent proxy issues an application synchronization instruction to the two agents. The synchronization instruction includes: the identifier of the other agent, task identifier, and agent service capability identifier. The old and new agents then negotiate and confirm the information to be synchronized, including the task identifier and agent service capability identifier. After verification, the information synchronization starts.

Furthermore, to improve the service efficiency of agents during multi-agent collaboration, if an agent completes the task it is responsible for, it can flexibly exit the task group in advance. To ensure the performance of the original task after such an early exit, the agent can add a new intermediate state, which is a transition state. In this state, the current agent can accept new task requests while still retaining the relevant information and context of the original task. The scheduling priority of agents in the transition state is higher than that of occupied agents and lower than that of idle agents. This can realize more efficient scheduling and utilization of each agent, make full use of the capabilities of each agent, and allows more users to be served.

6 Routing Protocol for the Internet of Agents

6.1 Agent Semantic Routing Protocol

Considering the agent service capability discovery mechanism, agent routing can be based on traditional routing systems, supporting flexible task group construction and multiple routing mechanisms such as unicast, anycast, and multicast. By supporting the agent routing protocol based on the agent service capability identifier, service discovery based on agent capabilities can be realized. A candidate list of agents that can provide services is searched through the agent service capability identifier, and the target agent is then determined in a distributed manner according to other dimensions.

By extending the computing-aware traffic steering routing protocol[15], a capability-aware agent routing mechanism can be realized. By advertising the supported capability information in the network, the anycast mechanism based on the

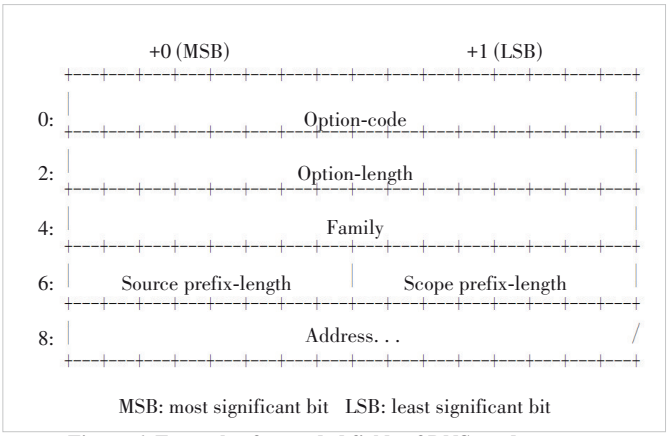

Figure 6. Example of extended fields of DNS used to carry demand information

agent service capability identifier could be realized. The agent proxy only needs to carry the target agent service capability identifier, and the entry gateway selects the optimal capability for it by combining location information, capability information, demand information, etc., which can ensure real-time and dynamic distributed capability discovery.

In addition, the agent routing protocol needs to support flexible task-oriented networking and construct a new task-based routing table. A collective communication group can be created based on the published task requirements to complete agent team formation, and further adaptively complete the task tree construction. According to the task tree, task release operator functions such as multicast broadcast and scatter are performed, and task execution results are summarized based on operators such as "gather" or "reduce" to achieve distributed task collaboration.

The Agent Semantic Routing Protocol is used in distributed agent collaboration scenarios, enabling related agents to discover target capabilities within a limited controlled scope. It performs capability-based routing directly via agent service capability identifiers in a decentralized manner, with high scalability and dynamics, and is more applicable to open, multi-domain, large-scale and dynamic agent interconnection scenarios.

6.2 Agent Cross-Domain Traffic Assurance Protocol

The agent wide-area Internet will bring a new traffic pattern. Different from the traditional client-server (C-S) communication traffic pattern, in the agent-centered traffic pattern, communication between agents may trigger call traffic between agents and tool libraries, introducing implicit traffic[13]. This may evolve into multi-segment traffic between agents, as well as between agents and tool libraries, among others. Therefore, the routing protocol needs to optimize such multi-segment traffic between agents, between agents and tool libraries, etc., in the same agent task to ensure unified service level agreement (SLA) assurance and to prevent the performance of any single traffic segment from affecting the overall task performance.

For the same service agent, when it interacts with different service agents, there may be different SLA assurance requirements. Therefore, it is necessary to adjust the SLA requirements for interacting with the peer agent and the corresponding tools according to the performance requirements of the different tasks in which the agent is involved. The SRv6 policy can be extended. The SRv6 controller identifies different segment sessions based on the network policy, performs session SLA association, and maps them to different policies. When the current agent interacts with other agents, if agent-invoked API traffic is introduced, the new session (identified by the agent-agent session) is maintained with the same priority as the current session. This can be identified by a triplet: the policy is uniquely identified by <Head end, Color, Endpoint>. The Endpoint can represent multiple destinations sharing the same policy group, supporting cross-domain traffic scheduling and ensuring that multi-segment sessions run under the same policy framework.

In addition, a single agent may establish connections with multiple agents at the same time to conduct sessions. Therefore, there is resource competition between multiple sessions of a single agent, including competition for network, computing and storage resources. It is necessary to clarify the priority of sessions and conduct resource planning for a single agent. Different types of agent sessions will correspond to different types of traffic. For short-term high-frequency traffic and long-term low-frequency large-data traffic, agents can negotiate different communication protocols. Therefore, a single agent needs to support the ability to adapt to different protocols and to support the simultaneous operation of different protocols.

7 Security Considerations

The introduction of agents brings new security and privacy challenges, including fake agent capability registration, discovery poisoning, performance signal spoofing, cross-domain trust issues, malicious identity spoofing, unauthorized service invocation, semantic routing hijacking, privacy leakage during capability discovery, and model or data attacks. These threats severely hinder the compliance of service calls and privacy protection of data interactions, which are crucial for building an open collaborative ecosystem. To address these issues, future research should focus on several key directions: developing trust evaluation and dynamic access control mechanisms for agent capabilities, designing decentralized cross-domain authentication and authorization systems, exploring privacy-preserving capability discovery and semantic routing technologies, establishing threat detection methods based on agent behavior analysis, constructing trusted execution environments for verifiable service invocation, and promoting the security standardization of capability identifier and namespace management.

8 Conclusions

The rise of agent technology marks a profound shift in Internet service models and communication paradigms, promoting the evolution of networks from "connecting information" to "connecting intelligence". Aiming at the management, control, and routing challenges faced by the IoA, this paper proposes a protocol framework for IoA. Through mechanisms such as unified identification registration, dynamic service discovery, and semantically aware routing, it provides a systematic protocol solution for efficient, secure, and scalable collaboration among multiple agents from different agent service providers and across multiple domains. In the future, with the continuous expansion of agent application scenarios, the actual deployment of the protocol still needs further ex-

ploration and verification in terms of security, real-time performance, and resource scheduling optimization.

Future work will focus on the detailed implementation of the IoA architecture, protocol performance simulation, and cross-domain experiments, aiming to advance the IoA from theoretical design to practical application and lay a foundation for the development of the next-generation intelligent network.

References

[1] Cheng Y H, Zhang C Y, Zhang Z W, et al. Exploring large language model based intelligent agents: definitions, methods, and prospects [PP/OL]. V1. arXiv (2024-01-07) [2026-01-10]. https://doi. org/10.48550/arXiv.2401.03428
[2] Yang Y X, Chai H C, Song Y Y, et al. A survey of AI agent protocols [PP/OL]. V1. arXiv (2025-04-23) [2026-01-10]. https://doi. org/10.48550/arXiv.2504.16736
[3] Chen W Z, You Z M, Li R, et al. Internet of agents: weaving a web of heterogeneous agents for collaborative intelligence [PP/OL]. V2. arXiv (2024-07-10) [2026-01-10]. https://doi.org/10.48550/arXiv.2407.07061
[4] Introducing the Model Context Protocol [EB/OL]. (2024-11-25) [2026-01-10]. https://www.anthropic.com/news/model-context-protocol
[5] Agent network protocol technical white paper [R/OL]. 2025-07-24. https://agent-network-protocol.com/specs/white-paper.html
[6] Agent2Agent (A2A) Protocol [EB/OL]. [2026-01-10]. https://google.github.io/A2A
[7] Agora [EB/OL]. [2026-01-10]. https://www.agora.io/en
[8] IETF RFC 8484. 2018 DNS queries over HTTPS (DoH) [S]
[9] IETF RFC 4271. 2006 A border gateway protocol 4 (BGP-4) [S]
[10] IETF RFC 2328. 1998 OSPF version 2 [S]
[11] Cisco. The internet of agents white paper [R/OL]. 2025: 1 – 14. https://outshift.cisco.com/the-internet-of-agents
[12] Liu J, Yu K, Chen K L, et al. ACPs: agent collaboration protocols for the internet of agents [PP/OL]. V1. arXiv (2025-05-18) [2026-01-10]. https://doi.org/10.48550/arXiv.2505.13523
[13] Duan X D, Sun T, Lu L, et al. Internet of agents: conception, architecture and key technologies [J]. Telecommunications science, 2025, 41 (10): 1 – 10. DOI: 10.11959/j.issn.1000-0801.2025221
[14] IETF RFC 1035. 1987. Domain names - implementation and specification [S]
[15] IETF. Official website of the IETF computing-aware traffic steering (cats) working group [EB/OL]. [2026-01-10]. https://datatracker.ietf.org/wg/cats

Biographies

Fu Yuexia is a researcher at the China Mobile Research Institute and serves as the Vice Chairman of FG AINN in ITU-T SG13. Her main research interests include computing force networks and new technologies of future networks.

Liu Peng is a senior engineer of the China Mobile Research Institute. His main research interests include next-generation IP technologies, computing-aware traffic steering routing, and new technologies and applications of integrated computing and networking.

Lu Lu (lulu@chinamobile.com) is the Deputy Director of the Department of Basic Network Technology at the China Mobile Research Institute, a leader of the core network group of CCSA TC5, and a Vice Chairman of ITU-T SG13. Her research interests include 5G-A/6G network architecture and computing force networks.

Duan Xiaodong is the Vice President of the China Mobile Research Institute and a leader of the network technology group of IMT-2030 (6G). His research interests include 5G/6G architecture, computing force networks, and new IP technologies.

The Dawn of 6G: Empowering a User-Centric Ecosystem with Agentic AI

Gao Yin[1,2], Chen Jiajun[1,2], Liu Yansheng[1,2], Xiang Jiying[1,3]

(1. State Key Laboratory of Mobile Network and Mobile Multimedia Technology, Shenzhen 518055, China;
2. Wireless Product R&D Institute (Shanghai Branch), ZTE Corporation, Shanghai 201203, China;
3. Wireless Product R&D Institute (Shenzhen Branch), ZTE Corporation, Shenzhen 518057, China)

DOI: 10.12142/ZTECOM.202602006

https://kns.cnki.net/kcms/detail/34.1294.TN.20260422.1331.002.html, published online April 22, 2026

Manuscript received: 2025-02-03

Abstract: The convergence of artificial intelligence (AI) with the physical world is reshaping the future of intelligent systems through real-time perception, interaction, and control within physical environments. To support this new paradigm, 6G networks are envisioned as critical enablers, offering ultra-low latency, high reliability, and service-aware intelligence to facilitate seamless human-machine collaboration. This paper proposes a functional framework that integrates Agentic AI into the 6G architecture, introducing the concept of Agentic AI-Enabled 6G Network Services (AA6NS). In this framework, user intents are translated and processed across the application layer, core network (CN), and radio access network (RAN), where Agentic AI dynamically manages task-level quality of service/quality of experience (QoS/QoE), orchestrates multi-device service groups, and enables real-time network adaptation. The proposed architecture with the new 6G techniques establishes a foundation for future physical AI applications across domains such as autonomous mobility, smart manufacturing, and remote robotics.

Keywords: AI/ML; Agentic AI; 6G network; physical AI

Citation (Format 1): Gao Y, Chen J J, Liu Y S, et al. The dawn of 6G: empowering a user-centric ecosystem with Agentic AI [J]. ZTE Communications, 2026, 24(2): 43 - 51. DOI: 10.12142/ZTECOM.202602006

Citation (Format 2): Y. Gao, J. J. Chen, Y. S. Liu, et al., "The dawn of 6G: empowering a user-centric ecosystem with Agentic AI," *ZTE Communications*, vol. 24, no. 2, pp. 43 - 51, Jun. 2026. doi: 10.12142/ZTECOM.202602006.

1 Introduction

The rapid proliferation of intelligent devices, the increasing complexity of digital ecosystems, and the emergence of new paradigms, such as next-generation wireless communication networks, the industrialization of intelligent agent devices, and ubiquitous artificial intelligence (AI), are stretching the limits of 5G capabilities. 6G networks are envisioned to address these challenges and serve as an intelligence-native infrastructure that supports real-time decision-making, automation, and context-awareness[1-2]. The transition to 6G is expected to further intensify these dynamic changes, placing higher demands not only on network management, optimization, and operational control, but also on enabling a user-centric ecosystem in the real physical world. As a result, the integration of AI with 6G networks has emerged as a transformative trend in networking[3].

During the 5G-A phase, by embedding AI capabilities across various network layers, AI/machine learning (AI/ML) functions have gradually found deployment in various network optimization use cases, including load balancing, energy saving[4], mobility optimization, network slicing, coverage and capacity optimization[5], channel state information (CSI) prediction, beam management, and positioning[6]. The 6G era demands a new AI paradigm—one that is not just embedded into the network but is native to it, capable of autonomous decision-making across distributed and multi-agent environments[7]. Ref. [8] introduces a novel framework to integrate Agentic AI with 6G networks to enable self-design, self-running, self-reflection, and self-recycling in the 6G core network (CN).

A new technological leap—physical AI—is emerging[9], where AI is no longer confined to the digital realm but increasingly integrates with the physical world. This paradigm envisions AI systems that can perceive, interact with, and influence the physical environment in real time. Physical AI enables intelligent interaction with the real world through systems such as robotic controllers, autonomous machines, and AI agents. In this context, future 6G networks can serve as a critical enabler, acting as the infrastructure layer that seamlessly connects humans, AI agents, and machines. By providing ultra-low latency, high reliability, and service-aware intelligence, 6G networks can facilitate real-time, bidirectional

communication between AI and physical systems, paving the way for seamless human-machine collaboration in domains such as smart manufacturing, smart transportation, smart healthcare, and remote robotics.

While current intelligent 5G networks and conceptual 6G AI architectures have made progress in integrating AI for network optimization, they lack real-world implementations and practical use cases involving cross-layer collaboration of Agentic AI. The absence of cross-layer AI agent collaboration hinders the realization of ubiquitous intelligence in 6G—a network that can autonomously understand, reason, and act. Motivated by these limitations, we propose a novel framework: Agentic AI-enabled 6G Network and Service (AA6NS). This architecture envisions the 6G network as a key component to achieve full-domain integrated AI within the network infrastructure that supports:

• Intent-driven service orchestration, where the network interprets high-level user intents and dynamically translates them into the service-aware information for cross-domain transfer;

• Adaptive real-time quality of service (QoS) management, allowing the network to proactively adjust network parameters in response to changing user goals and real-time environmental conditions;

• Task-level agent group management, enabling the dynamic formation and coordination of service groups to accomplish complex, multi-step tasks.

The remainder of this paper is structured as follows. Section 2 introduces the concepts of Agentic AI and AI agents, and reviews related work on AI/ML for next-generation radio access networks (NG-RAN) from the standard perspective. Section 3 presents the proposed integration framework for enabling Agentic AI in 6G networks and Section 4 describes a set of representative scenarios demonstrating the capabilities of the proposed AA6NS. Finally, Section 5 outlines the key technologies for future research and concludes the paper.

2 Background and Related Work

An AI agent is an automated, intelligent entity capable of interacting with its environment, acquiring contextual information, reasoning, self-learning, decision-making, and executing tasks, either autonomously or in collaboration with other AI Agents, to achieve a specific goal, as defined in 3GPP SA1 WG[10]. They can function across a wide range of domains, from autonomous vehicles to intelligent personal assistants, embodying behaviors with decision-making processes similar to those of humans.

Furthermore, Agentic AI refers to an autonomous, goal-oriented functional framework that empowers AI agents to perceive, reason, plan, and execute actions in dynamic environments. It provides the capability to orchestrate heterogeneous demands through intent-driven, multi-step tasks, involving multi-agent cooperation and autonomous optimization. The comparison between an AI agent and Agentic AI is summarized in Table 1.

Agentic AI represents a transformative shift in the design and deployment of intelligent systems. By equipping AI agents with autonomy, adaptability, and multi-agent collaboration capabilities, Agentic AI moves beyond the limitations of traditional AI, enabling intelligent behavior in unpredictable, real-world physical environments.

3 Integration Framework for Agentic AI in 6G

During the AI/ML for the NR-RAN phase of 3GPP 5G-A, the topic "AI/ML for NG-RAN" has been discussed from Release 17 through the current Release 20. The functional framework for RAN intelligence (as shown in Fig. 1a) and AI/ML-assisted use cases have been studied and specified in RAN3[11]. Additionally, RAN1 and RAN2 have designed their own functional frameworks for RAN intelligence on the air interface, as shown in Fig. 1b[5]. RAN3 focused more on data transmission, e.g., input, output and feedback, between AI/ML functions, while RAN1, besides data transmission, also emphasized model management within the lifecycle management (LCM).

Since AI in future 6G networks requires multi-domain collaboration, considering AI/ML functions from only a single layer limits the research on Agentic AI in 6G. Therefore, based on the existing functional framework, we propose a new functional framework for RAN Intelligence that integrates AI/ML data transmission, model management within LCM, and the increasingly important concept of Agentic AI in 6G.

Firstly, Agentic AI consists of several key components, encompassing the essential parts shown in Fig. 2.

• Perception: This enables the agent to perceive its network environment, allowing it to receive and process multimodal inputs such as text, images, audio, radio conditions or other data types.

Table 1. Comparison between AI agent and Agentic AI

Feature	AI Agent	Agentic AI
Autonomy	Reactive (requiring specific inputs or conditions to act)	Proactive (actively identifying intentions and preventing problems)
Processing	Rule-based (relying on pre-defined processes)	Goal-oriented (autonomously optimizing strategies)
Learning capability	Static (based on data for static modeling)	Dynamic (learning in real time from data and building knowledge bases across domains)
Architecture	Single agent	Multiple agents (including physical agents); orchestrating multiple agents
Application scenarios	Single-task execution	Collaboration with multiple agents across domains to handle complex and long-term tasks

AI: artificial intelligence

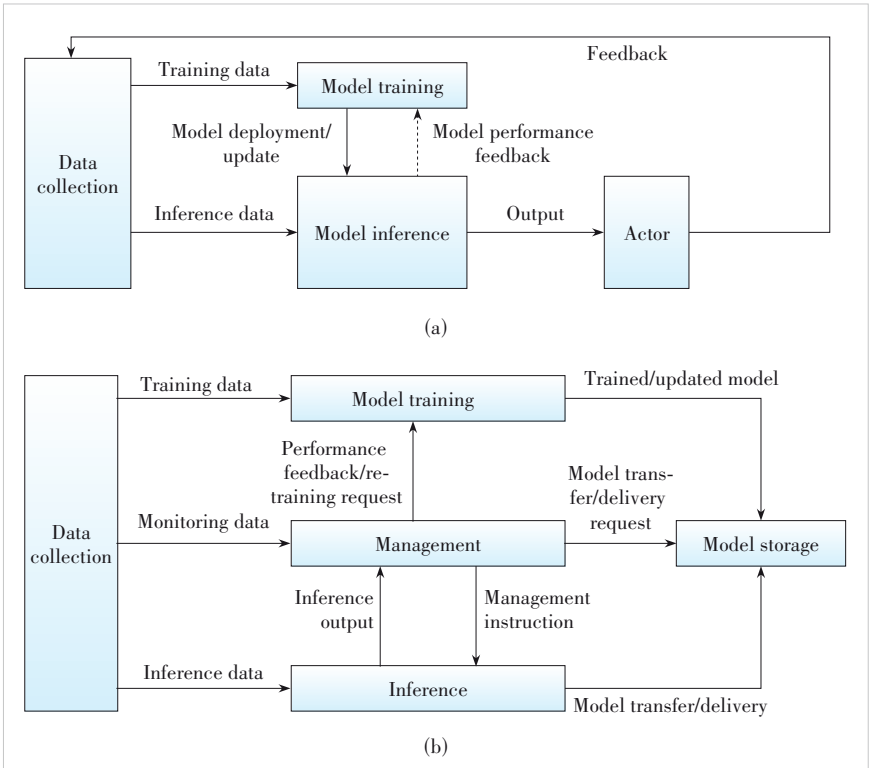

Figure 1. Functional framework for (a) RAN intelligence and (b) air interface

• Decision-making (Knowledge): This empowers the agent with autonomous decision-making and planning capabilities, enabling it to handle and execute more complex tasks effectively.

• Knowledge storage: This provides the agent's accumulated knowledge, skills, and experiences for reference and learning.

• Action: This equips the agent with the ability to interact with the network environment, allowing it to perform actions that, combined with perception, enable the autonomous completion of increasingly complex tasks.

Agentic AI can be deployed in all domains, including the CN, RAN and intelligent end devices.

Given this, we depict a new functional framework (Fig. 3) for 6G by combining the existing frameworks and the AI agentic architecture.

1) Data collection: This function provides input data to model training and model inference functions.

• Training data: data needed as input for the AI/ML model training function.

• Monitoring data: data required for the management of AI/ML models or functionalities, including data retrieval from the network environment to monitor the performance of AI/ML models or functionalities.

• Inference data: data needed as input for the AI/ML model inference function.

2) Model training: This function performs AI/ML model training, validation, and testing, generating model performance metrics that can be used as part of the model testing procedure. The model training function is also responsible for data preparation (e.g., pre-processing and cleaning, formatting, and transformation) based on the training data delivered by the data collection function, if required.

3) Model inference: This function generates outputs by applying AI/ML models or functionalities, using inference data provided by the data collection function as input. Similar to training, this function handles necessary data preparation (e.g., pre-processing and cleaning, formatting, and transformation) for the inference data.

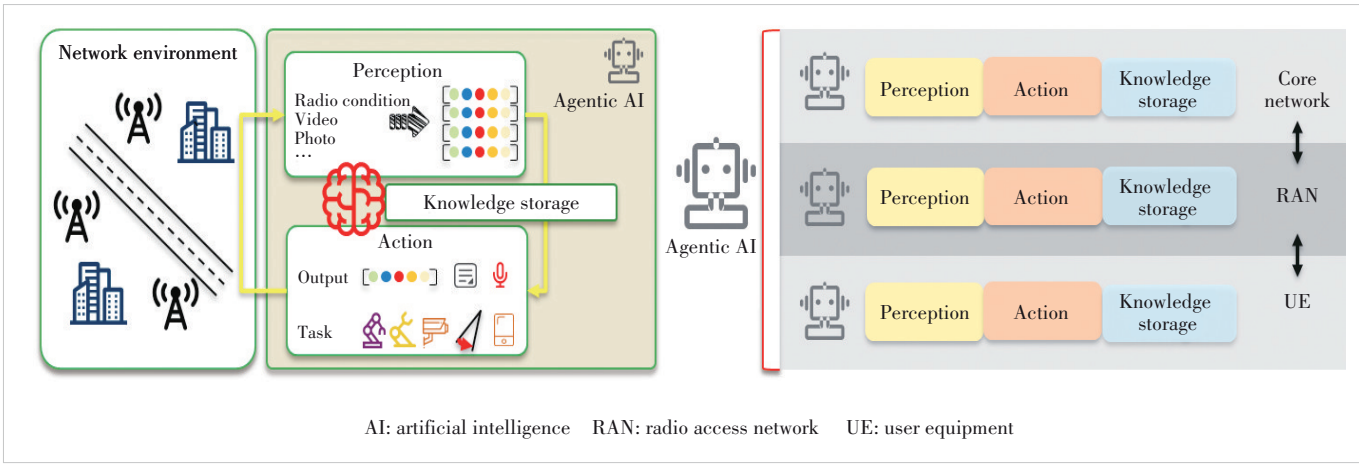

AI: artificial intelligence RAN: radio access network UE: user equipment

Figure 2. Agentic AI architecture in 6G

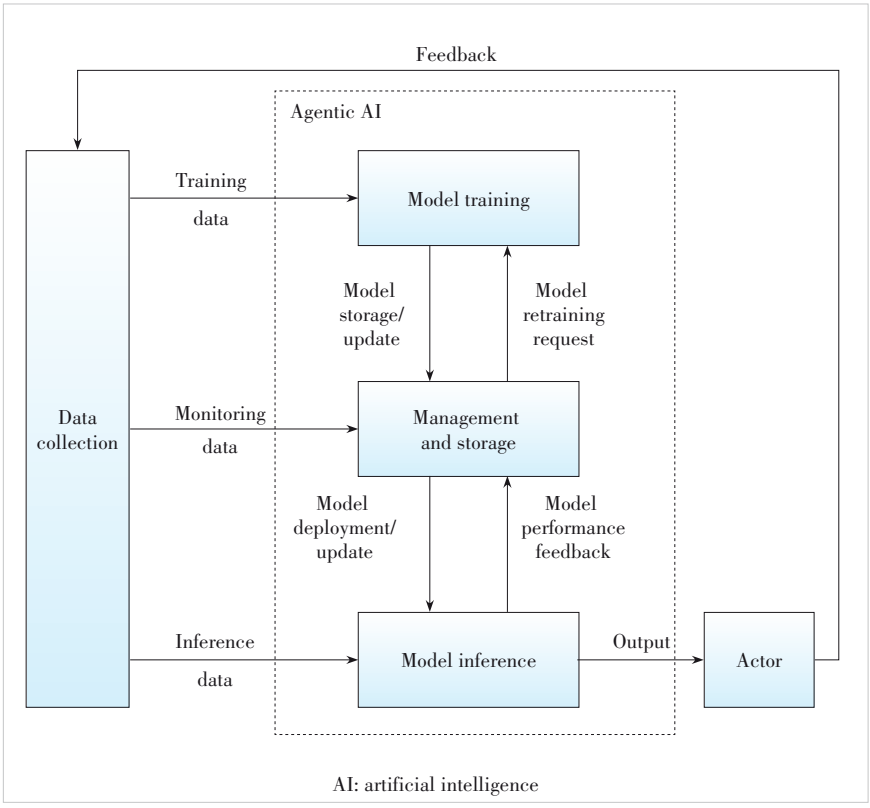

Figure 3. Functional framework for RAN intelligence in 6G

• Model storage/update: Trained or updated models are delivered to the management and storage function. Trained models are stored awaiting invocation, while updated models replace existing ones.

4) Management and storage: This function oversees the operation and monitoring of AI/ML models or functionalities, including the management of model training and inference, as well as orchestrating model collaboration between network elements. It also includes knowledge storage. For example, in a distributed learning architecture, this function coordinates the training and inference processes across various network elements.

• Model retraining request: Based on model performance feedback and monitoring data, model retraining can be triggered if the model's performance does not meet the requirements.

• Model deployment/update: It is used to initially deploy a trained, validated, and tested AI/ML model to the model inference function or to deliver an updated model to the model inference function.

Furthermore, compared with legacy AI/ML and Agentic AI, the short-term memory and long-term memory are critical for optimizing LLM performance. Therefore, the storage function here includes not only the AI/ML models but also the knowledge storage.

5) Actor: This function receives the output from the model inference function or Agentic AI, and triggers or performs corresponding actions. The actor may trigger actions directed toward other entities or the actor itself.

• Feedback: Information needed to derive training data and inference data, or to monitor AI/ML model performance and its impact on the network through key performance indicator (KPI) updates and performance counters.

6) Agentic AI: It refers to an autonomous, goal-oriented functional framework that empowers AI agents to perceive, reason, plan, and execute actions in dynamic environments, particularly in complex network systems. Agentic AI integrates advanced capabilities for model training and inference to enable real-time perception of the network environment. These models are grounded in a knowledge base and prior knowledge. Given that, Agentic AI can iteratively dynamically refine its decision-making, adapt to uncertainties, and orchestrate multi-entity collaborations to fulfil complex tasks.

4 Agentic AI-Enabled 6G Network and Service

Based on the concept of Agentic AI and the proposed Agentic AI functional framework above, AA6NS is proposed as a new paradigm to empower a user-centric ecosystem with Agentic AI. From a customer perspective, users can directly subscribe on-demand to personalized services provided by one or more Agentic AI-enabled service groups from operators or authorized service providers. Communities, schools, and airports utilize Agentic AI-enabled service groups to provide subscribed or customized services, as illustrated in Fig. 4.

For operators, AA6NS enables a transformative shift from traditional bit-pipe models to value providers through task- and attribute-based charging, e.g., billing based on device groups or AI compute usage. It supports multi-device collaboration via group capabilities and ensures security through a native, end-to-end 3GPP 6G security framework. For consumers—both businesses and individuals—AA6NS offers cost-effective deployment by orchestrating devices with specific capabilities (e.g., video, audio, flight capability, diving capability) instead of relying on expensive "do-it-all" devices. This approach enables proactive, always-on services, plug-and-play operation, service context-awareness, and flexible, customizable subscription models tailored to individual needs.

4.1 Applicable Scenarios

AA6NS supports a wide range of application scenarios in our daily lives. The following examples illustrate the capabili-

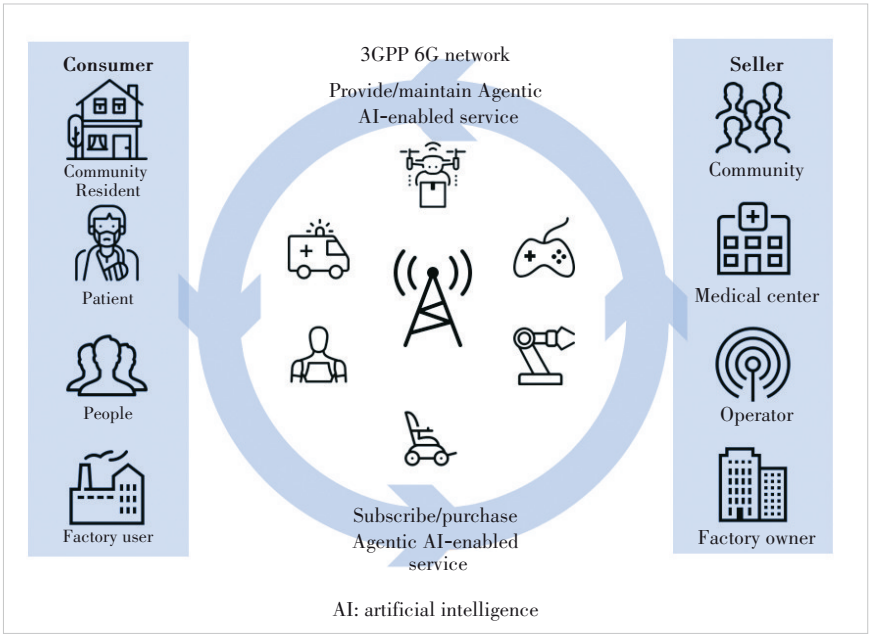

Figure 4. User-centric 6G ecosystem: empowering all scenarios with Agentic AI-enabled 6G networks and services

ties of the AA6NS.

1) Last meter delivery

In a 6G-enabled smart community as shown in Fig. 5, a user's natural language command, like "bring the package from the locker to my home", is instantly interpreted by the network into a precise, service-aware task with defined latency and security needs. Recognizing access restrictions, the system dynamically assembles an Agentic AI service group, e.g., a public robot for outdoor delivery and a private home robot for indoor handling, automating task distribution without user intervention. The network continuously adapts to real-world conditions. For instance, if it starts raining, it proactively updates robot behavior and allocates extra network and compute resources to maintain delivery speed, precision, and synchronization, ensuring seamless, end-to-end task execution from high-level intent to physical fulfillment.

2) Collaborative safe care

In this scenario, an elderly user is safeguarded by a dynamic Agentic AI service group, including a smartwatch, robot companion, and integrated sensing and communication (ISAC) sensor, driven by the high-level intent of ensuring continuous safety. When the user is distracted during a conversation and approaches a slippery surface, the ISAC device detects the risk and correlates it with the user's behavior. As shown in Fig. 6, the system triggers a rapid, coordinated response: devices communicate via ultra-low-latency wireless technologies, e.g., Device-to-Device (D2D) or network-assisted communication, to relay a hazard warning to the user. The accompanying robot then executes a real-time action to ensure user safety, which prevents accidents through proactive, autonomous collaboration within the group via 6G networks.

3) Emergency rescue

In a critical situation where a user suffers a sudden cardiac event, the local Agentic AI service group, initially just a smartwatch and support robot, detects the anomaly. The 6G network interprets the high-level intent as "Immediate Life Preservation" and translates it into actionable service needs, such as rapid automated external defibrillator (AED) delivery. The system in Fig. 7 dynamically expands the service group by recruiting a nearby delivery drone, which is allowed to override its original task. It reconfigures network resources for ultra-low latency and prioritizes control and video streams. The drone autonomously retrieves an AED and navigates the optimal route to the user, enabling a rapid, coordinated life-saving response.

Furthermore, all the above tasks can be regarded as individual subscription-based paid services or packaged as a whole subscription-based paid service, such as a "24-Hour

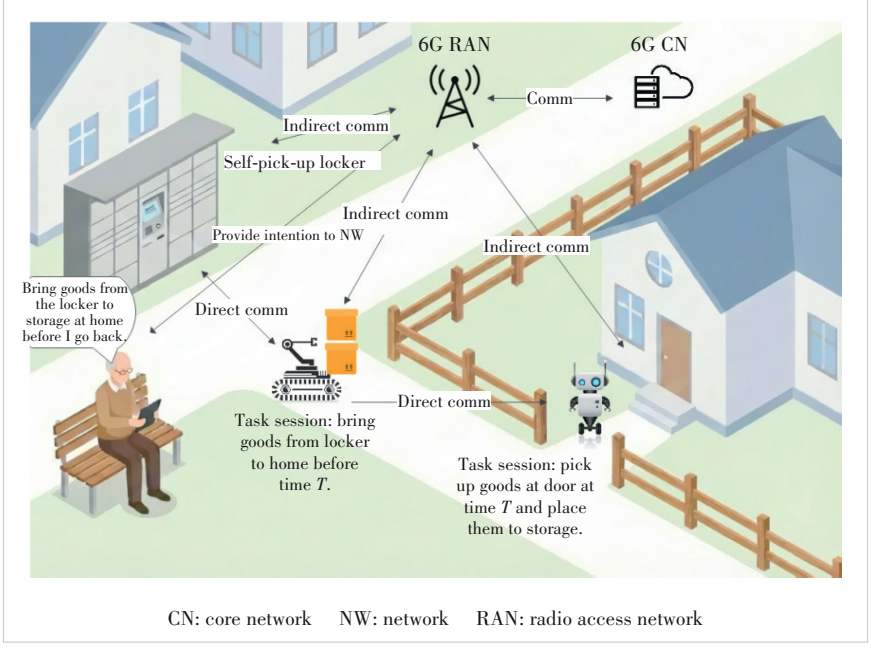

Figure 5. An illustration of last meter delivery

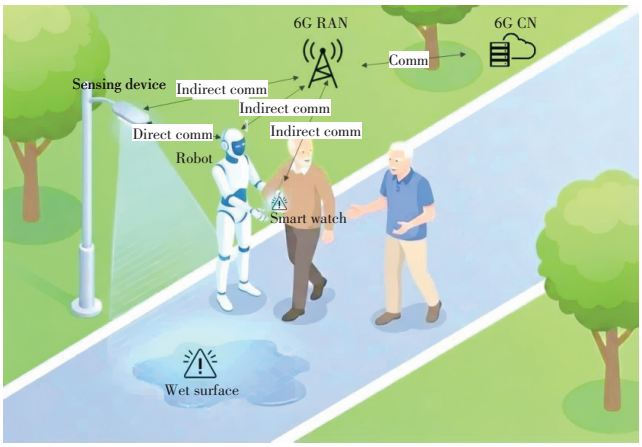

CN: core network RAN: radio access network

Figure 6. Collaborative safe care

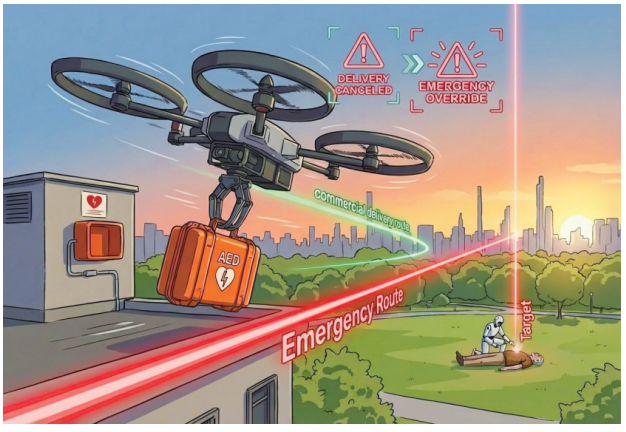

Figure 7. Emergency rescue

Community Butler". Users can directly subscribe to the service from operators or community property management, ultimately shaping a future society where all physical agents collaborate to serve people and fulfill user intents.

4.2 Architecture

By combining the proposed functional framework for RAN intelligence with the concept of AA6NS, the overall architecture integrated with Agentic AI is shown in Fig. 8. As explained above, customers first subscribe to the AA6NS from operators or third-party service providers (e. g., community property management, hospitals, and factories). Then, customers input intent requests to the application layer, which translates and forwards the intent to the 6G network leveraging the Agentic AI. After that, the 6G CN further analyzes the intent, triggers the corresponding protocol data unit (PDU) sessions toward multiple end devices, and provides the service-aware information to the RAN. Particularly, Agentic AI is deployed in each layer of the 6G network, facilitating knowledge sharing across domains. Thus, upon receiving service-aware information, the RAN can dynamically manage the real-time task-level QoS, perform the corresponding PDU sessions, monitor the task level QoS/QoE performance, and manage the collaborative Agentic AI-enabled service groups (e. g., express delivery, auto parking, intelligent care) to realize consumer intents. Agentic AI-enabled services are inherently performed with multiple tasks by multiple devices, which may require coordinated interactions among devices with differentiated capabilities within a service group. Task-associated PDU sessions are orchestrated accordingly, each provisioned with legacy QoS and task-level QoS parameters. Customers can also provide service quality feedback through the application layer. Network performance feedback and user performance feedback information can be collected within 6G networks and used for service quality evaluation or as part of the knowledge information.

4.3 Potential Technical Features

As previously discussed, the Agentic AI on applications may invoke 3GPP services based on the intent. In contrast, Agentic AI on 6G networks may provide the 3GPP service to customers or third parties based on the received service request, which will be triggered in the form of one or multiple task-associated PDU sessions towards one or multiple devices.

The 6G CN is capable of further analyzing intents from the application layer and triggering the corresponding PDU sessions toward multiple devices. As shown in Fig. 9, an Agentic AI-enabled service group is initiated based on the translation of user intents, service requirements and device capabilities.

To support AA6NS, the 6G network shall support the following basic functions: authorization and registration of task devices, service-aware information exposure, task-associated PDU session management and task-level QoS/QoE monitoring, and service group management, as illustrated in Fig. 10.

Agentic AI-enabled end devices report service capability information to the CN, which performs authorization and configures the set of allowed tasks for each device. Either the CN or the device may initiate service requests to establish a PDU session corresponding to certain tasks to achieve a specific Agentic AI enabled service. When the Agentic AI-enabled service is activated, service-aware information may be provided to the RAN for network performance monitoring and dynamic management of service group devices to meet specific task requirements. Task-associated PDU session management also includes PDU session setup, modification, and release. When the task-level QoS cannot be fulfilled, the RAN may also trigger the notification towards the CN. Additionally, task-level QoE/QoS monitoring for real-time status and performance tracking is also supported.

In addition, Fig. 11 illustrates the group management procedures. Initially, all participating devices join the Agentic AI-enabled service group, with Device1 and Device2 successfully

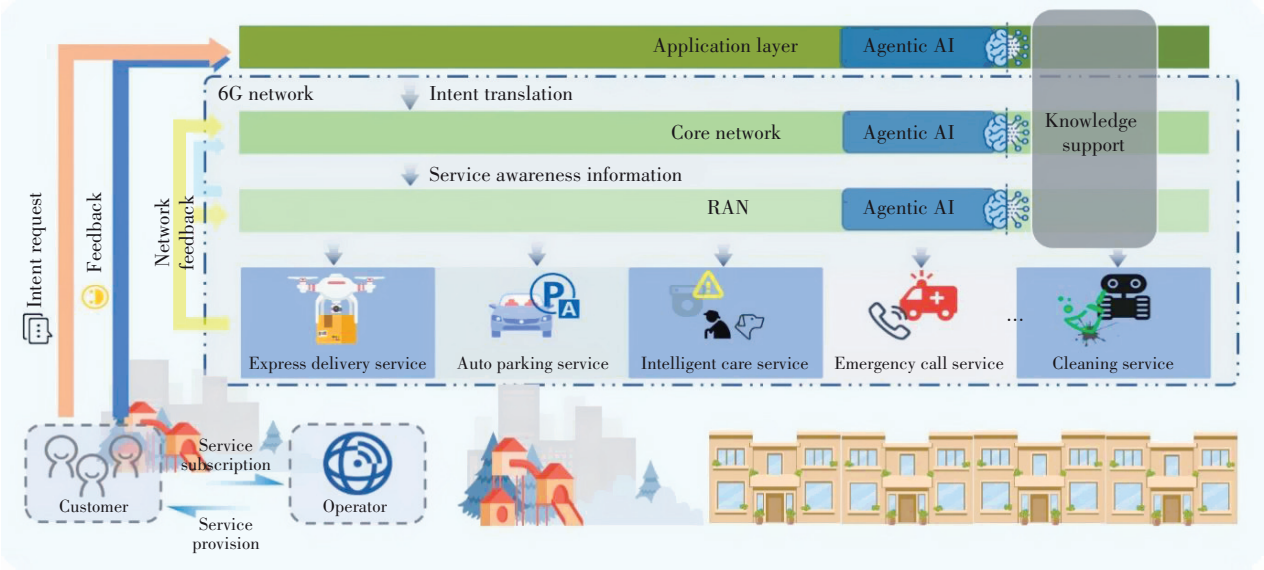

AI: artificial intelligence RAN: radio access network

Figure 8. Architecture of Agentic AI-enabled 6G networks and system

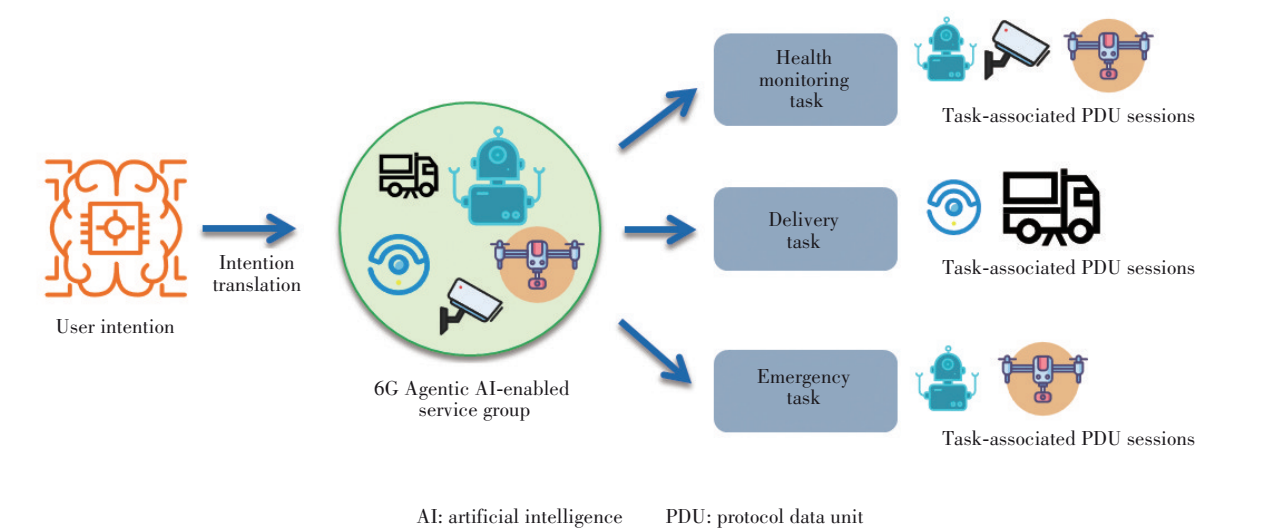

AI: artificial intelligence PDU: protocol data unit

Figure 9. Relation between Agentic AI-enabled service group and tasks

establishing task-level PDU sessions. Based on the data collected from devices and the network, the 6G network determines that Device2 is deemed no longer suitable for its assigned task. As a result, the 6G network initiates the establishment of a new task-level PDU session for Device3, and subsequently releases the PDU session associated with Device2.

Privacy and security protection is essential, especially as Agentic AI makes autonomous decisions based on sensitive user data. Techniques such as confidential computing, federated learning, and zero-knowledge proofs can enhance data protection, while subscriber identity module (SIM) identities ensure actions are traceable and auditable. This framework facilitates secure access control and ensures that only authorized device can interact on behalf of consumers.

The above outlines the technical features that we believe 6G networks need to possess in the future to support the proposed AA6NS.

5 Conclusions

The emergence of Agentic AI marks a transformative shift in the AI paradigm, bridging the gap between the digital and physical worlds. By enabling real-time perception, interaction, and actuation within the physical environment, 6G networks will play a foundational role as the intelligent infrastructure that

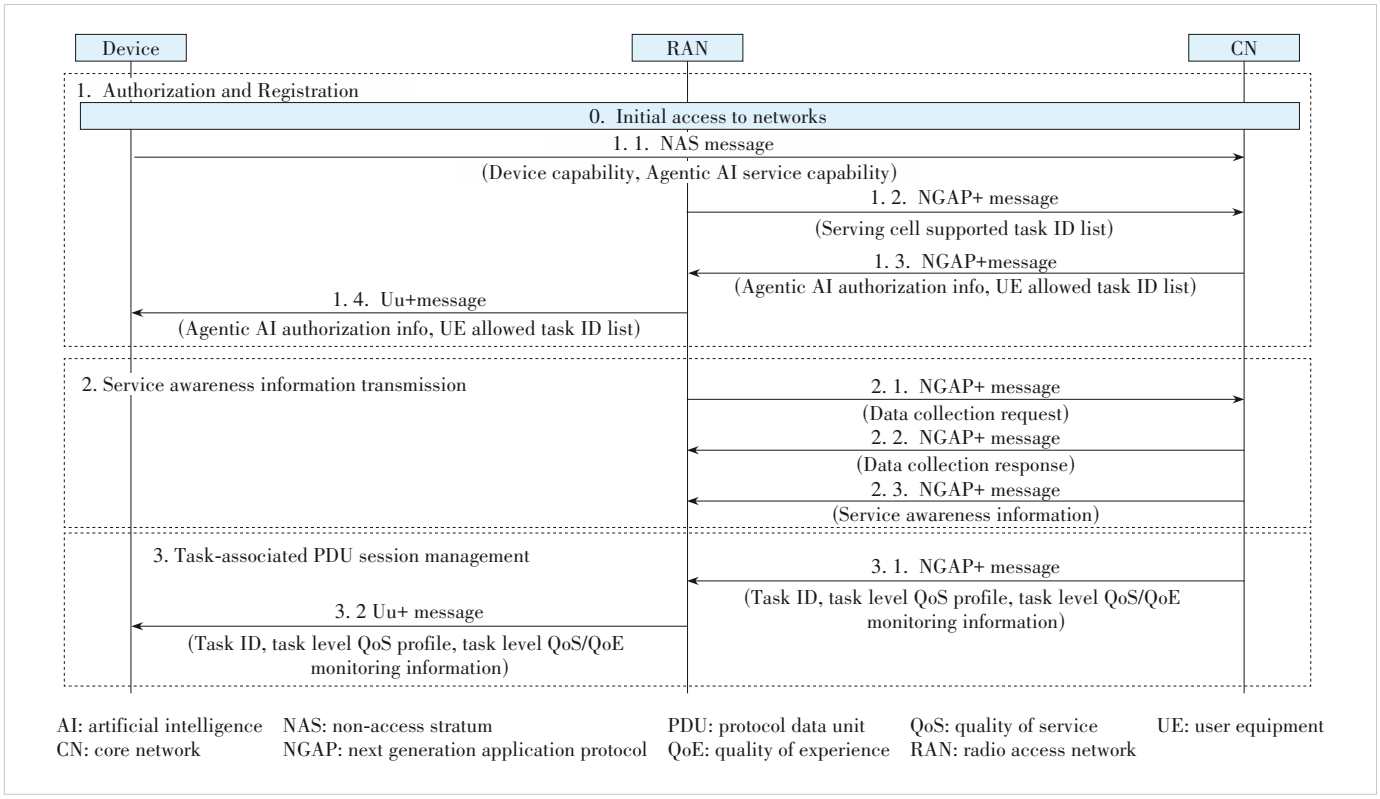

Figure 10. Examples of call flow on Agentic AI-enabled 6G networks and services

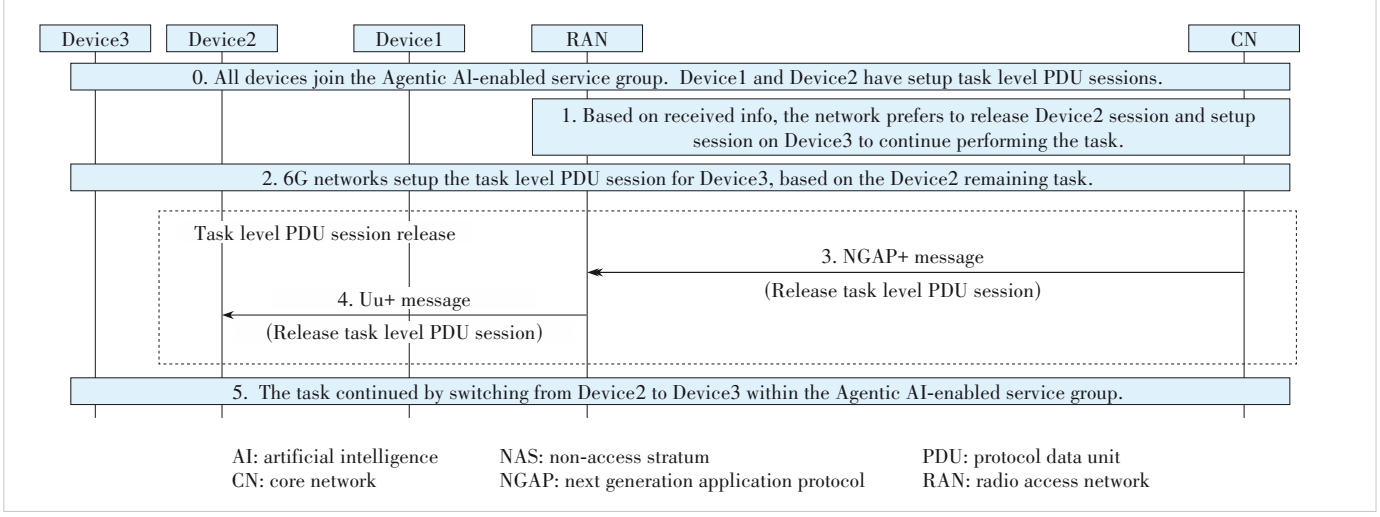

Figure 11. Call flow on group management

connects humans and Agentic AI-enabled machines through ultra-reliable, low-latency, and service-aware communication.

The proposed functional framework for RAN intelligence and the concept of AA6NS illustrate how future networks can dynamically manage intent-driven Agentic AI-enabled services. By utilizing Agentic AI across all layers of the 6G architecture, the network can interpret user intents, orchestrate multi-device and multi-step task execution, and ensure real-time task-level QoS and QoE performance.

As 6G networks evolve to support AA6NS, key enabling capabilities—such as authorization and registration of task devices, service awareness, task-associated PDU session management, task-level QoS/QoE monitoring, and service group management—become indispensable. Ultimately, this architecture lays the groundwork for a fully agentic, intelligent, and adaptive physical-digital ecosystem, where Agentic AI-

enabled networks and services can seamlessly meet human needs across diverse application scenarios, fulfilling the vision of a truly user-centric ecosystem.

References

[1] Saad W, Bennis M, Chen M Z. A vision of 6G wireless systems: applications, trends, technologies, and open research problems [J]. IEEE network, 2020, 34(3): 134 – 142. DOI: 10.1109/mnet.001.1900287
[2] Letaief K B, Chen W, Shi Y M, et al. The roadmap to 6G: AI empowered wireless networks [J]. IEEE communications magazine, 2019, 57 (8): 84 – 90. DOI: 10.1109/mcom.2019.1900271
[3] Bhat J R, Alqahtani S A. 6G ecosystem: current status and future perspective [J]. IEEE access, 2021, 9: 43134 – 43167. DOI: 10.1109/access.2021.3054833
[4] Chen J, Gao Y, Liu Z, et al. Future vision on artificial intelligence assisted green energy efficiency network [J]. ZTE communications, 2023, 21(2): 34 – 39. DOI: 10.12142/ZTECOM.202302006
[5] 3GPP TR 38.743: 2025 Study on enhancements for artificial intelligence (AI)/machine learning (ML) for NG-RAN [S]
[6] 3GPP TR 38.843: 2024 Study on artificial intelligence (AI)/machine learning (ML) for NR air interface [S]
[7] Çımen S, Karahan S N, Karhan D, et al. The integration of agentic AI in 6G wireless networks: state-of-the-art, challenges, and future perspectives [C]//Innovations in Intelligent Systems and Applications Conference (ASYU). IEEE, 2025: 1 – 6. DOI: 10.1109/asyu67174.2025.11208443
[8] Tong W, Huo W, Lejkin T, et al. A-core: a novel framework of agentic AI in the 6G core network [C]//International Conference on Communications Workshops (ICC Workshops). IEEE, 2025: 1104 – 1109. DOI: 10.1109/iccworkshops67674.2025.11162291
[9] Liu D C, Zhang J Y, Dinh A D, et al. Generative physical AI in vision: a survey [PP/OL]. arXiv (2025-04-19) [2026-02-16]. https://arxiv.org/abs/2501.10928
[10] 3GPP TR 22.870: 2025 study on 6G use cases and service requirements [S]
[11] 3GPP TR 37.817: 2022 Study on enhancement for data collection for NR and EN-DC [S]

Biographies

Gao Yin (gao.yin1@zte.com.cn) is the Standardization Director at ZTE Corporation and the former Chair of 3GPP RAN3 (2021 – 2025). She also serves as the Vice Chair of CCSA TC624 WG4 and is an expert at the State Key Laboratory of Mobile Network and Mobile Multimedia Technology, China. She has led and participated in multiple major national projects, focusing on wireless network technologies research and standardization for 3G/4G/5G/6G in SDOs, including 3GPP, CCSA, IMT-2020/2030, NGMN, and IEEE. She has initiated and completed multiple international and domestic standardization projects, and has served as a rapporteur for various international and domestic standards and technical reports.

Chen Jiajun received his master's degree in communication engineering from Shanghai University, China in 2019. He is currently a senior pre-research and standardization engineer at the R&D center of ZTE Corporation and the State Key Laboratory of Mobile Network and Mobile Multimedia Technology, China. He serves as the rapporteur for AI for NG-RAN in 3GPP RAN3 (Release 18, Release 19, and Release 20). His research interests include 5G/6G wireless communications, artificial intelligence assisted network, and Agentic AI-enabled networks.

Liu Yansheng received his bachelor's degree in petroleum engineering from Missouri University of Science and Technology, USA in 2015, and his MS degree in information technology from The University of New South Wales, Australia in 2018. Since 2019, he has been with ZTE Corporation, serving as a pre-research engineer and a delegate to 3GPP RAN3. His main research focuses on 3GPP standardization and 5G/6G network technologies, including UAV networks, QoE/QoS management, NCR, XR, AIoT, MBS, and 6G network architecture and interfaces.

Xiang Jiying is the Chief Scientist of ZTE Corporation, leading research and development initiatives across 3G, 4G, 5G, B5G, and 6G technologies. He is a recipient of the Special Prize and Second Prize of the The State Science and Technology Progress Award, as well as The State Technological Invention Award. He has also been honored with titles such as "Contributor to China's Communication Industry Technology" and "Outstanding Engineer of China".

Intent-Driven Control System for Heterogeneous Agent-Oriented Networking (HaoNet)

Wang Bowen[1], Lu Lu[2], Li Huimin[1], Yang Chungang[1]
(1. Xidian University, Xi'an 710071, China;
2. China Mobile Research Institute, Beijing 100053, China)

DOI: 10.12142/ZTECOM.202602007
https://kns.cnki.net/kcms/detail/34.1294.TN.20260519.0857.002.html, published online May 19, 2026
Manuscript received: 2026-03-11

Abstract: Empowered by advances in large language models, the growing integration of autonomous agents into industrial and daily-life sectors is turning them into new networking entities. Such agent-oriented networking features high interaction frequencies and emergent task-driven structures, necessitating strong network policy consistency and reliability within dynamic environments. To address these challenges, we propose a network control system that integrates Intent-Driven Network (IDN) into Heterogeneous Agent-Oriented Networking (HaoNet). IDN focuses on high-level task intents and provides flexible reconfiguration and adaptive optimization, thereby enhancing the effectiveness of agent-oriented networking. In this paper, we first summarize three key features of HaoNet: task-driven operation, distributed collaboration, and closed-loop intelligence. Furthermore, we propose a comprehensive system architecture, which includes the application layer, the intent layer, and the infrastructure layer, and investigate the associated key technologies. Finally, typical application scenarios are presented to demonstrate the practical value of the proposed system in enabling robust agent-oriented networking control.

Keywords: AI agent; agent-oriented networking; intent-driven network; network control

Citation (Format 1): Wang B W, Lu L, Li H M, et al. Intent-driven control system for heterogeneous agent-oriented networking (HaoNet) [J]. ZTE Communications, 2026, 24(2): 52 - 63. DOI: 10.12142/ZTECOM.202602007
Citation (Format 2): B. W. Wang, L. Lu, H. M. Li, et al., "Intent-driven control system for heterogeneous agent-oriented networking (HaoNet)," *ZTE Communications*, vol. 24, no. 2, pp. 52 - 63, Jun. 2026. doi: 10.12142/ZTECOM.202602007.

1 Introduction

The rapid advancement of large language models (LLMs) has fundamentally expanded the application landscape of artificial intelligence (AI), with the AI agent emerging as a dominant paradigm for translating LLM capabilities into actionable systems. AI agents are intelligent entities capable of environment perception, autonomous decision-making, and action execution, which leverage LLMs to accomplish tasks independently or collaboratively in complex environments while continuously optimizing their behavior[1]. In recent years, a diverse spectrum of agent-based applications has been developed in both industrial and consumer domains, exemplified by Manus[2] and Coze[3]. Agents can be broadly categorized into physical agents, which exist in physical forms such as robots and interact directly with the physical world, and digital agents, which operate within digital environments to provide more sophisticated decision support. To accomplish increasingly sophisticated tasks, heterogeneous agents across different domains must frequently collaborate, necessitating seamless inter-agent communication and robust networking. As agents proliferate across diverse environments, future networks will increasingly interconnect these agents rather than conventional end hosts, marking a paradigm shift in networked object composition and imposing new demands on network architecture, control mechanisms, and resource management.

To accommodate the evolving connectivity requirements of agents, Heterogeneous Agent-Oriented Networking (HaoNet) has significant research value. HaoNet aims to provide a globally interconnected and controllable network with on-demand enabling for information exchange and task collaboration among agents of various forms, capabilities, and users[4]. Unlike conventional networking paradigms, HaoNet is designed to support reliable agent access and interaction frequencies that far exceed those of traditional networks. Driven by the intrinsic autonomy of agents, HaoNet shifts from reactive connectivity to proactive, task-oriented networking, where links are established autonomously to fulfill specific task goals. Furthermore, HaoNet enables real-time, flexible network reconfiguration to navigate emergent tasks and dynamic environments.

Despite its potential, realizing the full capabilities of HaoNet presents significant technical challenges. First, addressing emergent and complex tasks requires deep semantic parsing of task-specific objectives and the subsequent mapping of these mission-level goals onto networking targets. Second, ensuring

policy consistency and reliability across diverse agents is critical, as any misalignment in intent interpretation could lead to network instability in dynamic environments. Third, the proactive nature of agents leads to highly frequent and bursty interactions, requiring continuous network policy adaptation. Finally, the disparity in functional capabilities and computational resources among agents demands a sophisticated orchestration mechanism capable of balancing global intent fulfillment with resource efficiency.

The Intent-Driven Network (IDN) is a novel paradigm centered on user intent, utilizing AI to accurately identify and rapidly respond to high-level user requirements[5]. By integrating core technologies such as intent refinement, policy generation, and intent assurance, IDN achieves a closed-loop mapping from user intent to network configuration, enabling the network to dynamically adapt and optimize itself without manual intervention. This inherent flexibility and self-optimization capability offer a promising pathway to overcome the bottlenecks of HaoNet. Specifically, the intent-centered paradigm provides a robust framework for parsing the semantic objectives of emergent tasks, effectively bridging the gap between mission-level goals and networking targets. Moreover, the adaptive architecture of IDN, supported by advanced techniques such as multimodal processing and semantic communication, is uniquely suited to maintain policy consistency and handle the highly frequent interactions characteristic of agents.

This paper aims to develop a network control system for HaoNet that operates under an intent-driven paradigm, fundamentally bridging the gap between high-level task objectives and autonomous network execution. By integrating IDN technologies, the proposed system ensures policy consistency and reliability while enhancing networking effectiveness and task efficiency for emergent tasks in dynamic environments. The main contributions of this paper are summarized as follows:

1) Characterization of HaoNet: We summarize three key features of HaoNet, namely task-driven operation, distributed collaboration, and closed-loop intelligence, establishing a conceptual foundation for agent-oriented networking.

2) System architecture and key technologies: We propose a comprehensive system architecture that integrates IDN, and investigates the associated key technologies required to enable autonomous network control.

3) Illustrative application scenarios: We provide typical application scenarios to demonstrate the practical value and feasibility of the proposed system in enabling robust agent-oriented networking.

2 Related Work

The rapid proliferation of agents has spurred diverse paradigms of agent-oriented networking. Gupta et al. proposed AgNet[6], a novel architecture that draws parallels with the World Wide Web by introducing specialized components such as the Agent Name Server and the Agent Text Transfer Protocol to facilitate discovery and interoperability. From a broader ecosystem perspective, the Internet of Agents[7] has been envisioned as a foundational framework for the seamless interconnection of heterogeneous agents at scale, focusing on capability notification and adaptive communication, and introducing emerging agent communication protocols including Model Context Protocol (MCP)[8] and Agent to Agent Protocol (A2A)[9]. To further integrate intelligence into the network fabric, Xiao et al. proposed AgentNet[10], a 6G-oriented framework that connects task-oriented agents by deploying dedicated agents across the physical, network, and application layers to enable cross-layer collaborative intelligence. Despite these advancements, systematic analysis[11] reveals that siloed agent designs lead to significant architectural fragmentation, hindering cross-domain interoperability and manageable scaling. Compounding this issue, existing frameworks[6–7, 10] primarily focus on defining static structural components while paying insufficient attention to specific operational mechanisms, particularly under dynamic task execution.

IDN has emerged as a transformative paradigm that automates network management by translating high-level user objectives into actionable configurations[12]. Recent research has increasingly focused on integrating Agentic AI to overcome the rigidity of traditional rule-based IDN systems. For instance, Jiang et al.[13] proposed a hierarchical multi-agent framework for 6G, where LLM-based agents employ reasoning-action cycles to decompose natural language intents into technically feasible network slice configurations. Similarly, Lee et al.[14] introduced a Generative-AI-empowered architecture that utilizes a chief agent to transform intents into dependency-aware execution graphs for autonomous telecom service reconfiguration. In specialized domains such as industrial automation, Romero et al.[15] integrated Agentic AI into the intent-based paradigm, utilizing specialized sub-agents to translate high-level human goals into autonomous actions aligned with Industry 5.0 principles. While these studies predominantly leverage Agentic AI as a tool to enhance the autonomy of IDN, the maturation of IDN capabilities provides a natural foundation for extending its robust intent-centered and self-optimization mechanisms to support agent-oriented networking. Applying these enhanced capabilities enables a strategic shift from using agents to manage the network to leveraging the network's inherent intelligence to proactively sustain the task-driven, bursty, and heterogeneous interactions of the agents themselves.

The integration of IDN into agent-oriented networking remains in its early stages. A preliminary attempt is GoAgentNet[16], which draws on the intent-driven paradigm to enable multi-agent collaboration by orchestrating their perception, communication, and computation. While it explores goal-oriented fulfillment, GoAgentNet lacks specific mechanisms to ensure dynamic intent-agent mapping and scalable collaborative orchestration of heterogeneous agents. To bridge these gaps, our research proposes an intent-driven control frame-

work for HaoNet, which incorporates diverse mechanisms such as LLM fine-tuning and adaptive collaboration patterns to ensure high network policy consistency and reliability within dynamic environments.

3 Networking Scenario and Design of HaoNet

This section presents the core foundations of HaoNet, ranging from key features to architectural implementation. We introduce a general networking scenario to establish context, followed by a summary of key features that serve as a conceptual foundation. Finally, we present the system architecture for HaoNet.

3.1 Networking Scenario

To provide a foundational understanding of HaoNet, we introduce a general networking scenario centered on collaborative infrastructure maintenance tasks, which can be analogized to other networking scenarios, as shown in Fig. 1. This scenario incorporates a heterogeneous agent society comprising unmanned aerial vehicle (UAV) agents, ground robotic agents, and virtual assistant agents, all operating collaboratively to ensure the operational integrity and safety of 5G/6G network-based urban or unmanned ad-hoc network-based industrial infrastructures.

The collaborative infrastructure maintenance process typically initiates with high-level operational objectives, including comprehensive structural health inspections. These objectives are systematically decomposed into granular subtasks and allocated to multiple agents, which then form task subnets for collaborative execution based on their capabilities and real-time spatiotemporal status. During this collaborative process, their localized interactions give rise to specific networking requirements, as the underlying communication infrastructure must adapt its resources to support the synchronization and data-intensive demands of agents.

Beyond preplanned task allocation, the network must accommodate spontaneous, peer-to-peer interactions within this dynamic environment. For instance, a ground robotic agent requiring an aerial perspective for a localized assessment can autonomously initiate a collaborative request to a nearby UAV, triggering a real-time massive data exchange. These emergent communication requirements necessitate on-demand reconfiguration, where logical links and physical resources are rapidly reconfigured into transient, task-aligned subnets.

It is important to note that 5G/6G networks and unmanned ad-hoc networks exhibit fundamentally different characteristics. Specifically, 5G/6G networks rely on well-established infrastructure, providing relatively stable topology, reliable connectivity, and support for centralized control. In contrast, unmanned ad-hoc networks operate without fixed infrastructure, featuring highly dynamic topology, intermittent connectivity, and a stronger reliance on distributed and self-organizing mechanisms. Although the key technical requirements differ across scenarios in terms of control strategies, resource management, and communication patterns, the proposed architecture and key technologies are designed to address common requirements while enabling flexible adaptation to scenario-specific characteristics.

3.2 Key Features

By distilling the fundamental requirements of HaoNet, we summarize three key features: task-driven operation, distributed collaboration, and closed-loop intelligence.

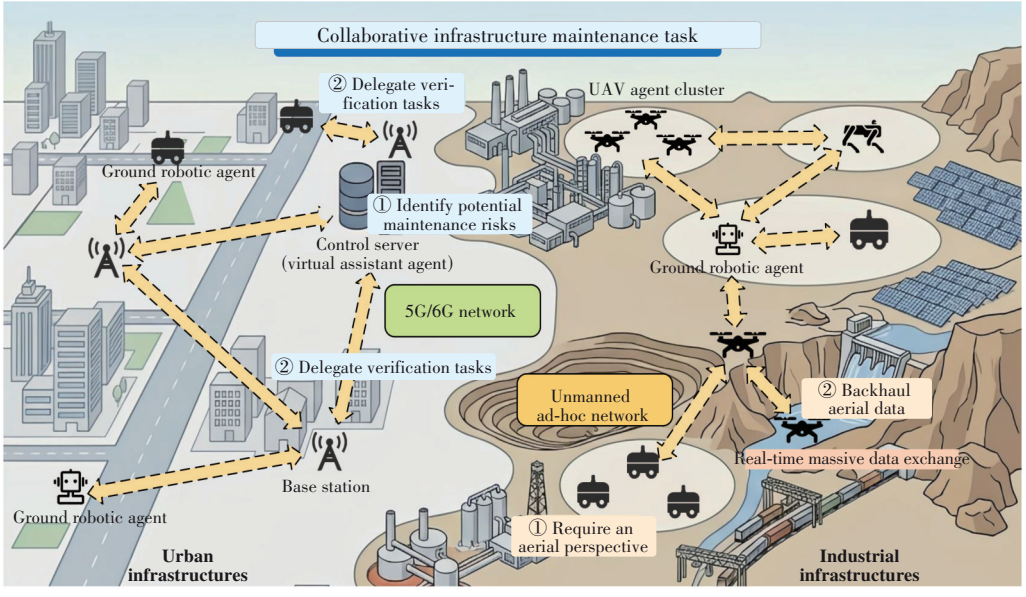

UAV: unmanned aerial vehicle

Figure 1. A general networking scenario of collaborative infrastructure maintenance in HaoNet

3.2.1 Task-Driven Operation

In HaoNet, task intent originating from the user or application serves as the core driving factor, guiding the agent network to enable adaptive task orchestration. Upon receiving a task intent, HaoNet performs intent refinement and decomposition to identify a group of agents that satisfy the task requirements based on agent capabilities. The resulting subtasks are then assigned to the selected agents to form a task-oriented agent subnet.

From the perspective of adaptive coordination in various environments,

HaoNet encompasses three task orchestration modes: centralized, distributed, and semi-distributed, as shown in Fig. 2. In the centralized mode, a central agent maintains a comprehensive global view of the network, covering agent capabilities, edge computing resources, network states, and related contextual information. Based on this view, it performs unified intent refinement and decomposition and assigns subtasks to appropriate agents. In the distributed mode, each agent is capable of intent refinement and decomposition; upon receiving a task intent, an agent autonomously processes the intent and collaborates with other agents through negotiation to accomplish the task. In the semi-distributed mode, a group of agents dynamically selects a central agent based on their intelligence levels. Task intents, together with relevant network information, are forwarded to the selected agent, which performs intent refinement and decomposition on behalf of the group.

These three orchestration modes are suitable for different scenarios and offer distinct advantages. Centralized orchestration is well-suited to relatively stable networks and tightly coupled tasks that require unified control. Distributed orchestration targets highly dynamic networks with numerous mobile nodes, where tasks exhibit weak dependencies and high requirements for flexibility and fault tolerance. Semi-distributed orchestration applies to agent networks that are locally centralized but globally distributed, aiming to balance the efficiency of centralized planning with the flexibility of distributed coordination.

3.2.2 Distributed Collaboration

Distributed collaboration signifies that agents are physically distributed and collaboratively accomplish tasks. Distributed agents execute assigned subtasks within a task subnet and continuously adjust their behaviors aligned with the task intent, collaborating and cooperating to achieve global task optimization.

To sustain such collaborative execution, the interplay between agents necessitates both information sharing and capability sharing. Information sharing encompasses the physical environment data perceived by agents, information regarding the capabilities of surrounding agents, and real-time network states. Through information exchange, agents within a task subnet can obtain a comprehensive view of subnet information. Capability sharing allows an agent to remotely leverage the capabilities of another agent to fulfill the current assignment.

Facing the challenge of massive data exchange among agents, distributed collaboration in HaoNet relies on semantic communication. To fulfill complex tasks, agents will exchange multi-modal information to achieve information unification, which inherently triggers massive data transmissions. Furthermore, the disparity in intelligence levels and functional capabilities leads to heterogeneous data modalities, creating a critical need for cross-modal transformation. To address these challenges, semantic communication is employed to provide expressive and flexible representations, such as embedding-based data transmission, ensuring efficient and seamless interoperability across agents.

3.2.3 Closed-Loop Intelligence

Closed-loop intelligence refers to the internal architecture of the agent that enables it to autonomously perform the full lifecycle of task intents, including environment perception, data processing, decision-making, and action execution. As shown in Fig. 3, a general agent consists of four core functional modules (perception, analysis, planning, and execution) supported by an internal knowledge base for data storage and inter-module interaction. To enhance the capabilities of each module, the agent integrates additional components such as LLMs, external knowledge bases, and external tools, thereby supporting comprehen-

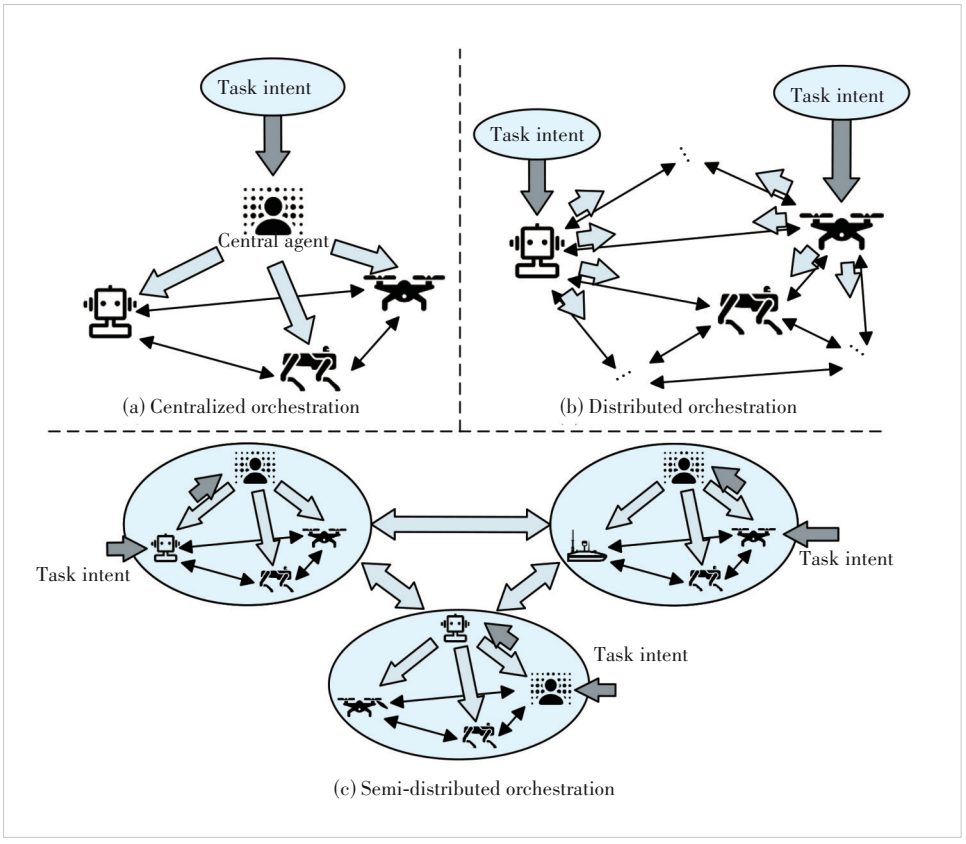

Figure 2. Three task orchestration modes in HaoNet

sive task completion[17].

The perception module monitors network connectivity, the physical environment, and agent capabilities. The analysis module handles intent recognition, conflict detection, intent refinement, and intent decomposition by utilizing LLMs and related processing tools. The planning module generates policies and resolves conflicts, drawing on analyzed data and other related tools to produce a new policy compatible with existing network policies. The execution module implements these policies using related execution tools to convert them into concrete configurations or actions. Interaction among these modules ensures reliable task execution and efficient collaboration with other agents.

3.3 Design of Architecture

Based on the above summarization, an architecture of an intent-driven control system for HaoNet is proposed, as shown in Fig. 4. The architecture comprises three layers: the application layer, the intent layer, and the infrastructure layer. The application and intent layers reside within each agent, while the agents and their surrounding physical and network environments form the infrastructure layer. The separation between the application and intent layers ensures modularity and functional clarity. The application layer handles user interaction and intent input, while the intent layer performs intent processing and decision-making, acting for closed-loop operation.

1) Application layer

The application layer is responsible for receiving task intents from users or applications. It supports flexible intent expressions through multi-modal inputs, including voice, text, and graphical interactions, thereby providing a user-friendly and intuitive interface. Serving as the entry point of the overall architecture, this layer abstracts the complexity of the underlying network.

2) Intent layer

The intent layer is responsible for interpreting task intents and transforming them into executable policies. It performs a complete technical workflow, including environment perception, intent refinement, intent decomposition, and policy generation, based on the agent's internal functional modules of Perception, Analysis, Planning, and Execution.

Environment perception collects heterogeneous contextual information from both the physical and network environments, providing essential inputs for subsequent processing. Intent re-

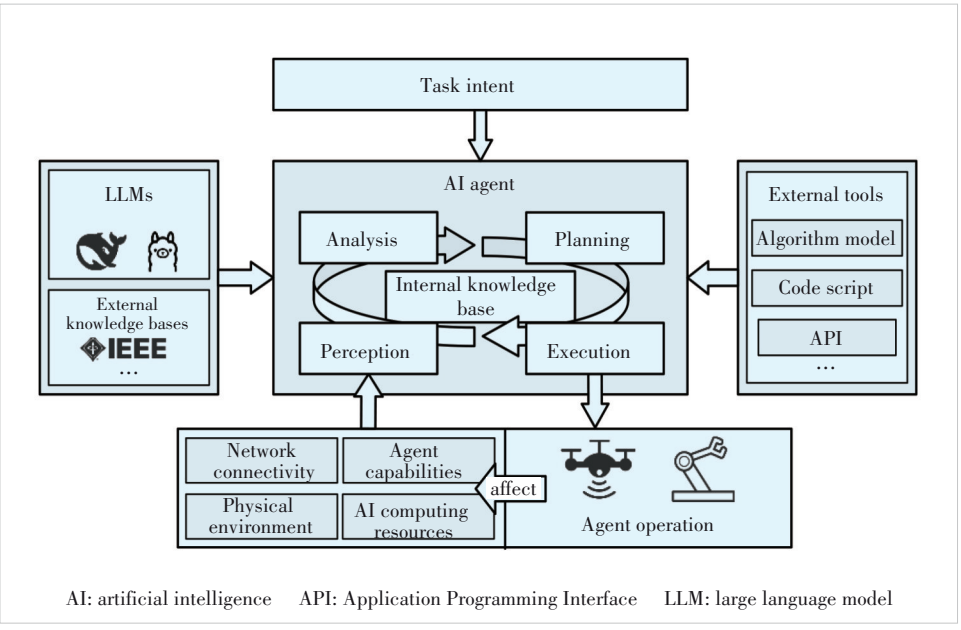

AI: artificial intelligence API: Application Programming Interface LLM: large language model

Figure 3. General internal architecture of agent

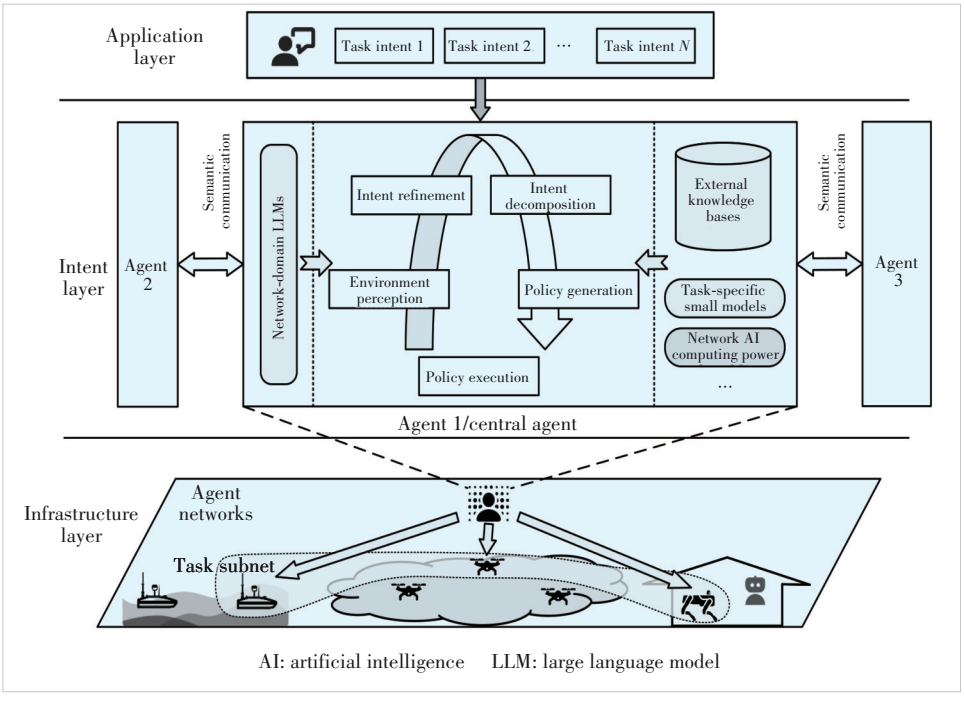

AI: artificial intelligence LLM: large language model

Figure 4. Architecture of an intent-driven control system for HaoNet

finement extracts explicit task requirements from user intents. Intent decomposition integrates the task requirements with environmental information to identify appropriate agent sub-groups, generate executable subtasks for individual agents, and coordinate their execution to optimize the fulfillment of the overall task intent. Based on the agent's current state and assigned subtask requirements, the policy generation function produces executable policies and delivers them to the execution module for concrete actions.

The intent layer incorporates semantic communication to support multi-modal and cross-modal information exchange among heterogeneous agents. Multi-modal inputs are encoded into unified semantic embeddings via modality-specific encoders, preserving task-relevant information for intent understanding, agent matching, and subtask coordination. These embeddings can be further transformed across modalities to ensure consistent interaction among agents with different capabilities. Structured interfaces based on MCP and A2A support context exchange, tool invocation, and task-level coordination, reducing redundant transmission and improving interoperability.

3) Infrastructure layer

The infrastructure layer is responsible for constructing task-specific subnets based on the matching results between agents and assigned subtasks, thereby enabling multi-agent collaboration. After receiving their respective subtasks, agents within a task subnet exchange information and adapt their execution policies in response to environmental dynamics, collectively working toward the optimal fulfillment of the overall task intent.

Built on the IDN framework, the architecture incorporates inter-agent semantic communication and implements workflows such as intent refinement and policy execution within the agents. Through continuous interactions within the three-layer architecture, the north – south direction realizes a full-lifecycle closed loop of task intent, from input and execution to assurance, while the east – west direction supports efficient collaboration among multiple agents, thus comprehensively ensuring the dynamic adaptability and flexible scheduling of HaoNet.

4 Key Technologies

To realize the intent-driven control system for HaoNet, this section presents the key technologies from three perspectives: Monitor-Analyze-Plan-Execute over a shared Knowledge (MAPE-K) based intent closed-loop and adaptive modes; LLM for intent recognition, refinement, decomposition, and mapping; and Coordination, Collaboration, and Cooperation (CoX) and large-small model collaboration mechanisms. These technologies form a general framework that can be flexibly adapted to different networks such as 5G/6G and unmanned ad-hoc networks.

4.1 MAPE-K Based Intent Closed-Loop and Adaptive Mode

To handle diverse task intents, agents must exhibit task adaptability and support closed-loop policy generation to ensure intent fulfillment. MAPE-K, an adaptive IDN architecture, consists of five components—Monitor, Analyze, Plan, Execute, and Knowledge—enabling autonomous management and intelligent optimization[18]. The internal MAPE-K architecture of the agent is shown in Fig. 5.

The Monitor, Analyze, Plan, and Execute components constitute the primary functional components of the agent. Knowledge serves as the data storage module, providing storage space for data interaction among the primary functional components. The Monitor captures environmental information through integrated sensors and data filtering tools. The Analyze component processes this data to perform intent refinement, decomposition, and conflict detection, leveraging LLMs and external knowledge bases to extract task requirements and generate subtasks while checking for conflicts with existing network policies. The Plan component generates executable policies by reconciling task requirements and detected conflicts, using LLMs and specialized small models. Finally, the Execute component implements these policies, employing code scripts and physical tools to carry out concrete task operations.

The MAPE-K architecture supports multiple patterns to accommodate different task scenarios, including coordinated control, information sharing, master-slave control, regional planning, and hierarchical control patterns[19]. In multi-agent collaboration, an MAPE-K based agent can dynamically select patterns according to task complexity, environmental conditions, and its own capabilities. The schematic diagrams of these five control modes across three task orchestration modes are shown in Fig. 6. While each agent in the figure contains all MAPE-K components, the diagrams highlight only the primary components utilized in each mode.

In the centralized orchestration mode, the main patterns are hierarchical control and master-slave control patterns. The hierarchical control pattern features a top-down structure, where the high level maintains a global network view and ensures long-term adaptive objectives, the middle level coordinates and manages multiple lower-level agents, and the low level handles direct execution, status monitoring, and short-term adaptive decisions. This pattern is well-suited for large-scale management systems, such as massive data centers, providing clear hierarchies but increasing management complexity. In contrast, the master-slave control pattern is simpler and easier to implement. The master agent handles analysis and planning, while slave agents focus on monitoring and execution. The master agent directly governs all slave agents, imposing higher stability requirements on the master and lacking the long- and short-term goal differentiation inherent to hierarchical control, making it better suited for small-scale agent networks.

In the distributed orchestration mode, the main patterns are coordination control and information sharing. The coordination control pattern emphasizes system consistency in intent execution. It requires the four MAPE-K components of each agent to

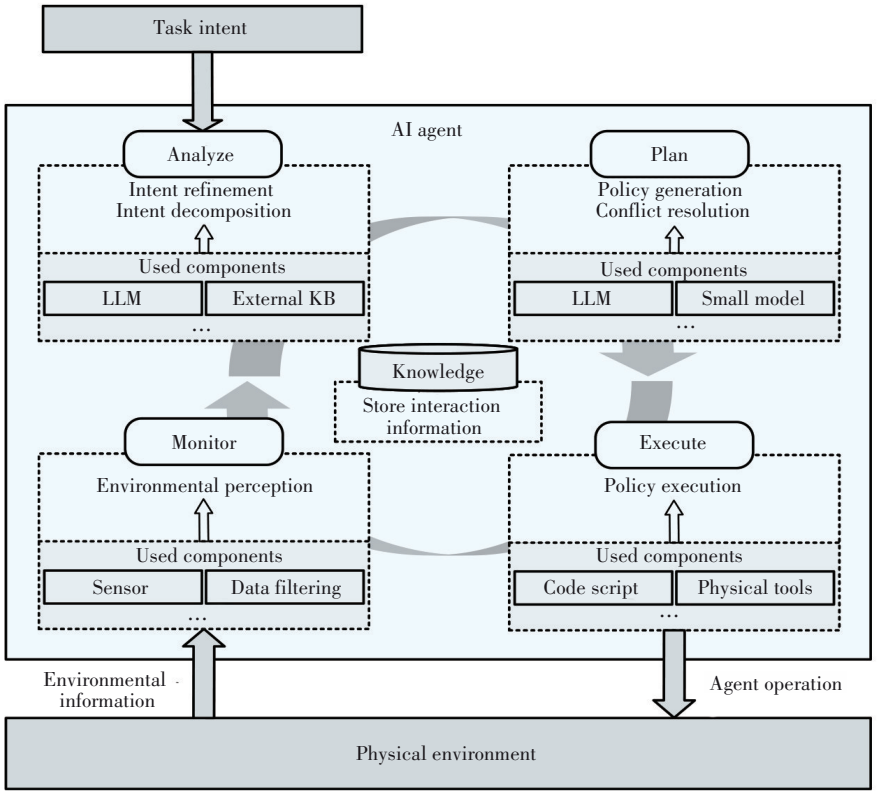

Figure 5. Internal MAPE-K architecture of the agent

interact with their counterparts in other agents. This pattern is suitable for tasks with high precision coordination requirements, but it also entails higher coordination costs. The information sharing pattern, by contrast, limits interaction to the Monitor component, while other components operate independently. It reduces complexity and inter-agent interactions, making it suitable for tasks such as distributed environmental monitoring, where information synchronization is prioritized over behavior.

In the semi-distributed orchestration mode, the main patterns are regional planning and master-slave control. In the regional planning pattern, a central agent is assigned the planning function within each region. Agent subnets achieve intra-domain objectives through local closed loops, while inter-domain objectives are accomplished via collaboration among the central agents of different regions. The master-slave control pattern integrates features of multi-regional planning, establishing master-slave control within each region while enabling collaboration among central agents across regions. Compared to master-slave control, regional planning provides greater autonomy to ordinary agents and reduces the computational burden on central agents, whereas master-slave control is more centralized, emphasizing the achievement of overall objectives. Both patterns are suitable for geographically dispersed tasks, balancing local adaptation with cross-regional optimization.

In large-scale agent-oriented networking scenarios, the scalability of the proposed control system is primarily enabled by the flexible adaptability of MAPE-K control patterns. Selecting appropriate patterns according to environmental characteristics ensures stable system operation. For example, in stable environments, hierarchical control provides large-scale structured collaboration, while in dynamic environments, information sharing and regional planning may enhance adaptability.

4.2 LLM for Intent Recognition, Refinement, Decomposition, and Mapping

For each task intent received by an agent, the processing workflows are performed in conjunction with its dependent LLM. The processing capability of the LLM largely represents the intelligence level of the agent. Therefore, to enhance the application of the LLM in specialized fields, this paper investigates the LLM for intent recognition, refinement, decomposition, and mapping, with the proposed technical architecture shown in Fig. 7.

In recent years, LLMs have attracted significant attention due to their powerful natural language processing capabilities, spurring extensive research on their application in networking[20–25]. However, deploying LLMs in highly specialized domains often faces challenges such as opaque internal mechanisms, limited interpretability, and hallucinations[26]. To improve reliability in professional network scenarios, mainstream approaches include fine-tuning[27] and prompt engineering[28]. Fine-tuning adjusts all or part of the model parameters on smaller, domain-specific datasets to enhance specialized performance, whereas prompt engineering operates at the input level, augmenting the user intent with additional information and instructions to elicit more accurate and comprehensive outputs.

This paper enhances the domain-specific performance of LLM through Parameter-Efficient Fine-Tuning (PEFT) and GraphRAG. PEFT trains only a subset of the LLM's parameters, with popular schemes including Prompt Tuning[29], LoRA[30], and Adapter Tuning[27]. An external knowledge base is constructed from network-domain documents, research papers, and expert knowledge, and is continuously updated as technology

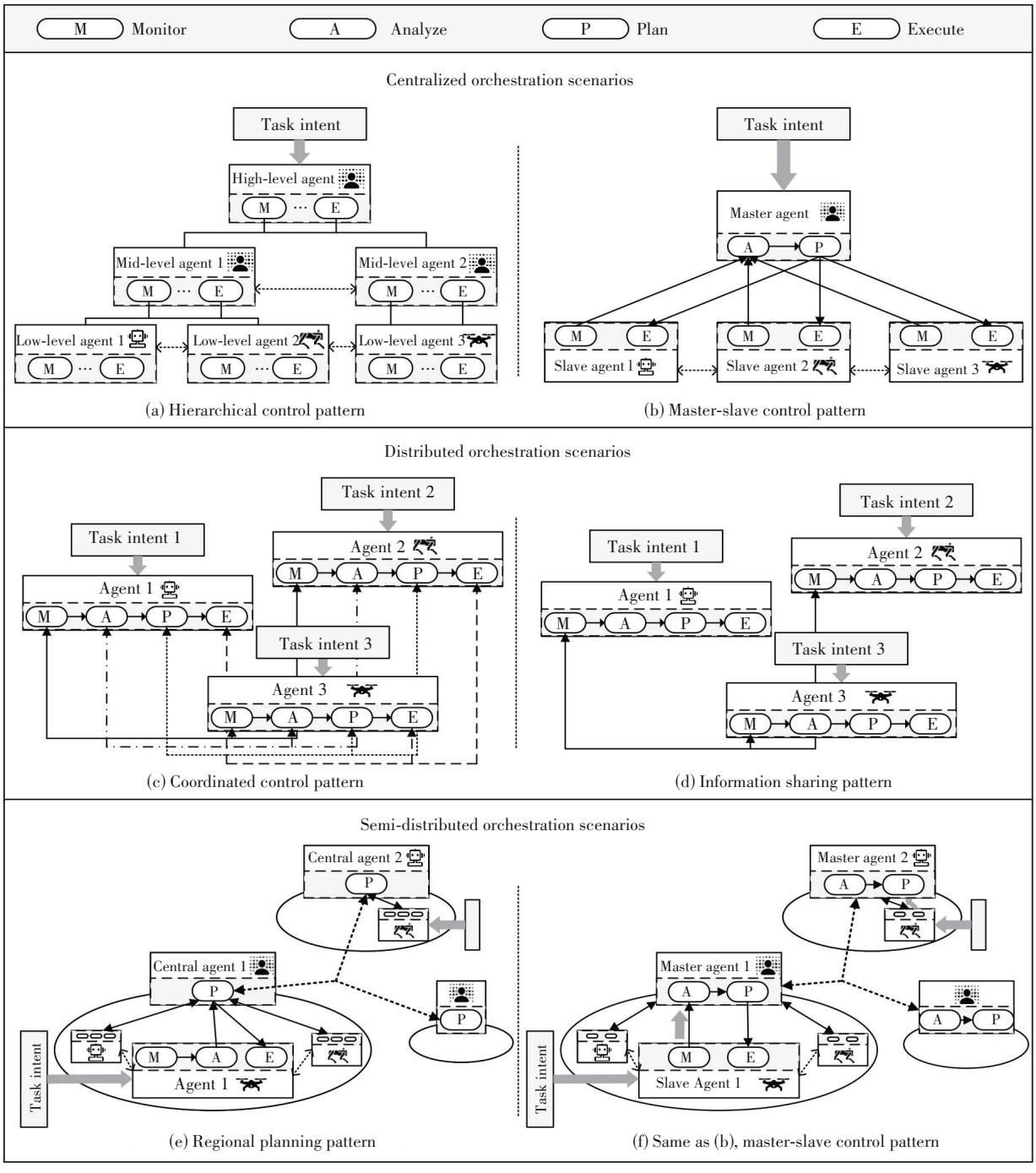

Figure 6. Five control patterns of MAPE-K across three task orchestration modes

evolves. The LLM is periodically fine-tuned using this knowledge base to achieve ongoing capability enhancement. GraphRAG[31–32], an extension of standard RAG and a prompt engineering technique, retrieves intent-related triplets from the knowledge base and performs graph-based expansions to enable contextual retrieval. The task intent, retrieved context, and relevant prompt templates are sequentially provided to the LLM according to the workflow. Combined with external model algorithms, this allows the LLM to perform task intent recognition, refinement, decomposition, and mapping. Additionally, environmental information collected by the agent's perception module is fed into the LLM to support comprehensive analysis and

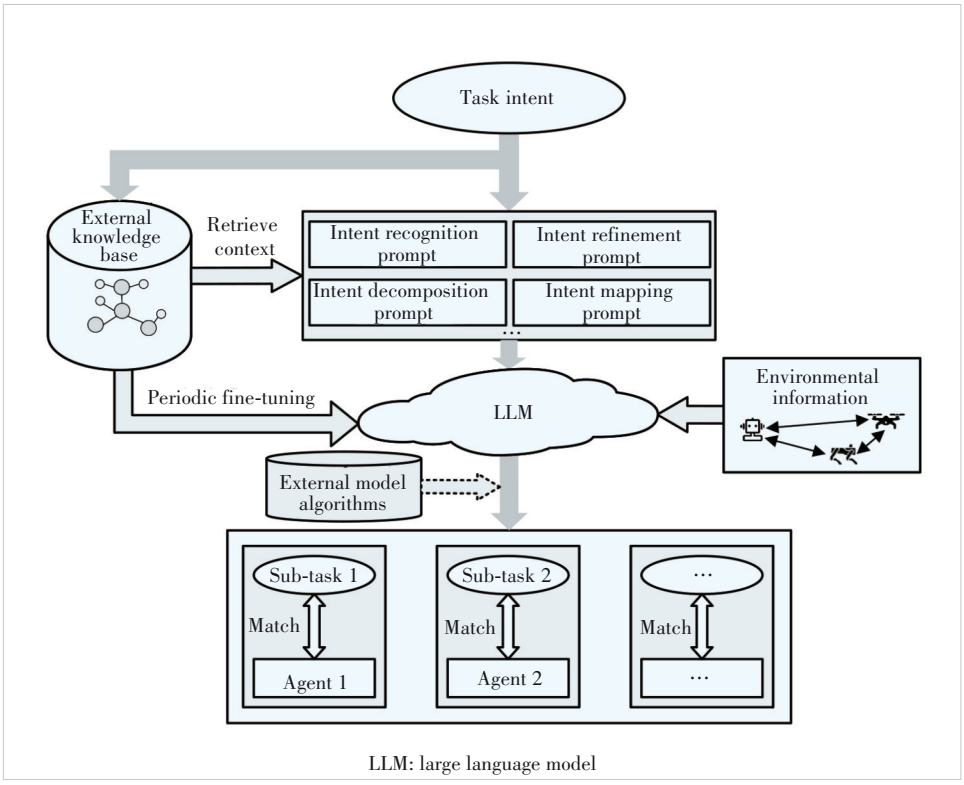

Figure 7. Technical architecture of LLM-based intent recognition, refinement, decomposition, and mapping

achieve optimal task-agent matching.

4.3 CoX and Large-Small Model Collaboration Mechanisms

To address challenges such as the difficulty of orderly governance over multiple agents, the design of the CoX mechanism is essential for ensuring reliable task intent execution. A schematic of the CoX mechanism within HaoNet is shown in Fig. 8.

Within the CoX mechanism, Coordination organizes and orchestrates agents, assigning subtasks to achieve complex objectives. Collaboration ensures that agents with distinct tasks work together to fulfill the overall mission, as individual efforts alone are insufficient. Cooperation allows idle agents to assist others when a subtask exceeds an agent's capacity[33]. In HaoNet, coordination refers to the rational partitioning of task intents into subtasks and their assignment to appropriate agents. Collaboration denotes that agents receiving subtasks form task subnets and interact according to orchestration specifications to ensure subtask execution and efficient realization of the overall task intent. Cooperation refers to scenarios in which an agent, when facing a subtask whose workload exceeds its reliable execution capability, seeks assistance from other idle agents with similar capabilities to jointly complete the subtask. Based on the CoX mechanism, task intents can be executed by multiple agents in a rational and orderly manner, ensuring the efficient operation of the AI-Agent Communication Network (ACN).

Within a single agent, a collaboration mechanism between large and small models is necessary to ensure efficient task execution. LLMs offer strong language understanding and generalization but incur high computational costs, slow inference, and limited specialization in decision-making. In contrast, small models are computationally efficient, fast, and excel at specialized decision-making, though they have weaker language processing and generalization. Additionally, Ref. [34] highlights that LLMs are insensitive to changes in numerical environmental conditions and lack precise decision-adjustment capabilities, motivating a symbiotic reinforcement learning approach with small models to achieve continuous optimization of the agent network. The large-small model collabora-

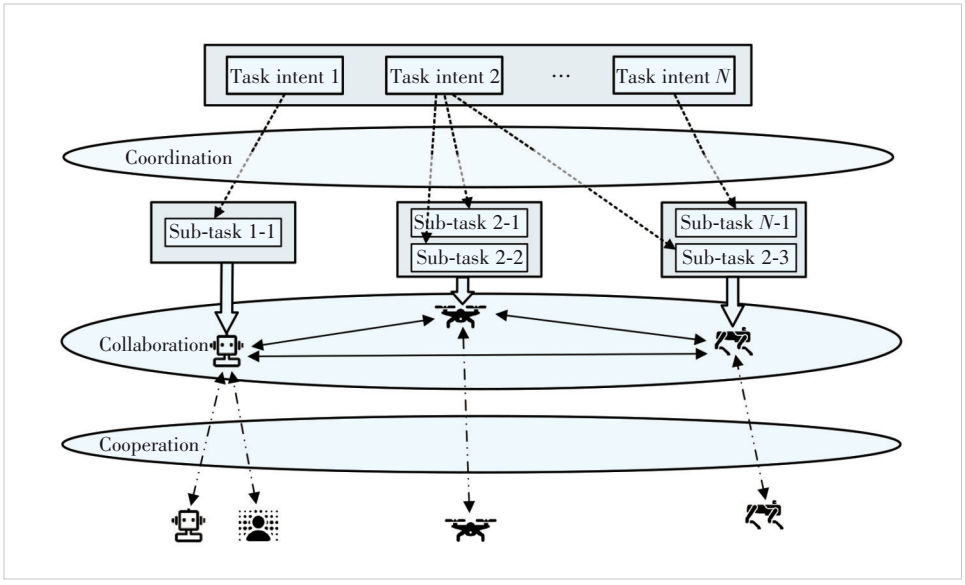

Figure 8. Schematic of CoX mechanism

tion mechanism is illustrated in Fig. 9.

The internal architecture of the agent integrates a domain-specific LLM for networking[23 - 24] and task-specific small models. Leveraging its natural language processing capabilities, the LLM identifies highly specialized tasks that require the expertise of a small model, initiates an invocation command, and forwards the request. By utilizing rule-based algorithms or pre-trained neural networks specific to concrete tasks within these small models, the system generates task policies that are professional and possess high real-time performance. Conversely, tasks involving extensive data analysis or language processing remain handled by the LLM itself. The final executable policy can either be directly generated by a task-specific small model or synthesized by the LLM based on feedback received from the small models. The large-small model collaboration mechanism combines the strengths of both, achieving adaptive selection of task processing strategies to support diverse tasks.

From a scalability perspective, the scalability of the proposed control system is primarily enabled by multiple MAPE-K control patterns. In addition, supporting mechanisms such as large-small model collaboration further improve system efficiency and responsiveness, facilitating practical deployment in complex scenarios. Together, these mechanisms enable the system to maintain performance as the system scales.

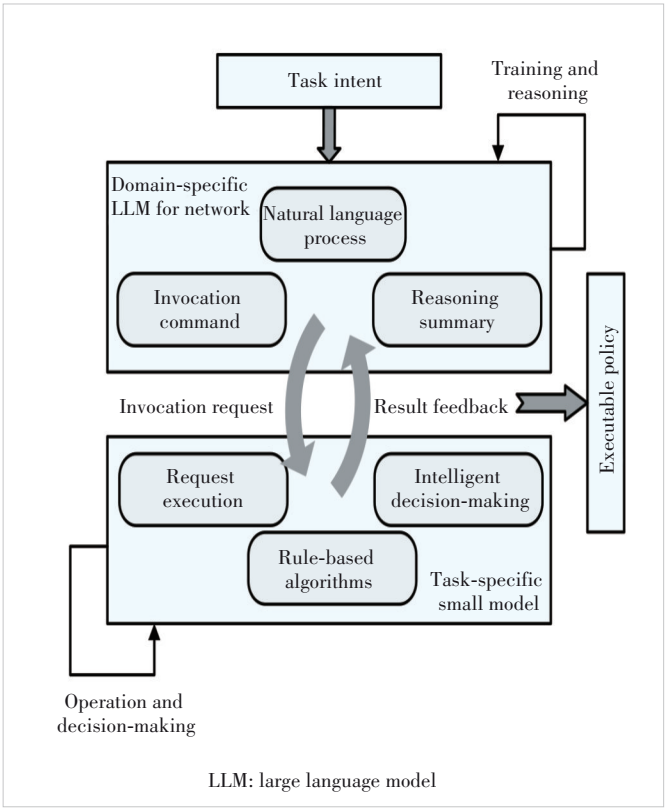

Figure 9. Schematic of large-small model collaboration mechanism

5 Application Scenarios

To demonstrate the practical value of the proposed system, we provide two representative application scenarios, as shown in Fig. 10.

1) Smart home scenario

Future smart homes are evolving from simple remote control and preset automation into complex ecosystems composed of multiple specialized agents. Consider a common return-home scenario in daily life: The system may include digital agents, such as home steward agents and health agents, as well as physical agents, such as robotic agents and quadruped robots. Before returning home, the user informs the home steward agent of the current intent: "Steward, I will be home in 30 minutes and I need a warm meal." Based on this intent, the home steward agent might assign a health agent to curate a nutritionally balanced recipe, command a quadrupedal robot to prepare the necessary ingredients, and finally delegate the cooking process to a robotic agent.

In this process, the proposed system plays a central role. When an unstructured intent is received, the intent layer performs intent refinement to identify specific task requirements. By referencing the real-time availability of agents based on the environment perception, the system executes an automated agent matching process and intent decomposition accordingly. Given the relatively stable and small-scale nature of smart home environments, the system utilizes the centralized task orchestration mode and selects the master-slave control pattern. Therefore, the home steward agent acts as the master agent, responsible for intent processing at the intent layer and for generating corresponding network policies according to the communication requirements among slave agents, thereby ensuring reliable communication during task execution.

Upon the successful formation of this task-specific subnet, the slave agents collaborate to complete their respective subtasks. After the overall task intent is fulfilled, the system systematically deallocates the dynamically configured resources and dissolves the task-specific subnet.

2) Smart factory scenario

Manufacturing factories are undergoing a digital transformation toward device-level intelligence, as they evolve into highly collaborative multi-agent networks. Consider a typical multi-production-line manufacturing scenario: Several production lines operate simultaneously, each managed by a dedicated main control agent. Under each main control agent, different types of agents are deployed to support production operations, including order reception agents, diagnostic agents, and robot agents. Meanwhile, the main control agents of different production lines exchange information and coordinate their actions to ensure balanced workloads and efficient collaboration across the entire factory.

Through continuous environment perception, the system obtains real-time information about the operational status of production lines, the availability of equipment agents, and the workload of embodied robots. Based on this information, the

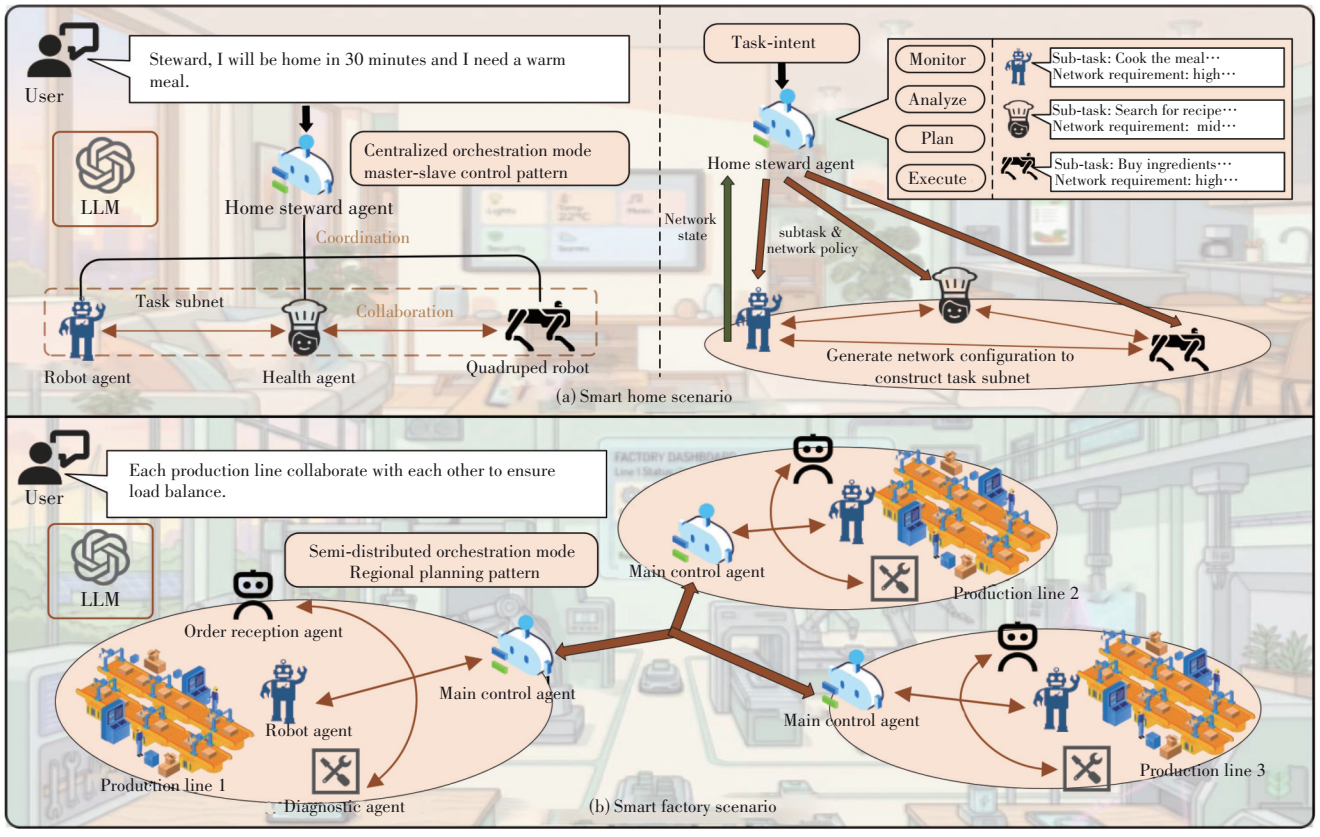

LLM: large language model

Figure 10. Two application scenarios of HaoNet: smart home and smart factory

system performs agent matching and intent decomposition, generating subtasks that are distributed to the corresponding agents within each production line. Considering the relatively large scale of industrial production systems and the need for both local autonomy and global coordination, the system adopts a semi-distributed task orchestration mode with a regional planning pattern. In this architecture, each production line is managed by its own main control agent responsible for local decision-making and for generating corresponding network policies according to the communication requirements among task agents, while inter-line communication among main control agents enables collaborative scheduling, load balancing, and global production optimization.

After the task-oriented subnet for a given production objective is established, the agents within each production line collaborate to complete their respective subtasks under the coordination of the local main control agent. Diagnostic agents continuously monitor production conditions, and robot agents perform the required physical manipulation tasks. Meanwhile, the main control agents exchange status information and coordinate resource allocation across production lines to maintain system-wide efficiency and stability. Through this mechanism, the proposed system supports flexible and intelligent coordination across heterogeneous agents, thereby improving production efficiency, operational reliability, and overall manufacturing adaptability in smart factory environments.

6 Conclusions

Heterogeneous agent-oriented networking aims to enable an interconnected and efficiently collaborative network for a large-scale population of heterogeneous agents. Leveraging the technical strengths of intent-driven networking, the proposed control system enhances networking effectiveness and task execution efficiency for heterogeneous agent-oriented networking, while enabling intent recognition, translation, and decomposition. By incorporating key technologies such as MAPE-K and the large-small model collaboration mechanism, it offers a novel architectural solution to advance future agent-oriented networking.

References

[1] ETSI GR ENI 051 v4.1.1: 2025 Experiential networked intelligence (ENI); study on AI agents based next-generation network slicing [S]
[2] Monica. Manus [EB/OL]. [2026-03-10]. https://manus.im
[3] Bytedance. Coze [EB/OL]. [2026-03-10]. https://www.coze.com
[4] China Mobile Think Tank. AI-agent communication network white paper [R]. Beijing: China Mobile, 2024

[5] Yang C G. Intent-driven autonomous network [M]. Beijing: Science Press, 2024
[6] Gupta M, Acharya V. Agnet: a novel AI agent network architecture [PP/OL]. SSRN [2026-03-10]. https://ssrn.com/abstract=5108385
[7] Wang Y T, Guo S L, Pan Y H, et al. Internet of agents: fundamentals, applications, and challenges [J]. IEEE transactions on cognitive communications and networking, 2026, 12: 4476 – 4501. DOI: 10.1109/TCCN.2025.3623369
[8] Anthropic. Model context protocol (MCP) [EB/OL]. [2026-03-10]. https://www.anthropic.com/news/model-context-protocol
[9] Google. Agent to agent protocol (A2A) [EB/OL]. [2026-03-10]. https://a2a-protocol.org/latest/
[10] Xiao Y, Shi G M, Zhang P. Toward agentic AI networking in 6G: a generative foundation model-as-agent approach [J]. IEEE communications magazine, 2025, 63(9): 68 – 74. DOI: 10.1109/MCOM.001.2500005
[11] Du C G, Wang C Y, Chao Y H, et al. AI agent communication from Internet architecture perspective: challenges and opportunities [PP/OL]. V1. arXiv (2025-09-02)[2026-03-10]. https://doi.org/10.48550/arXiv.2509.02317
[12] Minhas S, Jaswal R, Sharma A, et al. Revolutionizing networking: a comprehensive overview of intent-based networking [C]//Proceedings of International Conference on Emerging Innovations and Advanced Computing (INNOCOMP). IEEE, 2024: 463 – 468. DOI: 10.1109/INNOCOMP63224.2024.00081
[13] Jiang G Z, Wang K Z, Chen X M, et al. Agentic AI empowered intent-based networking for 6G [PP/OL]. V1. arXiv (2026-01-10)[2026-03-10]. https://doi.org/10.48550/arXiv.2601.06640
[14] Lee K Y. Intent-driven autonomous reconfiguration for telecom OSS: a generative-AI-empowered hierarchical multi-agent architecture [C]//Proceedings of 25th Asia-Pacific Network Operations and Management Symposium (APNOMS). IEEE, 2025: 1 – 6. DOI: 10.23919/APNOMS67058.2025.11181316
[15] Romero M L, Suyama R. Agentic AI for intent-based industrial automation [C]//Proceedings of 16th IEEE International Conference on Industry Applications (INDUSCON). IEEE, 2025: 437 – 444. DOI: 10.1109/INDUSCON66435.2025.11241317
[16] Chen S T, Liao Q, Aijaz A, et al. Goal-oriented multi-agent semantic networking: unifying intents, semantics, and intelligence [PP/OL]. V2. arXiv (2026-03-24)[2026-03-10]. https://doi.org/10.48550/arXiv.2512.01035
[17] Tong J W, Guo W, Shao J W, et al. WirelessAgent: large language model agents for intelligent wireless networks [PP/OL]. V1. arXiv (2025-05-02)[2026-03-10]. https://doi.org/10.48550/arXiv.2505.01074
[18] Dzeparoska K, Beigi-Mohammadi N, Tizghadam A, et al. Towards a self-driving management system for the automated realization of intents [J]. IEEE access, 2021, 9: 159882 – 159907. DOI: 10.1109/ACCESS.2021.3129990
[19] Weyns D, Schmerl B, Grassi V, et al. On patterns for decentralized control in self-adaptive systems [M]//Software Engineering for Self-Adaptive Systems II. Berlin, Heidelberg: Springer, 2013: 76 – 107. DOI: 10.1007/978-3-642-35813-5_4
[20] Jiang F B, Peng Y B, Dong L, et al. Large language model enhanced multi-agent systems for 6G communications [J]. IEEE wireless communications, 2024, 31(6): 48 – 55. DOI: 10.1109/MWC.016.2300600
[21] Saad W, Hashash O, Thomas C K, et al. Artificial general intelligence (AGI)-native wireless systems: a journey beyond 6G [J]. Proceedings of the IEEE, 2025, 113(9): 849 – 887. DOI: 10.1109/JPROC.2025.3526887
[22] Cui H W, Du Y Y, Yang Q, et al. LLMind: orchestrating AI and IoT with LLM for complex task execution [J]. IEEE communications magazine, 2025, 63(4): 214 – 220. DOI: 10.1109/MCOM.002.2400106
[23] Chen Y X, Li R P, Zhao Z F, et al. NetGPT: a native-AI network architecture beyond provisioning personalized generative services [PP/OL]. V4. arXiv (2024-03-09) [2026-03-10]. https://doi. org/10.48550/arXiv.2307.06148
[24] Zou H, Zhao Q Y, Tian Y, et al. TelecomGPT: a framework to build telecom-specific large language models [J]. IEEE transactions on machine learning in communications and networking, 2025, 3: 948 – 975. DOI: 10.1109/TMLCN.2025.3593184
[25] Wang X C, Ji S W, Li C. Research on intelligent computing network technology for large-scale pre-trained models [J]. Telecommunications science, 2024, 40(6): 160 – 172. DOI: 10.11959/j.issn.1000-0801.2024167
[26] Huang B, Wu S A, Wang W G, et al. KG-LLM-MCom: a survey on integration of knowledge graph and large language model [J]. Journal of Wuhan University (natural science edition), 2024, 70(4): 397 – 412. DOI: 10.14188/j.1671-8836.2024.0040
[27] Hu Z Q, Wang L, Lan Y H, et al. LLM-adapters: an adapter family for parameter-efficient fine-tuning of large language models [C]//Proceedings of the 2023 Conference on Empirical Methods in Natural Language Processing. Stroudsburg, PA, USA: ACL, 2023: 5254 – 5276. DOI: 10.18653/v1/2023.emnlp-main.319
[28] Mekrache A, Ksentini A. LLM-enabled intent-driven service configuration for next generation networks [C]//Proceedings of IEEE 10th International Conference on Network Softwarization (NetSoft). IEEE, 2024: 253 – 257. DOI: 10.1109/NetSoft60951.2024.10588881
[29] Lester B, Al-Rfou R, Constant N. The power of scale for parameter-efficient prompt tuning [C]//Proceedings of the 2021 Conference on Empirical Methods in Natural Language Processing. ACL, 2021: 3045 – 3059. DOI: 10.18653/v1/2021.emnlp-main.243
[30] Hu E J, Shen Y, Wallis P, et al. LoRA: low-rank adaptation of large language models [C]//International Conference on Learning Representations. ICLR, 2022: 1 – 20. DOI: 10.48550/arXiv.2106.09685
[31] Han H Y, Wang Y, Shomer H, et al. Retrieval-augmented generation with graphs (GraphRAG) [PP/OL]. V2. arXiv (2025-01-08) [2026-03-10]. https://doi.org/10.48550/arXiv.2501.00309
[32] Edge D, Trinh H, Cheng N, et al. From local to global: a graph RAG approach to query-focused summarization [PP/OL]. V2. arXiv (2025-02-19)[2026-03-10]. https://doi.org/10.48550/arXiv.2404.16130
[33] Ou Y Y. Intelligent intent policy refinement of space-terrestrial network [D]. Xi'an: Xidian University, 2023
[34] Liu Y Q, Liu G Y, Wang J C, et al. LAMeTA: intent-aware agentic network optimization via a large AI model-empowered two-stage approach [J]. IEEE journal on selected areas in communications, 2026, 44: 2462 – 2478. DOI: 10.1109/JSAC.2025.3642840

Biographies

Wang Bowen is currently pursuing his doctoral degree with the GUIDE family at Xidian University, China. His research interests include intent-driven networks, large AI models, and software-defined networks.

Lu Lu received her master's degree from Beijing University of Posts and Telecommunications, China. She is currently the Deputy Director of the Department of Basic Network Technology, China Mobile Research Institute; the leader of the Core Network Group, CCSA TC5; and the Vice Chair of ITU-T SG13. Her main research interests include 5G/6G network architecture and next-generation IP technology.

Li Huimin is currently pursuing a master's degree in the GUIDE family at Xidian University, China. Her research interests include intent-driven networks, agents, and software-defined networks.

Yang Chungang (guideyang2050@163.com) is a full professor at Xidian University, China. His research interests are AI-enabled 6G wireless mobile networks, intent-driven networks, space-terrestrial networks, and game theory for emerging communication networks.

Mitigating Semantic Drift in Multi-Agent Communication: A Dynamic Neuro-Symbolic Approach

Xie Linhao[1,2], Li Fan[3], Wu Mingxuan[4], Song Yong[1], Ouyang Ye[1]

(1. AsiaInfo Technologies, Beijing 100193, China;
2. Communication University of China, Beijing 100024, China;
3. China Unicom Beijing Branch Network Optimization Center, Beijing 100032, China;
4. CRSC Information Industry Co., Ltd., Beijing 100070, China)

DOI: 10.12142/ZTECOM.202602008

https://kns.cnki.net/kcms/detail/34.1294.TN.20260429.0945.002.html, published online April 29, 2026

Manuscript received: 2026-02-24

Abstract: The emergence of multi-agent systems (MAS) based on large language models (LLMs) has enabled autonomous collaboration on complex, goal-oriented tasks. However, effective interaction is frequently hindered by semantic drift, a phenomenon where heterogeneous agents assign conflicting meanings to shared terminology due to differing internal prompts or domain knowledge. Existing communication paradigms either rely on unconstrained natural language, which suffers from structural vagueness, or rigid symbolic schemas that fail to adapt to emergent concepts. To address this gap, we propose DOA, a novel dynamic ontology alignment framework that serves as a semantic mediation layer for MAS. DOA integrates a proactive semantic prober to detect conceptual mismatches and a neuro-symbolic aligner that reconciles local semantic structures in real time. By grounding fluid natural language dialogues in an evolving shared ontology, our framework ensures deterministic mutual understanding over long-horizon tasks. Empirical evaluations in cross-domain supply chain and healthcare coordination scenarios demonstrate that DOA improves task success rates by an average of 31.5% and reduces communication overhead (token consumption) by 50% compared to state-of-the-art baselines. Our results provide a robust and scalable foundation for semantic consistency in next-generation industrial-grade AI systems.

Keywords: DOA; multi-agent systems; neuro-symbolic AI; semantic drift; large language models

Citation (Format 1): Xie L H, Li F, Wu M X, et al. Mitigating semantic drift in multi-agent communication: a dynamic neuro-symbolic approach [J]. ZTE Communications, 2026, 24(2): 64 - 70. DOI: 10.12142/ZTECOM.202602008

Citation (Format 2): L. H. Xie, F. Li, M. X. Wu. "Mitigating semantic drift in multi-agent communication: a dynamic neuro-symbolic approach," *ZTE Communications*, vol. 24, no. 2, pp. 64 - 70, Jun. 2026. doi: 10.12142/ZTECOM.202602008.

1 Introduction

The rapid advancement of large language models (LLMs) has fundamentally transformed the landscape of artificial intelligence, shifting focus from individual generative tasks toward the development of autonomous, goal-oriented multi-agent systems (MAS). By simulating human-like organizational structures and collaborative reasoning, LLM-based agents have demonstrated unprecedented capabilities in solving multifaceted problems, ranging from automated software engineering to complex scientific discovery[1]. In these distributed environments, communication serves as the vital substrate that enables information exchange, task synchronization, and collective consensus[2]. However, as the complexity of collaborative tasks scales, the fundamental limitations of existing communication protocols have become increasingly apparent[3].

A critical yet often overlooked challenge in agent-to-agent interaction is the phenomenon of semantic drift, as illustrated in Fig. 1. Despite their linguistic fluency, LLM-based agents lack a shared, deterministic conceptual framework. Because agents are often initialized with different system prompts, role-specific instructions, or private domain knowledge, they frequently assign conflicting meanings to the same terminology. This "contextual drift" creates a subtle but destructive form of ambiguity, where agents operate under the illusion of agreement while pursuing divergent logical paths[4 - 5]. Recent studies have begun to quantify this drift, revealing that even minor misalignments in initial conceptual grounding can lead to significant reasoning hallucinations and a degradation in system reliability, particu-

This work is supported by Mobile Information Networks-National Science and Technology Major Project of China under Grant No. 2025ZD1304800.

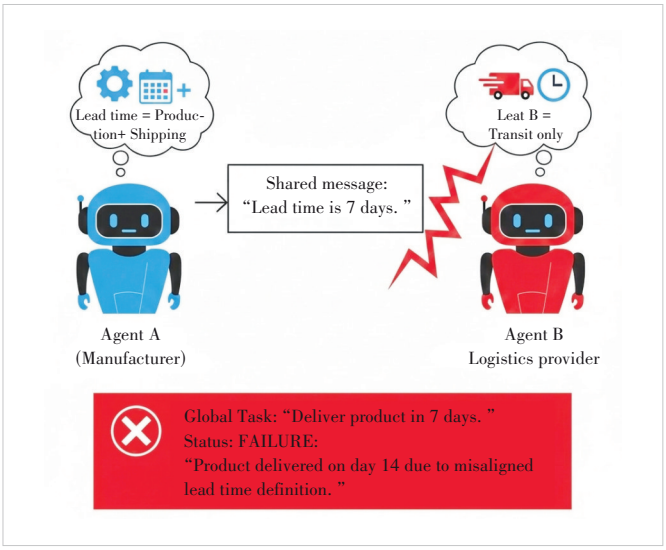

Figure 1. Semantic drift in multi-agent communication

larly in safety-critical applications such as autonomous healthcare or industrial supply chain management[6].

Research into agent communication has primarily oscillated between two suboptimal extremes. On one hand, unconstrained natural language communication offers maximum flexibility but suffers from structural vagueness and high computational overhead due to excessive token consumption[2]. On the other hand, traditional symbolic approaches, such as static ontologies, provide rigorous formalisms but are inherently too rigid to accommodate the emergent, non-predefined concepts that LLMs generate during real-time problem solving[7]. While recent efforts have explored using LLMs to assist in offline ontology matching[8-9], these methods fail to address the fluid nature of live agent-to-agent dialogues. This dichotomy necessitates a new paradigm that combines the logical rigor of formal ontologies with the adaptive reasoning of neural models[10].

To bridge this gap, we propose a novel framework called dynamic ontology alignment (DOA) for LLM-based multi-agent communication. Rather than imposing a predefined, "one-size-fits-all" global schema, our approach enables agents to autonomously negotiate and align their local semantic structures in real time as the dialogue progresses. The proposed DOA mechanism incorporates a proactive semantic probing protocol to detect conceptual mismatches at the onset of interaction, coupled with a neuro-symbolic alignment mediator that resolves conflicts by reasoning over hierarchical constraints. By dynamically grounding natural language communication in an evolving shared ontology, the DOA framework ensures that agents maintain semantic consistency across long-horizon tasks. Empirical evaluations in cross-domain collaborative scenarios demonstrate that our method significantly improves task success rates while reducing communication redundancy, providing a robust and scalable foundation for next-generation industrial-grade AI systems[11].

2 Related Work

The development of LLM-based MAS has necessitated a re-evaluation of how autonomous entities coordinate and share knowledge. Our work lies at the intersection of agent communication protocols[12-13], semantic alignment, and neuro-symbolic integration.

Existing communication protocols in LLM-based MAS fall into two main categories (also referred to as paradigms)[14]. The first is unconstrained natural language interaction, popularized by frameworks such as AutoGPT and MetaGPT, which leverage the linguistic flexibility of LLMs to simulate human-like collaboration. While versatile, these systems are prone to logical inconsistencies and "hallucinated" instructions. The second paradigm employs structured formats, such as JavaScript Object Notation (JSON) or predefined Application Programming Interface (API) schemas, to enforce syntactical consistency. However, these rigid structures often fail to capture the nuanced semantic relationships inherent in complex, multi-domain tasks, creating a "semantic gap" between the agent's internal reasoning and the external communication interface[15].

Ontology matching has evolved from classical algorithms to LLM-enhanced approaches[16-17]. Ontology matching is a well-established field in the Semantic Web community, traditionally focused on finding correspondences between heterogeneous metadata schemas. Classical approaches, such as LogMap and AgreementMakerLight (AML), utilize graph-based matching and lexical similarity to align static ontologies. While effective for stable datasets, these methods lack the contextual adaptability required for generative AI environments[18]. Recent studies, such as Agent-OM, have demonstrated that LLM-based agents can outperform traditional algorithms in identifying complex semantic mappings by leveraging their vast parametric knowledge. Nevertheless, most existing LLM-enhanced ontology matching methods, such as LLMs4om and Agent-OM, are primarily designed for offline alignment of static schema files. These approaches lack the temporal responsiveness and dynamic negotiation capabilities required for live, multi-turn agent dialogues where concepts emerge contextually. In contrast, DOA introduces a real-time mediation layer that specifically targets these "on-the-fly" semantic discrepancies. Semantic drift and the challenge of reaching consensus have been central to research on multi-agent collaboration[17]. A fundamental challenge in long-horizon agent interaction is semantic drift, where the shared understanding of a concept gradually diverges as the conversation progresses. Research into "Shared Mental Models" suggests that for effective collaboration, agents must maintain a synchronized internal representation of the task environment[19]. Becker et al.[5] quantified this drift in multi-turn interactions, noting that without an explicit grounding mechanism, agents frequently succumb to "Contextual Illusion", i.e., the false assumption of mutual understanding. Our work ad-

dresses this by introducing a dynamic re-alignment mechanism that acts as a continuous grounding layer, preventing the accumulation of semantic errors.

The landscape of semantic alignment has shifted significantly in 2024 and 2025 with the advent of more sophisticated reasoning frameworks. For instance, He et al.[20] provided a comprehensive vision for LLM-based MAS in software engineering, identifying semantic consistency as a critical bottleneck for long-horizon task coordination. Furthermore, the emergence of neuro-symbolic hybrids, as discussed by Bougzime et al.[21], underscores the necessity of combining generative flexibility with logical rigor, i.e., a principle that lies at the core of our DOA framework. Other recent works, like Kamali et al.[18], have explored compositional generalization in neuro-symbolic agents, further justifying our approach to dynamic concept grounding.

Neuro-symbolic integration and dynamic schema generation offer promising directions for robust agent communication[20]. The integration of neural models with symbolic reasoning (Neuro-Symbolic AI) provides a promising path toward more robust agent communication[21]. By grounding the "soft" reasoning of LLMs in the "hard" constraints of formal ontologies, systems can achieve both creativity and reliability[11]. Furthermore, emerging research in dynamic schema generation explores how systems can evolve their data structures in response to novel inputs. Our proposed DOA framework extends this concept by treating the ontology not as a static artifact but as a living protocol that is negotiated and refined through agent interaction, thereby combining the adaptability of neural agents with the precision of symbolic logic.

3 Methodology

The DOA framework serves as a semantic mediation layer that operates between an agent's internal reasoning engine and its external communication interface. It ensures that heterogeneous agents reach a state of mutual understanding by dynamically resolving conceptual discrepancies.

We define a MAS as a tuple $\mathcal{S} = (A, O, \Gamma)$, where $A = \{A_1, A_2, \cdots, A_n\}$ represents the set of autonomous agents, $O = \{O_1, O_2, \cdots, O_n\}$ denotes the set of local ontologies held by each agent, and Γ signifies the operational task context.

Each local ontology O_i is a structured graph (C_i, R_i, Σ_i), consisting of concepts C, relations R, and logical constraints Σ. Semantic divergence occurs when two agents A_i and A_j assign different internal representations to the same linguistic token T.

3.1 Definition of Semantic Drift Degree

Let C be a concept invoked in a message, and let $\sigma(C, O_i) \epsilon = \mathbb{R}^d$ be the semantic embedding of the concept derived from the LLM's parametric knowledge grounded in ontology O_i. The semantic drift δ between agents A_i and A_j regarding concept C is defined as:

$$\delta(A_i, A_j | C) = 1 - \frac{\sigma(C, O_i) \cdot \sigma(C, O_j)}{\left\| \sigma(C, O_i) \right\| \left\| \sigma(C, O_j) \right\|} \quad (1).$$

A mediation process is triggered if and only if $\delta > \tau$, where τ is a predefined tolerance threshold for semantic precision.

3.2 System Architecture

The DOA architecture comprises three primary modules:

• Semantic Prober: responsible for extracting concept snippets from outbound messages and identifying potential conflicts in inbound headers.

• Neuro-Symbolic Aligner: a hybrid reasoning engine that utilizes the LLM's zero-shot reasoning to propose mappings and a symbolic reasoner to verify logical consistency.

• Dynamic Consensus Vault (DCV): a volatile, session-based repository; in the implementation, it is referred to as the Volatile Consensus Vault (V). It caches established mappings $\varnothing$ to ensure temporal consistency and reduce redundant negotiations.

3.3 Dynamic Alignment Algorithm

The core logic for resolving semantic conflicts is encapsulated in the dynamic alignment algorithm. Unlike traditional batch-matching techniques, this algorithm operates on demand during the dialogue. Algorithm 1 delineates the end-to-end execution flow for resolving semantic discrepancies during active agent-to-agent dialogue. The process begins with a lightweight concept extraction phase, which isolates key predicates from the natural language stream. A critical component is the use of the semantic drift function (δ) in Step 2, which acts as a computational "trigger" to ensure that expensive reasoning resources are invoked only when conceptual divergence exceeds the tolerance threshold τ. By integrating a symbolic check in Step 4, the algorithm guarantees that the neural-generated mappings do not violate the hard logical constraints (Σ) of the domain, thereby preventing "hallucinated" alignments that often plague purely LLM-based systems. From a computational perspective, Step 2 (Compatibility Analysis) is a lightweight operation with a time complexity of $O(d)$, where d is the embedding dimension, typically executed on a CPU or a small-scale embedding model. In contrast, LLM_DeepReasoning is the primary consumer of resources, involving a forward pass of an LLM. Its GPU memory consumption scales with the context length of the source concept definition (D_{src}) and the local ontology (O_{rec}), though this cost is mitigated by the lazy alignment strategy described in Section 3.4.

Algorithm 1: LLM-driven dynamic alignment process

Input: Source message M_{src}, Source concept definition D_{src}, Recipient local ontology O_{rec}, Context Γ
Output: Alignment mapping rule $\varnothing$
1. **Step 1: Concept Extraction**

2. $E \leftarrow \text{Parse}(M_{src})$ //Extract primary predicate P and attributes {attr}
3. **Step 2: Compatibility Analysis**
4. $\delta \leftarrow \text{ComputeSemanticDrift}(P_{src}, P_{rec}, \Gamma)$
5. **If** $\delta > \tau$ **then**
6. $R_{deep} \leftarrow \text{LLM\_DeepReasoning}(D_{src}, O_{rec}, \Gamma)$// Invoke Neural Phase
7. **Step 3: Conflict Resolution**
8. **If** $\text{isSubset}(P_{src}, P_{rec})$ **then**
9. $\varnothing \leftarrow \text{DefineSubsumptionMapping}(P_{src}, P_{rec})$
10. **Else if** $\text{hasAttributeMismatch}(\{attr_{src}\},\{attr_{rec}\})$ **then**
11. $f \leftarrow \text{GenerateTransformation}(x)$ // e.g., unit conversion
12. $\varnothing \leftarrow \text{ApplyTransformation}(f)$
13. **End if**
14. **Else**
15. $\varnothing \leftarrow$ IdentityMapping
16. **End if**
17. **Step 4: Consistency Verification**
18. **If** $\text{SymbolicCheck}(\varnothing,\Sigma)$ is False **then**
19. $\varnothing \leftarrow \text{RefineMapping}(\varnothing,\Sigma)$ // Resolve logical contradictions
20. **End if**
21. **Step 5: Consensus Commitment**
22. $\text{UpdateDCV}(\varnothing)$ // Store in Dynamic Consensus Vault
23. $\text{NotifyAgents}(A_{src}, A_{rec}, \varnothing)$
24. **Return** $\varnothing$

3.4 Pseudo-Code Implementation

The following pseudo-code illustrates the implementation of the alignment mediator using a neuro-symbolic algorithm. Algorithm 2 formalizes the internal reasoning mechanism of the DOA mediator. The mediator follows a "lazy alignment" strategy facilitated by the Volatile Consensus Vault (V), which minimizes redundant negotiation by caching successful mappings within the session context. The architecture exemplifies a neuro-symbolic hybrid approach: Phase 2 leverages the zero-shot reasoning capabilities of LLMs to handle linguistic variety, while Phase 3 enforces logical rigor via symbolic verification. If a mapping fails the consistency check, the mediator initiates a recursive refinement loop, ensuring that the final consensus is both semantically rich and logically sound before it is committed to the shared environment.

Algorithm 2: Dynamic ontology alignment mediator

Input: Source concept C_{src}, Recipient concept C_{rec}, Task context Γ
Output: Aligned semantic mapping rule $\varnothing$

1. **Phase 1: Volatile Cache Lookup**
2. $key \leftarrow \text{concatenate}(C_{src}\cdot\text{uid}, C_{rec}\cdot\text{uid})$
3. **If** key $\in V_{consensus}$ **then**
4. **Return** $V_{consensus}[\text{key}]$ // Retrieve from shared consensus vault
5. **End if**
6. **Phase 2: Neuro-Symbolic Inference**
7. $\mathcal{P} \leftarrow \text{GenerateAlignmentPrompt}(C_{src}, C_{rec}, \Gamma)$
8. $\varnothing_{raw} \leftarrow \text{LLM\_Reasoning}(\mathcal{P})$ // **Neural Phase:** LLM-based semantic
9. **Phase 3: Symbolic Consistency Verification**
10. **If** $\text{SymbolicReasoner.check}(\varnothing_{raw}, C_{rec}\cdot\Sigma)$ **then**
11. $V_{consensus}[\text{key}] \leftarrow \varnothing_{raw}$ // Commit to volatile cache
12. **Return** $\varnothing_{raw}$
13. **Else**
14. // **Refinement Phase:** Recursive negotiation if logic verification fails
15. **Return** $\text{RefineNegotiation}(C_{src}, C_{rec})$
16. **End if**

3.5 Grounded Message Transformation

Once the mapping $\varnothing$ is established, the original message M is transformed into a grounded message M^*. This transformation is defined by a function $\mathcal{G}$:

$$M^* = \mathcal{G}(M, \varnothing, \Gamma) \tag{2}$$

In M^*, ambiguous natural language tokens are replaced or augmented with unique semantic identifiers, i.e., Uniform Resource Identifiers (URIs) from the aligned space. This ensures that Agent A_{rec} can deserialize the message into its internal state with deterministic accuracy, thereby eliminating downstream errors in the collaborative workflow.

4 Experimental Evaluation

In this section, we evaluate the DOA framework's efficacy in resolving semantic conflicts and improving collaborative performance in multi-agent systems. Our experiments aim to answer three key research questions (RQs):

RQ1: Does DOA improve the success rate of complex tasks compared to standard LLM-based communication?

RQ2: How robust is the framework against increasing levels of semantic drift?

RQ3: Does the neuro-symbolic alignment significantly reduce communication overhead (tokens) compared to raw natural language negotiation?

4.1 Experimental Setup

1) Datasets and environments

We utilized two distinct environments to simulate heterogeneous agent interactions:

• Cross-domain supply chain (CDSC): Agents represent a manufacturer (using ISO-based terminology) and a logistics provider (using proprietary transport schemas). The task requires synchronizing inventory levels and shipping schedules where units and lead times are intentionally mismatched.

• Autonomous healthcare coordination (AHC): Diagnostic agents and therapeutic agents must collaborate, using Systematized Nomenclature of Medicine—Clinical Terms (SNOMED CT) standard ontology[22] and International Classification for Diseases (ICD)-10 ontologies[23], respectively.

2) Baseline models

We compared DOA against three baselines:

• Raw-NL: unconstrained natural language communication;

• Fixed-Schema: Agents are forced to use a predefined JSON schema (static);

• LLM-Prompt-Only: Agents are prompted to "be clear and define terms" but have no formal alignment mechanism.

3) Implementation details

We used DeepSeek-R1 as the core LLM for the Neuro-Symbolic Aligner and used the Protege-OWL API for symbolic consistency checking. The drift threshold is set to τ = 0.3. Additionally, all experiments were conducted on a server equipped with dual NVIDIA H100 (80 GB) GPUs and an Intel Xeon Platinum 8480C CPU to ensure reproducible latency measurements.

4.2 Task Success Rate (RQ1)

We conducted 100 trials for each environment. A trial was marked as successful only if the final state matched the global goal without any constraint violations.

As shown in Table 1, DOA outperforms the best baseline (LLM-Prompt-Only) by over 25%. The failure of the Fixed-Schema in complex tasks highlights the inability of static structures to handle the emergent concepts required for multi-domain reasoning.

Unlike baseline methods that rely solely on the LLM's internal parametric knowledge (similar to the mechanism in LLM-Prompt-Only), DOA's superiority lies in its Neuro-Symbolic hybridity. While state-of-the-art LLM-based aligners often focus on lexical similarity, our framework ensures that proposed mappings are validated against hard logical constraints (Σ), preventing the reasoning hallucinations that often lead to task failure in purely neural approaches.

Table 1. Task success rate across frameworks in CDSC and AHC

Framework	CDSC/%	AHC/%	Average/%	Improvement over Baseline/%
Raw-NL	62.5	54.0	58.3	**31.5**
Fixed-Schema	45.0	38.5	41.8	**48.0**
LLM-Prompt-Only	67.5	61.5	64.5	**25.3**
DOA (Ours)	**91.5**	**88.0**	**89.8**	–

AHC: autonomous healthcare coordination
CDSC: cross-domain supply chain
DOA: dynamic ontology alignment
LLM: large language model
NL: natural language

4.3 Robustness to Semantic Drift (RQ2)

To evaluate the resilience of the DOA framework, we conducted a sensitivity analysis by manually injecting "semantic noise" into the agents' local ontologies. We controlled the semantic drift degree (δ) by perturbing concept embeddings with Gaussian noise and introducing disjoint taxonomic labels for identical concepts, ranging from δ = 0.1 (minor terminology variation) to δ = 0.6 (significant conceptual misalignment). The detailed success rates under different drift levels are shown in Table 2.

As illustrated in Fig. 2, there is a clear "performance cliff" for baseline methods.

• Breakdown of Raw-NL: When δ > 0.3, the performance of the Raw-NL baseline collapses. This confirms the "contextual illusion" hypothesis, i.e., agents continue to communicate using shared tokens but are unaware that their underlying logical grounding has diverged, leading to irreversible reasoning errors.

• DOA's graceful degradation: In contrast, the DOA frame-

Table 2. System success rate vs. semantic drift (δ)

Drift (δ)	Raw-NL/%	Fixed-Schema/%	LLM-Prompt-Only/%	**DOA (Ours)/%**
0.1 (Low)	90.3	88.0	92.5	**96.0**
0.2	75.5	72.8	83.3	**94.0**
0.3 (Threshold)	58.3	41.8	64.5	**89.8**
0.4	32.3	22.0	43.5	**88.3**
0.5 (High)	16.5	12.3	24.3	**82.5**
0.6 (Critical)	6.5	5.0	11.0	**65.8**

DOA: dynamic ontology alignment
LLM: large language model
NL: natural language

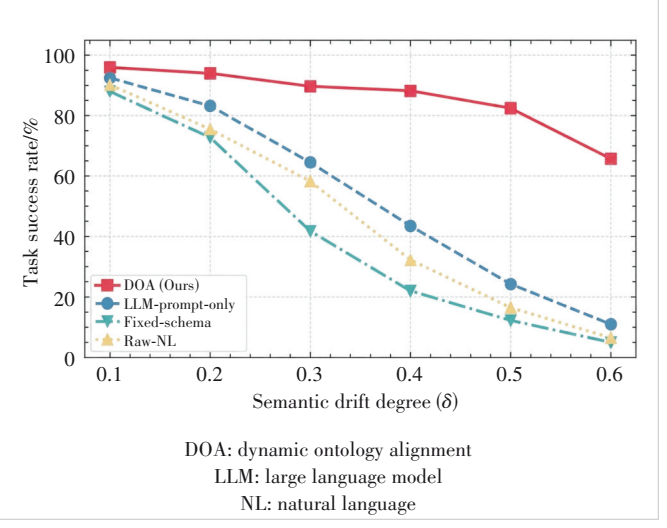

DOA: dynamic ontology alignment
LLM: large language model
NL: natural language

Figure 2. Robustness analysis of the impact of semantic drift δ on task success rate, where the DOA framework maintains stability compared to the sharp decline of baseline methods

work maintains a success rate above 80% even at high levels of drift (δ = 0.5). The stability of the curve is attributed to the semantic prober's proactive detection mechanism. By calculating the drift before the task execution begins, DOA triggers the Neuro-Symbolic Aligner to bridge the gap early.

• Symbolic anchor: Even at the "Critical" drift level (δ = 0.6), where natural language becomes almost deceptive, the symbolic consistency check ensures that the agents do not commit to contradictory plans, allowing the system to fail safely or request human intervention rather than proceeding with hallucinated consensus.

4.4 Communication Efficiency (RQ3)

One major concern with LLM-based negotiation is the "token explosion". We measured the average tokens consumed per successful task completion.

As shown in Table 3, while Fixed-Schema exhibits the lowest token consumption and latency due to its rigid structure, it fails to handle emergent semantic conflicts as previously shown in Table 1. Our DOA framework strikes an optimal balance: it incurs slightly higher initial overhead than Fixed-Schema due to the neuro-symbolic alignment phase. Although the observed alignment latency (1.4 s) is acceptable for supply chain coordination, it may pose challenges in ultra-high-stakes scenarios, such as robotic surgery or acute medical emergency coordination, where sub-second responses are mandatory. However, since DOA utilizes a "lazy alignment" strategy via the DCV, this latency is typically a one-time cost per concept, with subsequent interactions benefiting from cached mappings at near-zero overhead.

During our experiments, the peak GPU memory utilization for the Neuro-Symbolic Aligner was recorded at approximately 24 GB per instance when processing complex healthcare ontologies. The ComputeSemanticDrift function accounted for less than 1% of the total alignment latency, confirming that the gating mechanism successfully prevents unnecessary invocations of the more expensive neural reasoning phase.

Table 3. Communication overhead analysis: comparison of efficiency metrics per successful task completion

Metric	Raw-NL	Fixed-Schema	LLM-Prompt-Only	**DOA (Ours)**
Avg. turns to consensus	8.4	2.0*	6.2	3.1
Avg. tokens per task	4 200	1 200	3 850	1 950
Alignment latency / s	N/A	0.3	N/A	1.4

Notes: * Fixed-Schema achieves the lowest number of consensus turns among all frameworks, but it also has the lowest task success rate (see Table 1).

DOA: dynamic ontology alignment
LLM: large language model
NL: natural language

5 Conclusions and Future Work

In this paper, we introduce the DOA framework, a neuro-symbolic approach designed to mitigate semantic drift in LLM-based multi-agent systems. By combining the adaptive reasoning of LLMs with the formal rigor of symbolic consistency checking, our framework ensures that heterogeneous agents maintain synchronized conceptual grounding during real-time collaboration.

Our experimental results demonstrate that DOA increases task success rates by an average of 25.25% over natural language baselines, reduces token consumption by 50% through efficient grounded message transformation, and maintains robustness in the face of significant conceptual divergence.

Despite its efficacy in structured domains, a potential limitation of the current DOA framework lies in its performance on unconstrained open-domain dialogues. Specifically, when agents encounter "out-of-ontology" concepts that lack any formal parent-child relationship or attribute constraints in their local knowledge bases, the neuro-symbolic aligner may struggle to provide a verifiable mapping. In such cases, the system defaults to probabilistic neural alignment without the added guarantees of symbolic verification.

Beyond current evaluations, we recognize the necessity of validating DOA in domains with stricter real-time constraints and safety sensitivities. We intend to extend the framework to cooperative autonomous driving scenarios, where sub-second semantic alignment is critical for collision avoidance. Furthermore, we plan to incorporate active learning to allow local ontologies to evolve incrementally based on successful alignments.

References

[1] Qian C, Liu W, Liu H Z, et al. ChatDev: communicative agents for software development [C]//Proc. 62nd Annual Meeting of the Association for Computational Linguistics (Volume 1: Long Papers). ACL, 2024: 15174 – 15186. DOI: 10.18653/v1/2024.acl-long.810
[2] Xi Z H, Chen W X, Guo X, et al. The rise and potential of large language model based agents: a survey [J]. Science China information sciences, 2025, 68(2): 121101. DOI: 10.1007/s11432-024-4222-0
[3] Yang Y X, Chai H C, Shao S, et al. AgentNet: decentralized evolutionary coordination for LLM-based multi-agent systems [PP/OL]. V1. arXiv (2025-04-01)[2025-12-12]. https://doi.org/10.48550/arXiv.2504.00587
[4] Park J S, O'Brien J, Cai C J, et al. Generative agents: interactive simulacra of human behavior [C]//36th Annual ACM Symposium on User Interface Software and Technology. ACM, 2023: 1 – 22. DOI: 10.1145/3586183.3606763
[5] Becker J, Kaesberg L B, Stephan A, et al. Stay focused: problem drift in multi-agent debate [PP/OL]. V1. arXiv (2025-02-26)[2025-12-12]. https://doi.org/10.48550/arXiv.2502.19559
[6] Chen W Z, Su Y S, Zuo J W, et al. AgentVerse: facilitating multi-agent collaboration and exploring emergent behaviors [C]//International Conference on Learning Representations. ICLR, 2024: 1 – 43. DOI: 10.48550/arXiv.2308.10848
[7] Noy N F, McGuinness D L. Ontology development 101: a guide to creating your first ontology [EB/OL]. [2026-01-13]. http://protege.stanford.edu/publications/ontology_development/ontology101.pdf

[8] Giglou H B, D'Souza J, Engel F, et al. LLMs4OM: matching ontologies with large language models [PP/OL]. V2. arXiv (2024-04-23)[2026-01-14]. https://doi.org/10.48550/arXiv.2404.10317
[9] Qiang Z C, Wang W Q, Taylor K. Agent-OM: leveraging LLM agents for ontology matching [J]. Proceedings of the VLDB endowment, 2024, 18(3): 516 – 529. DOI: 10.14778/3712221.3712222
[10] Hitzler P, Sarker M K. Neuro-symbolic artificial intelligence: the state of the art [M]. Amsterdam: IOS Press, 2021. DOI: 10.3233/faia342
[11] Chang E Y. Multi-LLM agent collaborative intelligence: the path to artificial general intelligence [M]. New York: ACM, 2025. DOI: 10.1145/3749421
[12] Hong S R, Zhuge M C, Chen J, et al. MetaGPT: meta programming for a multi-agent collaborative framework [C]//International Conference on Learning Representations. ICLR, 2024: 1 – 29. DOI: 10.48550/arXiv.2308.00352
[13] Cancedda N, Dessi R, Dwivedi-Yu J, et al. Toolformer: language models can teach themselves to use tools [C]//Proceedings of Advances in Neural Information Processing Systems 36. Neural Information Processing Systems Foundation, Inc. (NeurIPS), 2023: 68539 – 68551. DOI: 10.52202/075280-2997
[14] Renney H, Nethercott M N, Renney N, et al. LLM-enabled multi-agent systems: empirical evaluation and insights into emerging design patterns & paradigms [PP/OL]. V1. arXiv (2026-01-06)[2026-02-01]. https://doi.org/10.48550/arXiv.2601.03328
[15] Wang Z, Moriyama S, Wang W Y, et al. Talk structurally, act hierarchically: a collaborative refinement framework for LLM multi-agent systems [J]. IEEE transactions on artificial intelligence, 2026: 1 – 11. DOI: 10.1109/tai.2026.3676025
[16] Jiménez-Ruiz E, Cuenca Grau B. LogMap: logic-based and scalable ontology matching [C]//The Semantic Web—ISWC 2011. Springer, 2011: 273 – 288. DOI: 10.1007/978-3-642-25073-6_18
[17] He Y, Chen J Y, Dong H, et al. Exploring large language models for ontology alignment [PP/OL]. V1. arXiv (2023-09-12)[2026-01-18]. https://doi.org/10.48550/arXiv.2309.07172
[18] Kamali D, Barezi E J, Kordjamshidi P. NeSyCoCo: a neuro-symbolic concept composer for compositional generalization [J]. Proceedings of the AAAI conference on artificial intelligence, 2025, 39(4): 4184 – 4193. DOI: 10.1609/aaai.v39i4.32439
[19] Schelble B G, Flathmann C, McNeese N J, et al. Let's think together! assessing shared mental models, performance, and trust in human-agent teams [J]. Proceedings of the ACM on human-computer interaction, 2022, 6: 1 – 29. DOI: 10.1145/3492832
[20] He J D, Treude C, Lo D. LLM-based multi-agent systems for software engineering: literature review, vision, and the road ahead [J]. ACM transactions on software engineering and methodology, 2025, 34(5): 1 – 30. DOI: 10.1145/3712003
[21] Bougzime O, Jabbar S, Cruz C, et al. Unlocking the potential of generative AI through neuro-symbolic architectures: benefits and limitations [PP/OL]. V1. arXiv (2025-02-16)[2026-02-23]. https://doi.org/10.48550/arXiv.2502.11269
[22] El-Sappagh S, Franda F, Ali F, et al. SNOMED CT standard ontology based on the ontology for general medical science [J]. BMC medical informatics and decision making, 2018, 18: 76. DOI: 10.1186/s12911-018-0651-5
[23] Möller M, Sintek M, Biedert R, et al. Representing the international classification of diseases version 10 in OWL [C]//International Conference on Knowledge Engineering and Ontology Development. KEOD, 2010: 50 – 59

Biographies

Xie Linhao is currently an undergraduate student at Communication University of China. He is also an intern at the Product R&D Center of AsiaInfo Technologies. During his university years, he received several awards, including the First Prize in the 2025 AI.Talk National College Student Artificial Intelligence Knowledge Competition, the Second Prize in the North China region of the 15th MathorCup Mathematical Application Challenge in 2025, and the National Third Prize in the 2024 National Mathematics Competition. His research interests include multi-agent systems, computer vision, and intelligent robotics.

Li Fan is a Senior Engineer at China Unicom Beijing Branch. She holds a Master of Engineering from Beijing University of Posts and Telecommunications, China. Her research interests include 4G/5G network optimization, mobile network digital operation, intelligentization of mobile communication networks, intelligent optimization and operation and maintenance, and emerging mobile communication technologies.

Wu Mingxuan received his MS degree from Peking University, China. He is currently the Deputy Manager of the Information Technology Department at CRSC Information Industry Co., Ltd., and holds the professional title of Engineer. His research interests include application of AI agents in vertical fields, digital transformation for large enterprises, and smart city solutions.

Song Yong (songyong@asiainfo.com) received his MS degree from Peking University, China. He is currently an algorithm expert at the Product R&D Center of AsiaInfo Technologies. He received the Second Prize of the Beijing Science and Technology Progress Award. His research interests include automatic ontology generation, multi-agent systems, and the Internet of Agents.

Ouyang Ye is a professor and an IEEE Fellow. He serves as the Chief Executive Officer and Chief Technology Officer at AsiaInfo Technologies. He holds a Bachelor of Engineering from Southeast University in China, a Master of Science from Tufts University in the United States, a second Master of Science from Columbia University in the United States, and a PhD from Stevens Institute of Technology in the United States. He has extensive experience in large-scale team management and R&D innovation in the ICT field. He focuses on cross-domain innovation and the commercialization of technologies in cellular networks, AI, and data science.

ACTap: Integrating Attention and Convolution for Network Modality Recognition

Ling Zihan[1], Zhang Tianwei[1], Ning Yuwei[1], Cao Yang[1], Shen Can[2]

(1. Huazhong University of Science and Technology, Wuhan 430074, China;
2. ZTE Corporation, Shenzhen 518057, China)

DOI: 10.12142/ZTECOM.202602009

https://kns.cnki.net/kcms/detail/34.1294.TN.20260522.1646.002.html, published online May 25, 2026

Manuscript received: 2025-08-14

Abstract: With the sustained growth of live video streaming, the demand for high-quality video services for mobile users across diverse network environments is increasing rapidly. In this paper, we define the network fluctuation characteristics in different environments as network modality. To comprehensively investigate network modality across different environments, we construct a network modality dataset by collecting multi-dimensional network metrics from various real-world scenarios and suggest that network modality exhibits separability. Therefore, network modality recognition, which aims to distinguish the scenarios where a user is located based on network modality sequences, is feasible and can be formulated as a multivariate time series (MTS) classification problem. To address this problem, we propose a novel neural network (NN)-based classification model called ACTap. Specifically, the model first integrates a two-stage attention (TSA) mechanism and a convolutional neural network (CNN) to extract features from network modality sequences. Then, it filters out noisy feature representations to learn discriminative class prototypes, and finally recognizes network modality based on the distance between their feature representations and class prototypes. Experimental results validate the separability of network modality and show that ACTap outperforms four benchmark models in terms of classification accuracy on the network modality dataset.

Keywords: network modality; multivariate time series classification; feature fusion; class prototype learning

Citation (Format 1): Ling Z H, Zhang T W, Ning Y W, et al. ACTap: integrating attention and convolution for network modality recognition [J]. ZTE Communications, 2026, 24(2): 71 - 82. DOI: 10.12142/ZTECOM.202602009
Citation (Format 2): Z. H. Ling, T. W. Zhang, Y. W. Ning, et al., "ACTap: integrating attention and convolution for network modality recognition," *ZTE Communications*, vol. 24, no. 2, pp. 71 - 82, Jun. 2026. doi: 10.12142/ZTECOM.202602009.

1 Introduction

The widespread popularity of mobile devices has spurred explosive growth in mobile video services. User demand for viewing experience is steadily increasing, with video streaming constituting a significant portion of network traffic. However, mobile users are often situated in environments with significant disparities in network modality (e. g. , malls, subways, basements), where pre-programmed adaptive bitrate streaming (ABR) algorithms (e.g. , the congestion control algorithm[1]) and offline learning models (e. g. , Pensieve[2]) cannot adapt to the highly heterogeneous networks[3]. To alleviate this issue, accessing current network modality information can aid in adapting ABR algorithms to dynamic network conditions. Therefore, network modality recognition is beneficial for providing low-latency and high-reliable mobile video services across diverse network environments.

Network modality can be reflected by multiple typical network metrics (e.g., bandwidth, latency, packet loss ratio). To dive deeper into network modality across different scenarios, we collect multi-dimensional network metrics across various real-world scenarios to construct a network modality dataset. Through the observations of network modality sequences from different scenarios in the dataset, we suggest that the network modality exhibits separability, which motivates the task of network modality recognition. The purpose of network modality recognition is to distinguish the scenarios where users are located based on the network modality sequences. Network modality sequences are multivariate time series (MTS), which consist of coevolving time series typically recorded over multiple attributes, since network metrics are measured over time and can be obtained simultaneously. Thus, network modality recognition can be formulated as an MTS classification problem that aims to identify labels for MTS. In general, the work on MTS classification can be roughly divided into pattern-based methods and neural network (NN)-based methods.

This work was supported in part by ZTE Industry-University-Institute Cooperation Funds under Grant No. IA20230728008 and the National Natural Science Foundation of China (NSFC) under Grant No. 62271224.

The pattern-based methods typically generate discriminative patterns for classification. In addition to the fact that the produced patterns may not be helpful for classification, they have two major limitations: 1) They rely on domain knowledge to carefully design the architectures for generating patterns; 2) they tend to select discriminative patterns from a large number of candidates, which may require sophisticated filtering mechanisms. In contrast, the NN-based methods can directly learn feature representations from MTS through deep NNs. They are more effective and do not involve domain knowledge. In this paper, we propose a novel NN-based model for network modality recognition, named ACTap which means integrating Attention and Convolution for extracting features from time series and utilizing them for attentional prototype learning.

Considering that most prior datasets[4–8] fail to provide high-level granularity of multi-dimensional network modality information across multiple scenes, which would be detrimental to the appropriate design of NN-based models and to showcasing their benefits, we collect multi-dimensional network metrics in various real-world scenarios with higher-level granularity. Moreover, due to the difference of measurement factors (e.g., packet size), there may be a gap between measured throughput and actual bandwidth, which is seldom considered in prior datasets. Here, to eliminate ambiguity, we define the term "throughput" as the rate at which data is successfully transmitted, and it is typically measurable, whereas the term "bandwidth" refers to the maximum rate that the path can provide to a flow, which is usually unobservable. Besides, some datasets rely on measuring Transmission Control Protocol (TCP) flows while neglecting testing with User Datagram Protocol (UDP) flows (e.g., online conferences[9] and live streaming[10]).

In this paper, we present a network modality dataset. Our dataset is logged with 100 ms granularity and contains 5-dimensional network modality information, including round-trip time (RTT), bandwidth, and packet loss ratio for both uplink and downlink. Moreover, during the measurement process, we adjust the packet size and rate to probe the full pipe (as detailed in Section 5.2), where measured throughput can be considered as bandwidth depending on whether the packet loss ratio exceeds a threshold. The performance of neural networks is highly correlated with the distribution of training data. Thus, obtaining bandwidth data that closely resembles real-world scenarios is beneficial for improving model performance during real-world deployment. Besides, we conduct real-time measurements using both UDP and TCP flows in six real-world scenes. The main contributions are as follows:

• We construct a network modality dataset by real-time collection of 5-dimensional network metrics in various real-world scenarios (e.g., subway, mall, and high-speed railway) using HoloWan[11]. Compared to prior datasets, ours is logged with higher-level granularity and considers the gap between measured throughput and bandwidth. In addition, we conduct measurements using both TCP and UDP. Subsequently, we suggest that network modality exhibits separability through observations from our dataset.

• We propose a novel NN-based model for network modality recognition, named ACTap, which integrates two-stage attention (TSA)[12] and convolutional neural networks (CNNs) to extract features from network modality sequences. Moreover, the model adopts a clustering algorithm and random sampling to filter out noisy feature representations for better class prototype learning.

• We conduct experiments using our dataset to compare ACTap with four benchmark models. The benchmark models include TapNet[13], which achieves classification accuracy of over 80% on a well-known MTS dataset, as well as several variants of ACTap. The results validate the separability of network modality and show that our proposed model achieves the highest classification accuracy compared to four benchmark models.

2 Related Work

2.1 Network Datasets

Prior related datasets focus on network metrics logged across a range of timescales and various mobility patterns. A comparison of these datasets is shown in Table 1. Raca et al.[4] recorded latency, throughput, and some physical information (e.g., signal strength) of video services during stationary (indoor, stationary car) and mobile (car in urban and suburban areas) scenarios at a granularity of 1 s, but it was only tested using TCP. Yang et al.[5] measured the throughput of various applications (including web browsing, instant messaging, music streaming, etc.) during usage, while other network modality information was neglected. Van et al.[6] collected throughput for six modes of transportation, namely walking, cycling, bus, light rail, train, and car, with a granularity of 1 s. Pan et al.[7] collected throughput, packet loss ratio, RTT, and physical information for video services on high-speed rails, with a granularity of 1 s, while other scenes were not measured. Kousias et al.[8] measured the throughput, packet loss ratio, delay, and physical information in three scenarios (indoor static, outdoor

Table 1. Comparison of network datasets

Dataset	Sampling Time Interval/s	Multi-Dimensional Modality Information	Multiple Scenes	Full Pipe	Protocol
Ours	0.1	√	√	√	UDP/TCP
Raca et al.[4]	1	√	√	×	TCP
Yang et al.[5]	unknown	×	√	×	UDP/TCP
Van et al.[6]	1	×	√	×	TCP
Pan et al.[7]	1	√	×	×	UDP/TCP
Kousias et al.[8]	millisecond-level	√	√	×	TCP

TCP: transmission control protocol UDP: user datagram protocol

walking, and outdoor driving) with millisecond-level granularity. All the above datasets do not carefully consider the gap between measured throughput and bandwidth; instead, they simply send large files to maximize link utilization.

2.2 MTS Classification

Many works on multivariate time series classification follow the direction of pattern-based classification models. Li et al.[14] adopt contrastive learning and K-means to select subsequences of MTS as patterns and employ SVM with a linear kernel for classification. Gao et al.[15] adopt reinforcement learning and Toeplitz inverse covariance-based clustering to select state changes in adjacent time steps of MTS as patterns and train a long short-term memory (LSTM) classifier. Moreover, NN-based methods achieve promising performance in multivariate time series classification tasks. Zhang et al.[13] adopt CNN and LSTM to extract features from MTS and use feature representations for classification. Khan et al.[16] build an end-to-end model called SE-FCN for MTS classification. They also hybridize an RNN-based model with their SE-FCN to make augmentations. Many variants of Transformer[17–18] have also been proposed for MTS classification. Although these models have shown great performance for MTS classification, they are often limited by insufficient data.

3 Dataset and Motivation

Using the specialized network metrics acquisition software HoloWan, we collect RTT, bandwidth, and packet loss ratio for both uplink and downlink with 100 ms granularity to construct the network modality dataset. RTT affects network responsiveness, bandwidth constrains the maximum transmission rate, and packet loss triggers data retransmission. Thus, these metrics can effectively reflect network conditions. Our dataset comprises measurement data spanning six and a half hours from six common scenarios with weak network conditions, including mobile environments (taxi, subway, and high-speed railway) and indoor environments (basement, mall, and elevator). This dataset faithfully logs the real-world network fluctuations under the influence of different communication scenarios, where different network modalities are expected to be present.

To illustrate the differences in network modalities across scenarios, we compare the measured downlink bandwidth across those scenarios in Fig. 1. From the comparison, we summarize the bandwidth fluctuation characteristics in different scenarios: 1) Bandwidth fluctuations in both basements and malls are significant, but those in basements exhibit more regular patterns, whereas those in malls do not (shown in Figs. 1a and 1b); 2) upon entering an elevator, there is a sudden

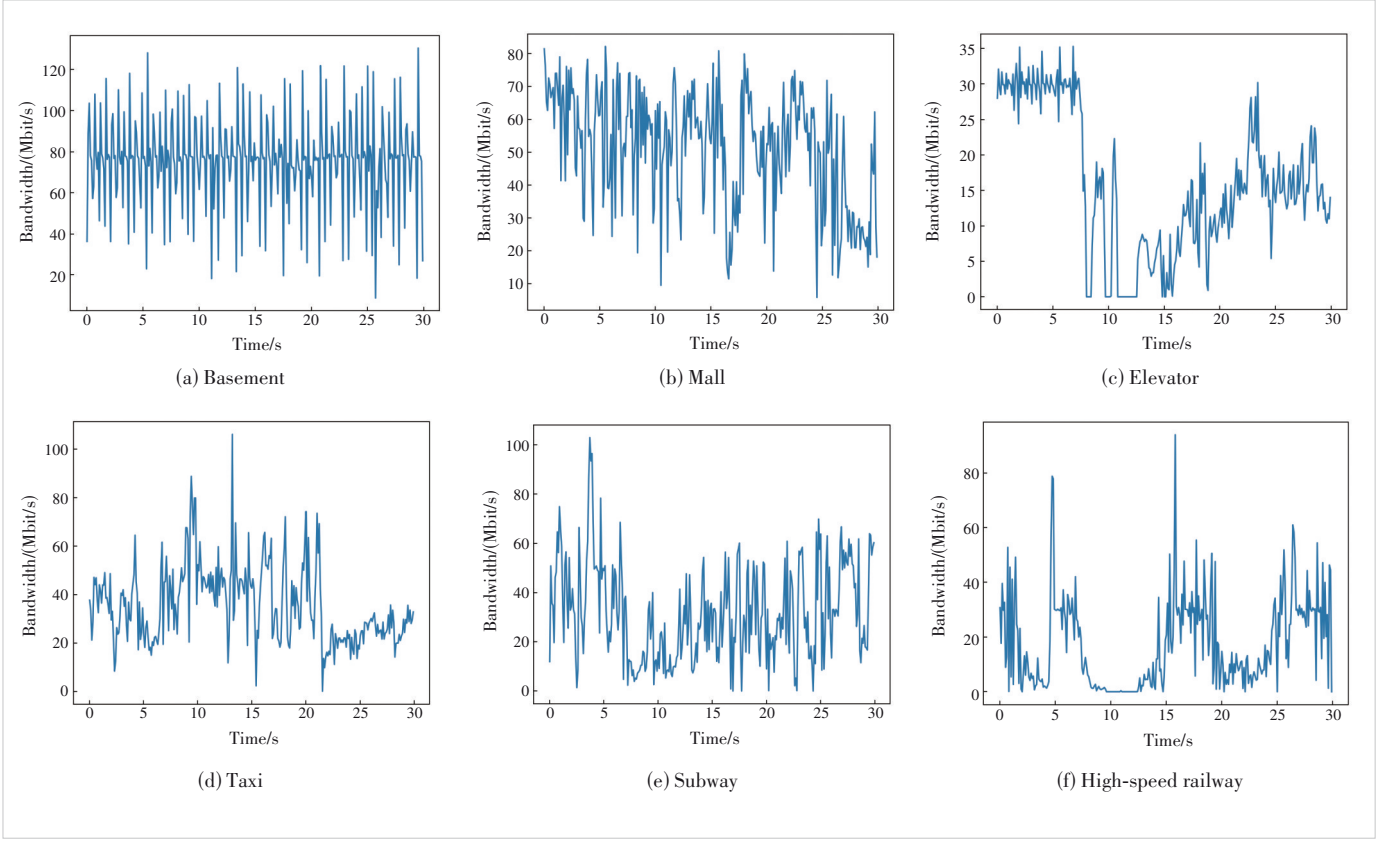

Figure 1. Bandwidth samples in six scenarios

drop in bandwidth (e.g., 1 – 10 s in Fig. 1c), and when the elevator doors open midway, the bandwidth increases (e.g., 20 – 25 s in Fig. 1c); 3) compared to indoor environments (e.g., basement and mall), users experience more instances of weak network conditions (e.g., bandwidth approaching 0) when moving outdoors, and as speed increases, the proportion of time spent in weak network conditions increases (shown in Figs. 1d – 1f); 4) similarly, outdoor mobile users experience longer RTT compared to indoor users (not shown in this paper).

Based on the above observations, we believe that network modality exhibits separability. Therefore, we propose the task of network modality recognition to identify the scenarios where mobile users are located based on network modality sequences. To achieve better recognition performance, we propose a novel NN-based model, ACTap. The network modality recognition approach presented in this paper can also provide new insights into ABR algorithms[19 – 21] with enhanced environmental adaptability, laying the foundation for lower-latency and more reliable video service in future research.

4 Network Modality Recognition Based on ACTap

In this section, we first formulate network modality recognition in Section 4.1. Then, we introduce the overall architecture of ACTap in Section 4.2. Afterwards, we explain each component of our proposed model in Section 4.3. Lastly, we elucidate class prototype learning in Section 4.4. The key notations are summarized in Table 2.

Table 2. Summary of notations

Symbol	Description
$\boldsymbol{X}_n$	The network modality sequence
$y_n \in \Omega$	The corresponding class label of the network modality sequence
L	The length of the network modality sequence
$\boldsymbol{F}_n$	The feature representation of the network modality sequence
f_{len}	The length of the feature representation
$\boldsymbol{s}_{d,i}$	The i-th segment in dimension d
seg_{len}	The length of segment
$\boldsymbol{h}_{d,i}$	The i-th feature vector in dimension d
d_{model}	The length of the feature vector
$\boldsymbol{H}$	The input of the TSA layer
$\boldsymbol{H}^{\text{time}}, \boldsymbol{H}^{\text{dim}}$	The outputs of the cross-time stage and cross-dimension stage, respectively
$\boldsymbol{F}_{\text{TSA}}, \boldsymbol{F}_{\text{CNN}}$	The extracted features of the TSA layer and CNN layer, respectively
$\boldsymbol{P}_k, \tilde{\boldsymbol{P}}_k$	The set of all representations and the set of selected representations, respectively
$\boldsymbol{W}_k$	The attention weight for class k
$\boldsymbol{c}_k$	The prototype of class k
$D(\boldsymbol{x}, \boldsymbol{c}_k)$	The distance between network modality sequence $\boldsymbol{x}$ and class prototype $\boldsymbol{c}_k$
$p(y = k\|\boldsymbol{x})$	The probability of network modality sequence $\boldsymbol{x}$ belonging to class k

CNN: convolutional neural network TSA: two-stage attention

4.1 Problem Formulation of Network Modality Recognition

Network modality can be represented as a sequence $\boldsymbol{X} = \{\boldsymbol{r}, \boldsymbol{l}_{\text{up}}, \boldsymbol{b}_{\text{up}}, \boldsymbol{l}_{\text{down}}, \boldsymbol{b}_{\text{down}}\}$, where $\boldsymbol{r}$ denotes RTT, $\boldsymbol{l}_{\text{up}}$ and $\boldsymbol{l}_{\text{down}}$ denote the packet loss ratios of uplink and downlink, respectively, and $\boldsymbol{b}_{\text{up}}$ and $\boldsymbol{b}_{\text{down}}$ denote the bandwidths of uplink and downlink, respectively. Each dimension of $\boldsymbol{X}$ is a time series of length L. For example, when we collect 5-dimensional network metrics with a length of 50 data points, the network modality can be represented as a matrix of size 5×50. Each network modality sequence $\boldsymbol{X}_n$ is associated with a class label $y_n \in \Omega$ indicating the corresponding network scenario. Our goal is to train a classification model $f: \boldsymbol{X}_n \rightarrow y_n$ to recognize a network modality sequence with an unknown label, given a set of network modality sequences and their corresponding labels.

4.2 Model Architecture Overview

Fig. 2 shows the overall architecture of ACTap, which comprises two main components: feature fusion of attention and convolution, and class prototype learning.

The input of our model is a set of 5-dimensional network modality time sequences. All dimensions of each sequence share the same temporal length, and the temporal length remains consistent across different network modality sequences. To capture cross-dimension and cross-time dependencies in network modality sequences, ACTap integrates TSA and a multi-layer CNN as the encoder. The basic idea of TSA is to extract features through a cross-time stage and a cross-dimension stage. The model then encodes the multi-dimensional network modality sequences into low-dimensional feature representations. For example, $\text{Encoder}(\boldsymbol{X}_n^{5\times L}) = \boldsymbol{F}_n^{1\times f_{\text{len}}}$, where L is the length of network modality sequences, and f_{len} is the length of feature representations. Further details of feature fusion are given in Section 4.3.

A class prototype is denoted as the benchmark feature representation of each class indicating the same real-world scene, and has the same size as the feature representations of training samples. After feature extraction and fusion, the feature representations of the training set are clustered and randomly sampled to filter out noisy representations. Then, the selected representations are used as input to learn the prototype for each class. Specifically, the class prototype is a weighted sum of the training samples belonging to the same class, where the weights of the training samples are trained by an attention layer. The intuition behind this is to learn a prototype for each class, which has smaller distances to the samples with the same class, but larger distances to others. A detailed description of class prototype learning can be found in Section 4.4.

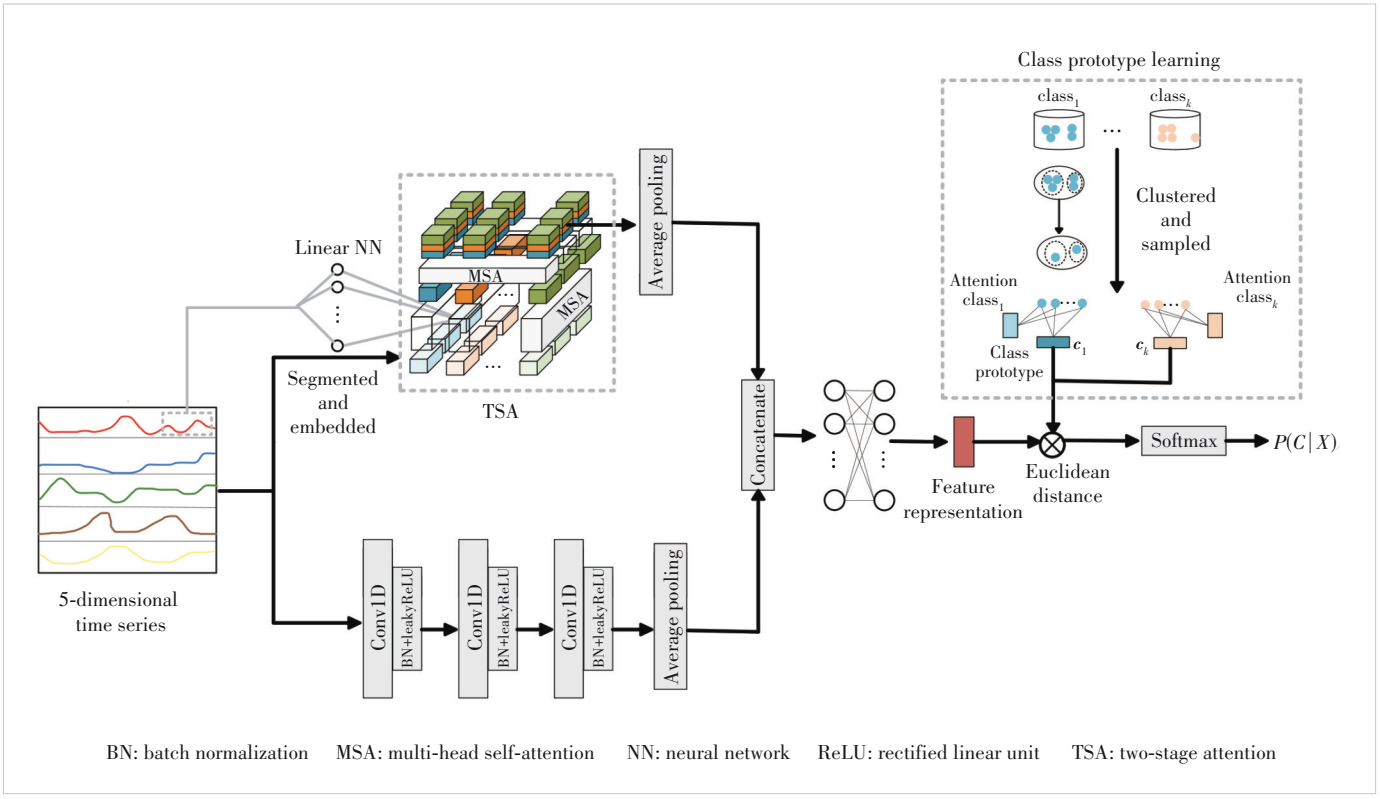

Figure 2. Overall architecture of ACTap

4.3 Feature Fusion of Attention and Convolution

Encoding a network modality sequence through neural network-based function $f_\theta(\boldsymbol{X})$ aims to learn a low-dimensional feature representation $\boldsymbol{F} \in R^{1 \times f_{\text{len}}}$, where θ denotes the set of parameters and $\boldsymbol{X} \in R^{5 \times L}$ is the network modality sequence. CNN and some Transformer-based models[22-23] can only capture cross-time dependencies in multivariate time series. Inspired by ViT[24], which splits an image into non-overlapping patches and rearranges these patches into a sequence, TSA can simultaneously capture cross-time and cross-dimension dependencies of multivariate time series. Thus, ACTap integrates TSA and multi-layer CNN for feature fusion.

4.3.1 Multi-Head Self-Attention

To utilize multi-head self-attention (MSA)[25] for feature extraction from the network modality sequences in subsequent sections, we briefly outline its process here. In practice, we compute the attention function on a set of queries, keys and values, packed together into matrices $\boldsymbol{Q}$, $\boldsymbol{K}$, $\boldsymbol{V}$, respectively:

$$\text{Attention}(\boldsymbol{Q}, \boldsymbol{K}, \boldsymbol{V}) = \text{softmax}\left(\frac{\boldsymbol{Q}\boldsymbol{K}^{\text{T}}}{\sqrt{d_k}}\right)\boldsymbol{V} \quad (1),$$

where $\sqrt{d_k}$ is the scaling factor. Then, instead of performing a single attention function with d_{model}-dimensional keys, values, and queries, Vaswani et al.[25] propose that it is beneficial to linearly project the queries, keys and values h times with different, learned linear projections to d_q, d_k and d_v dimensions, respectively. Afterwards, on each of these projected versions of queries, keys and values, we perform the attention function in parallel, yielding d_v-dimensional output values:

$$\text{MSA}(\boldsymbol{Q}, \boldsymbol{K}, \boldsymbol{V}) = \text{Concat}(\text{head}_1, \cdots, \text{head}_h)W^O \quad (2),$$

where $\text{head}_i = \text{Attention}(\boldsymbol{Q}W_i^Q, \boldsymbol{K}W_i^K, \boldsymbol{V}W_i^V)$, and the projections are parameter matrices $W_i^Q \in R^{d_{\text{model}} \times dq}$, $W_i^K \in R^{d_{\text{model}} \times d_k}$, $W_i^V \in R^{d_{\text{model}} \times d_v}$, and $W^O \in R^{hd_v \times d_{\text{model}}}$. In summary, MSA allows the model to jointly attend to information from different representation subspaces at different positions while a single attention head cannot achieve this.

4.3.2 Feature Extraction Based on TSA

Zhang et al.[12] propose that attention values of time series tend to be segmented, i.e., nearby data points have similar attention weights. Thus, it is more reasonable to first partition the network modality sequence in each dimension into non-overlapping segments (Fig. 3) and then embed them into feature vectors:

$$\boldsymbol{s}_{d,i} = \left\{ x_{d,t} \,\middle|\, (i-1) \times \text{seg}_{\text{len}} < t < i \times \text{seg}_{\text{len}} \right\} \quad (3),$$

where $\boldsymbol{s}_{d,i} \in R^{1 \times \text{seg}_{\text{len}}}$ is the i-th segment in dimension d with

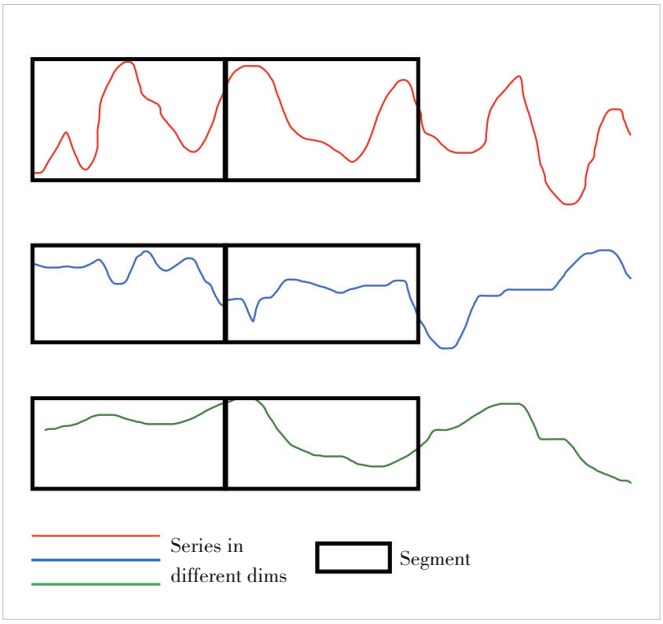

Figure 3. Partition of network modality sequence

length seg_{len}, and $x_{d,t}$ is the data of $\boldsymbol{X}$ in dimension d and time step t. For convenience, we assume that L is divisible by seg_{len}. Then each segment is encoded into a feature vector using a single-layer feedforward (SLF) neural network with position information:

$$\boldsymbol{h}_{d,i} = \text{SLF}(\boldsymbol{s}_{d,i}) + \mathbf{pos}_{d,i} \tag{4},$$

where $\boldsymbol{h}_{d,i} \in R^{1 \times d_{\text{model}}}$ is the i-th feature vector in dimension d with length d_{model} and $\mathbf{pos}_{d,i} \in R^{1 \times d_{\text{model}}}$ denotes the learnable position parameters for position (d, i). After encoding, we obtain $\boldsymbol{H} = \{h_{d,i} | 1 \leqslant d \leqslant 5, 1 \leqslant i \leqslant N\} \in R^{5 \times N \times d_{\text{model}}}$, where N is the number of segments in each dimension. Therefore, $\boldsymbol{H}$ is the input of the TSA layer.

The TSA layer contains two stages: cross-time stage and cross-dimension stage. For convenience, in the following, we use $\boldsymbol{H}_{:,i}$ to denote the feature vectors of all dimensions at time step i, and $\boldsymbol{H}_{d,:}$ for those of all time steps in dimension d. In the cross-time stage, MSA is applied to each dimension:

$$\hat{\boldsymbol{H}}^{\text{time}}_{d,:} = \text{LayerNorm}(\boldsymbol{H}_{d,:} + \text{MSA}^{\text{time}}(\boldsymbol{H}_{d,:})) \tag{5},$$

$$\boldsymbol{H}^{\text{time}} = \text{LayerNorm}(\hat{\boldsymbol{H}}^{\text{time}} + \text{MLP}(\hat{\boldsymbol{H}}^{\text{time}})) \tag{6},$$

where LayerNorm denotes layer normalization[25], MLP denotes multi-layer feedforward network, and $\hat{\boldsymbol{H}}^{\text{time}}_{d,:}$ and $\boldsymbol{H}^{\text{time}}$ denote the output of the MSA and MLP, respectively. All dimensions share the same MSA layer. Through the above process, feature vectors of each dimension can be fused across time range.

In the cross-dimension stage, MSA is also used to fuse feature vectors of each dimension at the same time step:

$$\hat{\boldsymbol{H}}^{\text{dim}}_{:,i} = \text{LayerNorm}(\boldsymbol{H}^{\text{time}}_{:,i} + \text{MSA}^{\text{dim}}(\boldsymbol{H}^{\text{time}}_{:,i})) \tag{7},$$

$$\boldsymbol{H}^{\text{dim}} = \text{LayerNorm}(\hat{\boldsymbol{H}}^{\text{dim}} + \text{MLP}(\hat{\boldsymbol{H}}^{\text{dim}})) \tag{8},$$

where $\hat{\boldsymbol{H}}^{\text{dim}}_{:,i}$ and $\boldsymbol{H}^{\text{dim}}$ denote the outputs of the MSA and MLP, respectively. We construct multiple TSA layers to further fuse features, with the output of a lower layer serving as the input of the layer above. Then, we operate average pooling on $\boldsymbol{H}^{\text{dim}} \in R^{5 \times N \times d_{\text{model}}}$ (the output of the top layer) to obtain the features $\boldsymbol{F}_{\text{TSA}} \in R^{N \times d_{\text{model}}}$ extracted by TSA.

4.3.3 Feature Fusion of CNN and TSA

Three one-dimensional CNN layers are employed to enhance the ability to capture cross-time dependencies in network modality sequences. Batch normalization[26] and leaky rectified linear unit (Leaky ReLU)[27] are operated after each convolutional layer. We set the number of filters for the three convolutional layers to 256, 256, and 256, with kernel sizes of 8, 5, and 3, respectively. The output $\boldsymbol{F}_{\text{CNN}} \in R^{1 \times d_f}$ is then generated after average pooling, where d_f is the filter size of the last convolutional layer.

Finally, the outputs of TSA and CNN are fused to obtain the feature representation of the network modality sequence. Specifically, $\boldsymbol{F}_{\text{TSA}}$ is flattened and concatenated with $\boldsymbol{F}_{\text{CNN}}$ as $\boldsymbol{F}_{\text{Comb}} \in R^{1 \times (N \times d_{\text{model}} + d_f)}$. Then, two fully connected layers are operated on $\boldsymbol{F}_{\text{Comb}}$ to generate the low-dimensional feature representation $\boldsymbol{F} \in R^{1 \times f_{\text{len}}}$.

4.4 Class Prototype Learning

To better recognize network modality, we adopt the idea of learning a prototype for each class and classifying the input network modality sequences based on their distance to these class prototypes[13]. Let $\boldsymbol{P}_k = \{\boldsymbol{x}_1, \cdots, \boldsymbol{x}_{|n_k|}\} \in R^{|n_k| \times f_{\text{len}}}$ denote the set of feature representations of training samples belonging to class k, where $|n_k|$ is the number of samples of class k.

Considering the fact that the number of feature representations used for class prototype learning can be large due to the big size of the training set, it is highly desirable to filter out the noisy feature representations and base classification on the most critical ones, which may improve the classification performance. In this paper, the K-means clustering algorithm[28] and random sampling are adopted to select discriminative feature representations. Specifically, at the beginning of each learning iteration, the model uses K-means to aggregate $\boldsymbol{P}_k$ into n clusters, and then randomly samples m feature representations from each cluster to form a new set $\tilde{\boldsymbol{P}}_k$. Thus, $\boldsymbol{c}_k$, the prototype of class k, can be expressed as a weighted sum of the feature representations in $\tilde{\boldsymbol{P}}_k$:

$$\boldsymbol{c}_k = \sum_i W_{k,i} \times \tilde{\boldsymbol{P}}_{k,i} \tag{9},$$

where $\tilde{\boldsymbol{P}}_{k,i}$ is the i-th feature representation in $\tilde{\boldsymbol{P}}_k$ and $W_{k,i}$ de-

notes its weight. The weight $W_{k,i}$ is not predefined but is learned according to $\tilde{\boldsymbol{P}}_{k,i}$. Specifically, for each feature representation, an attention-based multi-instance pooling method[13] is applied to learn its weight for the class prototype. The attention weights for class k are computed by:

$$\boldsymbol{W}_k = \mathrm{softmax}(\boldsymbol{\omega}_k^{\mathrm{T}} \times \tanh(V_k \tilde{\boldsymbol{P}}_k^{\mathrm{T}})) \tag{10},$$

where $\boldsymbol{\omega}_k \in R^{h \times 1}$ and $V_k \in R^{h \times f_{\mathrm{len}}}$ are trainable parameters for the attention model, and h is the size of hidden dimensions for them. Each class uses separate parameters $\{\boldsymbol{\omega}_k, V_k\}$ to accommodate the assumption that different classes may have distinct attentions on their feature spaces.

Afterwards, the squared Euclidean distance $D(\boldsymbol{x}, \boldsymbol{c}_k) = \|\boldsymbol{x} - \boldsymbol{c}_k\|^2$ is adopted to calculate the distance from a feature representation to each class prototype. Then, the model converts the distance into probability by a softmax layer:

$$p(y = k|\boldsymbol{x}) = \frac{e^{-D(\boldsymbol{x}, \boldsymbol{c}_k)}}{\sum_i e^{-D(\boldsymbol{x}, \boldsymbol{c}_i)}} \tag{11}.$$

We introduce a multiplicative coefficient before the distance function to align with the intuitive expectation: the smaller the distance between feature representations and a class prototype, the higher the probability of the sample being classified into that class. Moreover, we calculate the distance between prototypes of different classes:

$$d_{\mathrm{proto}} = \sum_{i=1}^{K} \sum_{j=1}^{K} D(\boldsymbol{c}_i, \boldsymbol{c}_j) \tag{12},$$

where K is the total number of classes. The overall loss function can be presented as:

$$\mathrm{loss} = -\log p(y = k|\boldsymbol{x}) - \alpha \times d_{\mathrm{proto}} \tag{13},$$

where α is the scale factor between the negative log probability and d_{proto}. Lastly, we train our model by minimizing the loss function via the Adam algorithm[29]. During the training process, feature representations gradually approach the prototype of their own class and move away from prototypes of other classes, thereby achieving network modality recognition with higher accuracy.

5 Data Collection

5.1 Setup

The collection campaign took place in Wuhan, China. During the implementation, we ran the HoloWan backend program on an Aliyun[30] cloud server. Concurrently, we enabled Android mobile devices with the HoloWan software to connect to a portable Customer Premise Equipment (CPE) equipped with a 5G SIM card, to ensure a strong and stable signal and to prevent interruptions during measurements. Fig. 4 shows the complete setup, which consists of the CPE, a portable power source for powering the CPE, and the mobile device with the HoloWan software.

5.2 Measurements

The above setup allows us to perform network metrics measurements. We measure 5-dimensional network metrics of real-world scenes multiple times as the network modality sequences. Then, we label them with the corresponding collection scenes to construct a network modality dataset. During the measurement process, mobile devices send data packets of a certain size to the cloud server through the CPE at a set time interval (e.g., 0.1 s), and the HoloWan software is used to measure and record the network metrics.

The HoloWan software supports UDP stream testing, transmitting uniform, reliable, constant-speed UDP traffic between the two ends of the network and enabling the acquisition of more detailed bandwidth fluctuation data. Besides, it also supports high-frequency TCP testing to measure network latency and packet loss ratio with better precision. Therefore, we simultaneously conduct UDP and TCP testing during the measurement. Moreover, HoloWan can accurately track the trajectory of each packet by utilizing the sequence number in the packets, thereby effectively detecting common issues such as data loss and packet reordering and making network measurement more precise.

The basic principle of bandwidth measurement is that when packet loss caused by network congestion occurs, the channel is at the full-pipe stage and the throughput can be regarded as the bandwidth[31]. The full pipe is identified by the following condition:

$$F_t = \mathbb{I}\{l_t \geqslant 5\%\} \tag{14},$$

where l_t denotes the packet loss ratio at time t. $\mathbb{I}\{z\}$ is the indicator function for logic z such that $\mathbb{I}\{z\} = 1$ when z is true, and 0 otherwise. Thus, $F_t = 1$ indicates the full pipe. Here,

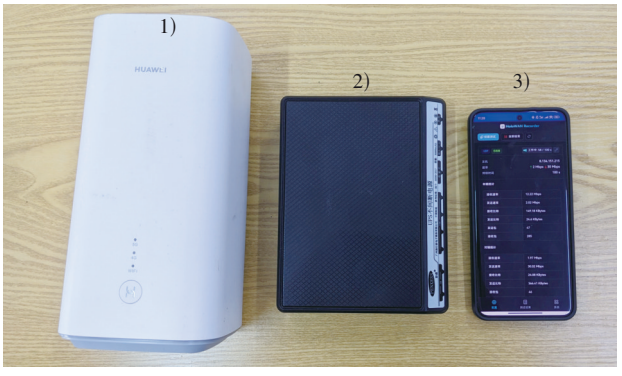

Figure 4. The measurement setup consists of 1) the CPE, 2) a portable power source, and 3) the mobile device with the HoloWan software

the threshold of 5% (see Ref. [1]) takes into account the presence of non-congestion packet loss, such as that caused by lossy wireless links.

At the initial stage of the measurement, we conduct multiple short-term measurements (e. g., for tens of seconds), gradually increasing the packet size and rate from small values to probe the full-pipe stage. Subsequently, we conduct long-term measurements (e.g., for tens of minutes) while maintaining the full-pipe configurations. Moreover, the packet size and rate should not be excessively large to avoid measurement interruptions. Afterwards, we remove the collected data points that satisfy $F_t = 1$, as the throughput observed at this time step does not reach the bandwidth of the channel.

We train and evaluate the proposed model on our network modality dataset, which contains higher-level granularity, more precise bandwidth data and more real-world scenarios than prior datasets. During training and evaluation, to mitigate the impact of noise in the measurement data, we sample one data point from every ten data points from the measurement data with 0.1 s interval to form the processed data with 1 s interval. Moreover, the processed data are divided into training and testing sets at a 6∶4 ratio. Then, we utilize a sliding window of size l with a stride of 1 to segment the data of the training/test set, generating sufficient network modality sequences.

6 Experiments

6.1 Environment

All models, including our proposed model ACTap and four benchmark models, are implemented in PyTorch[32]. All experiments were conducted on a server with an Intel(R) Xeon(R) Platinum 8352V CPU @ 2.10 GHz and a single NVIDIA RTX 4090 GPU with 24 GB memory, running Ubuntu 20.04. To avoid running out of memory, we set the batch size to 120. The learning rate is kept fixed at a low value of lr = 0.000 1, and the weight decay (regularization loss parameter) is set to 0.01, while the number of epochs for network training is 90.

6.2 Compared Methods

We compare ACTap with four different benchmark models, including the NN-based model named TapNet[13] and some variants of our proposed model. TapNet has been extensively tested on a well-known MTS dataset[33], and achieves a classification accuracy of over 80% on MTS classification tasks across multiple domains. The archive contains data collected from various domains, including human activity recognition, electrocardiogram signals, motion classification, etc. In this dataset, the dimensions of time series range from 2 to 963 and the lengths of time series range from 8 to 17 901.

The details of the benchmark models are provided as follows:

1) TapNet: an NN-based model for MTS classification. It consists of an LSTM layer, three one-dimensional CNN layers along with random dimension permutation to generate low-dimensional feature representations, and attention-based class prototypes learning.

2) CNNTap: a variant of our proposed model. It consists only of three one-dimensional CNN layers and class prototypes learning for classification.

3) AttentionTap: a variant of our proposed model. It consists only of the TSA layer and class prototypes learning.

4) ACMLP: a variant of our proposed model. It consists of the TSA layer and three one-dimensional CNN layers, but applies a multilayer perceptron for classification.

6.3 Accuracy Performance Evaluation

The classification accuracy of each model is shown in Table 3. Overall, our model outperforms all the other benchmark models in terms of classification accuracy.

1) ACTap vs. TapNet

Compared to TapNet, ACTap improves classification accuracy from 0.671 6 to 0.902 3 (an improvement of approximately 23.07 percentage points). This is mainly because ACTap can integrate cross-time and cross-dimension features of network modality sequences while TapNet cannot. Moreover, other experiments (not demonstrated in this paper) show that, for low-dimensional time series, random dimension permutation used in TapNet degrades classification performance.

2) Single feature extraction vs. feature fusion

To study the performance of our feature fusion, we compare ACTap with CNNTap and AttentionTap. Table 3 shows that ACTap achieves improvements of 5.23% and 8.90%, respectively. The results indicate that integrating TSA and multi-layer one-dimensional CNN achieves better network modality recognition than using either attention or convolution alone. This is mainly because the temporal dependencies extracted by the multi-layer one-dimensional CNN can complement the features extracted by TSA, thus enhancing the expressiveness of our model and improving classification performance.

3) Class prototype learning vs. MLP

To study the performance of class prototype learning, we compare ACTap with ACMLP, which applies a multilayer perceptron for classification. Table 3 shows that ACTap achieves a 5.44% improvement over ACMLP. The result indicates that learning class prototypes and classifying feature representa-

Table 3. Accuracy performance of models

Model	Accuracy
ACTap	**0.902 3**
TapNet	0.671 6
CNNTap	0.850 0
AttentionTap	0.813 3
ACMLP	0.847 9

Notes: CNNTap, AttentionTap, and ACMLP are variants of ACTap

tions based on Euclidean distance can better distinguish differences between different classes, thereby improving classification performance.

4) Varying the length of the network modality sequence

We compare the impact of different lengths of the network modality sequence on the final accuracy of ACTap. The chosen length l affects the total number of samples in the training set, and the number of selected samples needs to be predetermined. Thus, to mitigate the influence of sampling proportions on the experimental results, all samples in the training set are used directly to learn the class prototypes in this experiment. The set of lengths is {18, 36, 60, 72, 90, 108, 120}. Fig. 5 shows the accuracy for varying lengths of the network modality sequence. The accuracy increases rapidly as the length increases from 18 to 72, and then decreases slightly. Based on this observation, the default length of the network modality sequence is set to 72.

5) Varying cluster numbers

We compare the impact of different numbers of clusters on the final accuracy of ACTap. The set of cluster numbers is {5, 10, 15, 20, 50, and all}. Fig. 6 shows the accuracy for varying cluster numbers. The accuracy shows an increasing trend as the number of clusters increases from 5 to 15, since more feature representations can be learned, and then decreases gradually, since noisy features cannot be filtered out effectively, which degrades the discrimination of class prototypes. Based on this observation, the default number of clusters is set to 15.

6) All feature representations vs. random sampling vs. KNN

To study the effectiveness of K-means clustering algorithm for selecting feature representations in Section 4.4, we conduct an experiment to compare it with random sampling and no selection. The details of the three methods are as follows:

• K-means: This method aggregates the feature representations of the same class into n clusters through K-means and randomly sample m of representations from each cluster. It then uses the selected feature representations to learn the class prototype.

• Random: Without clustering, this method randomly samples the feature representations of the same class, keeping the total number of selected representations consistent with that in K-means. Then, it uses the selected ones to learn the class prototypes.

• All: Without selection, this method directly uses all the feature representations to learn the class prototypes. The number of clustering n and the number of samples per cluster m are set to 15 and 100, respectively.

The performance comparison is shown in Fig. 7. K-means achieves improvements of 2.20% and 2.30% over Random and All, respectively. The result indicates that K-means demonstrates its superior ability to filter out noisy features and select high-quality representations, leading to better performance.

7) Varying the size of the training set

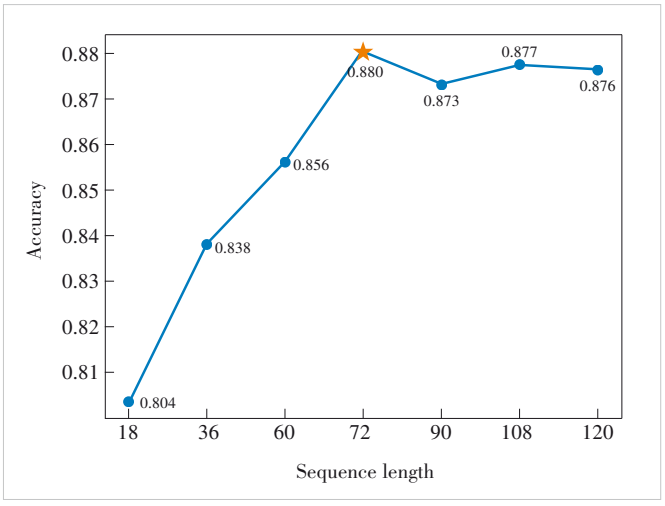

Figure 5. Performance comparison under different lengths of network modality sequence

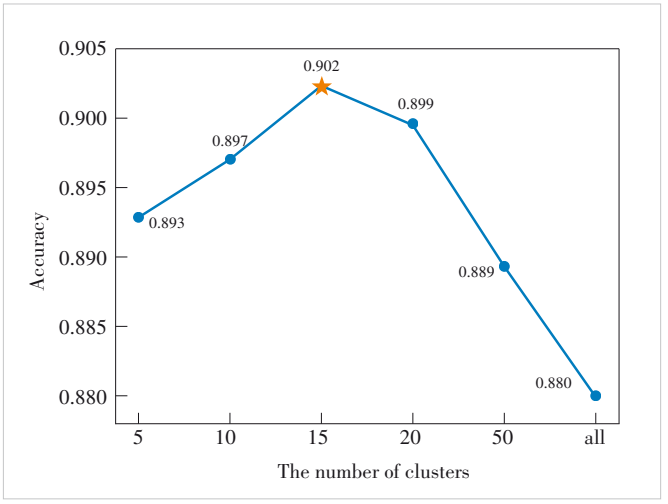

Figure 6. Performance comparison under different numbers of clusters

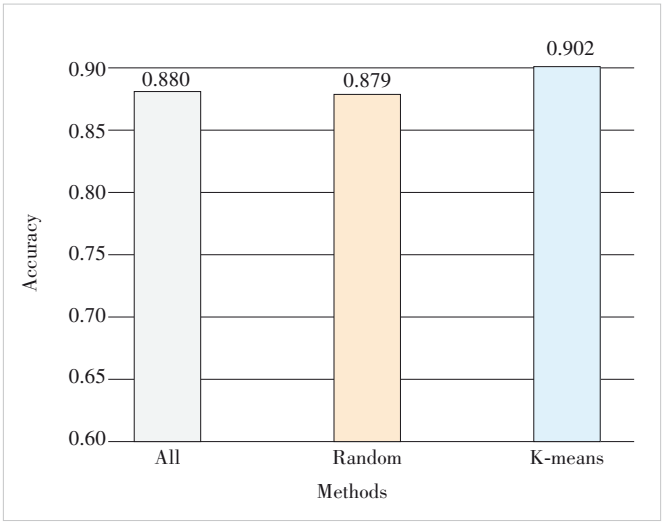

Figure 7. Performance comparison of feature selection methods

To investigate how much training data is needed for ACTap to achieve a high classification accuracy level (e.g., 80% or above), we train the model using training sets of varying sizes and evaluate the classification performance on the same test set. All represents a total of 7 784 network modality sequences in the training set, with a total duration of approximately 155 hours and 40 minutes. Ratios (e.g., 1/2) represent the proportion of the training set data being used. The test set comprises 5114 network modality sequences, with a total duration of approximately 102 hours and 16 minutes. Moreover, to adapt hyperparameters to different training set sizes, the number of training epochs and clusters are also scaled down proportionally with the size of the training set.

The performance comparison is shown in Fig. 8. As the proportion of the training set used decreases, the classification accuracy gradually decreases as well. When using a proportion of 1/15, comprising 519 network modality sequences (approximately 10 hours and 23 minutes), the classification accuracy falls below our expected threshold of 80%. Therefore, we should strive to ensure that the size of the training set exceeds this value.

8) Non-overlap vs. overlap

As indicated in Section 4.3.2, ACTap partitions the network modality sequence into non-overlapping segments. However, it is obvious that there are other segmentation methods for network modality sequences, for example, partitioning the sequence into multiple segments with a certain overlap using a fixed step size (as shown in Fig. 9). To further investigate the impact of different overlapping levels of segments on the final accuracy, we conduct an experiment to compare three overlapping levels: non-overlap (default), half overlap (the step size is half of the length of the segment), and almost full overlap (the step size is 1). Moreover, to prevent the GPU memory from being fully occupied, we train the model using 1/3 of the training set.

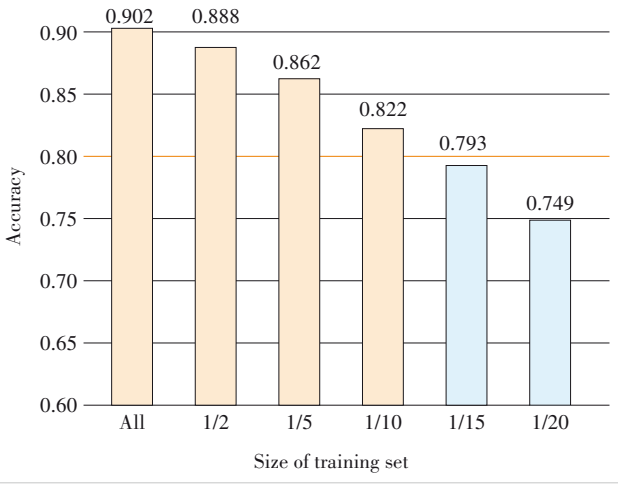

Figure 8. Performance comparison under different sizes of the training set

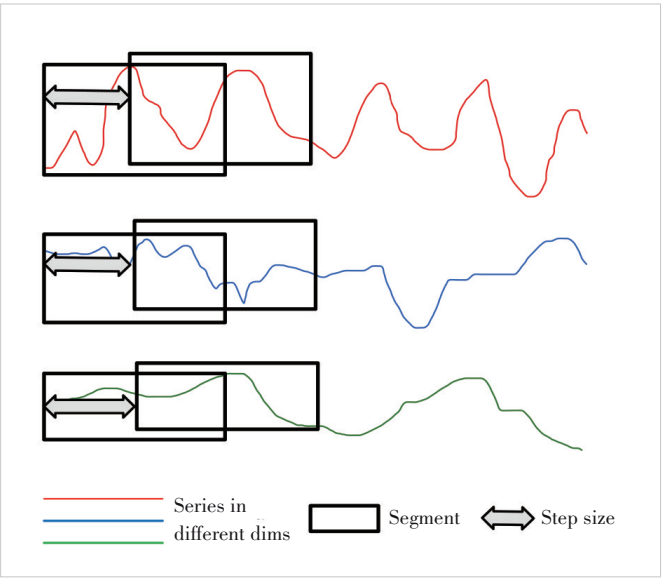

Figure 9. Partitioning the network modality sequence into overlapping segments

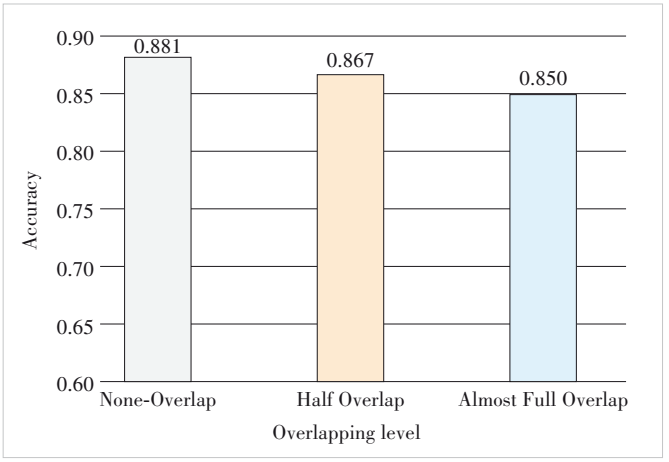

Figure 10. Performance comparison under different overlapping levels

The performance comparison is shown in Fig. 10. Non-overlap achieves improvements of 1.40% and 3.10% over Half Overlap and Almost Full Overlap, respectively. The result indicates that, as the overlapping level increases, the classification accuracy decreases gradually. We suspect that this may be due to the similarity between overlapping segments, thereby increasing the difficulty of learning attention weights for the TSA layer and leading to worse convergence of the model. Moreover, a higher overlapping level implies more data and longer training/testing time, while also resulting in poorer performance. Therefore, ACTap still adopts non-overlapping segmentation for network modality sequences.

9) Visualization

Lastly, we visualize the feature representations to demonstrate the effectiveness of our proposed model. We use the t-SNE algorithm[34] to visualize feature representations as two-

dimensional images and use different colors to distinguish different classes. Fig. 11 shows the ground truth and prediction results of ACTap. From the results, we can conclude that scenes including high-speed rail, elevator, and subway are well distinguished while other scenes like mall, basement and taxi are not. For example, network modality sequences of taxi are often misidentified as basement (as shown in the black circle area in Fig. 11b). We suspect that this may be due to the similarities between the different scenarios. For example, a basement and the ground floor of a mall may exhibit similarities. Similarly, when taxis pass through tunnels, the signals may be obstructed due to geographical factors, which may also share similarities with other scenes like basements. Therefore, ACTap may misjudge the network modality under these conditions. To mitigate this issue, in future work we intend to explore more detailed features, such as signal strength and handover events, to better distinguish between similar scenarios.

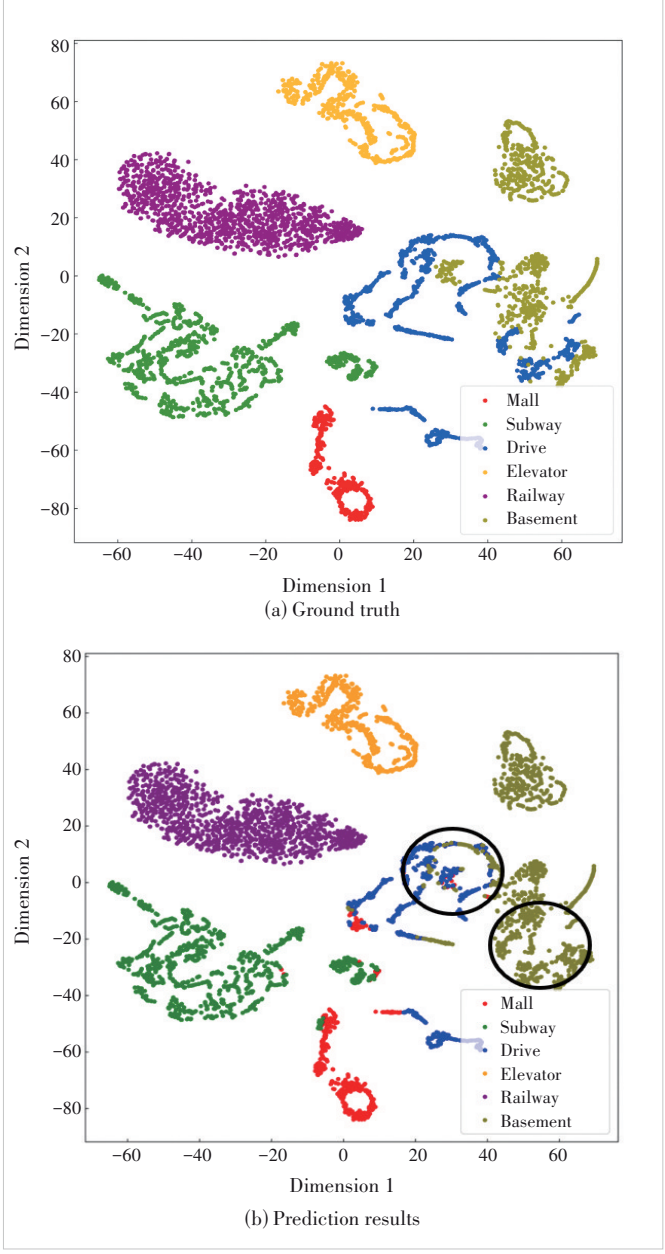

Figure 11. Classification visualization of ACTap

7 Conclusions

In this paper, we presented a network modality dataset collected from various real-world scenarios and suggested that network modality exhibits separability through observations. Subsequently, we proposed a novel NN-based model for network modality recognition, named ACTap. To improve classification performance, ACTap integrates TSA and multi-layer convolutional networks to extract cross-time and cross-dimension features of network modality sequences. Moreover, the model applies the K-means clustering algorithm and random sampling to filter out noisy features, thereby learning class prototypes with high discrimination. Lastly, the model recognizes network modality based on the Euclidean distance between feature representations and class prototypes. We conducted experiments on ACTap and four benchmark models using our dataset. The experimental results validate the separability of network modality and show that the accuracy of ACTap is the best among all the models compared. Moreover, we further explored the impact of multiple hyperparameters and the size of the training set on the classification accuracy of ACTap.

References

[1] Carlucci G, De Cicco L, Holmer S, et al. Analysis and design of the google congestion control for web real-time communication (WebRTC) [C]//Proceedings of the 7th International Conference on Multimedia Systems. ACM, 2016: 1 – 12. DOI: 10.1145/2910017.2910605

[2] Mao H Z, Netravali R, Alizadeh M. Neural adaptive video streaming with Pensieve [C]//Proceedings of the Conference of the ACM Special Interest Group on Data Communication. ACM, 2017: 197 – 210. DOI: 10.1145/3098822.3098843

[3] Zhang H H, Zhou A F, Lu J M, et al. OnRL: improving mobile video telephony via online reinforcement learning [C]//Proceedings of the 26th Annual International Conference on Mobile Computing and Networking. ACM, 2020: 1 – 14. DOI: 10.1145/3372224.3419186

[4] Raca D, Leahy D, Sreenan C J, et al. Beyond throughput, the next generation: a 5G dataset with channel and context metrics [C]//Proceedings of the 11th ACM Multimedia Systems Conference. ACM, 2020: 303 – 308. DOI: 10.1145/3339825.3394938

[5] Yang L, Yuan M X, Wang W, et al. Apps on the move: a fine-grained analysis of usage behavior of mobile apps [C]//Proceedings of the 35th Annual IEEE International Conference on Computer Communications. IEEE, 2016: 1 – 9. DOI: 10.1109/INFOCOM.2016.7524464

[6] van der Hooft J, Petrangeli S, Wauters T, et al. HTTP/2-based adaptive streaming of HEVC video over 4G/LTE networks [J]. IEEE communications letters, 2016, 20(11): 2177 – 2180. DOI: 10.1109/LCOMM.2016.2601087

[7] Pan Y Y, Li R H, Xu C R. The first 5G-LTE comparative study in extreme mobility [J]. Proceedings of the ACM on measurement and analysis of computing systems, 2022, 6(1): 1 – 22. DOI: 10.1145/3508040

[8] Kousias K, Rajiullah M, Caso G, et al. A large-scale dataset of 4G, NB-IoT, and 5G non-standalone network measurements [J]. IEEE communica-

tions magazine, 2024, 62(5): 44 – 49. DOI: 10.1109/MCOM.011.2200707
[9] Lu J G, Zheng Q F. Ultra-lightweight face animation method for ultra-low bitrate video conferencing [J]. ZTE communications, 2023, 21(1): 64 – 71. DOI: 10.12142/ZTECOM.202301008
[10] Xie L, Zhang X G, Huang C, et al. Markov based rate adaption approach for live streaming over HTTP/2 [J]. ZTE communications, 2018, 16(2): 37 – 41. DOI: 10.3969/j.issn.1673-5188.2018.02.007
[11] HoloWan APP [EB/OL]. [2024-08-01]. http://www.msytest.com
[12] ZHANG Y H, YAN J C. Crossformer: transformer utilizing cross-dimension dependency for multivariate time series forecasting [C/OL]// The Eleventh International Conference on Learning Representations. ICLR, 2022. https://openreview.net/forum?id=vSVLM2j9eie
[13] Zhang X C, Gao Y F, Lin J, et al. TapNet: multivariate time series classification with attentional prototypical network [J]. Proceedings of the AAAI conference on artificial intelligence, 2020, 34(4): 6845 – 6852. DOI: 10.1609/aaai.v34i04.6165
[14] Li G Z, Choi B, Xu J L, et al. ShapeNet: a shapelet-neural network approach for multivariate time series classification [J]. Proceedings of the AAAI conference on artificial intelligence, 2021, 35(9): 8375 – 8383. DOI: 10.1609/aaai.v35i9.17018
[15] Gao G, Gao Q T, Yang X, et al. A reinforcement learning-informed pattern mining framework for multivariate time series classification [C]//31st International Joint Conference on Artificial Intelligence. IJCAI, 2022: 2994 – 3000. DOI: 10.24963/ijcai.2022/415
[16] Khan M, Wang H Z, Ngueilbaye A, et al. End-to-end multivariate time series classification via hybrid deep learning architectures [J]. Personal and ubiquitous computing, 2023, 27(2): 177 – 191. DOI: 10.1007/s00779-020-01447-7
[17] Zerveas G, Jayaraman S, Patel D, et al. A transformer-based framework for multivariate time series representation learning [C]//Proceedings of the 27th ACM SIGKDD Conference on Knowledge Discovery & Data Mining. ACM, 2021: 2114 – 2124. DOI: 10.1145/3447548.3467401
[18] Zuo R D, Li G Z, Choi B, et al. SVP-T: a shape-level variable-position transformer for multivariate time series classification [J]. Proceedings of the AAAI conference on artificial intelligence, 2023, 37(9): 11497 – 11505. DOI: 10.1609/aaai.v37i9.26359
[19] Gao N Z, Yu Y F, Hua X H. A content-aware bitrate selection method using multi-step prediction for 360-degree video streaming [J]. ZTE communications, 2022, 20(4): 96 – 109. DOI: 10.12142/ZTECOM.202204012
[20] Li J X, Xu Y T, Cao Y, et al. Utility-driven joint caching and bitrate allocation for real-time immersive videos [J]. IEEE journal of selected topics in signal processing, 2023, 17(5): 1106 – 1118. DOI: 10.1109/JSTSP.2023.3295597
[21] Xu Y T, Du J H, Wang J H, et al. Panonut360: a head and eye tracking dataset for panoramic video [C]//Proceedings of the 15th ACM Multimedia Systems Conference. ACM, 2024: 319 – 325. DOI: 10.1145/3625468.3652176
[22] Du D Z, Su B, Wei Z W. Preformer: predictive transformer with multi-scale segment-wise correlations for long-term time series forecasting [C]// 2023 IEEE International Conference on Acoustics, Speech and Signal Processing (ICASSP). IEEE, 2023: 1 – 5. DOI: 10.1109/ICASSP49357.2023.10096881
[23] Zhou H Y, Zhang S H, Peng J Q, et al. Informer: beyond efficient transformer for long sequence time-series forecasting [J]. Proceedings of the AAAI conference on artificial intelligence, 2021, 35(12): 11106 – 11115. DOI: 10.1609/aaai.v35i12.17325
[24] Dosovitskiy A, Beyer L, Kolesnikov A, et al. An image is worth 16×16 words: transformers for image recognition at scale [PP/OL]. arXiv (2021-06-03) [2024-08-01]. https://doi.org/10.48550/arXiv.2010.11929
[25] Vaswani A, Shazeer N, Parmar N, et al. 2017. Attention is all you need [C]//Proceedings of the 31st International Conference on Neural Information Processing Systems. NIPS, 2017: 6000 – 6010. DOI: 10.48550/arXiv.1706.03762
[26] Ioffe S, Szegedy C. Batch normalization: accelerating deep network training by reducing internal covariate shift [C]//International conference on machine learning. PMLR, 2015: 448-456. DOI: 10.48550/arXiv.1502.03167
[27] Xu B, Wang N Y, Chen T Q, et al. Empirical evaluation of rectified activations in convolutional network [PP/OL]. V2. arXiv (2015-11-27). [2024-06-07]. https://doi.org/10.48550/arXiv.1505.00853
[28] MacQueen J. Some methods for classification and analysis of multivariate observations [C]//Berkeley Symposium on Mathematical Statistics and Probability, Volume 1: Statistics. University of California Press, 1967: 281 – 297
[29] Kingma D P, Ba J. Adam: a method for stochastic optimization [PP/OL]. V9. arXiv (2017-01-30) [2024-06-07]. https://doi. org/10.48550/arXiv.1412.6980
[30] Aliyun [EB/OL]. [2024-05-19]. https://cn.aliyun.com
[31] Cardwell N, Cheng Y, Gunn C S, et al. BBR: congestion-based congestion control [J]. Communications of the ACM, 2017, 60(2): 58 – 66. DOI: 10.1145/3009824
[32] Pytorch [EB/OL]. [2024-05-19]. https://pytorch.org
[33] Bagnall A, Dau H A, Lines J, et al. The UEA multivariate time series classification archive, 2018 [PP/OL]. V1. arXiv (2018-10-31)[2024-04-21]. https://doi.org/10.48550/arXiv.1811.00075
[34] van der Maaten L, Hinton G. Visualizing data using t-SNE [J/OL]. Journal of machine learning research, 2008, 9(86): 2579–2605. https://jmlr.org/papers/volume9/vandermaaten08a/vandermaaten08a.pdf

Biographies

Ling Zihan received his BE degree from the School of Microelectronics and Communication Engineering, Chongqing University, China in 2023. He is currently pursuing the MS degree at the School of Electronic Information and Communications, Huazhong University of Science and Technology, China. His current research interests include real-time VR video transmission, network modal analysis, and adaptive bitrate algorithms.

Zhang Tianwei received his MS degree in wireless communication systems from the University of Sheffield, UK in 2020. He is currently pursuing the PhD degree at the School of Electronic Information and Communications, Huazhong University of Science and Technology, China. His current research interests include real-time video transmission, video processing, and adaptive streaming.

Ning Yuwei is a third-year undergraduate student at Huazhong University of Science and Technology, China, supervised by Prof. Cao Yang. His research interests include deep learning, time series processing, and computer vision.

Cao Yang (ycao@hust.edu.cn) is currently an associate professor at the School of Electronic Information and Communications, Huazhong University of Science and Technology, China. From 2011 to 2013, he was a visiting scholar at the School of Electrical, Computer, and Energy Engineering, Arizona State University, USA. His research interests include immersive video transmission and edge/distributed computing. He has coauthored 50 papers in refereed IEEE journals and conferences. He received the CHINACOM Best Paper Award in 2010 and the Microsoft Research Fellowship in 2011.

Shen Can received his PhD degree in engineering in 1997 and has since been engaged in the research and development of audio and video technologies at ZTE Corporation. He has received the Second Prize of the National Science and Technology Progress Award, published 20 papers, and holds over 70 patents.

An Evanescent-Propagating Wave Conversion Method for Expanding the DoF in Holographic MIMO

Liu Guohao[1], Fang Min[2,3], Peng Lin[2,3], Luo Jun[2,3], Sun Zhi[1]

(1. Department of Electronic Engineering, Tsinghua University, Beijing 100084, China;
2. State Key Laboratory of Mobile Network and Mobile Multimedia Technology, Shenzhen 518055, China;
3. ZTE Corporation, Shenzhen 518057, China)

DOI: 10.12142/ZTECOM.202602010

https://kns.cnki.net/kcms/detail/34.1294.TN.20260422.1518.004.html, published online April 23, 2026

Manuscript received: 2025-02-03

Abstract: Holographic multiple-input multiple-output (HMIMO) systems deploy ultra-dense antennas in confined spaces, yet spatial degrees of freedom (DoF) fail to scale with element count. Only by harnessing evanescent waves can the potential gains of ultra-dense arrays be unlocked. However, in practical scenarios, antenna apertures are typically too small relative to communication distances to generate significant near-field effects for capturing these evanescent waves. This paper proposes a method to alter the dispersion relation via locally resonant metamaterials (LRM), thereby enabling the radiation of near-field evanescent wave components into the far field. This approach leverages the DoF gains offered by ultra-dense elements within a confined aperture. Full-wave simulations validate the effectiveness of the evanescent-propagating wave conversion method, demonstrating an increase in the spatial DoF radiated into the far field by the HMIMO system even with a limited aperture.

Keywords: spatial DoF; evanescent-propagating wave conversion; holographic MIMO

Citation (Format 1): Liu G H, Fang M, Peng L, et al. An evanescent-propagating wave conversion method for expanding the DoF in holographic MIMO [J]. ZTE Communications, 2026, 24(2): 83 - 93. DOI: 10.12142/ZTECOM.202602010
Citation (Format 2): G. H. Liu, M. Fang, L. Peng, et al., "An evanescent-propagating wave conversion method for expanding the DoF in holographic MIMO," *ZTE Communications*, vol. 24, no. 2, pp. 83 - 93, Jun. 2026. doi: 10.12142/ZTECOM.202602010.

Holographic multiple-input multiple-output (HMIMO), considered one of the potential technologies for 6G wireless communications, involves an antenna array with ultra-dense spacing within a confined aperture, which can be theoretically regarded as having an infinite number of antenna elements[1]. Although HMIMO consists of many antennas, the spatial degrees of freedom (DoF) are extremely limited. The antenna elements in HMIMO exhibit strong coupling, and thus are not independent of each other. This coupling has been modeled using a circuit model in Ref. [2], which also analyzes the spatial DoF. In existing HMIMO studies, the antenna apertures are often large, necessitating the use of near-field modeling[3]. However, when considering far-field communication scenarios, the Nyquist sampling theorem provides an upper bound on the spatial DoF for HMIMO[4]. In spatial signal processing, a sampling interval of half-wavelength is sufficient to recover spatial signal information without spatial aliasing, thereby preserving the spatial characteristics of the signal. Therefore, for far-field communications, an antenna arrangement denser than half a wavelength proves redundant[5].

Evanescent waves possess higher spatial frequencies, requiring denser spatial sampling and thereby increasing the DoF for a given aperture. Since evanescent waves exist only in the near-field region, utilizing them requires confining the communication distance to the near-field zone. As the size of the antenna array's aperture increases, the near-field region expands. If the communication distance remains within this region, evanescent waves can be exploited to achieve enhanced spatial DoF[6].

While evanescent waves can provide higher DoF for communication, it is physically challenging to utilize them in an HMIMO system with an infinitely large aperture. In practice, we can only deploy antennas within a limited space. This raises a question: is it possible to achieve spatial DoF exceeding the classical half-wavelength limit using ultra-dense antenna arrays (i.e., HMIMO) without increasing the antenna aperture size?

Due to the limited size of the antenna array aperture, the

This work was supported by ZTE Industry-University-Institute Cooperation Funds under Grant No. HC-CN-20200923014.

communication distance may not fall within the near-field range, where evanescent waves exhibit exponential decay and cannot directly reach the far field[7]. Therefore, evanescent waves must be converted into propagating waves to be utilized. This paper proposes a method to convert near-field evanescent waves of HMIMO into far-field propagating waves using locally resonant metamaterials (LRM), thereby enabling HMIMO transceivers to radiate additional DoF.

Previous studies have revealed the physical mechanisms of converting evanescent waves into propagating waves and have applied them in super-resolution imaging[8]. Physicists have developed a method to achieve sub-wavelength focusing by placing ultra-dense resonators, i.e., LRM, near the antenna[9]. These resonator units exhibit strong coupling, forming a frequency band with multiple resonance frequencies. When evanescent waves interact with these resonators, their sub-wavelength details are encoded as spectral information and radiated to the far field as propagating waves, enabling subwavelength focusing in super-resolution imaging[10].

However, to the best of our knowledge, no study has yet explained from a communication systems perspective how LRM can be used to convert the near-field evanescent waves of a limited-aperture HMIMO to achieve ultra-high spatial DoF. In this paper, we first reveal why a limited-aperture HMIMO transmitter cannot realize multiple streams. Then, we present the principle of extending the number of effective radiation modes to the far-field using LRM in the vicinity of the HMIMO. Finally, we verify through full-wave simulation software CST that an HMIMO composed of ultra-dense dipole antennas within a limited aperture can achieve spatial multiplexing.

The remainder of this paper is organized as follows. Section 2 details the HMIMO implementation and establishes the theoretical DoF limits for both HMIMO and discrete MIMO systems. It is demonstrated that the DoF in the radiative far field is solely dependent on the aperture size, indicating that densely deploying antennas, as in HMIMO configurations, results in redundancy. In Section 3, we introduce the theoretical framework for overcoming the DoF limitations of HMIMO using LRM. In Section 4, we perform full-wave simulations to verify the system where LRM enhances the DoF of HMIMO. Section 5 concludes the study.

Notation: a, $\boldsymbol{a}$, and $\boldsymbol{A}$ represent scalars, vectors, and matrices, respectively. $\boldsymbol{A}^T$, $\boldsymbol{A}^H$, and $\boldsymbol{A}^{-1}$ denote the transpose, Hermitian (conjugate transpose), and inverse, respectively. $\boldsymbol{A}_{i,j}$ or $[\boldsymbol{A}]_{i,j}$ represents the (i,j)-th element of $\boldsymbol{A}$. $\boldsymbol{a}_n$ represents the n-th element of $\boldsymbol{a}$. $|\cdot|$ and $(\cdot)^*$ denote the modulus and conjugate, respectively.

1 System Model

1.1 System Implementation of HMIMO

The HMIMO system examines a line-of-sight (LoS) MIMO communication scenario involving two continuous apertures of arbitrary shapes and positions in an infinite homogeneous medium. The modeling of continuous apertures and LoS channels is provided in Refs. [11] and [12], respectively. The current density $\boldsymbol{j}(\boldsymbol{s},t)$ at a source point $\boldsymbol{s}$ within the transmitting aperture S_t generates an electric field $\boldsymbol{e}(\boldsymbol{r},t)$ at a location $\boldsymbol{r}$ within the receiving aperture S_r. For only monochromatic sources and fields, the time-harmonic fields can be described by the phasors $\boldsymbol{j}(\boldsymbol{s})$ and $\boldsymbol{e}(\boldsymbol{r})$, with their relationship governed by the Green's function:

$$\boldsymbol{e}(\boldsymbol{r}) = jkZ_0 \int_{S_t} \boldsymbol{G}(\boldsymbol{r},\boldsymbol{s})\,\boldsymbol{j}(\boldsymbol{s})\,\mathrm{d}\boldsymbol{s}, \quad \boldsymbol{r} \in S_r \tag{1}$$

where $k = \omega/c = 2\pi/\lambda$ is the wavenumber (c being the speed of light), Z_0 is the characteristic impedance of the medium, and the Green's function $\boldsymbol{G}(\boldsymbol{r},\boldsymbol{s})$ is determined by the boundary conditions.

The continuous source and field on the transmitting and receiving apertures are expanded using orthogonal modes $\{\boldsymbol{\phi}_m(\boldsymbol{s});\, m = 1,\cdots,M\}$ and $\{\boldsymbol{\psi}_n(\boldsymbol{r});\, n = 1,\cdots,N\}$, respectively. As shown in Eqs. (2) and (3), the expansion coefficients x_m and $jkZ_0 y_n$ constitute the channel, where M and N are the dimensions of the input and output signal spaces, respectively.

$$y_n = \sum_{m=1}^{M} \boldsymbol{H}_{nm} x_m + z_n \,(n = 1,\cdots,N) \tag{2}$$

$$\boldsymbol{H}_{nm} = \int_{S_r}\int_{S_t} \boldsymbol{\psi}_n^{\mathrm{H}}(\boldsymbol{r})\,\boldsymbol{G}(\boldsymbol{r},\boldsymbol{s})\,\boldsymbol{\phi}_m(\boldsymbol{s})\,\mathrm{d}\boldsymbol{s}\,\mathrm{d}\boldsymbol{r} \tag{3}$$

Let $\boldsymbol{y} = [y_1,\cdots,y_N]^{\mathrm{T}}$ and $\boldsymbol{x} = [x_1,\cdots,x_M]^{\mathrm{T}}$. The equation can be expressed in the matrix form $\boldsymbol{y} = \boldsymbol{H}\boldsymbol{x}$, where $\boldsymbol{H} \in C^{N\times M}$ represents the channel matrix.

HMIMO uses orthogonal modes on continuous apertures to carry information, but practical implementation consists of a finite number of densely packed antennas. In this work, we select cosine and sine functions as orthogonal modes. The current distribution on an $M \times N$ antenna array used to construct orthogonal modes on an aperture $D_x \times D_y$ is described in Eq. (4).

$$\boldsymbol{J}_n(x,y) = \sum_{p,q} A_n^{pq} \boldsymbol{J}_d(x - qD_x, y - pD_y) \tag{4}$$

where A^{pq} describes the amplitude of the current on the (p,q)-th dipole, which is the sampled value of the orthogonal cosine and sine modes. The current amplitude of the (p,q)-th dipole in mode (m,n) is given in Eq. (5).

$$A_{mn}^{pq} = A_{0,mn}\sin(\pi m(p/(M+1) - 1/2))\sin(\pi n(q/(N+1) - 1/2)) \tag{5}$$

where $\boldsymbol{J}_d$ describes the current distribution on each dipole antenna. This distribution must satisfy boundary conditions where the current is zero at both ends, represented by a cosine distribution. The expression for $\boldsymbol{J}_d$ is given in Eq. (6):

$$\boldsymbol{J}_d(x,y) = \hat{\boldsymbol{y}} J_0 \cos\left(\pi \frac{y}{L}\right) \mathrm{rect}\left(\frac{y}{L}\right) \delta(x) \tag{6},$$

where L is the length of each dipole antenna.

The continuous function is achieved by interpolating current amplitudes A_{mn}^{pq} on the discrete antennas using the cosine-sine orthogonal basis, as described in Eq. (5). According to the sampling theorem, the current amplitudes extracted from $M \times N$ discrete antenna elements can perfectly reconstruct the superposition of $M \times N$ orthogonal mode currents on the continuous aperture. For example, Fig. 1 illustrates how the current distribution on densely packed discrete antennas is interpolated to form the current distribution on a continuous aperture. Fig. 1a depicts a 1×6 HMIMO array with an element spacing of 0.1λ, and the current distribution on it is plotted based on Eqs. (4) – (6). Fig. 1b shows the current distribution on a continuous aperture obtained by interpolating the current amplitudes of the discrete antennas in Fig. 1a.

1.2 DoF of HMIMO Transmitter with Limited Aperture

The DoF of HMIMO is determined by the number of orthogonal current modes M that can be effectively transmitted to the far-field on the aperture S_t. As illustrated in Fig. 2, to investigate the spatial DoF of the transmitter, the electromagnetic wave $\boldsymbol{y}(\boldsymbol{r},t)$ received in the far field is time-reversed as $\boldsymbol{y}^{\mathrm{TR}}(\boldsymbol{r},t) = \boldsymbol{y}(\boldsymbol{r},-t)$, which is then backpropagated. The electromagnetic field $\boldsymbol{x}^{\mathrm{TR}}(\boldsymbol{s})$ received again at the transmitting aper-

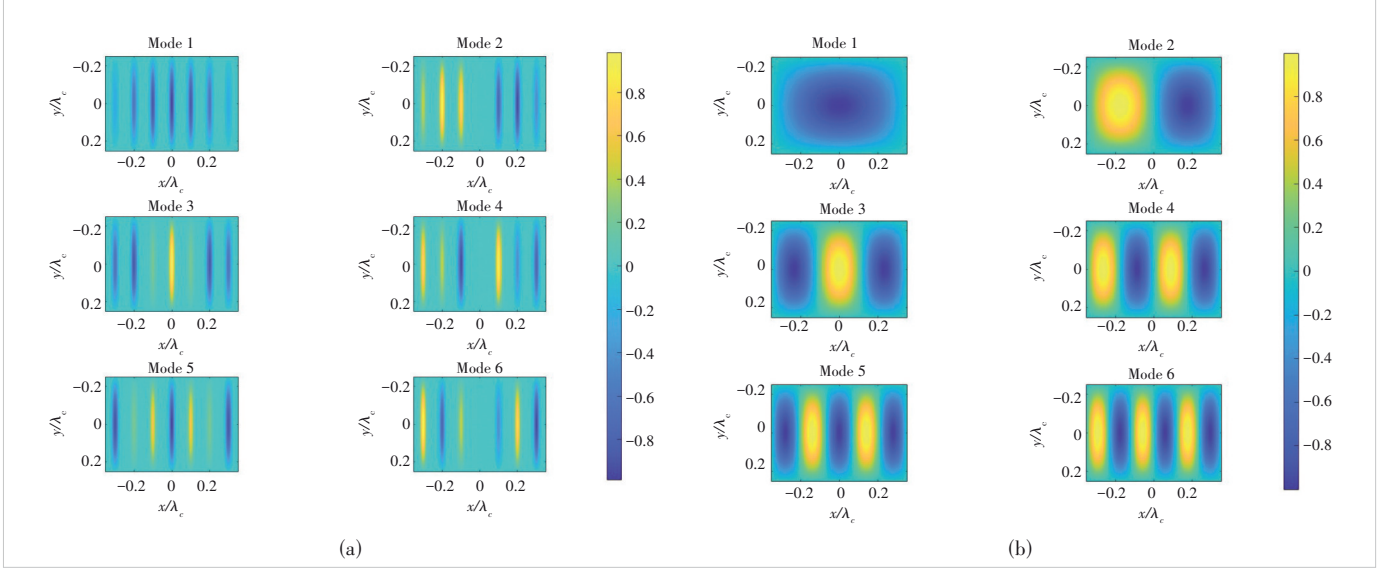

Figure 1. Current distribution on densely packed antennas and interpolated current distribution on a continuous aperture

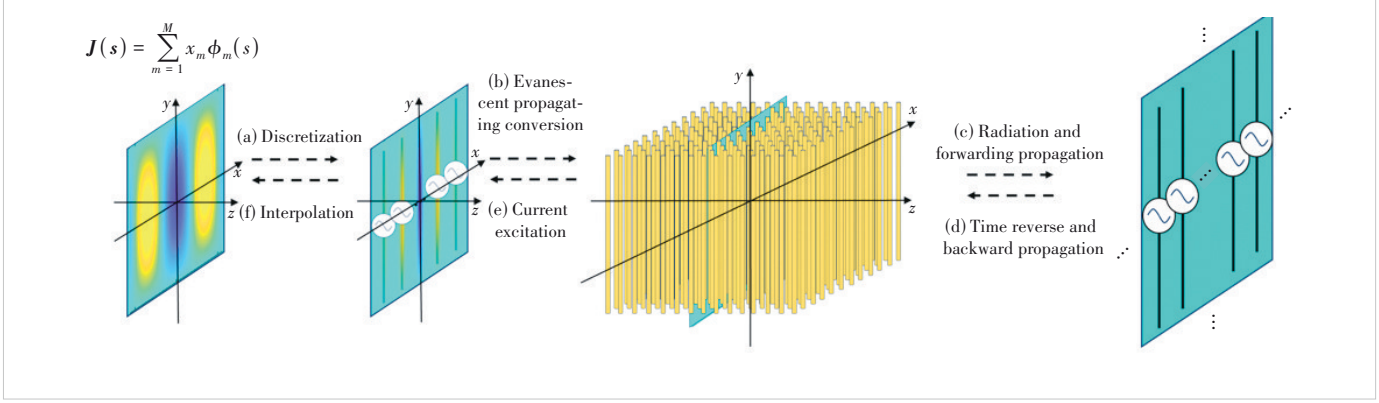

Figure 2. System model: (a) x_m is modulated onto the orthogonal basis of mode currents $\phi_m(s)$, where $m = 1,2,\cdots,M$, and is realized through a discretized dense dipole antenna array; (b) an LRM structure is employed to achieve the evanescent-propagating waves conversion; (c) the signal radiates and propagates forward into the far field; (d) the signal, received by an ideal aperture, undergoes time-domain reversal and is backpropagated; (e) the time-reversed field excites currents on the HMIMO transmitter; (f) the current distribution on the aperture is recovered through interpolation

ture can be projected onto the orthogonal basis to obtain $\boldsymbol{x}^{\mathrm{TR}}$. It can be proven (Appendix A*) that:

$$\boldsymbol{x}^{\mathrm{TR}} = \left(\boldsymbol{H}\boldsymbol{H}^{H}\right)^{T}\boldsymbol{x}^{*} \tag{7}$$

When the far-field receiving aperture ideally captures all radiated fields from the transmitting aperture, the rank and eigenvalue distribution of the matrix $\boldsymbol{H}\boldsymbol{H}^{H}$ constructed through time-reversal characterize the effectiveness of the orthogonal current modes in radiating into the far field.

For an HMIMO system with a limited aperture, the communication distance will be much greater than L/λ_0, where L is the aperture size of the HMIMO and λ_0 is the operating wavelength. In this case, the receiver is located in the far-field region of the HMIMO. The radiation from the HMIMO in the far-field region can be approximated as a plane wave, and thus the transformation from near-field (spatial domain) to far-field (wavenumber domain) is described by a Fourier transform (FT). Consequently, the minimum resolution in the wavenumber domain and the spatial domain are $\Delta k = 2\pi/L$ and $\Delta L = 2\pi/2k_0 = \lambda_0/2$, respectively. For propagating waves, the available range of wavenumbers in one direction is $|k_t| < k_0$, whereas wavenumbers beyond this range correspond to evanescent waves, which cannot propagate to the far field. As shown in Eq. (8), the number of independent channels can thus be estimated by the ratio of the wavenumber range to the minimum wavenumber resolution.

$$\mathrm{DoF} \leqslant \frac{2k_0}{\Delta k} = \frac{2L}{\lambda_0} \tag{8}$$

Therefore, for each $\lambda_0/2$-scale of the radiating aperture, there is only one spatial DoF. HMIMO systems with ultra-dense elements arranged within a limited aperture cannot achieve high spatial DoF, as reflected by the low effective rank of $\boldsymbol{H}\boldsymbol{H}^{H}$.

1.3 DoF of Conventional MIMO Transmitter

In the following, we compare HMIMO with conventional discrete MIMO and observe that the DoF of discrete MIMO is highly consistent with the theoretical bounds and limits of HMIMO.

Consider a discrete MIMO array composed of N elements. The radiation intensity of the n-th element in the direction (θ,φ) is given by $A_n f_n(\theta,\varphi) e^{i\boldsymbol{k}\cdot\boldsymbol{r}_n}$, where A_n is the amplitude of the n-th element, $f_n(\theta,\varphi)$ is the radiation pattern, $\boldsymbol{k}$ is the wave vector, and $\boldsymbol{r}_n$ is the position vector.

Consider that the radiation field of the N-element array undergoes time reversal of the far-field radiation and backpropagation, and is subsequently received by the same array. The transmitted signal from the n-th element, after time reversal, is received by the m-th element, forming the channel matrix $\boldsymbol{H}\boldsymbol{H}^{H}$ as shown in Eq. (9).

$$\left(\boldsymbol{H}\boldsymbol{H}^{H}\right)_{mn} = \frac{1}{4\pi}\int_0^{2\pi}\int_0^{\pi} f_m(\theta,\varphi) f_n^{*}(\theta,\varphi) e^{-i\boldsymbol{k}\cdot\boldsymbol{r}_m} e^{i\boldsymbol{k}\cdot\boldsymbol{r}_n} \sin\theta \mathrm{d}\theta\, \mathrm{d}\varphi \tag{9}$$

It can be easily shown that the spatial multiplexing DoF limitation of the array is the rank of the matrix $\boldsymbol{H}\boldsymbol{H}^{H}$ (Appendix B*), as shown in Eq. (10).

$$\mathrm{DoF} \leqslant \mathrm{rank}\left(\boldsymbol{H}\boldsymbol{H}^{H}\right) \tag{10}$$

For consistency throughout the paper, we consider a linear array composed of N half-wave dipoles, with an aperture size of $L = Nd$. In this case, the expression for $\left(\boldsymbol{H}\boldsymbol{H}^{H}\right)_{mn}$ is given in Eq. (11)[13].

$$\left(\boldsymbol{H}\boldsymbol{H}^{H}\right)_{mn} = \begin{cases} \dfrac{\sin[kd(n-m)]}{kd(n-m)}\left(1 - \dfrac{1}{[kd(n-m)]^2} + \dfrac{\cos[kd(n-m)]}{[kd(n-m)]^2}\right), \text{for } n \neq m \\ \dfrac{2}{3}\sin^2\theta, \text{for } n = m \end{cases} \tag{11}$$

For an HMIMO with the same aperture size, Eq. (8) provides the expression for its DoF limitation. Fig. 3 compares the DoF of a 1 000-element discrete MIMO linear array at various element spacings with that of an HMIMO array having the same aperture size. The high consistency between the two plot lines indicates

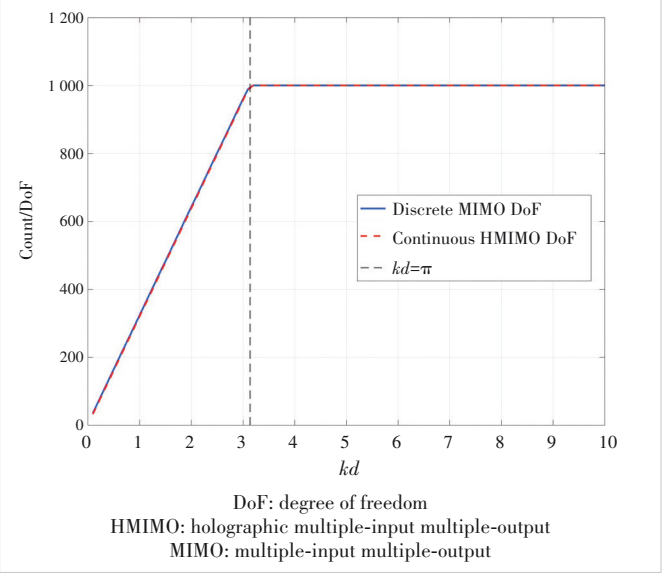

Figure 3. Comparison of a 1 000-element discrete MIMO array at different element spacings with an HMIMO array of the same aperture size, where the upper limit of the DoF of discrete MIMO is given by Eqs. (10) and (11), and the upper limit of the DoF of HMIMO is given by Eq. (8)

* The proofs of Eqs. (7) and (10) are provided in the supplementary material at the following link: https://zte.magtechjournal.com/EN/10.12142/ZTECOM.202602010.

that the DoF of the discrete MIMO array is equal to that of the HMIMO with the same aperture. When the element spacing is $\lambda/2$, the antenna elements are utilized most efficiently.

2 Principles for Expanding the DoF of HMIMO with Limited Aperture

In the previous section, we have established that the DoF of an HMIMO system with a limited aperture is inherently low. The primary reason for this low DoF is that, when the density of the antenna elements becomes excessively high, some current modes manifest as evanescent waves, which cannot effectively radiate to the far field. To address this issue, we propose principles for enhancing the DoF of HMIMO by converting evanescent waves into propagating ones, thereby enabling more modes to radiate effectively. These principles aim to optimize the system's capacity by increasing the number of effective spatial channels.

2.1 Number of Effective Radiation Modes

When N antennas are used to implement HMIMO, Eq. (4) indicates that N orthogonal modes can be constructed, yielding N spatial multiplexing DoF. However, in practice, not all N orthogonal bases can radiate into the far field.

To discuss the field distribution for each current excitation mode, it is necessary to consider the FT of the electric or magnetic field in the spatial domain. Using the equivalence principle, when the field on the opposite side of the planar aperture is set to zero, the field distribution on the aperture can be equivalently represented by an electric current distribution given by $\boldsymbol{J}_n = \hat{z} \times \boldsymbol{H}_n$, enabling quantitative description of the radiation field through the FT of the current distribution[14]. For the current distribution of an $M \times N$ array described by Eq. (4), the FT for mode (m,n) is given by Eq. (12), where $F_d\left(k_x,k_y\right)$ denotes the FT of the dipole current distribution.

$$\begin{aligned} F_{mn}\left(k_x,k_y\right) = {} & F_d\left(k_x,k_y\right)\left[\operatorname{sinc}\left(L_x k_x, L_y k_y\right) * \right. \\ & \sum_{p,q=-\infty}^{+\infty} \delta\left(k_x - q\frac{2\pi}{D_x}, k_y - p\frac{2\pi}{D_y}\right) * \\ & \left(\delta\left(k_x - \frac{n\pi}{L_x}\right) - \delta\left(k_x + \frac{n\pi}{L_x}\right)\right)\mathrm{e}^{-jk_x L_x/2} * \\ & \left.\left(\delta\left(k_y - \frac{m\pi}{L_y}\right) - \delta\left(k_y + \frac{m\pi}{L_y}\right)\right)\mathrm{e}^{-jk_y L_y/2}\right] \end{aligned} \tag{12}$$

In Eq. (12), the spectral distribution of the radiation field in the wavenumber domain for mode (m, n) is a translation and superposition of sinc functions.

In the $k_x - k_y$ wavenumber plane, the region within the circle $k_x^2 + k_y^2 = k^2$ is defined as the visible region. Inside the circle, the wavenumber in the propagation direction $k_z = \sqrt{k^2 - k_x^2 - k_y^2}$ is real, indicating that it can radiate into the far field. Outside the circle, the wavenumber in the propagation direction $k_z = j\sqrt{k_x^2 + k_y^2 - k^2}$ becomes purely imaginary. This implies that the wave decays exponentially in the z-direction and can only propagate along the $k_x - k_y$ plane, corresponding to evanescent waves that contribute to energy storage. Eq. (13) provides the spatial forms of electromagnetic waves along the z-direction in the $k_x - k_y$ wavenumber domain, for both the visible and invisible regions.

$$\begin{aligned} & \boldsymbol{E}\left(k_x,k_y,z\right) = \boldsymbol{E}\left(k_x,k_y\right)\mathrm{e}^{jk_z\left(k_x,k_y\right)z} = \\ & \begin{cases} \boldsymbol{E}\left(k_x,k_y\right)\mathrm{e}^{j\sqrt{k^2 - k_x^2 - k_y^2}\,z}, & k_x^2 + k_y^2 < k^2 \\ \boldsymbol{E}\left(k_x,k_y\right)\mathrm{e}^{-\sqrt{k_x^2 + k_y^2 - k^2}\,z}, & k_x^2 + k_y^2 \geqslant k^2 \end{cases} \end{aligned} \tag{13}$$

Thus, the radiation into the far field depends only on the portion of the source current's spatial FT that lies within the visible region.

Based on the visible region, the characteristic modes on the antenna array can be classified into radiation modes and evanescent modes. Radiation modes have their sinc functions' main peaks within the visible region, allowing them to radiate a significant amount of energy. Despite this, the infinite periodicity of the FT also results in peaks outside the visible region, corresponding to unavoidable evanescent waves that store energy in the near field. The number of radiation modes corresponds to the spatial DoF of the transmitter.

Evanescent modes are those whose sinc functions' main peaks lie outside the visible region, and thus all their main lobes generate evanescent waves, leading to greater energy storage. It should be noted that evanescent modes of a finite-sized array can still radiate a small amount of energy because all sinc functions in the wavenumber spectrum have sidelobes within the visible region. Theoretically, evanescent modes of an infinitely large array do not radiate energy, as the sinc function has a width close to zero, equivalent to a δ function without radiative sidelobes.

Consider a 1×5 linear array of electric dipoles to examine the changes in spatial DoF as the aperture gradually decreases, transitioning from an antenna array with standard half-wavelength spacing to an HMIMO system with a limited aperture. We observe the k_x direction for the 1×5 dipole array and plot the complete wavenumber spectrum of each mode, formed by the superposition of sinc functions at different element spacings, as shown in Fig. 4. In this figure, the red dashed box indicates the visible region. Based on the above classification criterion, the modes of the 1×5 dipole array with different element spacings are classified as shown in Table 1, indicating the corresponding spatial DoF.

For a conventional array with an element spacing of $\lambda/2$, the period of the shifted sinc functions equals the diameter of the visible region. This configuration excludes any evanescent modes, thereby fully exploiting the DoF provided by the num-

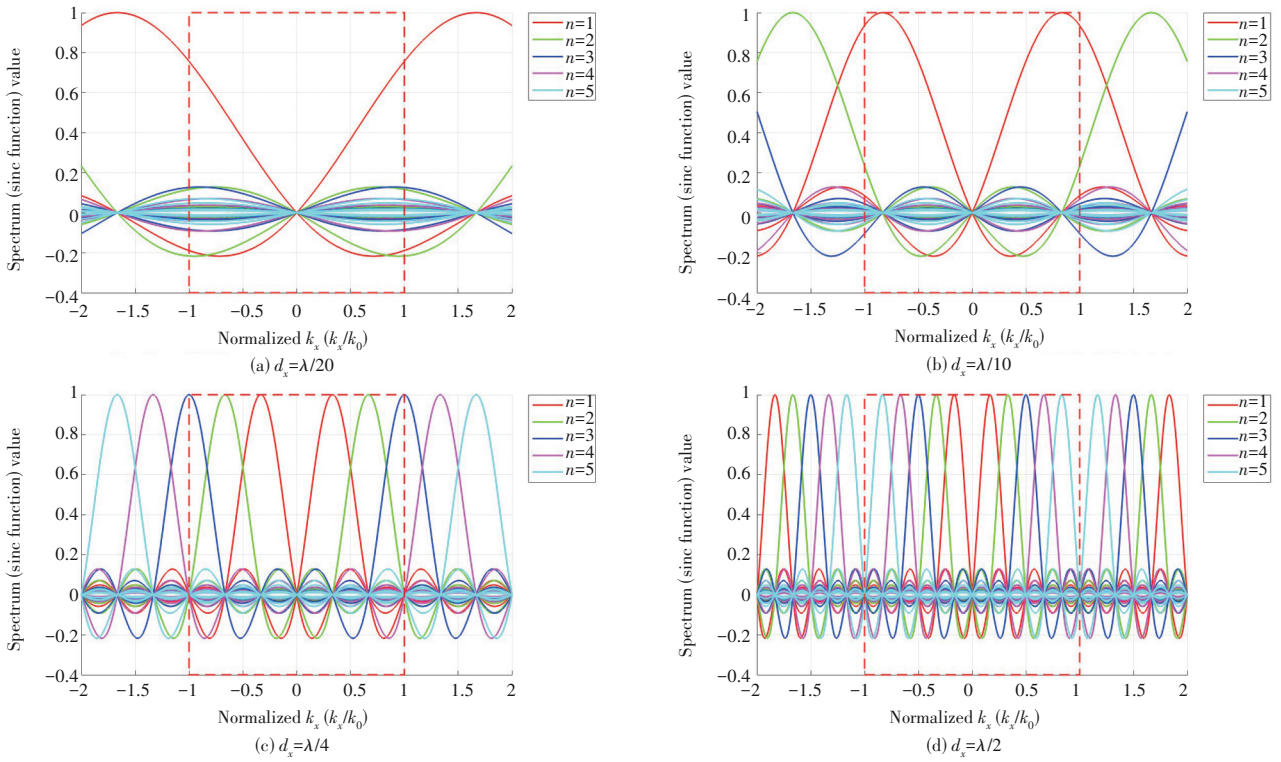

Figure 4. Spatial spectrum of each mode under element spacings: (a) d_x = λ/20, (b) d_x = λ/10, (c) d_x = λ/4, and (d) d_x = λ/2, where each color represents the spatial spectrum components of a current distribution mode and the red dashed box indicates the visible region

Table 1. Classification of patterns for a 1×5 dipole array

Element Spacing	λ/20	λ/10	λ/4	λ/2
Radiating mode	/	Mode 1	Modes 1 – 2	Modes 1 – 5
Evanescent mode	Modes 1 – 5	Modes 2 – 5	Modes 3 – 5	/
DoF	<1	1	2	5

DoF: degree of freedom

ber of antennas. In contrast, for an HMIMO system with ultra-dense element spacing and a limited aperture, the spatial DoF is extremely limited.

2.2 Expansion of DoF in Limited-Aperture HMIMO

To radiate more modes of HMIMO into the far field, it is necessary to effectively expand its visible region, i.e., convert the high-frequency oscillating components that originally existed as evanescent waves into propagating waves.

LRM with periodic structures can convert evanescent components into propagating waves. For example, an LRM consisting of $N \times N$ metallic wires of the same length L can achieve this effect[10].

The LRM is placed within the near-field region of the HMIMO, and the coordinate system is defined in Fig. 2. According to the Floquet theorem, the periodicity in the transverse plane gives the fields $E_{xz}(x_{xz})$, $E_y(x_{xz})$, $H_{xz}(x_{xz})$, and $H_y(x_{xz})$ the form of a Bloch wave solution:

$$U(x_{xz}) = e^{ik_{xz}x_{xz}}U_p(x_{xz}) \quad (14),$$

where k_{xz} is the Bloch wavenumber, and $U_p(x_{xz})$ represents the periodic part of the decomposed transverse components of the electric or magnetic field.

By applying Maxwell's equations in conjunction with the perfect electric conductor (PEC) boundary conditions, the dispersion relations for the transverse electric (TE) and transverse electromagnetic (TEM) modes described in Eq. (15) are derived as depicted in Fig. 5a.

$$\text{TE: } k_{xz}^2 + k_y^2 = \frac{\omega^2}{c^2};\ \text{TEM: } k_y^2 = \frac{\omega^2}{c^2} \quad (15).$$

Thus, the transverse wavenumber k_{xz} for TEM modes propagating along the y-direction can take any value. This allows high-frequency oscillating evanescent wave components from HMIMO to propagate within the metallic medium, which acts as a waveguide supporting the propagation of high-frequency components.

Further analysis of all transverse and longitudinal electromagnetic components, as shown in Fig. 5b, reveals that,

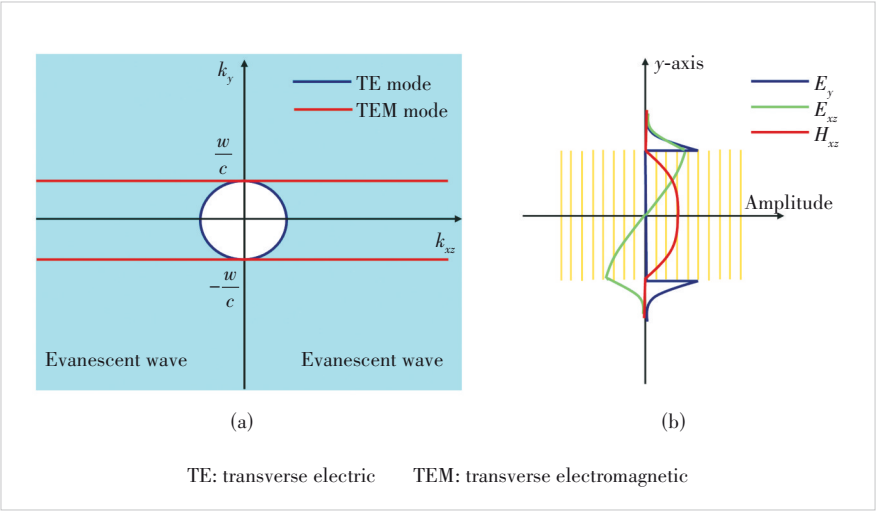

Figure 5. Locally resonant metamaterials: (a) dispersion relations for TE and TEM modes and (b) electromagnetic field distribution

near the y-axis adjacent to the metallic medium, the electric field exhibits strong polarization in the y-direction and decays exponentially as an evanescent wave, preventing energy from escaping through the top or bottom interfaces of the structure and allowing radiation only from the transverse interface[10]. The y-component of the electric field can be modeled as small dipoles located at $y = \pm L/2$. The spatial distribution of these small dipoles is determined by the y-component of the TEM mode at the interface, which radiates energy outward.

To understand how the spatial frequency of evanescent waves corresponds to the frequency of the radiated propagating waves, it is necessary to explore the dispersion relation between the radiated field frequency and the transverse wave vector component. When a TEM wave propagates along the y-axis and the metallic wire array, it encounters an interface between the metallic waveguide and air. At this interface, the wave undergoes both reflection and refraction. Between the two reflective surfaces located at $y = L/2$ and $y = -L/2$, the wave reflects back and forth, creating an effective Fabry-Perot cavity. This results in Fabry-Perot resonance for each propagating mode. The effective length of the Fabry-Perot cavity is determined by the energy entering the air, calculated in Eq. (16), where δ is the evanescent penetration depth associated with total internal reflection at the interface.

$$l_{\text{eff}} = l + 2\delta = l + \frac{2}{\sqrt{k_{xz}^2 - k^2}} \tag{16}$$

With the condition for Fabry-Perot resonance $l_{\text{eff}} = n\lambda/2$, the dispersion relation is obtained in Eq. (17), where $k_0 = \pi/l$ and $f_0 = c/2l$ denote the initial wavenumber and frequency of the first-order Fabry-Perot resonance, respectively.

$$\frac{f_0}{f} = 1 + \frac{2}{\pi}\left[\left(\frac{k_{xz}}{k_0}\right)^2 - \left(\frac{f}{f_0}\right)^2\right]^{-\frac{1}{2}} \tag{17}$$

This yields the dispersion characteristic describing the relationship between the high-spatial frequency components and the radiation frequency. As shown in Fig. 6c, compared to free space, the bending of the dispersion curve induced by the LRM results in a larger visible region in the wavenumber domain at the same radiation frequency. As the visible region for HMIMO modes expands, high-frequency components that would otherwise remain evanescent waves can now radiate into the far field as propagating waves, further increasing the DoF.

3 Simulation Results

We employ full-wave simulation software CST to validate the theoretical derivation regarding the expansion of the visible region of an HMIMO antenna array using LRM. As illustrated in Fig. 6a, we consider an HMIMO system consisting of five dipole antennas spaced approximately $\lambda_c/36$ apart, with an aperture width of $\lambda_c/9$ and a center operating frequency of $f_c = 340$ MHz. Focusing solely on the spatial multiplexing DoF of the transmitting HMIMO antenna, we employ the time-reversal method discussed in Section 2. By examining the eigenvalue distribution of the $\boldsymbol{HH}^H$ matrix, we determine the number of orthogonal eigenmodes that can be radiated into the far field by the transmitter, thereby evaluating the DoF.

3.1 Determination of the Visible Region

In the absence of LRM, the far-field time-reversal array completely surrounds the transmitting antenna, allowing electromagnetic waves radiated in all directions to be received. Thus, in free space, the visible region is defined as $[-k_0, k_0]$.

When LRM is present, the size of the visible region must be determined by measuring the frequency bands of the resonance peaks in the radiation field. As shown in Figs. 6b and Fig. 6c, the resonant frequencies of the electromagnetic waves radiated to the far field by the LRM are measured. This determines the visible region to be $[-98.3, 98.3]\ \text{m}^{-1}$ based on the dispersion relation.

3.2 Measurement of Transmit Spatial DoF

Based on the size of the visible region, the spatial DoF of the transmitting antenna with and without the LRM is determined to be 5 and 1, respectively. Simulations are performed for modes 1 to 5 under the same simulation environment, comparing the time-reversed signal distribution and the spatial distribution of the transmitted signal for scenarios with and

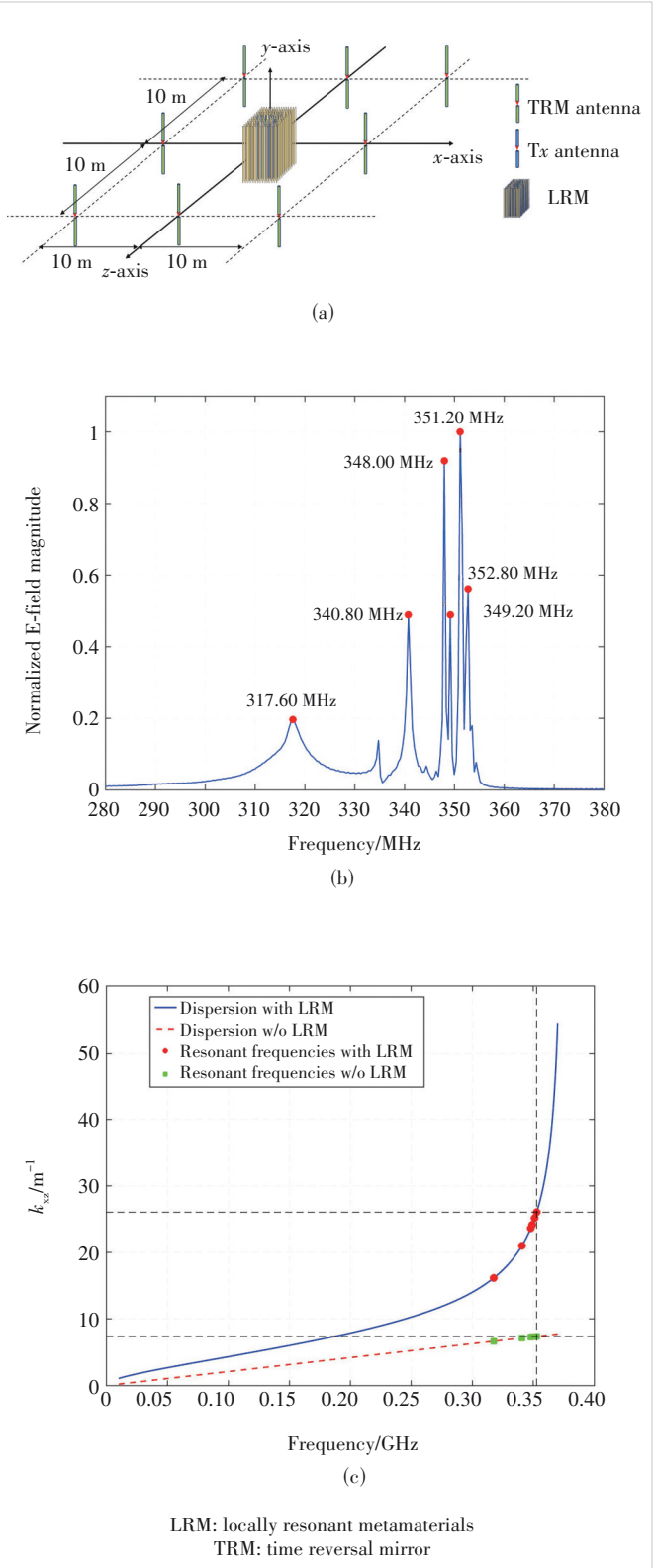

Figure 6. Simulation model and results: (a) simulation scenario, (b) normalized E-field magnitude with resonance frequencies and (c) visible region on the dispersion curve; in both scenarios (with and without LRM), the transverse wave number associated with the highest resonance frequency defines the range of the visible region

without LRM, as shown in Fig. 7. The blue line depicts the distribution of current modulus values for spatial signals transmitted on an ultra-dense antenna array. The green and red lines depict the reconstruction of time-reversed signals by the ultra-dense antenna array without and with LRM, respectively. All curves are normalized to their maximum values.

It is evident that, compared to the free-space scenario, the presence of a near-field LRM effectively enhances the spatial DoF of the radiated field in an HMIMO system composed of an ultra-dense linear antenna array, thereby enabling multi-stream transmission in a confined space.

Using the time-reversal method described in Section 2, we analyze the eigenvalue distribution of the channel matrix $\boldsymbol{HH}^H$ for an HMIMO system with five orthogonal basis modes to determine the spatial DoF at the transmitter side. When the transmitted signal is represented by $\boldsymbol{s}_i = \boldsymbol{e}_i$, i = 1,2,3,4,5, (where $\boldsymbol{e}_i$ are unit vectors), the time-reversed signal corresponds to the projection of the received signal onto each orthogonal basis, allowing us to compute the channel matrix $\boldsymbol{HH}^H$.

In the presence of a near-field LRM, the eigenvalue distribution obtained after eigenvalue decomposition is 1.252, 0.804, 0.397, 0.130, 0.049 ($\times 10^{-6}$). In the free-space scenario, the eigenvalue distribution is 8.769 8, 0.010 8, 0, 0, 0. It can be observed that in the presence of a near-field LRM, the rank of the channel matrix is 5, and the eigenvalue distribution is relatively uniform. If we consider channels with eigenvalues greater than 10% of the maximum eigenvalue as effective channels, the number of effective independent orthogonal channels in the system is 4. In contrast, without the near-field LRM, the number of effective channels is only 1. However, this enhancement comes at the cost of a certain degree of energy loss introduced by the LRM.

To better quantify the number of effective channels, the effective rank is employed as an evaluation metric, defined in Eq. (18), where λ_i represents the i-th eigenvalue of $\boldsymbol{HH}^H$, and N is the number of antenna elements. When calculating the effective rank, we normalize the time-reversed current distribution before projecting it onto an orthogonal basis to compute $\boldsymbol{HH}^H$. Consequently, the resulting eigenvalues differ from those previously discussed. This approach solely assesses mode recovery without considering energy differences.

$$\text{Effective Rank} = \frac{\left(\sum_{i=1}^{N}\lambda_i\right)^2}{\sum_{i=1}^{N}\lambda_i^2} \tag{18}$$

The effective rank quantitatively measures the uniformity of the eigenvalue distribution, the dimensionality of the signal subspace, and the system's ability to effectively distinguish between different signal sources. A higher effective rank indi-

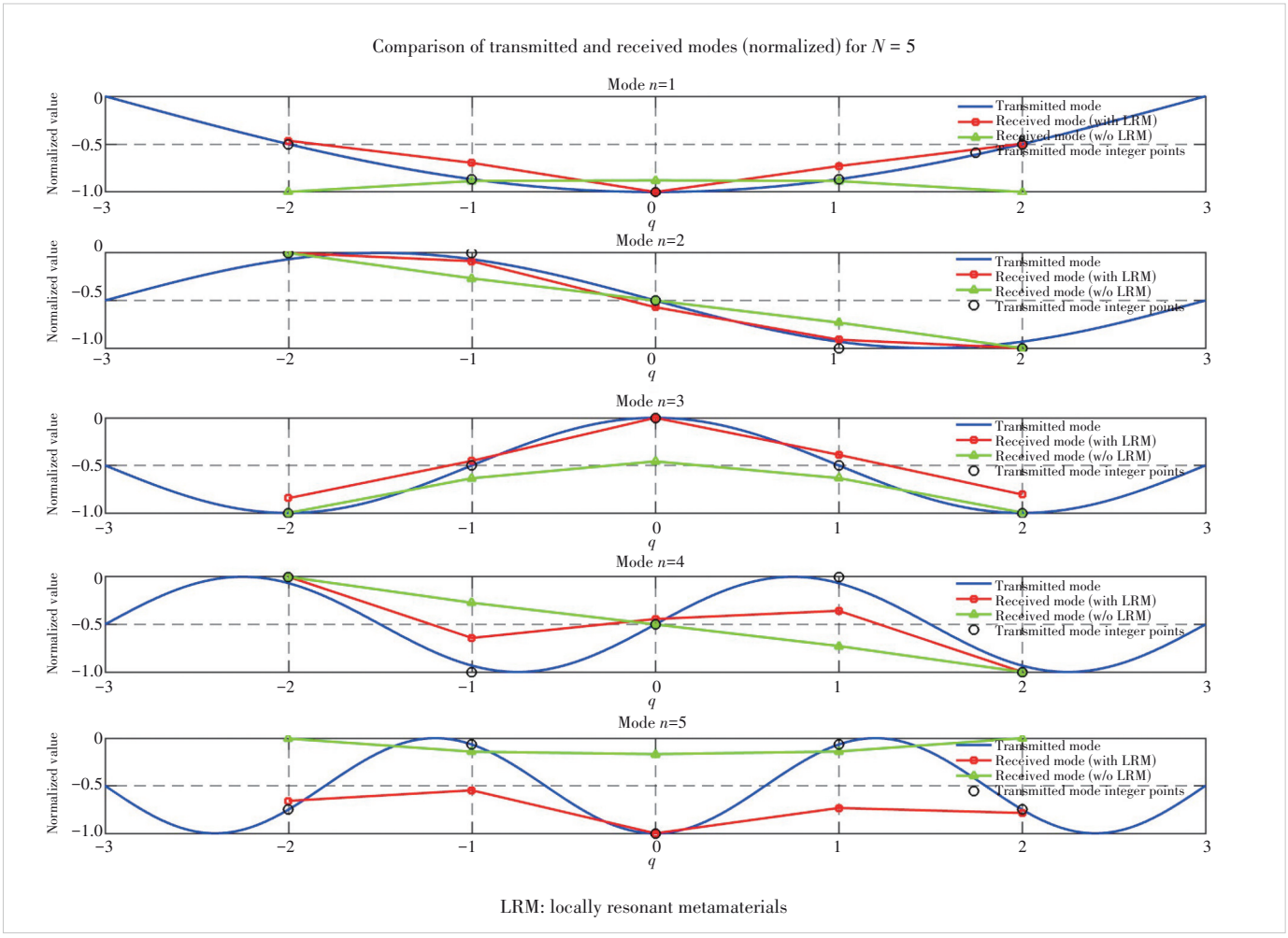

Figure 7. Normalized current magnitude distribution of time-reversal signals and transmitted signals

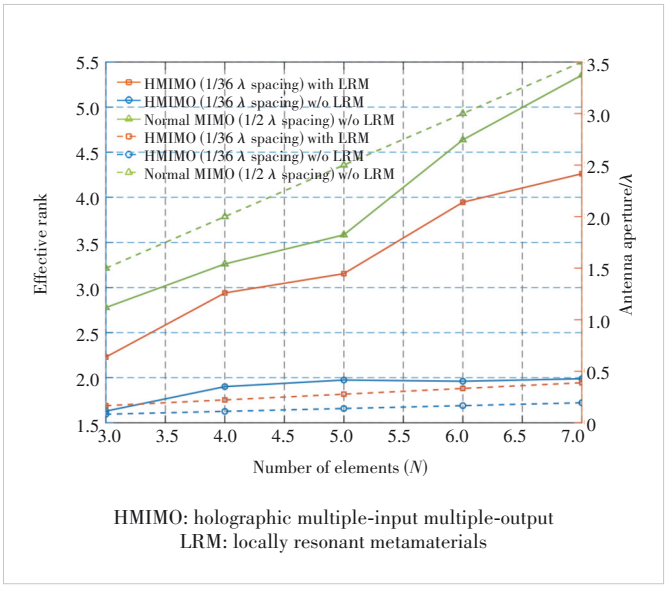

Figure 8. Relationship between effective rank(solid lines) and antenna aperture (deshed lines) as the number of elements varies

cates a system with greater DoF. We conduct simulations of HMIMO systems with LRM under different element spacings and compare them with HMIMO systems without LRM, as shown in Fig. 8. It is evident that HMIMO with a surrounding LRM significantly enhances the DoF by more than twofold compared to HMIMO without LRM, while being only slightly below the DoF of discrete MIMO with half-wavelength spacing used as a benchmark. Notably, the aperture size of HMIMO with LRM is reduced to approximately one-sixth of that of the discrete MIMO with half-wavelength spacing. It is important to note that, theoretically, the DoF of discrete MIMO with half-wavelength spacing equals the number of antenna elements. However, in our simulations, the time-reversal mirror utilized consists of only eight far-field antennas, which cannot achieve ideal performance, resulting in measured DoF values lower than the theoretical predictions. Through these simulations, we demonstrate that the LRM significantly enhances the DoF of the HMIMO system with a limited aperture, enabling high-dimensional multi-stream transmission.

4 Conclusions

HMIMO is implemented using ultra-dense antenna arrays. However, the upper limit of spatial multiplexing DoF in HMIMO is no longer determined by the number of antennas but by the size of the visible region defined by the laws of electromagnetic wave propagation. Placing LRM in the near field alters the spatial dispersion relation, converting the high-frequency evanescent wave components into propagating waves radiated into the far field. This effectively expands the visible region in the wavenumber domain, significantly enhancing the spatial multiplexing DoF of HMIMO. The theory of visible region expansion has been validated through full-wave simulation software. In the future, super-resolution multi-stream technology is expected to find wide-ranging applications in numerous domains. For instance, in smart factory environments, an HMIMO system deployed on agents can facilitate real-time data transmission and high-precision control with high efficiency and improved spatial utilization.

References

[1] Huang C W, Hu S, Alexandropoulos G C, et al. Holographic MIMO surfaces for 6G wireless networks: opportunities, challenges, and trends [J]. IEEE wireless communications, 2020, 27(5): 118 – 125. DOI: 10.1109/MWC.001.1900534
[2] Sun Y Q, Jian M N, Yang J, et al. Degree of freedom analysis for holographic MIMO based on a mutual-coupling-compliant channel model [J]. ZTE Communications, 2024, 22(1): 34 – 40. DOI: 10.12142/ZTECOM.202401005
[3] Yuan J D, Ngo H Q, Matthaiou M. Towards large intelligent surface (LIS)-based communications [J]. IEEE transactions on communications, 2020, 68 (10): 6568 – 6582. DOI: 10.1109/TCOMM.2020.3009115
[4] Pizzo A, de Jesus Torres A, Sanguinetti L, et al. Nyquist sampling and degrees of freedom of electromagnetic fields [J]. IEEE transactions on signal processing, 2022, 70: 3935 – 3947. DOI: 10.1109/TSP.2022.3183445
[5] Pizzo A, Marzetta T L, Sanguinetti L. Degrees of freedom of holographic MIMO channels [C]//The 21st International Workshop on Signal Processing Advances in Wireless Communications (SPAWC). IEEE, 2020: 1 – 5. DOI: 10.1109/spawc48557.2020.9154219
[6] Ji R, Chen S, Huang C W, et al. Extra DoF of near-field holographic MIMO communications leveraging evanescent waves [J]. IEEE wireless communications letters, 2023, 12(4): 580 – 584. DOI: 10.1109/LWC.2023.3234003
[7] Gong T R, Gavriilidis P, Ji R, et al. Holographic MIMO communications: theoretical foundations, enabling technologies, and future directions [J]. IEEE communications surveys and tutorials, 2024, 26(1): 196 – 257. DOI: 10.1109/COMST.2023.3309529
[8] Malyuskin O, Fusco V. Far field subwavelength source resolution using phase conjugating lens assisted with evanescent-to-propagating spectrum conversion [J]. IEEE transactions on antennas and propagation, 2010, 58 (2): 459 – 468. DOI: 10.1109/TAP.2009.2037713
[9] Lerosey G, de Rosny J, Tourin A, et al. Focusing beyond the diffraction limit with far-field time reversal [J]. Science, 2007, 315(5815): 1120 – 1122. DOI: 10.1126/science.1134824
[10] Lemoult F, Lerosey G, de Rosny J, et al. Resonant metalenses for breaking the diffraction barrier [J]. Physical review letters, 2010, 104(20): 203901. DOI: 10.1103/physrevlett.104.203901
[11] Sanguinetti L, D'Amico A A, Debbah M. Wavenumber-division multiplexing in line-of-sight holographic MIMO communications [J]. IEEE transactions on wireless communications, 2023, 22(4): 2186 – 2201. DOI: 10.1109/TWC.2022.3208961
[12] Gong X W, Yuan Z F, Xu J, et al. Line-of-sight MIMO for next-generation microwave transmission systems [J]. ZTE communications, 2012, 10(4): 33 – 38
[13] Altshuler E E, O'Donnell T H, Yaghjian A D, et al. A monopole superdirective array [J]. IEEE transactions on antennas and propagation, 2005, 53(8): 2653 – 2661. DOI: 10.1109/TAP.2005.851810
[14] King A J. Characteristic mode theory for closely spaced dipole arrays [D]. Ann Arbor: University of Michigan, 2015

Biographies

Liu Guohao received his BS degree from the Department of Electronic Engineering, Tsinghua University, China in 2024, where he is currently pursuing his PhD degree. His current research interests include electromagnetics-based communication theory and communication systems based on novel antenna designs.

Fang Min received her PhD degree from the Department of Electronic Engineering, Tsinghua University, China in 1999. She joined ZTE Corporation in 2004 and has been engaged in innovation in new technologies and standardization for next-generation wireless communications. She led ZTE's standard team to accomplish the 3GPP LTE Release 8 standardization and ZTE's first UMTS FDD work item. She also made a significant contribution to the ZTE's 5G R&D on the Pre5G massive MIMO technology, which won both the Best Mobile Technology Breakthrough and the CTO Choice Awards in MWC 2016. She is currently coordinating the wireless prototyping activities on new traffic models, novel architectures, and key technologies such as ultra-massive MIMO, mmWave coverage, and agent-based communication for 6G and beyond.

Peng Lin received his BS degree in information engineering, and MS degree in electromagnetic fields and microwave techniques from the Nanjing University of Science and Technology, China in 2004 and 2006, respectively. Since 2006, he has been with ZTE Corporation, where he engages in wireless communications. His current research interests include beyond-5G and 6G technology, millimeter-wave and terahertz communication, and intelligent reflecting surface for wireless applications.

Luo Jun received his BS degree in electronic science and technology from the University of Electronic Science and Technology of China in 2016, and MS degree in electromagnetic fields and microwave technology from Southeast University, China in 2019. He is currently a senior engineer with ZTE Corporation, and his research interests include RIS, near-field communication, novel MIMO antenna systems, and millimeter-wave and terahertz technologies.

Sun Zhi (zhisun@ieee.org) received his BS degree in telecommunication engineering from Beijing University of Posts and Telecommunications, China in 2004, MS degree in electronic engineering from Tsinghua University, China in 2007, and PhD degree in electrical and computer engineering from Georgia Institute of Technology, USA in 2011. Since 2021, he has been a tenured associate professor with Tsinghua University, China. Prior to that, he was a tenured associate professor at the University at Buffalo, The State University of New York, USA, which he joined as an assistant professor in 2012. His research interests include AI-enabled 6G wireless communication systems, underground and underwater wireless communications and networking, and communication systems based on novel antenna designs. He received the NSF CAREER Award in 2017, the Best Demo Award at IEEE INFOCOM 2017, and the Best Paper Award at IEEE GLOBECOM 2010. He has served as an editor for *IEEE Transactions on Mobile Computing*, *IEEE Transactions on Wireless Communications*, and *Computer Networks*.

5G-R Core Network Cyber Security Assessment Method Based on Attack Graphs

Dong Congtang[1], Xu Hang[1], Sun Bin[2,3], Ding Jianwen[1], Wang Wei[4]

(1. State Key Laboratory of Advanced Rail Autonomous Operation, Beijing Jiaotong University, Beijing 100044, China;
2. Key Laboratory of Railway Industry of Broadband Mobile Information Communications,Beijing Jiaotong University, Beijing 100044, China;
3. School of Electronic and Information Engineering, Beijing Jiaotong University, Beijing 100044, China;
4. ZTE Corporation, Shenzhen 518057, China)

DOI: 10.12142/ZTECOM.202602011

https://kns.cnki.net/kcms/detail/34.1294.TN.20260422.1331.002.html, published online April 22, 2026

Manuscript received: 2025-02-03

Abstract: With the rapid advancement of 5G network technology, cyber security threats are intensifying. The fifth-generation mobile communication for railways (5G-R), as a product of the deep integration of the railway industry with 5G technology, plays a crucial role in ensuring the operational safety of railways. Cyber security assessment is one of the key components in safeguarding network security, and attack graphs are one of the mainstream models for cyber security assessment methods. This paper focuses on optimizing the method for assessing the security of the 5G-R core network based on attack graphs. By integrating the business security requirements of the 5G-R core network, this paper optimizes the parameters for the conventional vulnerability assessment methods and the influencing indicators of atomic attack success probability. It also constructs a formula for calculating the atomic attack success probability based on the fuzzy analytic hierarchy process (AHP). By setting up a simulated environment of the 5G-R core network within a network target field, this paper conducts the feasibility verification of the assessment method for 5G-R core cyber security. Comparative experiments with the conventional common vulnerability scoring system (CVSS) and methods used in existing literature prove the validity and superiority of the proposed model.

Keywords: 5G-R; cyber security; attack graph; AHP; security assessments

Citation (Format 1): Dong C T, Xu H, Sun B, et al. 5G-R core network cyber security assessment method based on attack graphs [J]. ZTE Communications, 2026, 24(2): 94 - 103. DOI: 10.12142/ZTECOM.202602011
Citation (Format 2): C. T. Dong, H. Xu, B. Sun, et al., "5G-R core network cyber security assessment method based on attack graphs," *ZTE Communications*, vol. 24, no. 2, pp. 94 - 103, Jun. 2026. doi: 10.12142/ZTECOM.202602011.

1 Introduction

With the ongoing deployment and advancement of the 5G "New Infrastructure" strategy, a series of technological innovations related to the next-generation railway mobile communication are being actively developed in China[1]. The fifth-generation mobile communication for railway (5G-R) system, based on 5G technology and designed to meet the demands of railway communication services, is the next-generation railway mobile communication system[2]. Network security is critical to the safe and reliable operation of the 5G-R system and its underlying services, serving as a vital foundation for its high-quality development. Cyber security assessment constitutes one of the key steps in ensuring information system security[3]. It is an important measure to enhance cyber security, prevent malicious attacks and data leakage, and reduce security risks. For the 5G-R system and the railway industry, the importance of cyber security assessment technology cannot be overstated. It is significant in ensuring the normal operation of 5G-R network services, preventing the leakage of sensitive data, defending against network attacks, and maintaining the availability, reliability, and security of the 5G-R network.

Although certain cyber security assessment methods are prescribed in standards like ISO 27000[4], these methods require a comprehensive understanding of vulnerabilities pres-

This research was supported by State Key Laboratory of Advanced Rail Autonomous Operation under Grant No. RAO2023ZZ004, the Project of China State Railway Group under Grant No. N2024B004, and ZTE Industry-University-Institute Cooperation Funds under Grant No. W23L01180.

ent within a network. Additionally, their assessment results tend to be single-dimensional, making it difficult to obtain key information such as attack paths[5-8] and vulnerability scores. Moreover, these methods fail to meet the particular security and service requirements when applied to specific networks such as the 5G-R network. Therefore, for 5G-R cyber security, introducing attack graphs to analyze network vulnerabilities and attack paths enables a more comprehensive and in-depth assessment of the 5G-R core network security.

In 1998, Phillips et al.[9] introduced the concept of attack graphs, which involves simulating network attacks, predicting potential attack paths, and analyzing network vulnerabilities. This method relies on inputting the network's structural information, configurations, attacker actions, and attack patterns to construct a directed graph representing the state of the network. Thus, it analyzes various attack paths that an attacker might take and their effects.

As the demand for efficient generation of attack graphs grows, particularly in large network environments, reducing attack graph complexity and developing more efficient generation tools have become focal points in attack graph research. Ritchey et al.[5] constructed attack paths using the symbolic model verifier (SMV), a method capable of generating only one path at a time, thereby limiting coverage of all possible paths. In contrast, Lippmann et al.[6] developed the Network Security Planning Architecture (NetSPA) tool, leveraging graph theory principles. This tool employs a simple attack description language and utilizes a forward depth-first search algorithm to rapidly generate attack graphs. However, it relies on manually constructed rule bases and generates attack graphs containing multiple loops. The topological vulnerability analysis (TVA) tool developed by Noel et al.[10] faces similar issues: although offering TVA, it still depends on manually constructed rule bases and lacks automated generation methods. Sheyner et al.[7] developed the Attack Graph Toolkit for the Linux system, featuring a state attack graph generation tool. However, its state attack graphs are difficult to scale to large networks due to algorithmic complexity and state explosion issues. The MulVAL tool developed by Ou et al.[8] utilizes vulnerability scan results and describes relevant information using the Datalog programming language. It performs modeling and analysis using its rule base and employs the Graphviz tool to draw attack graphs. While it offers high accuracy, scalability, and has gained widespread recognition, it still faces issues such as rule base updates and the expression of attack types.

In recent years, with more in-depth research, attack graphs have been increasingly applied to cyber security across various domains. For instance, Ref. [11] combines attack graphs with the cyber security of power system networks, constructing a risk assessment method suitable for such networks. Ref. [12] introduces an optimized attack graph-based cyber security risk assessment method, achieving cross-domain dynamic security risk analysis for industrial control systems. Ref. [13] presents an attack path discovery method based on hierarchical task networks, addressing the performance shortcomings of attack graphs in large networks.

In summary, utilizing attack graphs as the theoretical model for security assessment of the 5G-R core network has its merits. On one hand, attack graphs enable structured analysis and identification of vulnerabilities within the 5G-R core network. Security assessments based on attack graphs can identify and prioritize paths most likely to be exploited by attackers, enhancing the specificity and efficiency of defensive measures. On the other hand, attack graphs support dynamic security assessments, adapting to the complex situations of the 5G-R core network environment. Updated attack graphs reflect new security statuses, making them particularly suitable for networks like 5G-R, which requires continuous monitoring and rapid response. Therefore, employing attack graphs as the theoretical model for 5G-R core cyber security assessment can help establish a robust cyber security assessment framework.

However, current security assessment models based on attack graphs still have the following shortcomings:

1) Vulnerability assessment indicators are relatively fixed, and their values are not comprehensive enough. The fixed nature of assessment indicators may result in assessment results that do not adequately reflect the real cyber security situation.

2) The influence of atomic attack probability is singular. Current assessment models rely only on one or a few simple probability values to estimate the success rate of each atomic attack, ignoring the reality that the success of an attack may be influenced by various factors.

To address the deficiencies of the current cyber security assessment models, this paper proposes the following optimization strategies:

1) Adding relevant assessment indicators: To improve the adaptability and comprehensiveness of vulnerability assessment indicators, assessment methods, and indicators can be adjusted and expanded by introducing related indicators based on specific scenarios and security needs of the network.

2) Multidimensional attack probability estimation: By introducing a multi-factor assessment model that takes into account the nature of the vulnerability itself and the influencing factors during the attack process, a method for calculating the probability of success for atomic attacks can be constructed.

2 Optimization of 5G-R Core Cyber Security Assessment Method Based on Attack Graphs

Attack-graph-based cybersecurity assessment technology is founded upon the attack graph model. Through detailed model analysis, it enables comprehensive evaluation of the cyber security status. This methodology mainly includes two key components: vulnerability assessment based on the attack graph and the quantification of node compromise probabilities.

This section focuses on optimizing the general attack graph

cyber security assessment method to develop a comprehensive assessment framework for 5G-R core networks. The overall architecture is shown in Fig. 1.

2.1 Vulnerability Assessment Method

This section investigates vulnerability assessment methods for the 5G-R core network. By integrating the security requirements of the 5G-R core network and expert knowledge, parameter indicators are optimized to better align the refined assessment method with practical cybersecurity needs. The vulnerability assessment method is illustrated in Fig. 1a.

The proposed optimization strategies focus on two aspects. First, the exploitability score values are optimized by expanding the exploitability scoring indicators, thereby improving assessment accuracy. Second, the impact scoring indicators are optimized by constructing a business security impact metric to measure the security influence of vulnerabilities in the 5G-R core network, which caters to cyber security needs.

1) Optimization of exploitability scoring indicators

For the conventional exploitability scoring indicator, attack vector $\boldsymbol{E}_{av}$, the values include Network N , Adjacent Network A , Local Network L, and Physical Access P. To meet the security needs of the 5G-R core network, Wireless Access W_v is added as a new value for the attack vector. Other attack vector classifications are consistent with the common vulnerability scoring system (CVSS). Since the definition of Wireless Access is similar to that of Network Access, it is assigned a weight of $W_v = N$. The level divisions for the 5G-R core network scoring system are consistent with the CVSS system, resulting in the weight order of $N > A > L > P$.

The attack complexity values for the 5G-R core network are divided into four levels: Low (L), Medium (M), High (H), and Very High (H_e). Among these, Medium (M) and Very High (H_e) are two new levels added specifically for assessing 5G-R core network vulnerabilities, designed to refine the difficulty in exploiting different vulnerabilities. Other attack complexity classifications are consistent with CVSS.

2) Optimization of impact scoring indicators

Conventional vulnerability impact scoring indicators focus solely on the impact on information security. In contrast, the vulnerability impact scoring indicators for the 5G-R core network comprehensively consider two main dimensions: one is the impact on information security, namely confidentiality (I_c), integrity (I_i), and availability (I_a); the other is the impact on business security, namely business confidentiality (B_s), business integrity (B_i) , and business continuity (B_c) . Regarding impact scoring, this paper adopts the same weight values and calculation methods as the CVSS scoring system. The calculation method for information security impact is shown in Eq. (1):

$$S_{\text{imp}} = 6.42 \times \left\{1 - \left[\left(1 - I_c\right) \times \left(1 - I_i\right) \times \left(1 - I_a\right)\right]\right\} \quad (1).$$

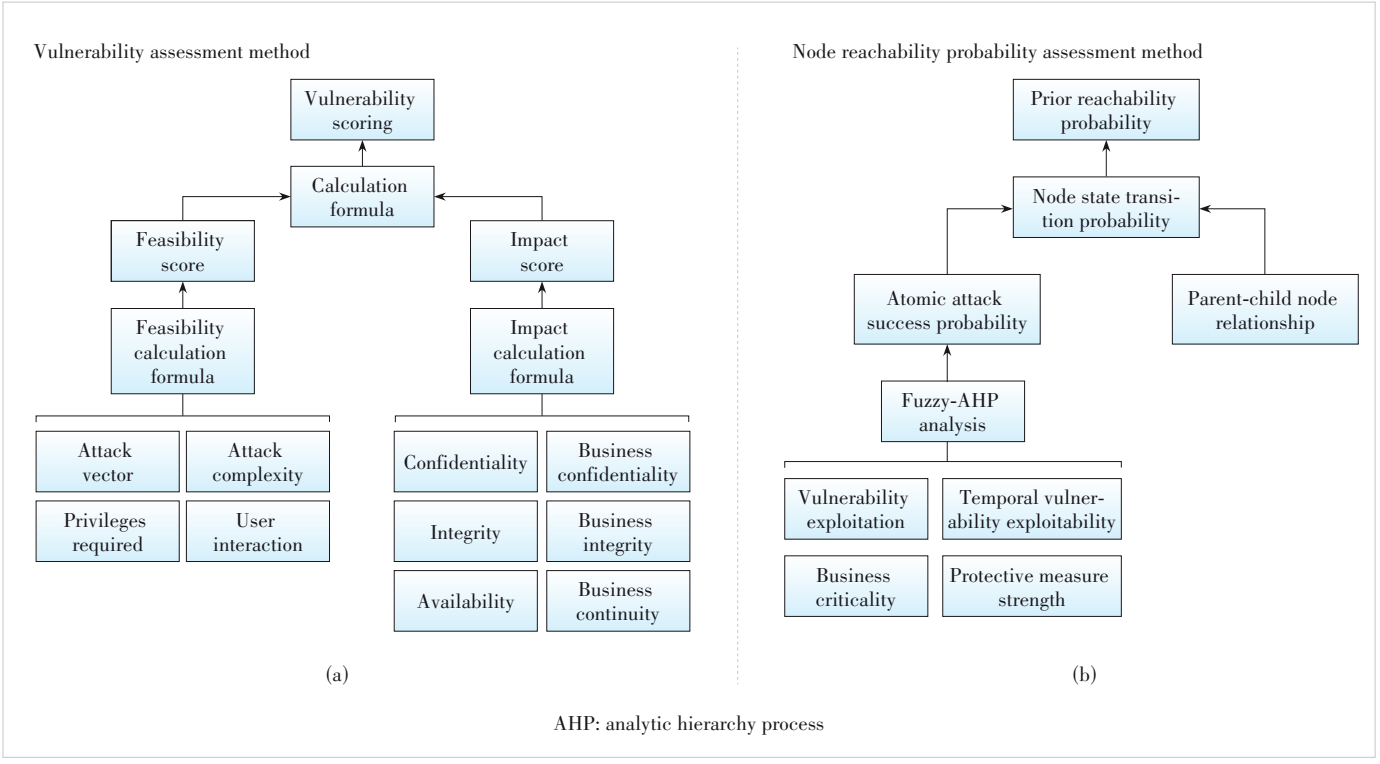

Figure 1. Overall framework of 5G-R core cyber security assessment based on attack graphs

Based on Eq. (1), the specific calculation method for business security impact assessment is shown in Eq. (2):

$$S_B = 1 - \left[\left(1 - B_c\right) \times \left(1 - B_i\right) \times \left(1 - B_s\right)\right] \quad (2).$$

Furthermore, given that the proposed vulnerability assessment model is tailored for 5G-R core network security and that the 5G-R system is a business-critical system, business security indicators are allocated a weight of 0.6, and information security indicators a weight of 0.4, based on past experience and expert advice. Building upon Eq. (1), the vulnerability impact score is calculated as follows:

$$S_{\text{Imp}} = 6.42 \times \left(0.6 \times S_B + 0.4 \times S_I\right) \quad (3),$$

where S_{Imp} represents the vulnerability impact score, S_B the business security impact score, and S_I the information security impact score.

For the 5G-R core network vulnerability assessment model, information and business security indicators are divided into three levels: High, Low, and None, which represent the potential damage to information and business security from the exploitation of 5G-R core network vulnerabilities. Information security indicators are consistent with CVSS, and new business security indicators grading criteria are shown in Table 1.

In summary, the specific values for the exploitability and impact scoring indicators in the 5G-R core network vulnerability assessment model are shown in Table 2. The values of the indicators are derived by combining the CVSS scoring system with related materials and expert judgment.

2.2 Node Reachability Probability Calculation Method

This section explores an optimization method for calculating the node reachability probability in the 5G-R core network. By optimizing influencing indicators of the atomic attack success probability for the 5G-R core network, a formula for calculating atomic attack success probability based on the fuzzy analytic hierarchy process (AHP) is constructed, which enables optimized node reachability probability to more accurately reflect the security requirements of the 5G-R core network.

The overall architecture of the 5G-R core network attack graph node reachability probability calculation model is shown in Fig. 1b.

The optimization of the node reachability probability primarily focuses on the calculation of the atomic attack success probability. On one hand, the influencing factors of atomic attack success probability are considered, where additional influencing indicators are introduced on top of conventional methods. On the other hand, a formula for calculating the atomic attack success probability based on expert experience and fuzzy AHP is constructed.

2.2.1 Vulnerability-Related Elements Research

The influencing factors of atomic success probability of the 5G-R core network attack graph can be mainly divided into two aspects: vulnerability exploitability within the 5G-R core network that attackers utilize during attacks, and the attacker's intent regarding vulnerability exploitation. This section optimizes the calculation methods for vulnerability exploitability and temporal exploitability, and defines indicators to measure attack intent.

1) Vulnerability exploitation

From the dynamic perspective of actual attack paths, attack-

Table 1. Consequences of vulnerability exploitation on business security indicators in the 5G-R core network

Level	Business Confidentiality	Business Integrity	Business Continuity
High	Serious threats to the business due to the leakage of critical information in the 5G-R core network	Illegal modification, destruction, or deletion of business data or system functions, seriously affecting business processes	Key business services unavailable for a long time, requiring an extended recovery period
Low	Minor leakage of non-critical business information, with relatively minor impacts	Minor unauthorized modification of business data or system functions	Temporary business interruption or delay
None	No information leakage	No modification of business data or system functions	No impact

Table 2. Vulnerability assessment indicator values

Indicator Category	Indicator Level	Quantitative Value
Attack vector	Network, wireless access, adjacent network, local, physical	(0.85, 0.85, 0.62, 0.55, 0.20)
Attack complexity	Very high, High, Medium, Low	(0.22, 0.44, 0.56, 0.77)
Business confidentiality	High, Low, None	(0.27, 0.62, 0.85)
Business integrity	High, Low, None	(0.27, 0.62, 0.85)
Business continuity	High, Low, None	(0.27, 0.62, 0.85)

ers inevitably obtain the necessary preconditions (such as privileges) and environmental conditions required to exploit vulnerabilities. Therefore, when dynamically considering the exploitability of vulnerability nodes in the 5G-R core network attack graph, to ensure the accuracy and non-redundancy of the inference results, the indicators of attack vector and required privileges should be excluded.

Thus, the vulnerability exploitability V_a calculation formula for the nodes in the 5G-R core network attack graph is:

$$V_a = E_{ac} \times E_{ui} \quad (4),$$

where E_{ac} represents attack complexity and E_{ui} means user interaction.

2) Temporal vulnerability exploitability

To assess the temporal exploitability of vulnerabilities in the 5G-R core network attack graph, it is necessary to optimize temporal exploitability indicators in the CVSS scoring system. The optimized indicators for 5G-R attack graph nodes are "Technical Maturity" and "Mitigation Level", corresponding to CVSS indicators "Vulnerability Exploitability" and "Mitigation Level", respectively. The calculation method for temporal exploitability V_{ta} of vulnerability nodes in the 5G-R core network attack graph is shown in Eq. (5).

$$V_{ta} = E_{tm} \times E_{rl} \times E_{rc} \quad (5),$$

where E_{tm} represents the technical maturity level of the attack against the node; E_{rl} corresponds to the mitigation level against the node vulnerability, which falls into four levels; and E_{rc} represents the confidence in the reports related to node vulnerability. The specific grading standards for the corresponding indicators are shown in Table 3.

3) Attack intent

This paper proposes two indicators to measure the attackers' intent toward nodes in the 5G-R core network attack graph: business criticality and the strength of protective measures, which are used to assess the potential gains from an attack and the associated risks, respectively.

• Business criticality

This section defines the business criticality of vulnerabilities in the 5G-R core network attack graph as the degree of importance, direct or indirect, of the network components involved in vulnerabilities to the continuity, stability, and efficiency of 5G-R network services. The main factors affecting the business criticality indicator include service impact scope, data sensitivity, and the effect of failure. The classifications and assigned values for business criticality levels in the 5G-R core network attack graph are shown in Table 4.

• Protective measure strength

This section defines the strength of protective measures in the 5G-R core cyber security assessment as the capacity and robustness of related components or systems in the 5G-R core network to resist attacks and threats. Factors that influence the protective measure strength indicator include technical deployment, physical security, data backup, restoration, etc. The classifications and assigned values for the protective measure strength levels in the 5G-R core network are presented in Table 5.

Table 3. Grading criteria for corresponding indicators

Indicator Category	Level	Classification Criteria
Technical maturity	High (H)	Widely used tools or methods exist; the attack process is fully automated, requiring no complex configuration.
	Automatable (A)	Automated tools requiring basic configuration; attack scripts or code may have been developed and shared, needing minor modifications.
	Verified (V)	Verified in certain environments but not widely automated; requiring technical adjustments to existing tools.
	Unverified (V_u)	Only proposed in theory; requiring highly customized development, involving complex research and testing.
Mitigation level	Non-remediable (N_R)	Currently, no known patches or tools that can mitigate the risk.
	Indirectly remediable (N_{DR})	Although no direct remedy is available, the risk can be mitigated by implementing additional protective measures.
	Low remediation (L_{DR})	Methods are available to address the vulnerability, but they either only partially alleviate the risk or are complex to implement.
	High remediation (H_{DR})	The vulnerability can be effectively addressed with existing methods and tools; patches or remedial measures are already available.
Report confidence	Confirmed (C)	Existence and details are verified through reliable means; it has been exploited in observed attacks or detailed reports provided by relevant organizations.
	Unconfirmed (C_u)	The report is not fully verified; it may originate from unverified third-party claims or automated scanning tools, requiring further verification.
	Unknown	There have been no reports related to this vulnerability.

Table 4. Business criticality value classification

Value Range	Classification Criteria
0.8 – 1.0	Extensive impact scope: involves crucial data; failure causes a severe breakdown of the entire system.
0.6 – 0.8	Broad impact scope: involves highly sensitive data; failure may result in prolonged business interruption.
0.4 – 0.6	Moderate impact scope: components handle sensitive data; failure causes temporary business interruption.
0.2 – 0.4	Limited impact scope: data is moderately sensitive; failure has a minor impact on network stability.
0.0 – 0.2	Negligible impact scope: data is public or non-sensitive; failure has virtually no impact on the network.

Table 5. Protective measure strength value classification criteria

Value Range	Classification Criteria
0.8 – 1.0	Integrates advanced security protection technologies; physical security meets high standards, possessing comprehensive data backup and rapid recovery capabilities.
0.6 – 0.8	Adopts multi-layered protective technologies; physical security has advanced preventative measures, with strong data backup and recovery capabilities.
0.4 – 0.6	Deploys a range of defense technologies; moderate physical security measures are implemented, with certain data recovery capabilities.
0.2 – 0.4	Configured with basic security controls; physical security relies on generic solutions, lacking the ability for quick recovery.
0.0 – 0.2	Unprotected or features only basic default settings; lacks physical security controls, data backup, and recovery mechanisms.

2.2.2 Atomic Attack Success Probability Calculation Method Research

This paper identifies four indicators—vulnerability exploitability, temporal vulnerability exploitability, business criticality, and the strength of protective measures—as the influencing factors for the atomic attack success probability in the 5G-R core network attack graph. When constructing a formula to calculate the atomic attack success probability, it is necessary to determine the relative weight of each influencing factor due to their varying degrees of influence. The calculation formula for the atomic attack success probability of the 5G-R core network attack graph is shown in Eq. (6).

$$P(E_i) = VA_i^{1-w_1} \times VT_i^{1-w_2} \times BC_i^{1-w_3} \times (1 - SP_i)^{1-w_4} \quad (6),$$

where $P(E_i)$ represents the success probability of the atomic attack for the i-th vulnerability exploitation; VA_i, VT_i, BC_i, and SP_i represent the i-th vulnerability's exploitability, temporal exploitability, business criticality, and the strength of protective measures indicators, respectively; w_1, w_2, w_3, and w_4 represent the relative weights corresponding to vulnerability exploitability, temporal vulnerability exploitability, business criticality, and the strength of protective measures.

To determine the relative weights of the indicators affecting the atomic attack success probability, this paper uses the fuzzy AHP to analyze the weights for the atomic attack success probability calculation formula of the 5G-R core network attack graph and determine the relative weights of each indicator in Eq. (6).

The fuzzy analysis of factors influencing the atomic attack success probability primarily considers four indicators: the vulnerability exploitability of nodes in the attack graph, the temporal vulnerability exploitability, business criticality, and the strength of protective measures. The fuzzy judgment matrix built based on expert experience is shown in Table 6.

Based on the matrix in Table 6, following the analysis process of the fuzzy AHP, the relative weights for the atomic attack success probability are obtained as 0.205 2, 0.121 8, 0.166 8, and 0.172 8, respectively. Substituting these into Eq. (6), we obtain w_1 = 0.205 2, w_2 = 0.121 8, w_3 = 0.166 8 and w_4 = 0.172 8. Therefore, the final formula for calculating the atomic attack success probability of nodes in the 5G-R core network attack graph is as follows:

$$P(E_i) = VA_i^{0.794\,8} \times VT_i^{0.878\,2} \times BC_i^{0.833\,2} \times (1 - SP_i)^{0.827\,2} \quad (7),$$

where E_i represents the atomic attack on the i-th vulnerability in the 5G-R core network attack graph, $P(E_i)$ represents the atomic attack success rate for the i-th vulnerability exploitation, and VA_i, VT_i, BC_i, and SP_i respectively denote the exploitability, temporal exploitability, business criticality, and the strength of protective measures of the i-th vulnerability.

In summary, the specific values of the indicators involved in the node reachability probability calculation method for the 5G-R core network are shown in Table 7.

3 Method Validation

To verify the effectiveness of the proposed 5G-R core cyber security assessment method based on attack graphs, as well as

Table 6. Fuzzy judgement matrix for atomic attack success probability

	Vulnerability Exploitability	Vulnerability Temporal Availability	Business Criticality	Strength of Protective Measures
Vulnerability exploitability	(0.5, 0.5, 0.5)	(0.7, 0.8, 0.9)	(0.6, 0.7, 0.8)	(0.5, 0.6, 0.7)
Vulnerability temporal availability	(0.1, 0.2, 0.3)	(0.5, 0.5, 0.5)	(0.3, 0.3, 0.4)	(0.2, 0.3, 0.4)
Business criticality	(0.2, 0.3, 0.4)	(0.6, 0.6, 0.7)	(0.5, 0.5, 0.5)	(0.3, 0.5, 0.5)
Strength of protective measures	(0.3, 0.4, 0.5)	(0.6, 0.7, 0.8)	(0.6, 0.6, 0.8)	(0.5, 0.5, 0.5)

Table 7. Node reachability probability indicator values

Indicator Category	Indicator	Quantitative Value
Technical maturity	High, automatable, verified, unverified	(1.00, 0.97, 0.94, 0.91)
Level of remediation	Non-remediable, indirectly remediable, low remediation level, high remediation level	(1.00, 0.97, 0.96, 0.95)
Report confidence	Confirmed, unconfirmed, unknown	(1.00, 0.96, 0.92)

the rationality of the optimization methods, this study conducts a comprehensive evaluation. We compare the performance of the proposed method with traditional assessment approaches to demonstrate its superiority. Specifically, a testbed was constructed to simulate the network environment, facilitating the generation of the corresponding attack graphs. By applying the attack probability quantification method for the 5G-R core network, we calculate the attack success probability and node reachability. The experimental results confirm the validity and robustness of the proposed framework.

3.1 Vulnerability Assessment Method Analysis

The analysis of the 5G-R core network vulnerability assessment method comprises two parts: feasibility analysis and performance analysis.

1) Feasibility analysis

To verify the effectiveness of the 5G-R core network vulnerability assessment method in Section 2.2, we evaluate 10 typical vulnerabilities identified both in the 5G-R core network and the CVSS database. Using the optimized scoring method developed in this paper, we rate these vulnerabilities and compare the results with CVSS scores. Comparison results are shown in Table 8.

Based on the comparative results of Table 8, vulnerabilities with a potentially significant impact on network services in the 5G-R core network, such as CVE-2017-9445 and CVE-2021-41794, receive higher scores in this assessment method. Vulnerabilities that are less associated with the 5G-R core network's services, or have a smaller business impact, such as CVE-2019-13272, receive lower scores in this assessment. However, all score changes remain within the same level of severity as the CVSS scores, indicating that within an acceptable range, the method provides a more differentiated understanding of the security level with respect to business impact, thereby demonstrating its superiority.

Table 8. Vulnerability comparison for the proposed method and CVSS

Vulnerability	CVSS	5G-R Core Network Vulnerability Assessment Method
CVE-2017-9445	7.5	8.8
CVE-2019-13272	7.8	7.1
CVE-2020-35658	5.3	5.6
CVE-2020-8554	5.5	7.5
CVE-2020-13777	7.5	7.5
CVE-2020-3556	7.5	8.1
CVE-2021-21985	9.8	9.8
CVE-2021-1732	7.8	6.8
CVE-2021-41794	7.5	8.1
CVE-2023-23846	7.5	8.1

CVE: common vulnerabilities and exposures
CVSS: common vulnerability scoring system

2) Performance analysis

To comprehensively verify the performance of the proposed 5G-R core network vulnerability assessment method, this section uses MATLAB to conduct a statistical analysis on the combined results of all indicator weights for both models. The score distributions of the CVSS model and the 5G-R core network vulnerability assessment model are presented respectively in Fig. 2.

Compared with the CVSS model, the score distribution curve of the proposed 5G-R vulnerability assessment method changes more gradually and has fewer extreme values. This indicates that the model provides higher consistency and stability in scoring, ensuring consistent risk quantification across different vulnerabilities and security threats. Moreover, the score distribution of the proposed method approximates a normal distribution, further highlighting its superiority.

To summarize, the proposed 5G-R vulnerability assessment method demonstrates superior characteristics in terms of stability, distribution smoothness, and the ability to capture the natural distribution of vulnerabilities.

3.2 Attack Probability Calculation Method Analysis

To verify the validity of the proposed optimization scheme for calculating the node reachability probability in 5G-R core network attack graphs, this section employs a network testbed to build a simplified simulation environment. Based on the corresponding attack graph, the probability of potential node risk occurrence is evaluated. Additionally, comparative experiments are conducted against the methods from Refs. [14] and [15] under an identical experimental setup. The 5G-R core network architecture, constructed using the Open5GS open-source platform, is shown in Fig. 3.

Based on the same simulation environment (Fig. 4) and the attack graph (Fig. 5), Fig. 6 compares the atomic attack success probabilities calculated by integrating the proposed method with the calculation methods in Refs. [14] and [15].

As shown in Fig. 6, there are significant differences in the

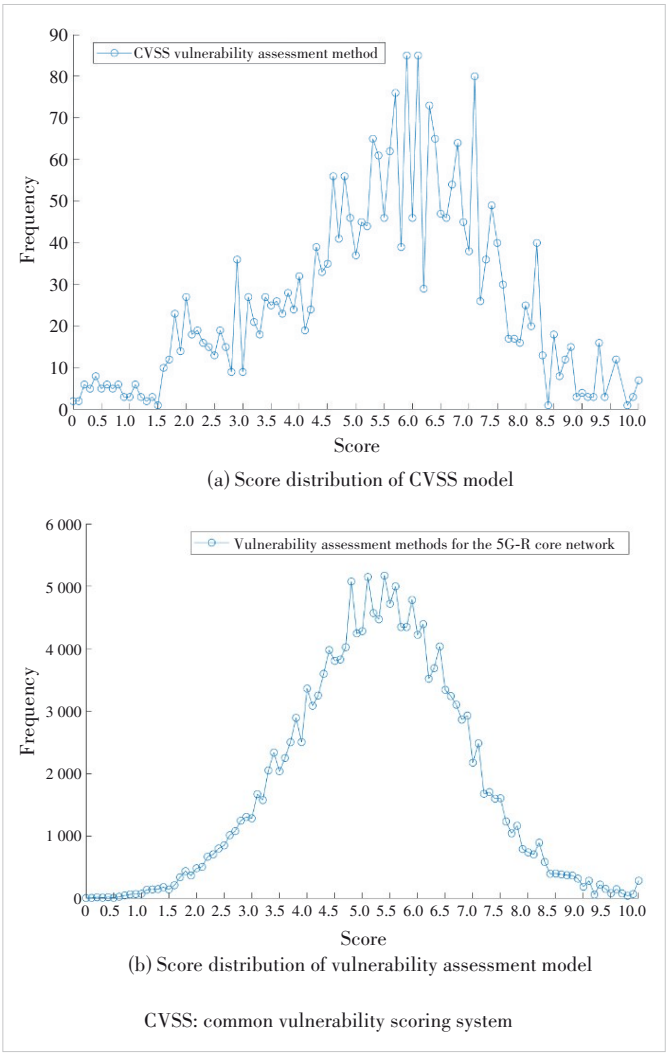

Figure 2. Score distribution diagram of CVSS model and vulnerability assessment model for 5G-R core network

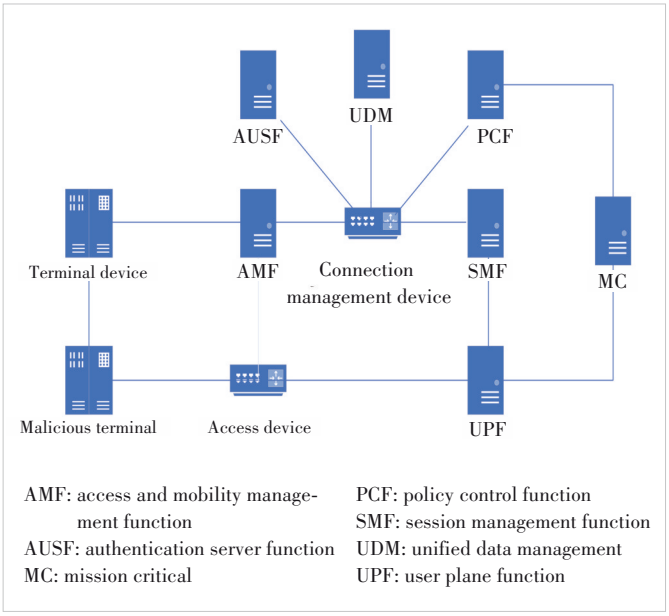

Figure 3. Network architecture diagram of 5G-R core network built-in cyber range

results produced by the three calculation methods, which can be attributed to the following reasons:

1) The method proposed in Ref. [14] is overly simplistic regarding the influencing indicators of the atomic attack success probability. It allows the vulnerability's own exploitability to dominate the probability of a successful atomic attack, while other important indicators are overlooked, resulting in an overestimation of the success probabilities for most atomic attacks.

2) Regarding the vulnerability source discussed in Ref. [15], since the vulnerabilities in the 5G-R core cyber security mostly stem from 5G network technologies, factors such as market share and user numbers are not appropriate for assessing the vulnerabilities of 5G network technologies.

3) Theoretically, attacker behaviors and defensive measures can significantly affect the probability of atomic attack success. Therefore, the calculation of atomic attack success probability in this paper is consistent with theoretical analysis and common understanding, demonstrating its rationality and superiority compared with other methods.

4 Conclusions

This paper presents a comprehensive methodology for 5G-R core cyber security assessment based on attack graphs, which comprises two main components: 1) A vulnerability assessment using an optimized CVSS method. Three elements of business security impact were introduced as optimization indicators, and the values of other indicators were optimized. The exploitability and impact indicators that conform to the network characteristics and security requirements of the 5G-R core network were investigated, resulting in a vulnerability assessment method specifically suited for the 5G-R core network; 2) A method for calculating the probability of successful attacks on nodes in the 5G-R core network attack graph. The fuzzy AHP was combined with the security requirements and actual network environment to optimize the calculation of atomic attack success probabilities. With the incorporation of Bayesian theory, the reachability probability of nodes in the attack graph was further processed, resulting in the determination of the node reachability probability for the 5G-R core network attack graph.

To verify the effectiveness and rationality of the proposed method, this paper selected conventional security assessment methods and approaches cited in existing literature for comparative analysis. A simplified 5G-R core network simulation environment was set up in a network range, and simulation validation based on the attack graph was carried out. The ex-

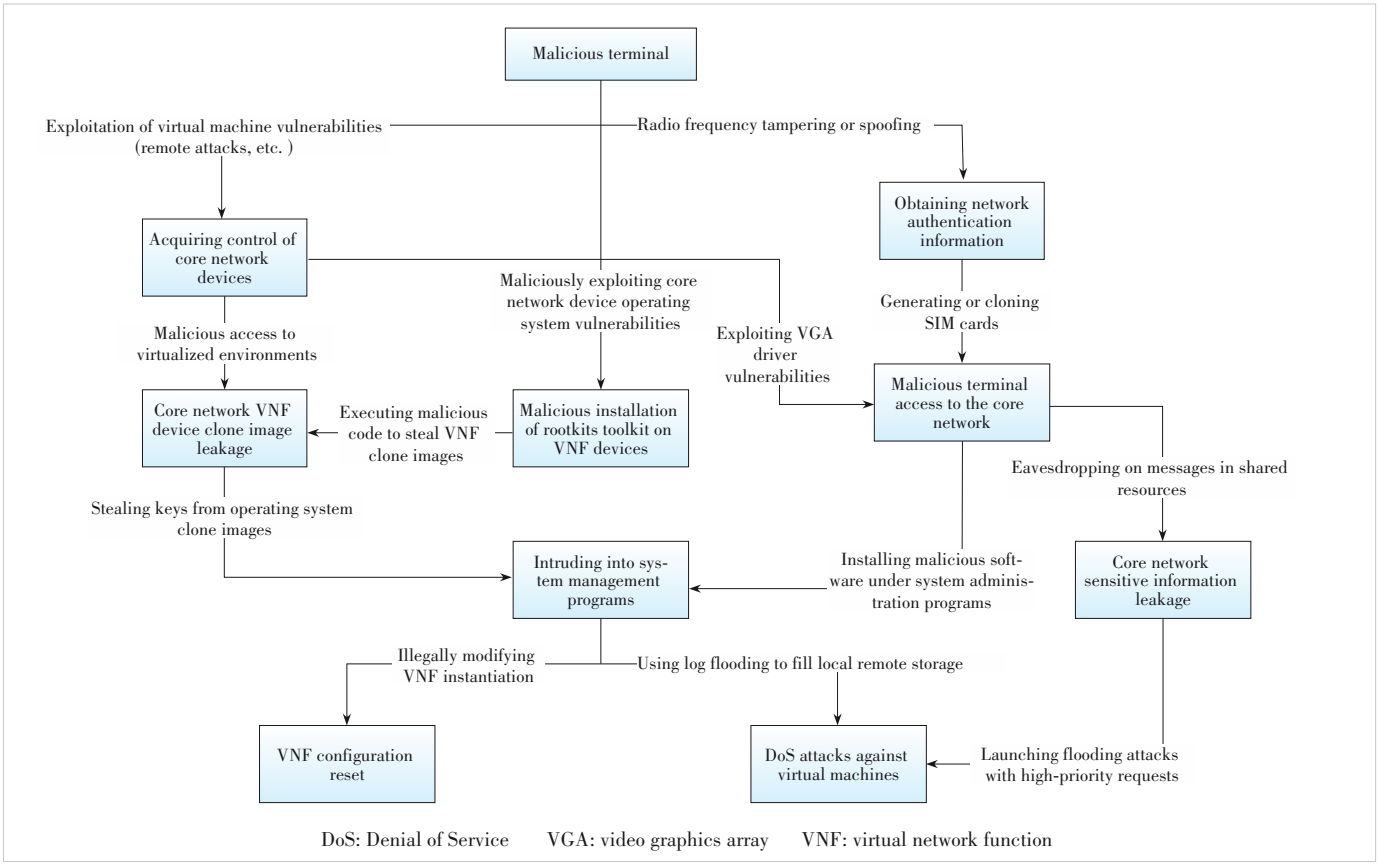

Figure 4. Attack graph of 5G-R core network in simulation environment

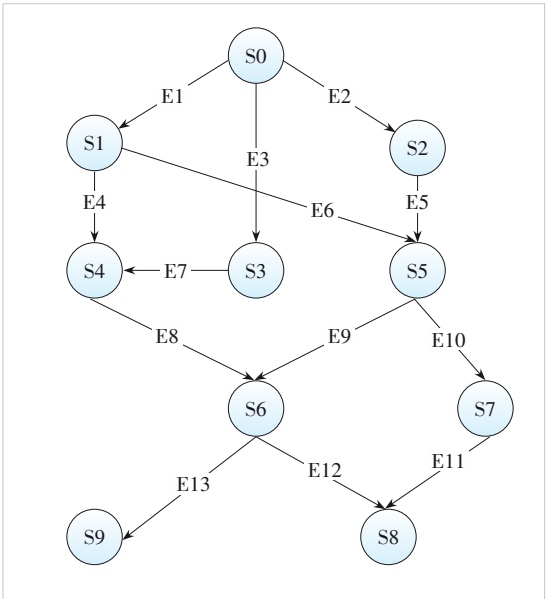

Figure 5. Equivalent form of attack graph

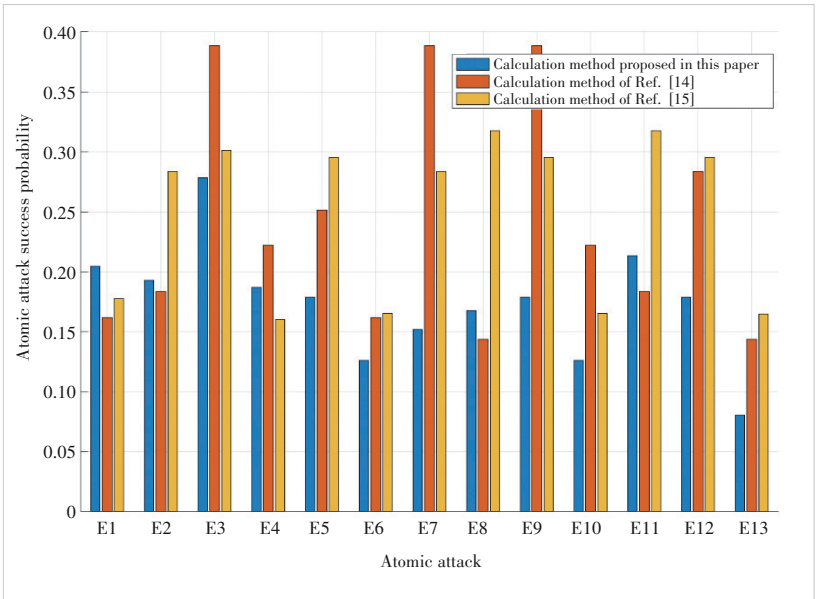

Figure 6. Comparison diagram of atomic attack probabilities

perimental results prove that the vulnerability assessment model in the proposed method outperforms existing approaches, and the node reachability probability calculation method is more comprehensive and rational. Therefore, the 5G-R core cyber security assessment method based on attack graphs is rational and demonstrates clear superiority.

References

[1] Ding J W, Liu Y, Liao H J, et al. Statistical model of path loss for railway 5G marshalling yard scenario [J]. ZTE communications, 2023, 21(3): 117 - 122. DOI: 10.12142/ZTECOM.202303015
[2] He R S, Ai B, Zhong Z D, et al. 5G for railways: next generation railway dedicated communications [J]. IEEE communications magazine, 2022, 60 (12): 130 - 136. DOI: 10.1109/mcom.005.2200328
[3] Sun Z T. Hierarchical and complex parallel network security threat situation quantitative assessment method [C]//The 6th International Conference on Computing Methodologies and Communication (ICCMC). IEEE, 2022: 276 - 279. DOI: 10.1109/ICCMC53470.2022.9753819
[4] ISO 27000: 2018 Information technology—security techniques—information security management systems—overview and vocabulary [S]
[5] Ritchey R W, Ammann P. Using model checking to analyze network vulnerabilities [C]//Symposium on Security and Privacy. IEEE, 2000: 156 - 165. DOI: 10.1109/SECPRI.2000.848453
[6] Lippmann R, Ingols K, Scott C, et al. Validating and restoring defense in depth using attack graphs [C]//IEEE Military Communications Conference. IEEE, 2006: 1 - 10. DOI: 10.1109/MILCOM.2006.302434
[7] Sheyner O, Wing J. Tools for generating and analyzing attack graphs [M]// Formal methods for components and objects. Berlin, Heidelberg: Springer, 2004: 344 - 371. https://doi.org/10.1007/978-3-540-30101-1_17
[8] Ou X, Govindavajhala S, Appel A W. MulVAL: a logic-based cyber security analyzer [C]//The 14th USENIX security symposium. USENIX, 2005: 113 - 128. DOI: 10.5555/1251398.1251406
[9] Phillips C, Swiler L P. A graph-based system for network-vulnerability analysis [C]//The 1998 Workshop on New Security Paradigms. ACM, 1998: 71 - 79
[10] Jajodia S, Noel S, O'berry B. 2005. Topological analysis of network attack vulnerability [M]//Managing cyber threats: issues, approaches, and challenges. Boston: Springer US, 2005: 247 - 266
[11] Wang J F, Guo Y B. Cyber security risk assessment of physical information systems based on attack graphs [J]. Science technology and engineering, 2023, 23(28): 12175 - 12181. DOI: 10.12404/j. issn. 1671-1815.2023.23.28.12175
[12] Pu J Y, Li Y H, Zhou C J. Method for cross-domain dynamic security risk analysis of industrial control systems based on probabilistic attack graphs [J]. Information cyber security, 2023, 23(9): 85 - 94. DOI: 10.3969/j. issn.1671-1122.2023.09.008
[13] Wang Z B, Zhang Y F, Chen Y L, et al. Method for discovering attack paths based on hierarchical task networks [J]. Computer science, 2023, 50(9): 35 - 43. DOI: 10.11896/jsjkx.230500025
[14] Wang S E, Liu C X, Liu S X, et al. A method for assessing 5G cyber security risk based on attack graphs [J]. Computer applications and software, 2023, 40(04): 289 - 296+335. DOI: 10.3969/j. issn. 1000-386x.2023.04.046
[15] Zeng K L, Zhang N, Li W H, et al. Network asset security assessment model based on Bayesian attack graph [J]. Computer science, 2023, 50 (12): 349 - 358. DOI: 10.11896/jsjkx.221000019

Biographies

Dong Congtang received his BE degree in communication engineering from Shandong Normal University, China in 2022. He is currently pursuing a master's degree at the State Key Laboratory of Advanced Rail Autonomous Operation, Beijing Jiaotong University, China. His research interests include cyber security, AIOps and 5G-R.

Xu Hang received his BE degree in communication engineering from China University of Petroleum in 2022 and his ME degree from Beijing Jiaotong University, China in 2024. His research interests include network security and 5G-R.

Sun Bin (bsun@bjtu.edu.cn) received his BS and MS degrees in electronic engineering from Beijing Jiaotong University, China in 2004 and 2007, respectively. From 2007 to 2015, he was an R&D manager with BeiJing Liujie Technology Co., Ltd. He is currently an assistant researcher with the School of Electronic and Information Engineering, Beijing Jiaotong University. His main research interest is the interconnection and interworking of core networks for dedicated railway mobile communication systems.

Ding Jianwen received his BS and MS degrees from Beijing Jiaotong University, China in 2002 and 2005, respectively. He is currently a professor at the School of Electronic and Information Engineering, Beijing Jiaotong University. He received the Second Prize of the China Railway Society Science and Technology Progress Award. His research interests include broadband mobile communications and personal communications, dedicated mobile communication systems for railway, and safety communication technology for train control systems.

Wang Wei is the Technical Director of LTE-R at ZTE Corporation and an expert in railway wireless communication systems. He has extensive experience in GSM-R system design, with in-depth insights into both GSM-R and LTE-R technologies. He has led and participated in several major railway wireless communication projects.

The 2nd Youth Expert Committee
for Promoting Industry-University-Institute Cooperation

Director **Chen Wei,** Beijing Jiaotong University

Deputy Director **Qin Xiaoqi,** Beijing University of Posts and Telecommunications

Lu Dan, ZTE Corporation

Members (Surname in Alphabetical Order)

Cao Jin	Xidian University
Chen Li	University of Science and Technology of China
Chen Qimei	Wuhan University
Chen Shuyi	Harbin Institute of Technology
Chen Siheng	Shanghai Jiao Tong University
Chen Wei	Beijing Jiaotong University
Gao Zhen	Beijing Institute of Technology
Guan Ke	Beijing Jiaotong University
Han Chong	Shanghai Jiao Tong University
Han Kaifeng	China Academy of Information and Communications Technology
He Zi	Nanjing University of Science and Technology
Hou Tianwei	Beijing University of Posts and Telecommunications
Hu Jie	University of Electronic Science and Technology of China
Huang Chen	Purple Mountain Laboratories
Huo Jiahao	University of Science and Technology Beijing
Li Ang	Xi'an Jiaotong University
Li Li	University of Science and Technology of China
Liu Fan	Southeast University
Liu Junyu	Xidian University
Lu Dan	ZTE Corporation
Lu Youyou	Tsinghua University
Mei Weidong	University of Electronic Science and Technology of China
Ning Zhaolong	Chongqing University of Posts and Telecommunications
Pan Cunhua	Southeast University
Qi Liang	Shanghai Jiao Tong University
Qin Xiaoqi	Beijing University of Posts and Telecommunications
Qin Zhijin	Tsinghua University
Shi Yao	Harbin Institute of Technology
Shi Yinghuan	Nanjing University
Tang Wankai	Southeast University
Wang Jingjing	Beihang University
Wang Xinggang	Huazhong University of Science and Technology
Wang Yongqiang	Tianjin University
Wen Miaowen	South China University of Technology
Wu Qingqing	Shanghai Jiao Tong University
Wu Yongpeng	Shanghai Jiao Tong University
Xia Wenchao	Nanjing University of Posts and Telecommunications
Xiang Luping	Nanjing University
Xu Mengwei	Beijing University of Posts and Telecommunications
Xu Tianheng	Shanghai Advanced Research Institute, Chinese Academy of Sciences
Yang Chuanchuan	Peking University
Ye Yinghui	Xi'an University of Posts and Telecommunications
Yin Haifan	Huazhong University of Science and Technology
You Changsheng	Southern University of Science and Technology
Yu Jihong	Beijing Institute of Technology
Zhang Jiao	Beijing University of Posts and Telecommunications
Zhang Jiayi	Beijing Jiaotong University
Zhang Yuchao	Beijing University of Posts and Telecommunications
Zhao Yizhe	University of Electronic Science and Technology of China
Zhao Yuda	Zhejiang University
Zhao Zhongyuan	Beijing University of Posts and Telecommunications
Zhou Yi	Southwest Jiaotong University
Zhu Bingcheng	Southeast University
Zhu Guangxu	Shenzhen Research Institute of Big Data
Zhu Zhengyu	Zhengzhou University

ZTE COMMUNICATIONS
中兴通讯技术(英文版)

ZTE Communications has been indexed in the following databases:

- Abstract Journal
- China Science and Technology Journal Database
- Chinese Journal Fulltext Databases
- Index Copernicus
- Scopus
- Ulrich's Periodicals Directory
- Wanfang Data
- WJCI 2021–2025

ZTE COMMUNICATIONS
Vol. 24 No. 2 (Issue 95)
Quarterly
First Issue Published in 2003

Supervised by:
Anhui Publishing Group

Sponsored by:
Time Publishing and Media Co., Ltd.
Shenzhen Guangyu Aerospace Industry Co., Ltd.

Published by:
Anhui Science & Technology Publishing House

Edited and Circulated (Home and Abroad) by:
Magazine House of ZTE Communications

Editorial Correspondence:
Add: 12F Kaixuan Building, 329 Jinzhai Road,
Hefei 230061, P. R. China
Tel: +86-551-65533356
Email: magazine@zte.com.cn
Website: http://zte.magtechjournal.com

Annual Subscription: RMB 120
Printed by:
Anhui Tianjin Printing Technology Co., Ltd.
Publication Date: June 25, 2026

China Standard Serial Number: ISSN 1673–5188 / CN 34–1294/TN